

Masaryk University Brno

Faculty of Medicine

Department of Anatomy

**NERVE INJURY INDUCED NEUROPATHIC PAIN AND
SPREAD OF INFLAMMATORY RESPONSE TO REMOTE
STRUCTURES OF THE NERVOUS SYSTEM**

Habilitation thesis

(Collection of Articles)

MUDr. Marek Joukal, Ph.D.

2019

Abstract

Peripheral nerve injury may result in neuropathic pain represented by spontaneous allodynia and thermal hyperalgesia. It has been found that unilateral nerve injury induces cellular and molecular changes not only in the structures anatomically related with the injured nerve but also in structures of the nervous system unrelated with the site of injury. The Cellular and Molecular Research Group at the Department of Anatomy, that I am a member, was the first who gave an evidence that sciatic nerve injury induces cellular and molecular changes in remote cervical dorsal root ganglia (DRG). These changes correspond with induction of pro-regenerative state in the remote DRG. Moreover, we found that descending modulation of pain perception is mediated via CCL2/CCR2 signaling pathway in the periaqueductal gray and the rostral ventromedial medulla. Therefore, there is compelling evidence indicating that neuroinflammatory response after nerve injury may spread to structures of the nervous system not only transynaptically via the sensory pathway but also through the nervous system barriers. In a field of the nervous system barriers, our experiments revealed that subarachnoid space filled with cerebrospinal fluid directly communicates with the DRG giving anatomical background for spread of inflammatory molecules to remote structures of nervous system via cerebrospinal fluid. In addition, we found that peripheral nerve injury induces immune reaction in the choroid plexus where is localized the blood-cerebrospinal fluid barrier indicating its possible alteration after nerve injury. Presented habilitation thesis is written as a collection of published articles with a commentary introducing the topic and describing current state of knowledge.

Acknowledgments

I would like to thank to all my co-authors and colleagues who guided my research career. Especially, I would like to thank to prof. RNDr. Petr Dubový, CSc. for mentorship and support in my research activities. Most of all I would like to thank my family for their support, love and patience.

Table of Contents

1. Introduction and aims	1
2. Nociceptive pathway	2
2.1. Peripheral nociceptive receptors.....	2
2.2. The primary nociceptive neurons	2
2.3. Nociceptive afferentation in the spinal cord.....	3
2.4. Tertiary nociceptive neurons	4
2.5. Cortical projections of nociceptive pathway	5
2.6. Descending modulatory pathways.....	6
3. Peripheral neuropathic pain models	8
3.1. Experimental peripheral nerve injury	9
3.1.1. Sciatic nerve transection.....	9
3.1.2. Chronic constriction injury	9
3.1.3. Partial sciatic nerve ligation	10
3.1.4. Spared nerve injury.....	11
3.1.5. Segmental L5/L6 spinal nerve ligation.....	12
3.2. Experimental spinal nerve root injury	12
3.2.1 Dorsal root compression.....	12
3.2.2. Dorsal rhizotomy	13
3.2.3. Ventral rhizotomy.....	13
4. Wallerian degeneration.....	15
4.1. Axon degeneration.....	15
4.2. Wallerian degeneration as sterile inflammatory reaction	16
5. Reaction of the DRG to peripheral nerve injury.....	17
5.1. Cellular reactions in DRG induced by peripheral nerve injury	17
5.2. Molecular reactions in DRG induced by peripheral nerve injury	18

5.2.1. Cytokines and chemokines involved in neuropathic pain development and maintenance	18
5.2.2. Nerve injury-induced regeneration state in the DRG	20
6. Reaction of the spinal cord and brain stem to nerve injury	21
6.1. Inflammatory reactions in the spinal cord of neuropathic pain models	22
6.2. Pain processing and modulation in the brain stem	25
6.2.1. The gracile and cuneate nucleus	25
6.2.2. Rostral ventromedial medulla.....	26
6.2.3. Pons	27
6.2.4. Mesencephalon	28
7. Diencephalon and its reaction to nerve injury	30
7.1. Thalamus	30
7.2. Hypothalamus.....	30
8. Pain processing and modulation in the telencephalon.....	31
8.1. Basal ganglia	31
8.2. Anterior cingulate cortex	32
8.3. Ventrolateral orbitofrontal cortex	32
8.4. Insular cortex	33
8.5. Somatosensory cortex.....	34
9. Barriers of the nervous system, their alteration and contribution to spread of inflammatory reaction after nerve injury.....	35
9.1. The blood-nerve barrier	35
9.2. The blood-DRG barrier	36
9.3. The cerebrospinal fluid-DRG barrier	37
9.4. Blood-brain and blood-spinal cord barrier	40
9.5. Blood-cerebrospinal fluid barrier	43
10. Conclusions and future perspectives	46
11. References	48

12. Collection of articles.....	70
13. Full list of author's publications in impacted journals.....	159

1. Introduction and aims

Neuropathic pain is defined as a chronic pain condition that occurs and persists in a heterogeneous group of etiologically different diseases characterized by primary lesions or dysfunction of the peripheral or central nervous system ¹. The World Health organization has estimated that 22% of the world's primary care patients have chronic debilitating pain making chronic pain a problem to be addressed by all physicians and health professionals ².

Peripheral neuropathic pain is manifested by spontaneous pain, hyperalgesia and allodynia, arises as a result of various types of nerve damage, e.g., diabetic neuropathy, HIV neuropathy, post-herpetic neuralgia, drug-induced neuropathy and traumatic nerve injury ^{3,4}.

It is generally accepted that the unilateral injury of the peripheral nerve causes wide range of inflammatory reactions alongside the neuroaxis. These reactions are not only restricted on the structures that are anatomically related to the injured sciatic nerve but also remote structures such as cervical dorsal root ganglia (DRG) ^{5,6} or rostral ventromedial medulla and periaqueductal grey ⁷. These changes might be caused by spread of the proinflammatory chemokines and cytokines via blood circulation and/or cerebrospinal fluid ^{8,9}.

The goal of presented habilitation thesis is to provide an overview of present knowledge about the nerve injury induced neuropathic pain and spread of the inflammatory response to the central nervous system (CNS) and to summarize results of my experimental work in this field. Details about design of experiments and used methods can be found in attached publications (Chapter 12).

2. Nociceptive pathway

The nociceptive pathway begins on the peripheral nociceptive receptors and contains three neurons; the primary neuron is located in the DRG, the secondary neuron in the spinal cord and the tertiary neuron in the thalamus. The nociceptive pathway terminates in the sensory cerebral cortex.

2.1. Peripheral nociceptive receptors

The sensation of pain begins on high-threshold receptors (nociceptors) as a reaction on tissue damage. Nociceptors are free nerve endings different with regard to stimulus specificity. Some nociceptors react on intense mechanical stimulus (mechanical nociceptors), others respond to extreme heat or coldness (cold and heat nociceptors) and some nociceptors respond to chemical stimuli, e.g. inflammatory state. However, many nociceptors are polymodal responding to several kinds of stimuli. Nociceptive fibers are predominantly thinly myelinated and unmyelinated ($A\delta$ and C fibers) with conduction velocity 5 – 30 m/s for $A\delta$ fibers and 0.4 – 1.4 m/s for C fibers ^{10,11}.

2.2. The primary nociceptive neurons

The primary sensory neuron of the nociceptive pathway has its cell bodies in the DRG. Since the bodies of primary neurons are pseudounipolar, they send their peripheral branches to the peripheral nerves and central branches to the spinal cord forming the dorsal root. The axons of different kind of receptors are intermingled in peripheral nerves and the dorsal root, while they are grouped according to their thickness as soon as they enter the spinal cord. Heavily myelinated $A\alpha$ and $A\beta$ fibers enter the spinal cord medially while thinly myelinated $A\delta$ fibers and unmyelinated C fibers laterally ¹².

2.3. Nociceptive afferentation in the spinal cord

Afferent fibers reach the spinal cord and form the Lissauer tract to synapse with the second-order neurons distributed alongside the dorsal horn of spinal cord. The nociceptive neurons respond to specific noxious stimuli and they are found in laminae I, II, V and VI. Inputs for these neurons are high threshold A δ nociceptive fibers and polymodal C nociceptive fibers with somatotopic organization mainly in lamina I¹³⁻¹⁵.

Axons of the secondary nociceptive neurons pass through the anterolateral funiculus and posterior funiculus. These afferent bundles transmit nociceptive stimuli to the structures of the brain stem and diencephalon^{14,16}.

The bodies of neurons sending their axons to form the spinothalamic tract are localized mainly in lamina I and V of the spinal cord. In addition, scattered neurons are also found more ventrally in laminae VII and VIII.^{12,17,18} Most of the neurons project to the contralateral thalamus although a small group of cells projects ipsilaterally. Based on the origin and the projection, the spinothalamic tract can be divided into three bundles. The first is monosynaptic neospinothalamic pathway or ventral spinothalamic tract directly projected to the lateral part of the thalamus that carries fibers involved in the sensory-discriminative component of pain. The second, dorsal spinothalamic tract, is multisynaptic paleospinothalamic pathway that terminates on intralaminar and dorsal nuclei of the thalamus involved in the motivational-affective aspects of pain. The third tract is projected directly to the medial central nucleus of the thalamus that is responsible for affective component of pain^{14,16}.

The spinoreticular tract starts on neurons localized in the deep layers of the dorsal horn of spinal cord as well as in laminae VII and VIII of the ventral horn^{16,19}. The tract has two components,

the first projects to the precerebellar nucleus involved in motor control. The other component is involved in nociception and projects to the medial pontobulbar reticular formation. The pontocerebellar tract is believed to play a role in motivational-affective characteristics and neurovegetative responses to pain ^{13,14}.

The spinomesencephalic tract originates in lamina I, IV and V as well as the ventral horn and lamina X. Spinomesencephalic projections run to several areas of the midbrain including nucleus cuneiformis, intercolliculus nucleus, deep layers of the superior colliculus, nucleus of Darkschewitsch, pretectal nuclei, red nucleus, Edinger-Westphal nucleus, interstitial nucleus of Cajal. Moreover, the spinomesencephalic tract also terminates in periaqueductal gray that play important role in descending modulatory system for attenuation of pain ^{14,16}.

2.4. Tertiary nociceptive neurons

Tertiary nociceptive neurons are found in the thalamus that is the main relay station for ascending tracts directed to the cortex. The thalamus receives fibers involved in perception, integration, and transfer of the pain mainly via the spinothalamic tract that projects to both medial and lateral nuclear complex. Many spinothalamic fibers terminate in the ventral posterolateral nucleus that is somatotopically organized. The ventral posterolateral nucleus has interconnections with the primary sensory cortex responsible for localization of the pain and its intensity.

The spinothalamic tract has also terminations on the neurons of the ventral posteromedial nucleus that send axons to the prefrontal cortex. Since the ventral posteromedial nucleus receives fibers from the parabrachial nucleus and has interconnections with the amygdala, hypothalamus and periaqueductal grey, it is believed to be involved in emotional aspects and

vegetative response to the pain. In addition, the spinothalamic fibers end on the posterior nucleus, the intralaminar nuclei (e.g. central lateral nucleus) and mediodorsal nucleus ^{12,14}.

2.5. Cortical projections of nociceptive pathway

The painful stimuli activate multiple cortical areas, namely primary sensory cortex, secondary sensory cortex, insula, anterior cingulate cortex and prefrontal cortex. The afferent fibers from the thalamus form the medial and lateral system of the nociceptive pathway based on the projection sites from medial and lateral thalamic nuclear complexes (Fig. 1). Although the division of the afferent nociceptive pathway to the lateral and medial system is oversimplification, it is useful because of grouping of the cerebral regions that seem to have similar role in pain perception. The lateral system is believed to play a role in perception of the location and intensity of the pain while the medial system in affective component of the pain ²⁰⁻²².

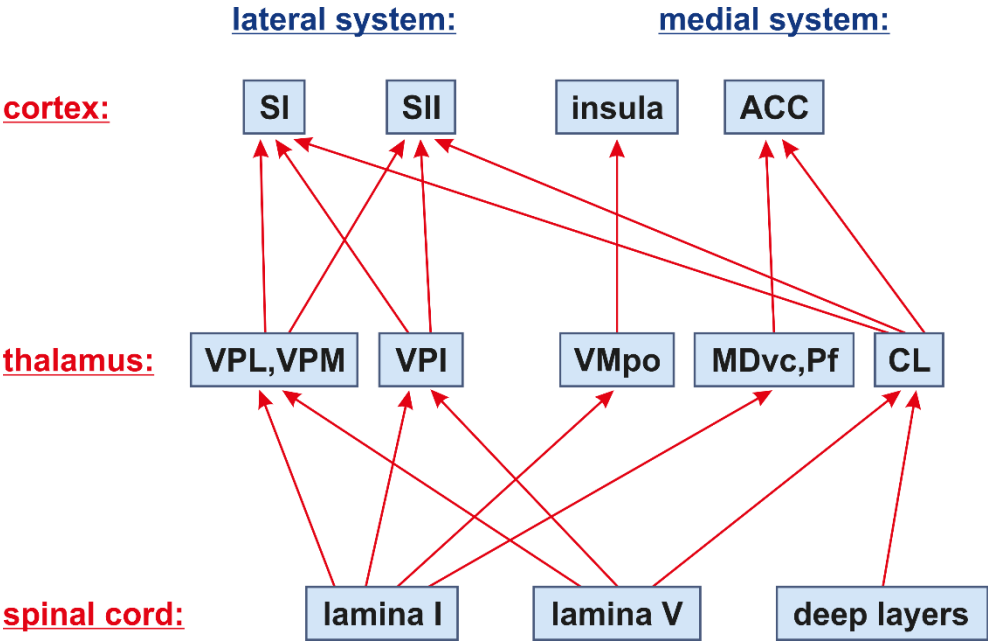


Figure 1. The cortical projections of nociceptive pathways ²². VPL – ventral posterior lateral nucleus; VPM – ventral posterior medial nucleus; VPI – ventral posterior inferior nucleus;

VMpo – posterior part of ventromedial nucleus; MDvc – ventrocaudal part of medial dorsal nucleus; Pf – parafascicular nucleus; CL – centrolateral nucleus; SI – primary somatosensory cortex; SII – secondary somatosensory cortex; ACC – anterior cingulate cortex.

2.6. Descending modulatory pathways

Pain is modulated by descending modulatory circuit that receives inputs from several areas of the central nervous system, e.g. the hypothalamus, cingulate cortex or amygdala. However, pivotal role in nociceptive modulation plays the periaqueductal gray in the midbrain. The periaqueductal gray has columnar functional organization with ventrolateral and dorsolateral columns. It has been found that stimulation of the ventrolateral column evokes active defense behavior and opioid-dependent analgesia (abolished by injection of naloxone). In contrast, stimulation of the dorsolateral column causes freezing reaction and opioid-independent analgesia²³. Axons of the periaqueductal gray have their synapses in the rostral ventromedial medulla on neurons of the nucleus raphe magnus and the nucleus reticularis gigantocellularis. These neurons have connections with the spinal cord forming the raphespinal tract that directly or indirectly modulates nociceptive afferentation^{12,24} (Fig. 2).

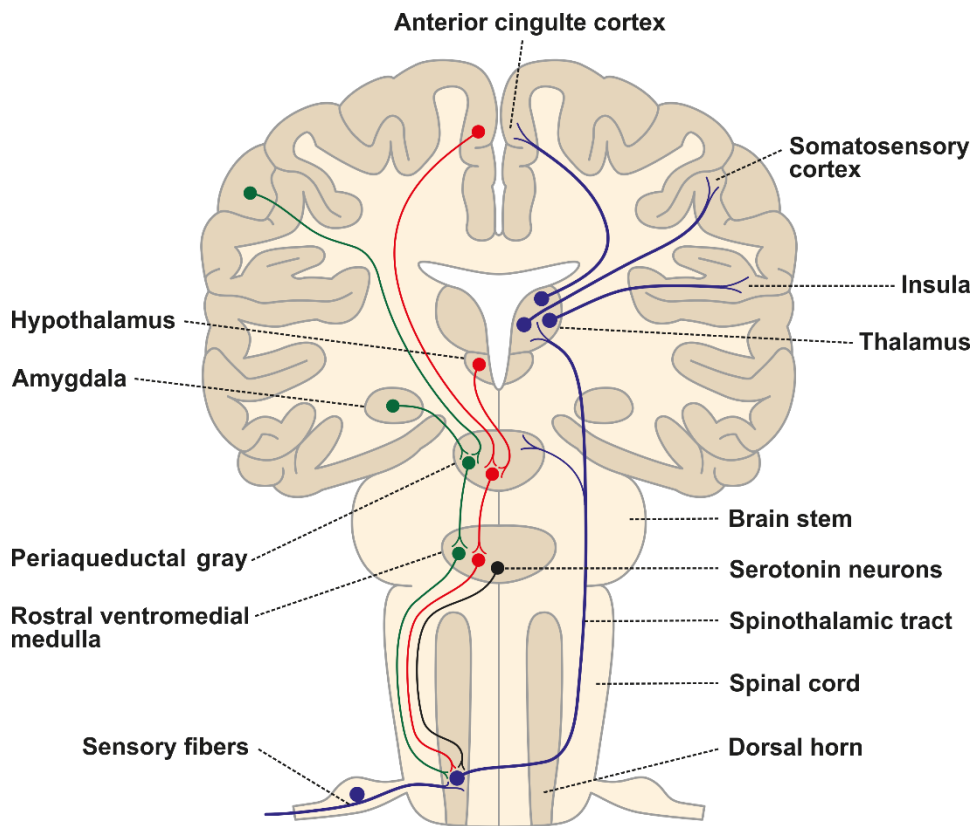


Figure 2. Scheme of the nociceptive pathway on the right (purple) and descending modulatory pathways on the left. Red neurons induce inhibition while green mediate facilitation of nociception. Modified from Brodal ¹².

3. Peripheral neuropathic pain models

Peripheral nerve injury frequently results in development of the neuropathic pain that may differ depending upon the type of nerve damage and the individual. Our knowledge of cellular and molecular events in the nervous system following peripheral nerve injury is based on various types of experimental nerve lesions in animal models.

Peripheral nerve injury causes cellular and molecular changes in primary afferent neurons, their peripheral and central branches. Severity and form of molecular and cellular changes depends on many factors including type and lesion position. Generally, reaction of neurons in corresponding DRG is more intensive when the nerve damage is closer to the neuronal perikaryon and prognosis of recovery is much poorer in comparison to lesions far from the perikaryon^{25,26}. Total axotomy produces more severe reaction than peripheral nerve ligation when continuity of the axons is not disrupted²⁷. In addition, age of the organism plays important role in reaction to the injury. Experimental studies revealed that peripheral nerve injury in young animal causes more intensive reaction of the nervous system than in older animals^{28,29}.

Numerous experimental models were developed to study neuropathic pain induction as a consequence of molecular and cellular changes in the nervous system. In general, the experimental models can be divided according to position of the lesion (spinal nerve roots, DRG, spinal nerve or peripheral nerve) and the type of lesion (transection, compression by loose or tight ligation, cryoneurolysis, stimulation of perineuronal inflammation, tumor cells invasion or laser radiation)³⁰.

Because of favorable anatomical organization, majority of experimental models are undertaken on the hind limb of rodents which is innervated from L3 – L6 spinal segments^{31,32}.

3.1. Experimental peripheral nerve injury

The sciatic nerve is the most commonly used peripheral nerve for the nerve lesions having the maximum amount of neuronal perikarya in rat DRG of the L4 and L5 segments ³³.

3.1.1. Sciatic nerve transection

The model of sciatic nerve transection described Wall with colleagues ³⁴ to mimic the “phantom pain” well known in patients undergoing the amputation or transverse spinal lesion. Transection of the sciatic nerve is performed in the middle of thigh. The proximal stump is either ligated or inserted to the polyethylene tube or a 5-8 mm long segment of the nerve is removed to prevent reinnervation. The axotomy causes immediate loss of both sensory and motor innervation in area innervated by the sciatic nerve. The whole distal stump undergoes molecular and cellular changes well known as the Wallerian degeneration. Since the axotomy results in blockade of retrograde transport and interruption of the blood-nerve barrier, the Wallerian degeneration products (cytokines, chemokines and cellular debris) are easily transported via blood circulation. The disadvantage of this model is impossibility of behavioral testing including allodynia and hyperalgesia in denervated limb. In addition, deafferentation of the limb results in “self-attack”, the autotomy. It is questionable if this phenomenon is a sign of spontaneous pain ³⁵ or a response to total denervation of the hind paw.

3.1.2. Chronic constriction injury

Bennet and Xie ³⁶ as the first described the chronic constriction injury. In its original form, four tight ligatures of chromic gut (4-0) were placed on the sciatic nerve in the middle of thigh. The chromic gut causes local inflammatory response and subsequent nerve edema inducing an increased compression of axons. Nerve inflammation caused by the chromic gut is accompanied

by immune reaction ³⁷ with invasion of immune cells ³⁸. Therefore, the chronic constriction injury using the chronic gut is not suitable to distinguish between inflammatory reaction induced by the chronic gut and that produced during Wallerian degeneration ^{30,39}.

Nevertheless, use of sterilized material (e.g. Prolen) to prevent inflammatory response and edema of the nerve has disadvantage in non-uniform amount of injured and uninjured axons. To prevent this disadvantage, it is possible to use polyethylene “cuff” with standardized diameter placed on the sciatic nerve. Tissue reaction between the nerve and cuff can be minimalized using biocompatible material ⁴⁰.

Chronic constriction injury causes loss of both sensory and motor fibers. Considerable loss of heavily myelinated A α and A β axons and smaller amount of A δ and C fibers with partial deafferentation of the hind limb was demonstrated following the sciatic nerve ligation ^{41,42}. The DRG associated with the nerve ligation contain a mixture of neurons with injured and uninjured axons. The uninjured axons distal to the ligation are exposed to the Wallerian degeneration products (cytokines, chemokines) from injured fibers. These molecules can be retrogradely transported by uninjured axons to corresponding DRG neurons. Therefore, the nerve ligation is suitable model for studying contribution of the Wallerian degeneration to neuropathic pain induction.

3.1.3. Partial sciatic nerve ligation

Partial sciatic nerve ligation is also known as “Seltzer’s ligation” ⁴³ that mimic nerve contusion. Partial sciatic nerve ligation is performed using curved needle and silk thread (8-0) at the mid-thigh with the aim to affect approximately one third to one half of nerve fibers. In comparison to the chronic constriction injury, majority of heavily myelinated axons remains unaffected and contributes to development of mechanical allodynia. Partial nerve ligation induces lower

inflammatory component than the chronic constriction injury model with chronic gut. However, variability of number of affected axons, inconsistent manner of damaged endoneurial cells by needle penetration and random mixture of L4-L5 spinal nerve afferent injuries are considered to be disadvantageous in this model.

3.1.4. Spared nerve injury

Spared nerve injury is a model of partial limb denervation with minimal variability of nerve damage. Rat's hind limb plantar area is innervated by three branches of the sciatic nerve, the common fibular, the tibial and the sural nerves⁴⁴. Classical spared nerve injury model described by Decosterd and Woolf⁴⁵ in rats was based on transection of the tibial and the common fibular nerves while sural nerve was left intact. In mice, the dynamics of mechanoallodynia and thermal hyperalgesia after spared sural nerve does not correlate with those seen in rats. Therefore, variations of spared nerve injury when the common peroneal or the tibial nerve is left intact were studied⁴⁶. Reinnervation of axotomized nerves was prevented by tight ligation of the proximal stump and removal of 2-4 mm segment of appropriate nerve. In contrast to aforementioned models of peripheral nerve injury, spared nerve injury model produces the most constant degree of axonal damage. In addition, the direct contact of injured and uninjured axons is avoided in peripheral nerve. However, there is considerable co-mingling of injured and uninjured neurons in corresponding DRG. This situation allows studies of potential paracrine signaling in DRG and its contribution to neuropathic pain development. It is important to note that even only two branches out of three are axotomized there are changes in all neurons in DRG associated with the sciatic nerve. Advantage of this model is possibility of behavioral testing in the skin region innervated by non-affected branch of the sciatic nerve.

3.1.5. Segmental L5/L6 spinal nerve ligation

The spinal nerve ligation is performed using tight (3-0) ligature distally to corresponding DRG on the L5-L6 spinal nerves while leaving the L4 spinal nerve intact⁴⁷. This model is based on experimental paradigm that there is population of axotomized and intact neurons in one DRG. Since the L4 spinal nerve is intact it is possible to investigate changes in sensitivity in corresponding plantar dermatomes.

Although spinal nerve ligation produces uniform changes in associated DRG, an extensive surgical approach to vertebral foramina and tissue damage near intact L4 spinal nerve are disadvantageous in this model. Therefore, evaluation of molecular changes including inflammatory is very problematic.

3.2. Experimental spinal nerve root injury

In contrast to peripheral nerve injury models, experimental models of spinal root injury are more difficult to achieve. Overall range of surgical approach is the biggest limitation. Before the spinal root lesion it is necessary to retract the paravertebral muscles, remove the transverse processes, provide hemilaminectomy and open the dural sac.

3.2.1 Dorsal root compression

The dorsal root of spinal nerve contains primary central arms of afferent fibers. Therefore, there is no motor defect in case of the dorsal root injury. Model of the dorsal root compression simulates the compressive radiculopathy. Original model described Tabo with colleagues⁴⁸ when the silk ligature (7-0) was placed on the dorsal roots of L4-L6 spinal segments. Corresponding DRG contain populations of affected and unaffected primary sensory neurons.

Some of the fibers proximal to the lesion undergoes Wallerian degeneration while a mixture of injured and uninjured axons is found distal to the lesion.

There were developed alternative methods of the dorsal root compression to guarantee constant force on the axons. The dorsal root can be compressed using the steel bar inserted to the intervertebral foramen⁴⁹ or tube containing material that can expand following fluid absorption⁵⁰. Temporal cellular and molecular changes during compressive radiculopathy and subsequent decompression can be studied using combination of epidural catheter and nylon rod⁵¹.

3.2.2. Dorsal rhizotomy

Dorsal rhizotomy mimics an avulsion of the dorsal root nerve out of the spinal cord frequently caused by traction mechanism. The model is based on complete transection of the dorsal root of spinal nerve between the cervical/thoracic or lumbar/sacral segments⁵² that affects all primary sensory neurons in corresponding DRG. Moreover, there is deafferentation to associated segment of the spinal cord resulting in various degree of self-mutilation in experimental animals. Although complete transection of the dorsal root causes deafferentation of the spinal segments, allodynia and hyperalgesia are present in experimental animals in similar degree to the dorsal root compression model⁵³.

3.2.3. Ventral rhizotomy

Ventral rhizotomy is the first model of neuropathic pain where afferent sensory fibers remain intact. The model is based on complete transection of the ventral root of spinal nerve. Motor axons distal to the lesion undergo Wallerian degeneration and generate cellular and molecular changes that affect intact afferent fibers. Ventral rhizotomy causes morphological and

metabolic changes in corresponding DRGs represented by invasion of macrophages and increased expression of tumor necrosis factor α (TNF- α)^{54,55}.

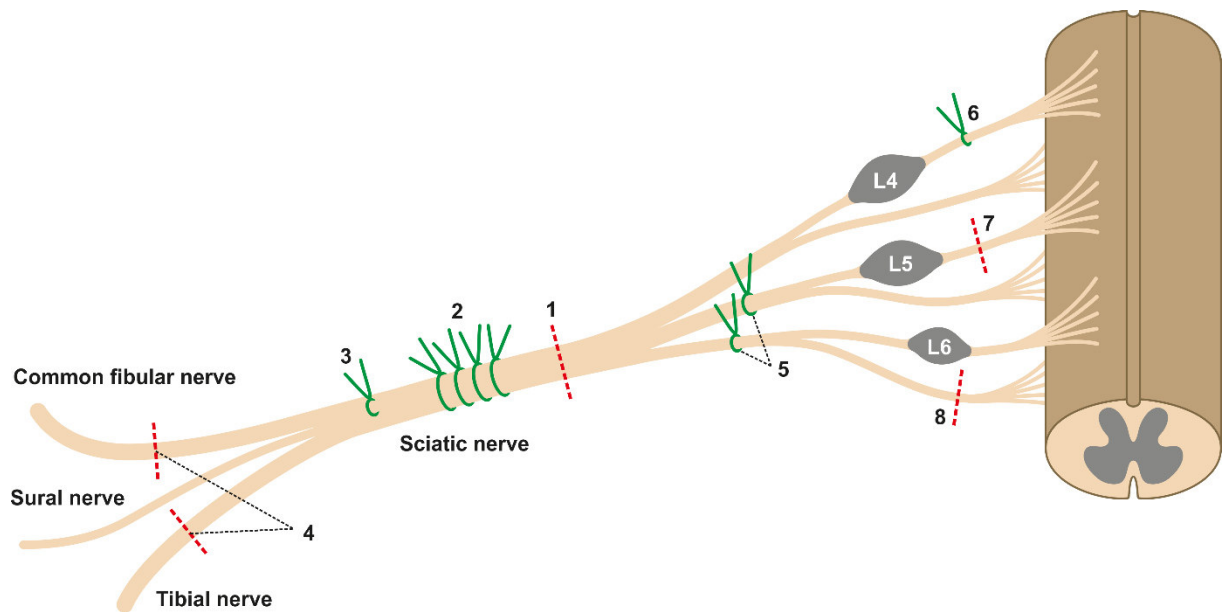


Figure 3. Schematic drawing of the peripheral neuropathic pain models. 1 – Sciatic nerve transection; 2 – Chronic constriction injury; 3 – Partial sciatic nerve ligation; 4 – Sural nerve injury; 5 – Segmental L5/L6 spinal nerve ligation; 6 – Dorsal root compression; 7 – Dorsal rhizotomy; 8 – Ventral rhizotomy. Modified from Klusáková and Dubový³⁰.

4. Wallerian degeneration

In 1850, dr. Augustus Waller described degeneration of the cranial nerves after injury in frog⁵⁶. Therefore, cellular and molecular changes after peripheral nerve injury are well known as Wallerian degeneration. These events form convenient environment for regeneration of axons and thus provide an important precondition for reinnervation.

Injury of the nerve and axons causes cascade of events including proliferation of Schwann cells⁵⁷, invasion of circulating macrophages⁵⁸, alteration of the blood-nerve barrier⁵⁹, changes in the endoneurial extracellular matrix⁶⁰ and elevation of cytokine production⁶¹.

4.1. Axon degeneration

The axotomy induces degeneration of axoplasm, axolemma and myelin distal to nerve lesion. Degeneration of axon is an active event independent on non-neuronal cells surrounding the axons⁶². Degeneration of the axon is possibly triggered by impaired axonal transport⁶³. Increased free intracellular Ca^{2+} and activation of calpains leads to decrease of microtubular and neurofilament protein levels⁶⁴. These events result to axonal fragmentation in 48 hours⁶⁵.

Schwann cells play crucial role in initiation of the Wallerian degeneration. Fragments of the myelin sheath appear within Schwann cell cytoplasm as ovoids and small whorls of myelin debris and the Schwann cell displayed numerous lipid droplets. Then, the myelin debris is phagocytized by the recruited macrophages^{66,67}.

Circulating macrophages infiltrate epineurium of the lesion site 3 days after injury while endoneurium is infiltrated 5 to 7 days after injury⁶⁸. Then, the macrophages spread to entire distal stump of injured nerve and reach maximum number 14 days after injury⁶⁹. Beside myelin phagocytosis, macrophages secrete mitogenic factors for Schwann cells and fibroblasts⁵⁸.

Beside the macrophages, Wallerian degeneration is accompanied by invasion of mast cells, neutrophils and lymphocytes to the site of nerve lesion. Mast cells degranulate within the endoneurium of the injured nerve and thus contribute to recruitment of macrophages and neutrophils⁷⁰. Moreover, they participate on initiation of inflammatory reaction and development of hyperalgesia⁷¹. Neutrophils are responsible for production of a wide range inflammatory cytokines and chemokines in injured nerve. They are attracted by factors of degranulated resident mast cells⁷².

4.2. Wallerian degeneration as sterile inflammatory reaction

Tissue injury leads to inflammatory reaction that is characterized by increased expression of immune mediators responsible for wound healing⁷³. Nerve injury induces not only production of neurotrophic factors but also induction of inflammatory response accompanied by production of cytokines, chemokines and transcription factors⁷⁴. Beside immune cells, activated glial cells contribute to secretion of cytokines and chemokines in nervous system⁶¹. The first cytokines secreted after nerve injury are TNF- α , interleukin 1 α (IL-1 α) and IL-1 β ⁷⁵ because they play crucial role in microphage recruitment to the site of nerve injury⁷⁶. Cytokines produced during Wallerian degeneration have mainly negative effect on neuropathic pain induction^{77,78}. However, *in vitro* experiments revealed that some cytokines like TNF α , IL-1 β , IL-4 and IL-6 have a synergic effect with neurotrophic factors to induction axon outgrowth⁷⁹.

5. Reaction of the DRG to peripheral nerve injury

Peripheral nerve injury induces cellular and molecular changes in the DRG that contribute to induction and maintenance of neuropathic pain⁸⁰. The DRG contain bodies of primary sensory neurons that are surrounded with satellite glial cells. Since the primary sensory neurons are pseudounipolar they send off peripheral and central branches. The peripheral branches are localized within peripheral nerves and reach peripheral terminals in target tissue while the central branches run in the dorsal roots to the CNS.

5.1. Cellular reactions in DRG induced by peripheral nerve injury

The cellular changes induced by peripheral nerve injury are related with proliferation and activation of the satellite glial cells^{81,82} as well as invasion of macrophages and lymphocytes to corresponding DRG⁸³. Primary stimuli inducing invasion of macrophages to ipsilateral DRG seems to be triggered by retrograde signaling from injured nerve⁸⁴. Injury-induced invasion of macrophages is probably triggered also by release of CX3CL1 (fractaline)⁸⁵ and CCL2 from axotomized DRG neurons⁸⁶.

Numbers of macrophages immunoreactive for major histocompatibility system II increase in the corresponding DRG 1 week after a nerve transection and remain elevated for 3 months. In early phase, macrophages are diffusely distributed in the DRG and later are concentrated around injured sensory neurons^{55,87}. Activated ED1+ macrophages frequently invade the satellite glial cell-neuron unit in corresponding DRG after nerve injury. Thus, the satellite glial cells together with invaded macrophages have ideal position for modification of the neuron environment⁵⁵.

There is an evidence that activated ED1+ macrophages invade not only the ipsilateral but also contralateral DRG⁵⁵.

5.2. Molecular reactions in DRG induced by peripheral nerve injury

Molecular reactions in the DRG following the peripheral nerve injury represent double-edge sword. On one side, these reactions participate on neuropathic pain development and maintenance. However, on the other side, the same reactions give background for reactivation of the neuronal regeneration program important for successful recovery of the injured peripheral nerve. Our lab is focused on both events and published articles in highly impacted journals.

5.2.1. Cytokines and chemokines involved in neuropathic pain development and maintenance

The cytokines and chemokines are secreted in corresponding DRG after peripheral nerve injury from immune cells, neurons and satellite glial cells. They have been implicated to play role in neuropathic pain process by two mechanisms. Firstly, they may act directly on primary sensory neurons, and secondly, they can indirectly act via activation of signaling pathways in immune cells⁸⁸. From the pathophysiological point of view, the cytokines and chemokines might be divided to two groups, pro- and anti-inflammatory.

The pro-inflammatory cytokine IL-1 β is produced and secreted by macrophages, monocytes and microglia as a part of stress reaction. Expression of the IL-1 β receptor has been detected in DRG suggesting IL-1 β autocrine and paracrine effect on sensory processing^{89,90}. It has been found that application of endogenous IL-1 receptor antagonist reduces pain-associated behavior suggesting the central IL-1 β effect on hyperalgesia⁹¹.

TNF- α is pro-inflammatory cytokine that initiates cascade of activation of other cytokines, chemokines and growth factors. Expression of TNF- α and its receptors (TNF- α receptor 1 and 2) in DRG has been proved in different models of peripheral neuropathic pain⁹²⁻⁹⁴. Importantly, unilateral chronic constriction injury induced enhanced expression of TNF- α not only in ipsilateral but also in contralateral and remote cervical DRG⁶. In addition, enhanced expression

of TNF- α receptor in the injured nerve was detected after chronic constriction injury and nerve crush ⁹⁵. Direct application of TNF- α to the sciatic nerve that produced dose-dependent ectopic firing in afferent axons ⁹⁶ suggesting the role of TNF- α in neuropathic pain processing.

Expression of the pleiotropic pro-inflammatory cytokine IL-6 is associated with hyperalgesia and allodynia in models of peripheral nerve injury ⁹⁷⁻⁹⁹. Increased IL-6 mRNA levels were detected in DRG after chronic constriction injury. In addition, IL-6 knockout mice displayed attenuation of hyperalgesia compared with wild type mice after chronic constriction injury ⁹⁹. Intrathecal application of IL-6 antagonist attenuated nerve-injury induced hyperalgesia ¹⁰⁰. Moreover, it has been found that expression of IL-6 is increased not only in nerve injury-affected DRG but also in remote DRG ¹⁰¹. Upon binding the specific receptor, IL-6 brings together the intracellular regions of gp130 to initiate signal transduction through STAT3 signaling pathway ¹⁰². We found that intrathecal application of IL-6 caused nuclear translocation of STAT3 and its phosphorylation at the tyrosine-705 and serine-727 in lumbar and cervical DRG. Interestingly, similar reaction was displayed in remote cervical DRG after chronic constriction injury. These findings suggest spread of inflammatory response from nerve injury-affected DRG to remote DRG through CSF in subarachnoid space ⁵ (**Chapter 12, Article A**).

The IL-10 is anti-inflammatory cytokine with suppressor effect on many pro-inflammatory cytokines including e.g. IL-1 and TNF- α ^{103,104}. It has been found that peripheral nerve injury induces increased bilateral expression of IL-10 not only in the homonymous DRG but also in the heteronymous DRG unassociated with the injured nerve ⁶.

5.2.2. Nerve injury-induced regeneration state in the DRG

Peripheral nerve injury induces significant changes in metabolism, survival, excitability and neurotransmitter functions of affected neurons¹⁰⁵. These events may lead to reactivation of intrinsic regenerative program as a part of functional recovery in injured peripheral nerves. The DRG provide very potent *in vitro* and *in vivo* model for testing of mechanisms regulating reactivation of silent regenerative program.

Regenerative state in the DRG neurons can be detected by expression of regeneration-associated molecules like cortical cytoskeleton associated protein 23 (CAP-23), growth associated protein 43 (GAP-43), superior cervical ganglion 10 (SCG-10) or small proline-rich repeat protein 1A (SPRR-1A). These molecules are important intrinsic determinants of the increased regenerative ability of the DRG neurons^{106,107}. However, different populations of the DRG neurons may respond differently with respect to their regeneration capacity and expression of molecular markers. Therefore, we aimed in our research to describe expression of aforementioned markers with respect to size of neurons and their phenotype.

We found that immunohistochemical detection of GAP-43 recognizing both phosphorylated and dephosphorylated forms is not sufficient as a marker for recognition of all types of neurons with regenerating axons. Moreover, this marker cannot be used for detection of regenerating axons in early periods after nerve injury. Contrary to GAP-43, SCG-10 is more reliable for detection of neurons with reactivated regeneration program and regenerating sensory axons. Another markers that could be used as a good alternative for recognition of neurons with regenerating axons are ATF3 and STAT3¹⁰⁸ (**Chapter 12, Article B**).

In our second experimental work, we were focused on induction of pro-regenerative state in the DRG non-associated with injured nerve. We correlated expression of GAP-43 and SCG-10 with length of regenerating axons in crushed ulnar nerve after prior sciatic nerve injury. Seven days

after sciatic nerve compression or transection, our experiments revealed increased bilateral expression of GAP-43 and SCG-10 not only in primary sensory neurons of the lumbar DRG (L4-L5) associated with injured nerve, but also in remote cervical DRG (C6-C8). Moreover, increased expression of pro-regenerative proteins in the cervical DRG was associated with the greater length of regenerated axons 1 day after ulnar nerve crush following prior sciatic nerve injury as compared to controls with only ulnar nerve crush. To confirm axonal regeneration capacity of the cervical DRG we used neurite outgrowth assay of *in vitro* cultivated DRG neurons. In next part of experiments, we found that the IL-6 signaling pathway plays a key role in activating the pro-regenerative state in remote DRG. Our results revealed that the pro-regenerative state induced in remote primary sensory neurons non-associated with the injured nerve reflects a systemic reaction of these neurons to unilateral sciatic nerve injury possibly due to spread of inflammatory reaction via the cerebrospinal fluid ¹⁰⁹ (**Chapter 12, Article C**).

6. Reaction of the spinal cord and brain stem to nerve injury

Central branches of the DRG primary sensory neurons enter the posterolateral sulcus of spinal cord through dorsal root. Heavily myelinated A fibers involved in mediation of non-noxious somatosensory inputs enter the spinal cord medially and travel through the dorsal columns projecting ipsilateral to second order cells in the brainstem, including cells in the nucleus gracilis and nucleus cuneatus ¹¹⁰. Lightly myelinated (A δ) and unmyelinated (C) fibers enter spinal cord laterally and most of them terminate on grey matter of the homonymous or segment. The grey matter of the dorsal horn may be divided into 10 laminae on which low-threshold mechanoreceptors terminate in laminae III and IV, high-threshold nociceptors in laminae I, II and V and unmyelinated C-fibers in lamina II ^{13,111,112}.

6.1. Inflammatory reactions in the spinal cord of neuropathic pain models

It was demonstrated that the peripheral nerve injury-induced hyperalgesia is associated with cellular and molecular changes in the dorsal horn of the spinal cord in segments corresponding to injured nerve. These changes are related with activation of microglial cells and astrocytes as well as alteration of pro- and anti-inflammatory cytokines produced by neurons, microglia, astrocytes and invading immune cells ^{72,113–116}.

It is generally accepted that microglial cells are considered to be immune cells of the CNS playing a key role as scavenger cells in inflammation, infection, trauma, ischemia and neurodegeneration in the CNS ^{117,118}. Since the microglial cells belong to monocyte-macrophage lineage, they form clusters around cell bodies of injured neurons, similar to macrophages in the DRG ^{117,119}. The peripheral nerve injury induces robust activation of microglia in the dorsal horn of spinal cord that precedes to activation of astrocytes. It was found that specific molecular markers for microglial activation TLR4, ITGAM and CD14 are upregulated in the dorsal horn early after nerve injury ¹²⁰. Activated microglia is immunohistochemically detected by OX-42 antibody directed against a complement receptor 3 antigen (CD11b/c) or antibody against ionized calcium binding adapter molecule 1 (Iba1) ^{121,122}.

Activation of the resident microglia in the spinal cord as a response to nerve injury can be mediated via three pathways; fractalkine (CX3CL1) mediated pathway through the CX3CR1 receptor, CCR2 pathway and Toll-like receptors (TLR). Fractalkine (CX3CL1) is a neuronal transmembrane glycoprotein from which a soluble chemokine domain can be cleaved by proteolysis. However, fractalkine is biologically active in both membrane-bounded and soluble form ¹²³. Role of the fractalkine/CX3CR1 signaling pathway in neuropathic pain was studied by intrathecal administration of fractalkine and CX3CR1 neutralizing antibody. Intrathecal injection of the fractalkine induced mechanical allodynia and contrary, the CX3CR1 neutralizing antibody decreased mechanical allodynia after nerve injury ⁸⁵. Member of the CC

chemokine family CCL2 has the ability to recruit immune cells including macrophages and microglia to the site of neuronal injury¹²⁴. It has been found that CCL2 is a key mediator in development of neuropathic pain. The peripheral nerve injury induces upregulation of CCL2 in the DRG that is transported and released in the dorsal horn of spinal cord. Moreover, lumbar application of CCL2 induces mechanical allodynia and microglial activation in naïve rats and inhibition of endogenous CCL2 following nerve injury attenuates both phenomena⁸⁸. TLR are 12 evolutionary conserved membrane receptors that initiate innate immune response by recognizing molecules shared by different pathogens. Signaling pathway mediated by TLR leads to activation of NF- κ B, subsequently to upregulation of interferons and expression of pro-inflammatory cytokines and chemokines^{123,125}. It has been found that activation of TLR2 and TLR4 plays crucial role in microglial activation and production of proinflammatory cytokines after nerve injury. Inhibition of TLR2 and TLR4 signaling pathway lead to attenuation of microglial reaction and neuropathic pain-like behavior in nerve-injured animals^{126,127}.

Astrocytes are the most abundant glial population participating in immune reactions. They have been investigated mainly because of their supportive functions for neurons. Astrocyte hypertrophy and activation expressed by GFAP upregulation has been found in the dorsal horn of spinal cord after nerve injury^{128,129}. In contrast to microglial reaction, activation of astrocytes is more persistent and can last for more than 150 days⁸⁶. Activated astrocytes are a major source of pro-inflammatory cytokines that contribute significantly to induction and maintenance of peripheral neuropathic pain^{130,131}.

It has been found that peripheral nerve injury induces upregulation of proinflammatory cytokines and downregulation of anti-inflammatory cytokines in activated microglial cells and astrocytes related with induction and maintenance of peripheral neuropathic pain^{72,116,132}. The major pro-inflammatory cytokines that affect peripheral neuropathic pain are IL-1 β , IL-6 and TNF- α ¹³³. Expression of IL-1 β following the nerve injury is enhanced in microglia and

astrocytes of the CNS structures ¹³⁴. Moreover, it has been found that intraplantar application of IL-1 β to naïve animals produces hyperalgesia ¹³⁵. Mechanical allodynia and thermal hyperalgesia are associated with IL-6 expression. Intrathecal application of IL-6 induces onset of neuropathic pain-like behavior in naïve animals. Conversely, intrathecal administration of IL-6 inhibitor relieves pain in nerve injured animals ^{97,100,133}. Receptors for TNF- α , TNFR1 and 2, are present in both neurons and glia ¹³⁶. There is an evidence that at injured nerve sites, TNF- α is retrogradely transported and released at the terminals in the dorsal horn of spinal cord ¹³⁷. In contrast to IL-1 β , IL-6 and TNF- α , the major cytokines with anti-inflammatory effect are IL-4 and IL-10. It has been found that the expression of both IL-4 and IL-10 is decreased in the dorsal horn of spinal cord after nerve injury ^{138,139}. Since low blood levels of IL-4 and IL-10 were found in patients with chronic widespread pain, they seem to be crucial for onset and maintenance of the chronic pain ¹⁴⁰. IL-4 is pleiotropic anti-inflammatory cytokine that is produced by various types of immune cells including CD4+ T lymphocytes, mast cells, eosinophils and basophils ¹⁴¹. There is growing body of evidence that even IL-4 inhibits macrophage activation it also upregulates transcription of μ - and δ -opioid receptors. Therefore, IL-4 may attenuate nociception through endogenous opioid system ^{142,143}. IL-10 is very potent anti-inflammatory cytokine repressing the expression of pro-inflammatory cytokines (IL-1 β , IL-6 and TNF α). Acute administration of IL-10 has ability to suppress development of pain ¹⁴⁴. In our research about the reaction of the spinal cord on nerve injury, we were focused on attenuation of behavioral hyperalgesia using intrathecal application of the CD200 fusion protein ¹¹⁶. CD200 is a membrane glycoprotein with immune suppression effect via its receptor CD200R. CD200 is mainly expressed on neurons while CD200R preferentially on myeloid cells including microglia ¹⁴⁵. Increased level of CD200 is associated with less activated monocytes and increasing expression of IL-10 in the CNS in experimental model of autoimmune encephalomyelitis ¹⁴⁶. Conversely, CD200^{-/-} mice displayed immune cells dysregulation,

increased activation of microglial cells and enhanced susceptibility of autoimmune encephalomyelitis^{147,148}. In our experimental study we found increased mRNA levels of pro-inflammatory cytokine (IL-1 β , IL-6 and TNF α) and decreased mRNA levels of anti-inflammatory cytokines (IL-4 and IL-10) in spinal cord of L4-5 segments after chronic constriction injury. We proved that intrathecal application of CD200 fusion protein diminished elevation of pro-inflammatory cytokine mRNA and simultaneously ameliorated deficit of anti-inflammatory cytokines after chronic constriction injury. Moreover, intrathecal CD200 fusion protein application suppressed activation of microglial cells and astrocytes after nerve injury. In agreement with cellular and molecular changes the CD200 fusion protein also attenuated mechanical allodynia and thermal hyperalgesia in nerve-injured animals. However, the anti-inflammatory effect of CD200 fusion protein was only transient and dropped at 24h after intrathecal application (**Chapter 12, Article D**).

6.2. Pain processing and modulation in the brain stem

6.2.1. The gracile and cuneate nucleus

Innocuous information such as touch, pressure and vibration are conveyed via the dorsal columns and transmitted in the in medulla oblongata. The gracile nucleus receives information from the lower part of the body while the cuneate nucleus from the upper part of the body. It has been found that both nuclei are involved in neuropathic pain development and maintenance¹⁴⁹.

Increased GABA synaptic uptake together with robust astrogliosis was reported in the gracile nucleus after spared nerve injury¹⁵⁰. Moreover, it has been found that gracile nucleus plays a role in central sensitization by up-regulation of phosphorylated NMDA receptor 1 in neurons

¹⁵¹ and phosphorylated-p38 MAPK-immunopositive microglia ¹⁵². Role of the medulla oblongata in neuropathic pain processing was also confirmed by experiments using nerve injury of the median nerve. These experiments revealed important role of astrocyte activation expressed by increased GFAP immunoreactivity in the cuneate nucleus after median nerve injury ¹⁵³. Furthermore, it has been demonstrated that median nerve injury induces increased neuropeptide Y immunoreactivity and c-fos expression in the cuneate nucleus corresponding with behavioral signs of the neuropathic pain ^{154,155}.

6.2.2. Rostral ventromedial medulla

Rostral ventromedial medulla (RVM) is composed of nucleus raphe magnus and gigantocellularis. Their neurons are involved in descending attenuation of pain perception as was described in chapter 2.8. According to their pharmacological and physiological properties, the neurons of RVM can be divided to three groups, “On-cells”, “Off-cells”, and “neutral cells”. The “On-cells” increase their firing rate before the nocifensive reflexes and enhance response to the pain. Contrary to the “On-cells”, the “Off-cells” decrease firing rate before the nocifensive reflexes and inhibit nociception. Remaining cells that display no changes in firing rate are “neutral cells” ¹⁴⁹. In neuropathic pain conditions, balance of circuitry within the RVM shift to domination of the “On-cells” over the “Off” and “neutral cells” ^{156,157}. However, sensitization of both “On” and “Off-cells” to innocuous and noxious mechanical stimuli was demonstrated to facilitate allodynia and hyperalgesia ^{149,158}.

Since activation of glial cells affect neuronal activity via cytokines and chemokines, activation of astrocytes and/or microglia in RVM may affect modulatory role of descending pathways in neuropathic pain maintenance. Early transient activation of microglia and delayed reaction of astrocytes in RVM related to mechanical hyperalgesia was reported after chronic constriction

injury of the infraorbital nerve ¹⁵⁹. However, after spinal nerve ligation strong activation of microglia was displayed 10 days after injury ¹⁶⁰.

In the light of these findings, we focused our research on changes of glial cells in RVM following different types of peripheral nerve damage, namely chronic constriction injury and transection of the sciatic nerve. We used OX-42 immunostaining for detection of activated microglia and GFAP for activated astrocytes. Our results showed that both types of the nerve injury induced microglial activation while only nerve transection caused strong astrogliosis in PAG. Consequently, we wanted to answer a question what causes activation of glia in RVM after nerve injury. Therefore, we focused on candidate chemokine CCL2 with its receptor CCR2 (see chapter 6.1.). Our results revealed that CCL2 immunoreaction was present in neurons and activated GFAP+ astrocytes while the CCR2 was displayed in OX-42 positive microglial cells ⁷ (**Chapter 12, Article E**).

6.2.3. Pons

The main structure involved in pain processing in the pons is the locus coeruleus. Neurons of the locus coeruleus are capable to produce noradrenaline that is known to act on α_2 -adrenoreceptors in the spinal cord with antinociceptive effect ¹⁶¹. Noradrenaline reuptake inhibitors and gabapentin are used as approved treatments of chronic pain ^{162,163}. It has been demonstrated that gabapentin acts directly within the locus coeruleus via glutamate dependent mechanism to alleviate pain behavior after spinal nerve ligation ^{149,164}. However, on the other hand, there are experimental works that revealed opposite role of the locus coeruleus in pain processing ^{165,166}. It has been found that lesion of the locus coeruleus prevented autotomy in animals after sciatic and saphenous nerve transection ¹⁶⁶.

6.2.4. Mesencephalon

Two structures are involved in pain processing in the midbrain, the periaqueductal grey and the red nucleus. The red nucleus is well known as an important structure of the extrapyramidal system participating in e.g. motor learning, postural corrections and recovery after spinal nerve injury^{167,168}. However, experimental studies demonstrated its role in neuropathic pain regulation. It has been shown that glutamate and IL-6 in red nucleus are related with induction and maintenance of mechanical allodynia after spared nerve injury^{169,170}. Moreover, it has been demonstrated that cytokine levels including TNF- α , IL- β and nerve growth factor (NGF) in red nucleus correlate with severity of behavioral changes after spared nerve injury^{149,171–173}.

Periaqueductal gray plays very important role in descending modulatory pathways with its connections in rostral ventromedial medulla (see chapter 2.8.). Reynolds¹⁷⁴ demonstrated that electrical stimulation of the periaqueductal grey produces analgesia in rats undergoing surgery. Further experiments revealed that local application of opiates to the periaqueductal grey produces pain relieve after spared nerve injury¹⁷⁵. It is well known that glial activation contributes to development and maintenance of chronic pain after nerve injury¹⁴⁴. However, most of the experimental studies about glial contribution on pain states were observation performed in the dorsal horn of the spinal cord^{176,177}. Therefore, the main idea of our research was focused on reaction of astrocytes and microglia after chronic constriction injury and transection of the sciatic nerve in the periaqueductal grey. Our results revealed more extent activation of astrocytes in periaqueductal grey of in nerve-injured animals when compared with naïve and sham groups. Increased astrocyte activation was found on ipsilateral side of ventrolateral periaqueductal grey than on contralateral side. More robust activation of astrocytes was found after nerve transection than chronic constriction injury. However, in contrast to astrocyte activation, microglial cells displayed bilateral activation after nerve injury⁷. In the

light of these results, we wanted to answer a question: what is the signaling pathway that contributes to the glial activation in the periaqueductal grey? One of the candidate signaling pathway may be the CCL/CCR2 pathway (reviewed in chapter 6.1.) with its ability to recruit microglial cells to the site of nerve injury ¹²⁴. Similar to the rostral ventromedial medulla (see chapter 6.2.1.), we found CCL2 immunoreaction in neurons and astrocytes while the CCR2 was displayed in OX-42 positive microglial cells. Taken together, our results revealed that CCL2/CCR2 signaling is involved in glia-glia and neuron-glia interactions in the descending modulatory system including the RVM and the periaqueductal grey after nerve injury related to chronic pain ⁷ (**Chapter 12, Article E**).

7. Diencephalon and its reaction to nerve injury

7.1. Thalamus

The thalamus contains the third-order neurons receiving information from the spinal cord about the pain and temperature via the spinothalamic tract. Therefore, thalamic nuclei play crucial role in chronic pain development and processing. It has been found that nerve injury induces decreased neuronal activity in contralateral thalamus in patients with chronic neuropathic pain¹⁷⁸. However, increased spontaneous and mechanically evoked activity of neurons in the ventral posterolateral nucleus in different neuropathic pain models^{179,180}. Electrical stimulation of the ventral posterolateral nucleus alleviate mechanical allodynia in rats after partial sciatic nerve ligation¹⁸¹. Moreover, lesions or block of the intralaminar or the medial thalamic nuclei attenuated neuropathic pain-like behavior in rats after spared nerve injury. These results suggest involvement these nuclei in neuropathic pain processing¹⁸².

It has been found that not only neurons but also glia in thalamus contribute to neuropathic pain development. Increased glial activation in thalamus was found in patients with chronic low back pain suggesting a role of thalamic glia in neuropathic pain development¹⁸³. Moreover, increased thalamic activity was also found in patients after peripheral nerve injury¹⁸⁴. These results suggest that thalamus and glia activation play a key role in rearrangement of cortical representational maps.

7.2. Hypothalamus

The hypothalamus receives afferent nociceptive fibers and sends off efferent projections to the brainstem and the spinal cord¹⁴⁹. It has been found that chronic constriction injury induces decreased expression of substance P and activation of microglia in the hypothalamus suggesting

their role in development of neuropathic pain ¹⁸⁵. Conversely, stimulation of the posterior part of the hypothalamus exhibit analgesic effect in animals after chronic constriction injury ^{149,186}. Magnocellular part of the paraventricular nucleus and the supraoptic nucleus produce oxytocine playing physiological role in partuation and milk ejection reflex. However, there is compelling evidence indicating participation of oxytocine in endogenous analgesia. Electrical stimulation of the paraventricular and supraoptic nuclei inhibits pain perception ¹⁸⁷. Moreover, intrathecal injection of oxytocine attenuates nociception after spinal nerve ligation ¹⁸⁸.

8. Pain processing and modulation in the telencephalon

Painful stimuli are processed in different areas of the telencephalon including primary and secondary somatosensory cortices, the insular cortex, the anterior cingulate cortex and the orbitofrontal cortex. It is believed that primary and secondary somatosensory cortices play role in sensory-discriminative aspect of pain. The insular cortex and anterior cingulate cortex are involved in the affective-emotional aspects of pain and cognitive aspects of pain are associated with activation of the prefrontal areas. Furthermore, changes in basal ganglia activity are also present in painful states ¹⁸⁹.

8.1. Basal ganglia

It is well known that basal ganglia are mainly involved in motor functions. However, experimental and clinical studies revealed also their role in processing of non-noxious and noxious somatosensory information ¹⁹⁰.

The amygdala is formed by group of nuclei that are counted as a part of limbic forebrain system. Therefore, these nuclei play a role in emotional-affective aspects of pain ¹⁴⁹. It has been reported that activation of GABA-A receptors in amygdala attenuates affective processing after

peripheral nerve injury ¹⁹¹. Spared nerve injury induces neuroplasticity in the amygdala resulting in increased total volume of amygdalar nuclei. These findings suggest a role of the amygdala in depressive-like symptoms well known in cases of patients with chronic pain ¹⁹².

Striatum (putamen and the caudate nucleus) and striatal dopamine D2 receptors play a role in modulation of pain sensation both in clinical conditions and experimental models ¹⁹³. Microinjection of dopamine D2 receptor agonist quinpirol attenuates neuropathic hypersensitivity in spared nerve injury-operated animals ¹⁹⁴. In addition, it was demonstrated that the striatum plays dual role on neuropathic sensitivity in animals after spinal nerve ligation. Activation of noradrenergic α_2 -adrenoceptors and downregulation of dopamine D receptors reduce hypersensitivity while activation of striatal NMDA receptors promotes hypersensitivity ¹⁹⁵.

8.2. Anterior cingulate cortex

The anterior cingulate cortex responds to painful stimuli both in humans and animals ¹⁴⁹. Using functional magnetic resonance imaging it was found that neuronal activity within the anterior cingulate cortex is increased in chronic pain states ¹⁹⁶. Electrical stimulation of the anterior cingulate cortex produces analgesic effect in rats subjected to spared nerve injury ¹⁹⁷. However, nerve injury induces neuronal caspase-dependent apoptosis triggered by NMDA receptor the anterior cingulate cortex ¹⁹⁸. In addition, spared nerve injury causes astrocyte activation which contributes to painful state ¹⁹⁹.

8.3. Ventrolateral orbitofrontal cortex

The ventrolateral orbitofrontal cortex is involved in sensory integration and pain modulation. It has connections with the thalamic nucleus submedius, hypothalamus, periaqueductal gray and

RVM^{149,200,201}. Functional imaging techniques revealed that the ventrolateral orbitofrontal cortex is activated in patients with chronic pain²⁰². Block of neuronal activity in the ventrolateral orbitofrontal region induces attenuation of allodynia and hyperalgesia in animals after spared nerve injury²⁰³. Chemical inhibition induced by local application of morphine, GABA or lidocaine to the ventrolateral orbitofrontal attenuated pain-like behavior in rats after formalin injection to the hind-paw²⁰⁴. In addition, increased expression of pro-inflammatory and pro-apoptotic genes correlated with allodynia and hyperalgesia were found after spared nerve injury²⁰⁵.

8.4. Insular cortex

The insular cortex is involved in emotion, cognitive functions, motor control as well as processing and modulation of pain¹⁴⁹. It receives afferent fibers mainly from the thalamus and sends efferent fibers to different regions including the amygdala, hypothalamus, periaqueductal gray and rostral ventromedial medulla^{201,206}. It has been found that regional cerebral blood flow in the insular cortex correlates with pain experience and noxious stimuli²⁰⁷ and lesion in the insular cortex alleviate neuropathic pain-like behavior after sciatic nerve injury²⁰⁸. There is growing body of evidence that opioid, GABA and dopamine are key neurotransmitters playing a role in nociceptive modulation in the insular cortex^{201,209}. Local administration of morphine to the insular cortex induced analgesia in animals after formalin injection to the hind-paw²¹⁰. Locally increased presence of GABA produces lasting analgesia by enhancing inhibition of the spinal nociceptive neurons. However, activation of GABA_B-receptor-bearing insular neurons induces hyperalgesia via projection to the amygdala²¹¹. Moreover, local application of the dopamine re-uptake inhibitor to the insular cortex produces inhibition of the spinal nociceptive neurons and analgesia²¹².

8.5. Somatosensory cortex

The primary and secondary somatosensory cortices are involved in the sensory-discriminative aspect of pain^{201,213}. Imaging techniques revealed that painful heat stimuli induced significant activation of both primary and secondary somatosensory cortices²¹⁴. Electrical stimulation of the secondary somatosensory cortex reduced formalin-induced nociceptive behavior in experimental animals²¹⁵. Spinal cord injury-induced neuropathic pain causes contralateral somatosensory cortex reorganization and its amount is dependent on pain intensity²¹⁶. It has been found that modulation of pain perception relates to metabotropic glutamate receptors and opioid receptors in both primary and secondary somatosensory cortices²¹⁷.

9. Barriers of the nervous system, their alteration and contribution to spread of inflammatory reaction after nerve injury

Barriers of the nervous system play an essential role in maintaining of neural microenvironment. However, the barriers within the nervous system react during different diseases with alteration of their protective function. In this chapter, I would like to focus on changes of the nervous system barriers induced by nerve injury that may play a role in spread of inflammatory reaction alongside the neuroaxis.

9.1. The blood-nerve barrier

The blood-nerve barrier forms interface between the endoneurial compartment, surrounding tissue and blood. The barrier is localized at the innermost layer of the perineurium and endoneurial microvasculature in the peripheral nerve. The microvessels are continuous capillaries where the endothelial cells are sealed with tight junctions and covered by the basal lamina with surrounding pericytes ²¹⁸.

It has been shown that the blood-nerve barrier is impermeable for large molecules in physiological conditions. However, the endoneurial microvessels become permeable for labeled albumin after nerve injury. The main site of the barrier alteration is found in distal stump of injured nerve undergoing Wallerian degeneration ^{219,220}. Breakdown of the blood-nerve barrier after nerve injury is associated with changes of tight junctions proteins, namely claudin-1, claudin-5, occluding, VE-cadherin and connexin 43 ²²¹. However, the alteration of blood-nerve barrier is only temporary with the highest permeability 7 days after nerve injury and approximately one month after injury the barrier is reconstituted ²²². Alteration of the blood-nerve barrier is double-edged sword. On the one hand, it is positive allowing macrophage invasion to remove myelin debris and regenerate damaged axons. However, on the other hand,

Wallerian degeneration products may enter blood and thus spread to remote tissue including the CNS.

9.2. The blood-DRG barrier

The DRG are supplied with fenestrated capillaries with fenestration size between 60 to 80 nm²²³. Microvascular density in the dorsal root ganglia is 7 times higher than in peripheral nerve and nerve roots. It has been found that the highest capillary density within the DRG is present in the neuronal body-rich area²²⁴. In contrast to axonal compartment of the DRG, the neuronal body-rich area contains capillaries with high density of tight junctions²²⁵. Experimental studies on intact animals revealed penetration of intravenously injected tracers including horseradish peroxidase, Evans blue albumin and fluorescein to the DRG²²⁵⁻²²⁷. Therefore, the blood-DRG barrier is incomplete in physiological conditions and is opened for large molecules mainly because of fenestrated capillaries (Fig. 4). However, nerve injury induces proliferation of capillaries in the DRG forming nests around neurons with damaged axon²²⁸.

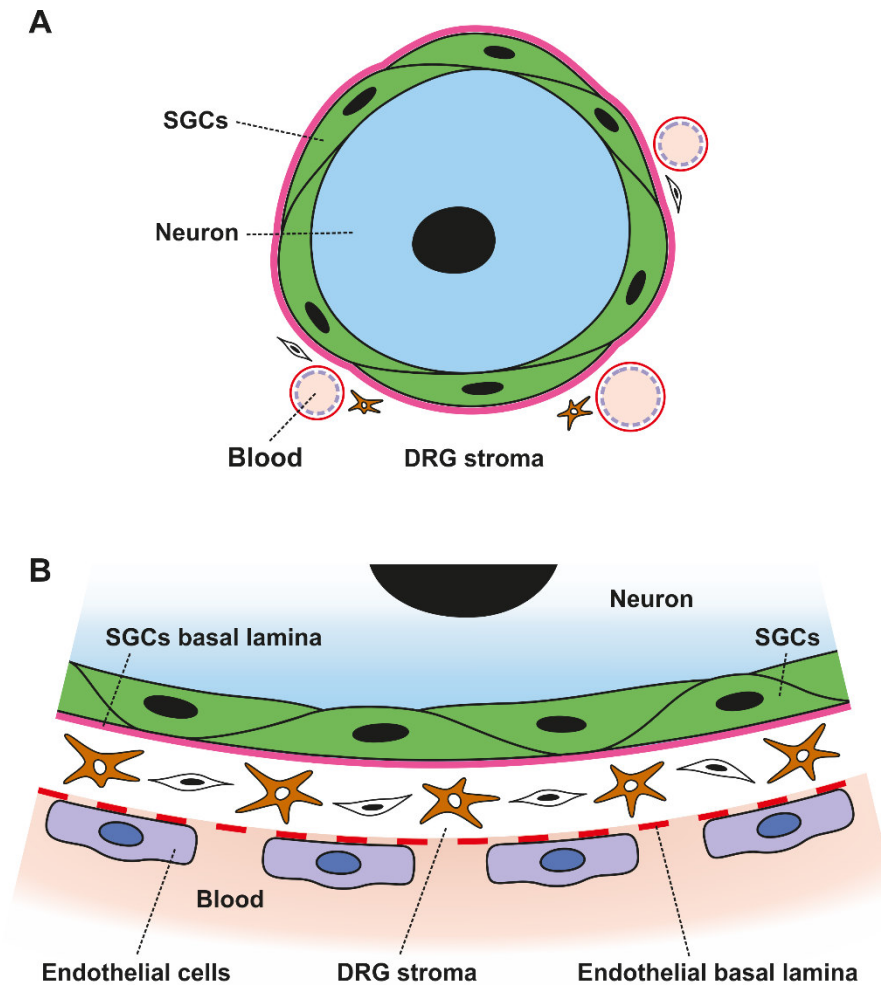


Figure 4. A simplified scheme of the blood-DRG barrier. The DRG are supplied with fenestrated capillaries that allow free movement of solutes, molecules and cells between blood and the DRG stroma (A). Detail of the barrier organization on B. SGCs – satellite glial cells.

9.3. The cerebrospinal fluid-DRG barrier

The barrier between the cerebrospinal fluid and the DRG is formed by meninges, especially arachnoid that limits subarachnoid space filled with the cerebrospinal fluid, and by capsule of the DRG. The lateral boarder of the subarachnoid space localized at transition of the dorsal and ventral roots and the DRG is called subarachnoid angle. At this place, perineurium of the peripheral nerve leaves surface of the nerve and runs between the dura mater and arachnoid.

Microscopic organization of the subarachnoid angle and communication with the peripheral nerve explains a pathway for spread of inflammation to the CNS ²²⁹.

The arachnoid villi were found in the subarachnoid angle giving anatomical substrate for communication with the epidural space. These findings may correspond with spread of anesthetics in epidural anesthesia ²³⁰. In addition, important site for penetration of anesthetics is the spinal nerve root cuff forming lateral prolongations of the the dura mater and the arachnoid membrane enclosing spinal nerve roots in their way through the epidural space to the vertebral foramina ²³¹. At this place, layers of leptomeninges fuse together and continue as the perineurium of peripheral nerves while the dura mater corresponds with the epineurium ²³² (Fig. 5).

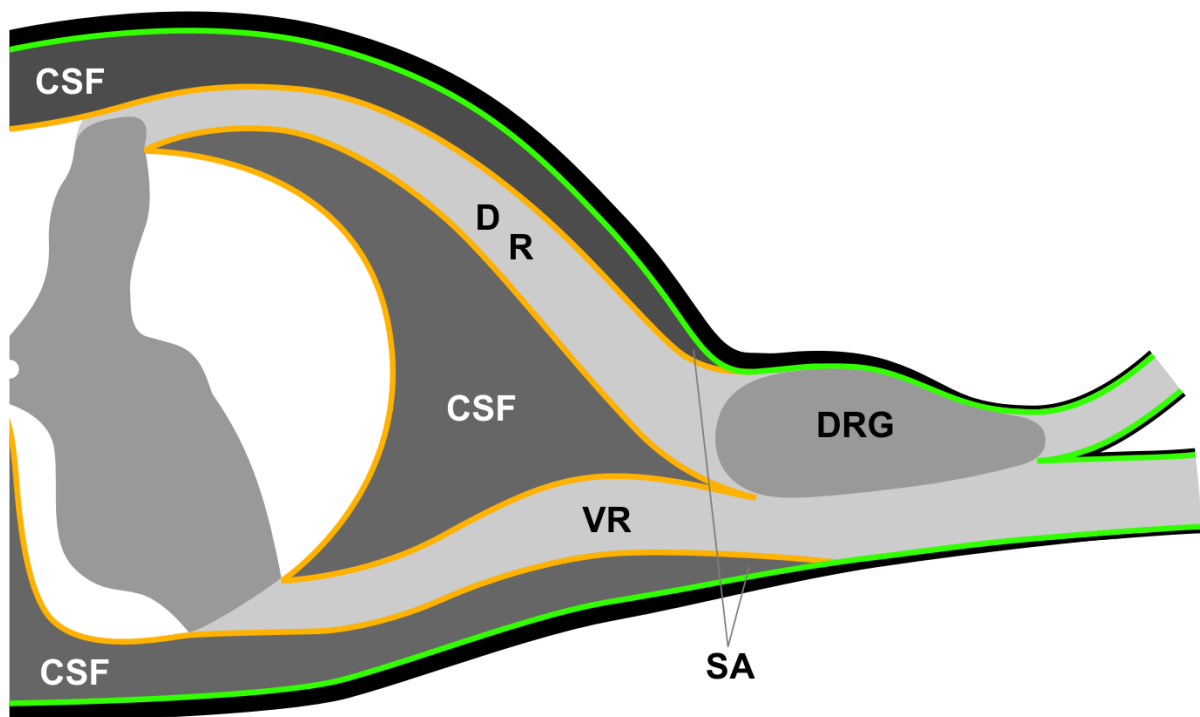


Figure 5. Schematic drawing of the subarachnoid angle (SA) position with respect to meninges, spinal nerve roots (ventral root – VR, dorsal root – DR) and the DRG. Dura mater is depicted in black, arachnoid membrane in green and pia mater in yellow.

It has been found that the cerebrospinal fluid-DRG barrier is permeable for tracer fluorescein after its intrathecal injection. Fluorescein was accumulated in the subarachnoid angle and diffused to the DRG with proximo-distal gradient. Nerve injury induced accumulation of fluorescein in the neuronal body-rich area of the DRG ²²⁷.

In our experiments we used intrathecal administration of fluorescent-conjugated dextran FluoroEmerald (FE; MW=10 kDa) to investigate whether the cerebrospinal fluid-DRG barrier is permeable for molecules of a size of cytokines. We found particles of FE in the cells of the DRG capsule, satellite glial cells, interstitial space, as well as in small and medium-sized neurons. Penetration of lumbar-injected FE into the cervical DRG was greater than that into the lumbar DRG after intrathecal injection of FE into the cisterna magna. Moreover, FE induced an immune reaction in the DRG with presence of the particles in antigen-presenting cells (MHC-II+), activated (ED1+) and resident (ED2+) macrophages, and activated satellite glial cells (GFAP+). Since we found FE inside the DRG, we wanted to answer a question whether there is morphologic background for direct communication of the subarachnoid space with the DRG. Therefore, we used intrathecal injection of methylene blue and DPP-IV immunostaining to visualize position of the subarachnoid space and arachnoid in relation to the DRG. The subarachnoid space delimited by the arachnoid mater was extended up to the capsule of DRG in a fold-like recess and reached approximately half of the DRG length. The arachnoid was found in direct contact to the neuronal body-rich area in the angle between dorsal root and DRG as well as between spinal nerve roots at DRG. Our results clearly demonstrated direct communication between the DRG and cerebrospinal fluid that can create another pathway for possible propagation of inflammatory and signaling molecules from DRG primary affected by peripheral nerve injury into DRG of remote spinal segments ⁸ (**Chapter 12, Article F**).

9.4. Blood-brain and blood-spinal cord barrier

Both the blood-brain barrier and the blood-spinal cord barrier are composed of continuous type of microvessels. The endothelia are sealed with tight junctions, enveloped by the basal lamina with surrounding pericytes and astrocytic end-feet²³³. Compared to the blood-nerve barrier, the complex of the endothelia/basal lamina/pericytes is surrounded by the second basal lamina called glia limitans perivascularis^{218,234} (Fig. 6).

The main component of these barriers are endothelial tight junctions composed of several proteins including occludin, many subtypes of claudins, zonulins. Claudins and occludin are the main transmembrane molecules mediating the epithelial contact²³⁵. Occludin is a tetraspan integral protein of tight junctions that is functionally important for barrier function^{236,237}. There is an evidence that occludin seals the tight junctions because its downregulation leads to disruption of tight junction permeability²³⁸. Claudins form a large family of membrane proteins that have four transmembrane domains forming several subgroups. It has been found that the brain endothelial cells express claudin 1, 3 and 5²³⁹⁻²⁴¹. Zonulin (ZO) is the cytoplasmic protein associated with transmembrane proteins. The blood-brain endothelia displays positivity for ZO-1, ZO-2 and ZO-3²³⁷. Integrity of the blood-brain barrier after peripheral nerve injury was assessed using intravenous injection of Evans blue albumin and horseradish peroxidase. Chronic constriction injury, sciatic nerve transection as well as electrical stimulation of peripheral nerve induced increased permeability of the blood-brain barrier. Interestingly, increased permeability can be prevented by injecting local anesthetic lidocaine to the site of the nerve injury or prior to electrical stimulation²⁴².

Tight junctions of the blood-spinal cord barrier are mainly constituted of occludin, claudin-1 and -5 as well as ZO-1. In contrast to the blood-brain barrier, the blood-spinal cord barrier is more permeable for cytokines and tracers. Increased permeability would be explain by lower level of occludin and ZO-1 as well as less number of pericytes in comparison with the brain

^{243,244}. It has been found that peripheral nerve injury induces opening of the blood-spinal cord barrier for small and large molecules associated with down-regulation of ZO-1 and claudin-5²⁴⁴.

Interaction of astrocytes and endothelia plays a key role in correct function of the blood-brain and the blood-spinal cord barrier. The astrocytes are capable to secrete humoral agents that might increase permeability of the blood-brain barrier e.g. endothelin-1, glutamate, IL-1 β , IL-6, TNF- α , MIP-2, nitric oxide^{245,246}. However, role of astrocytes in regulation of the blood-brain barrier permeability after peripheral nerve injury is still unclear.

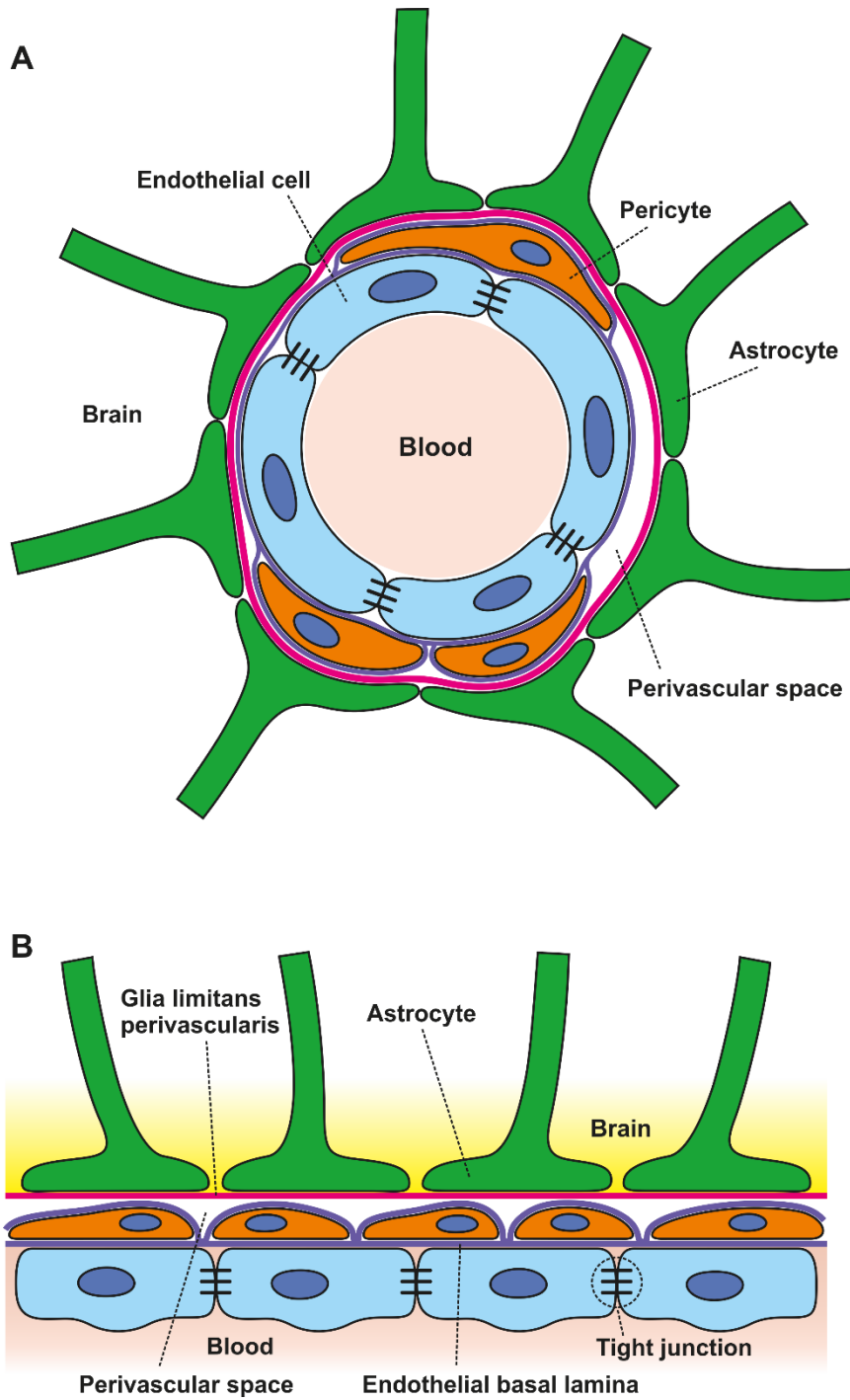


Figure 6. A simplified scheme of anatomical organization (A) and detail (B) of the blood-brain barrier²¹⁸. The endothelial cells (light blue) are linked with tight junctions (cross-links) and embedded together with pericytes in basal lamina (purple). The second basal lamina (pink; glia limitans perivascularis) serves for attachment of astrocytic end-feet and surrounds

the complex of endothelia, pericytes and the first basal lamina. Glia limitans perivascularis and the first basal lamina limit the perivascular space.

9.5. Blood-cerebrospinal fluid barrier

The blood-cerebrospinal fluid barrier is localized in the choroid plexus of brain ventricles that is epithelio-endothelial convolute composed of highly vascularized core, connective tissue stroma and epithelial cells ²⁴⁷⁻²⁴⁹ (Fig. 7). The vascularized core is formed by fenestrated capillaries with fenestrations ranged from 60 to 80 nm and is surrounded by connective tissue stroma with immune cells. They were recognized as resident (ED2+) and activated (ED1+) macrophages expressing major histocompatibility complex class II antigen as well as dendritic OX 62+ cell ^{250,251}. The ventricular side of the of stroma is covered by a single layer of cuboidal epithelial cells ^{247,248}. Epiplexus (Kolmer) cells adhere on the ventricular side of epithelial cells ²⁵². Kolmer cells have a various shape from cells with fibrous processes radiating from the centrally located cell body to cells with a few pseudopod-like processes. These cells have ability to phagocyte and they seem to be a scavengers in the cerebrospinal fluid ²⁵³. There is an evidence that the choroid plexus support trafficking of leukocytes to the cerebrospinal fluid ²⁵⁴⁻²⁵⁷.

The major role for regulation of the blood-cerebrospinal fluid barrier permeability play the apical tight junctions of cuboid cells responsible for regulation of paracellular diffusion of water soluble molecules ^{233,258}. Tight junctions are composed of proteins associated with the cellular membrane ²⁵⁹. The first described integral protein of tight junctions in the cuboidal cells of choroid plexus was occludin ^{261,262}. In addition, the choroid plexus epithelial cells express also claudin-1-6, 9-12, 19, 22 ^{260,262,263} and Zo proteins, Zo-1 ^{264,265}, Zo-2 ^{266,267} and Zo-3 ^{268,269} that bind occludin and claudin to actin filaments ^{270,271}.

It has been found that the choroid plexus plays a key role in pathophysiology of many disorders including inflammatory, neurodegenerative, infectious, traumatic, neoplastic and systemic diseases^{247,272}. However, it is unknown whether barrier function of the choroid plexus is altered after nerve injury. Therefore, we focused on cellular changes of the choroid plexus after peripheral nerve injury. We used ED1 and ED2 immunostaining to investigate epi-choroid plexus cell changes in rat choroid plexus after chronic constriction injury and sham-operated animals in comparison with the choroid plexus of naïve animals. We found significantly increased numbers of ED1+ cells in the choroid plexus of sham-operated rats in all periods of survival when compared with naïve animals while the number of ED2+ increased only at 3 days from operation. However, the number of ED1+ and ED2+ cells in the epi-choroid plexus position increased gradually with the duration of nerve compression. We detected no or negligible cell proliferation in the choroid plexus after sham- or nerve injury operation. This suggests that increased number of ED1+ and ED2+ cells in the epi-choroid plexus position of the choroid plexus is derived from peripheral monocytes passing through altered blood–cerebrospinal fluid barrier. The changes in epi-choroid plexus cells indicate that the choroid plexus reacts to tissue injury after the surgical approach itself and that the response to peripheral nerve lesion is greater. This suggests a role for an altered blood-cerebrospinal fluid barrier allowing propagation of signal molecules produced by damaged tissue and nerve to the CNS⁹ (**Chapter 12, Article G**).

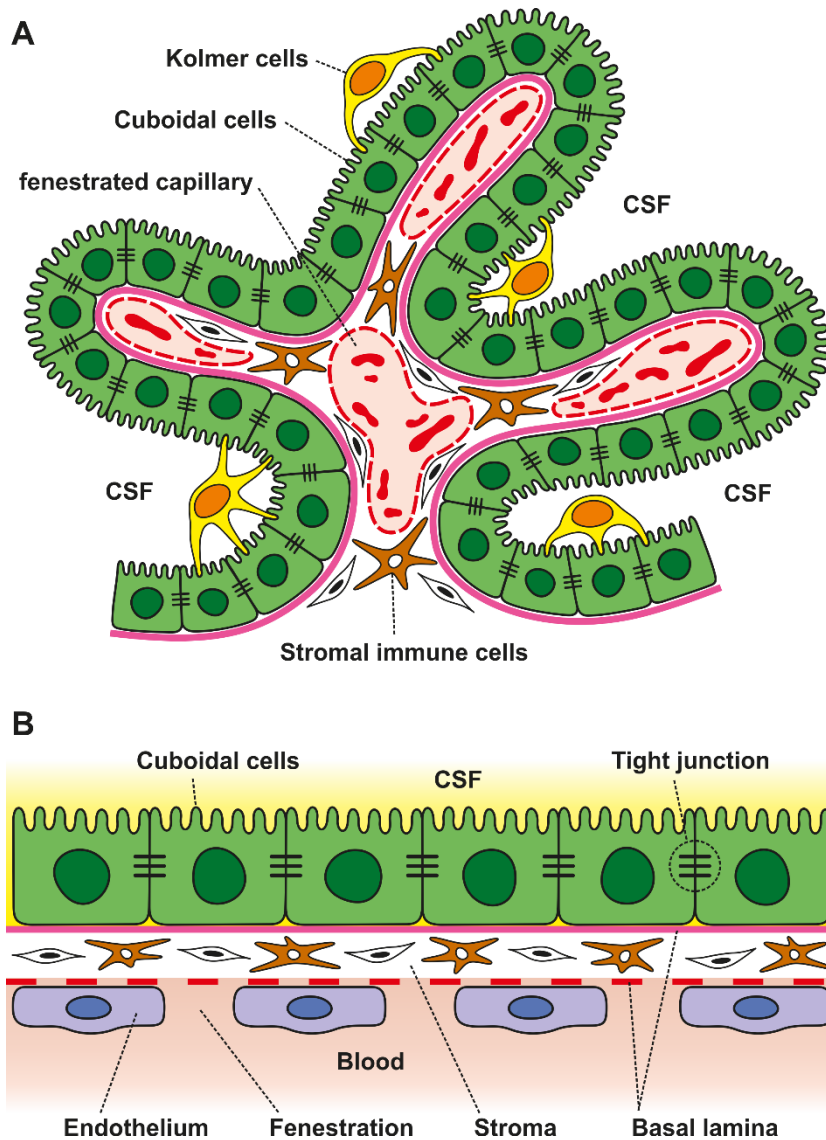


Figure 7. Scheme of anatomical organization (A) and detail (B) of the blood-cerebrospinal fluid barrier. The blood-cerebrospinal is localized in the choroid plexus of the brain ventricles composed of fenestrated capillaries surrounded with connective tissue stroma and and cuboidal epithelial cells with adhering Kolmer cells (A). The main site of the barrier is on the level of the cuboidal epithelial cells that are linked by tight junctions.

10. Conclusions and future perspectives

My habilitation thesis integrates important findings in the field of spread of inflammatory reaction after nerve injury to the CNS. Spread of inflammatory response from the site of injury may happen via two pathways or their combination. Firstly, “on-wire” pathway count with transsynaptic spread via sensory pathway to the the centers of the CNS. Secondly, “wire-less” pathway involve spread of pro-inflammatory cytokines and chemokines via blood stream or cerebrospinal fluid. This pathway represents my main research direction emphasizing generalized reaction of the nervous system on peripheral nerve injury. This reaction may play important role not only in neuropathic pain induction but also in nerve regeneration after nerve injury. However, the full range of mechanisms and reasons of generalized raction of nervous system still remains to be elucidated.

In summary, we provided the first evidence that:

- Peripheral nerve injury induces activation of STAT3 bilaterally in the DRG neurons of both lumbar and cervical spinal cord segments.
- IL-6 released to the subarachnoid space has ability to penetrate to the DRG and activate STAT3.
- Intrathecal application of CD200 fusion protein has ability to attenuate gliosis and inflammatory reaction in the spinal cord after peripheral nerve injury.
- CD200 fusion protein induces rapid but temporary suppression of mechanical allodynia and thermal hyperalgesia in neuropathic pain model.
- Peripheral nerve injury induces pro-regenerative state in primary sensory neurons non-associated with injured nerve.
- IL-6 signaling pathway plays a key role in activating the pro-regenerative state in the DRG non-associated with injured nerve.

- Peripheral nerve injury induces activation of astrocytes and microglia in the periaqueductal gray and the rostral ventromedial medulla.
- Microglial activation in the the periaqueductal gray and the rostral ventromedial medulla following nerve injury is mediated via CCR2 due to neuronal as well as astrocytal release of CCL2.
- Subarachnoid space reaches the dorsal root ganglion as a fold-like recess that gives anatomical background for changes of molecules between the dorsal root ganglion and the cerebrospinal fluid.
- Intrathecal application of the fluorescence-conjugated dextrane FE penetrates to the DRG and induces immune reaction.
- Peripheral nerve induces cellular changes in the choroid plexus represented by increased number of activated and resident macrophages in the epiplexus position.
- Not only nerve injury but also surgical approach itself induces cellular changes in the choroid plexus.

In future research, I would like to continue with experiments focused on changes of the blood-cerebrospinal fluid barrier after nerve injury emphasizing role of tight junctions. Moreover, the choroid plexus seems to be candidate structure of CNS suitable for gene manipulation. This would allow manipulation with choroid plexus permeability rate or secretory function.

In addition, I would like to continue with electrophysiological experiments of ex vivo model of skin and preserved nerve. I learned this model in the lab of prof. Christopher Honda during my Fulbright scholarship at the University of Minnesota.

11. References

1. Colombo B, Annovazzi POL, Comi G. Medications for neuropathic pain: current trends. *Neurol Sci.* 2006;27(2):s183-s189. doi:10.1007/s10072-006-0598-7.
2. Jean-Pierre L, Mike B. The epidemiology of pain in depression. *Hum Psychopharmacol Clin Exp.* 2004;19(S1):S3-S7. doi:10.1002/hup.618.
3. Woolf CJ, Mannion RJ. Neuropathic pain: aetiology, symptoms, mechanisms, and management. *The Lancet.* 1999;353(9168):1959-1964. doi:10.1016/S0140-6736(99)01307-0.
4. Jensen TS, Gottrup H, Sindrup SH, Bach FW. The clinical picture of neuropathic pain. *Eur J Pharmacol.* 2001;429(1-3):1-11. doi:10.1016/S0014-2999(01)01302-4.
5. Dubový P, Hradilová-Svíženská I, Klusáková I, Kokošová V, Brázda V, Joukal M. Bilateral activation of STAT3 by phosphorylation at the tyrosine-705 (Y705) and serine-727 (S727) positions and its nuclear translocation in primary sensory neurons following unilateral sciatic nerve injury. *Histochem Cell Biol.* February 2018:1-11. doi:10.1007/s00418-018-1656-y.
6. Jancalek R, Dubovy P, Svizenska I, Klusakova I. Bilateral changes of TNF-alpha and IL-10 protein in the lumbar and cervical dorsal root ganglia following a unilateral chronic constriction injury of the sciatic nerve. *J Neuroinflammation.* 2010;7:11. doi:10.1186/1742-2094-7-11.
7. Dubový P, Klusáková I, Hradilová-Svíženská I, Joukal M, Boadas-Vaello P. Activation of Astrocytes and Microglial Cells and CCL2/CCR2 Upregulation in the Dorsolateral and Ventrolateral Nuclei of Periaqueductal Gray and Rostral Ventromedial Medulla Following Different Types of Sciatic Nerve Injury. *Front Cell Neurosci.* 2018;12:40. doi:10.3389/fncel.2018.00040.
8. Joukal M, Klusáková I, Dubový P. Direct communication of the spinal subarachnoid space with the rat dorsal root ganglia. *Ann Anat - Anat Anz.* 2016;205:9-15. doi:10.1016/j.aanat.2016.01.004.
9. Joukal M, Klusáková I, Solár P, Kuklová A, Dubový P. Cellular reactions of the choroid plexus induced by peripheral nerve injury. *Neurosci Lett.* 2016;628:73-77. doi:10.1016/j.neulet.2016.06.019.
10. Dubin AE, Patapoutian A. Nociceptors: the sensors of the pain pathway. *J Clin Invest.* 2010;120(11):3760-3772. doi:10.1172/JCI42843.
11. Djouhri L, Lawson SN. A β -fiber nociceptive primary afferent neurons: a review of incidence and properties in relation to other afferent A-fiber neurons in mammals. *Brain Res Rev.* 2004;46(2):131-145. doi:10.1016/j.brainresrev.2004.07.015.
12. Brodal P. *The Central Nervous System: Structure and Function.* 4th ed. New York: Oxford University Press; 2010.
13. Millan MJ. The induction of pain: an integrative review. *Prog Neurobiol.* 1999;57(1):1-164. doi:10.1016/S0301-0082(98)00048-3.

14. Almeida TF, Roizenblatt S, Tufik S. Afferent pain pathways: a neuroanatomical review. *Brain Res.* 2004;1000(1):40-56. doi:10.1016/j.brainres.2003.10.073.
15. Schaible H-G, Grubb BD. Afferent and spinal mechanisms of joint pain. *Pain.* 1993;55(1):5-54. doi:10.1016/0304-3959(93)90183-P.
16. Willis WD, Westlund KN. Neuroanatomy of the Pain System and of the Pathways That Modulate Pain. *J Clin Neurophysiol.* 1997;14(1):2.
17. Willis WD, Kenshalo DR, Leonard RB. The cells of origin of the primate spinothalamic tract. *J Comp Neurol.* 1979;188(4):543-573. doi:10.1002/cne.901880404.
18. Apkarian AV, Hodge CJ. Primate spinothalamic pathways: I. A quantitative study of the cells of origin of the spinothalamic pathway. *J Comp Neurol.* 1989;288(3):447-473. doi:10.1002/cne.902880307.
19. Kevetter GA, Haber LH, Yeziarski RP, Chung JM, Martin RF, Willis WD. Cells of origin of the spinoreticular tract in the monkey. *J Comp Neurol.* 1982;207(1):61-74. doi:10.1002/cne.902070106.
20. Bushnell MC, Duncan GH, Hofbauer RK, Ha B, Chen J-I, Carrier B. Pain perception: Is there a role for primary somatosensory cortex? *Proc Natl Acad Sci.* 1999;96(14):7705-7709. doi:10.1073/pnas.96.14.7705.
21. Brooks J, Tracey I. REVIEW: From nociception to pain perception: imaging the spinal and supraspinal pathways. *J Anat.* 2005;207(1):19-33. doi:10.1111/j.1469-7580.2005.00428.x.
22. Treede R-D, Kenshalo DR, Gracely RH, Jones AKP. The cortical representation of pain. *PAIN.* 1999;79(2):105-111. doi:10.1016/S0304-3959(98)00184-5.
23. Behbehani MM. Functional characteristics of the midbrain periaqueductal gray. *Prog Neurobiol.* 1995;46(6):575-605. doi:10.1016/0301-0082(95)00009-K.
24. Ossipov MH, Dussor GO, Porreca F. Central modulation of pain. *J Clin Invest.* 2010;120(11):3779-3787. doi:10.1172/JCI43766.
25. Rich KM, Disch SP, Eichler ME. The influence of regeneration and nerve growth factor on the neuronal cell body reaction to injury. *J Neurocytol.* 1989;18(5):569-576. doi:10.1007/BF01187077.
26. Wong J, Oblinger MM. A comparison of peripheral and central axotomy effects on neurofilament and tubulin gene expression in rat dorsal root ganglion neurons. *J Neurosci.* 1990;10(7):2215-2222. doi:10.1523/JNEUROSCI.10-07-02215.1990.
27. Lieberman AR. Some factors affecting retrograde neuronal responses to axonal lesion. In: Bellairs R, Gray EG, eds. *Essays on the Nervous System.* Oxford: Clarendon Press; 1974.

28. Whiteside G, Doyle CA, Hunt SP, Munglani R. Differential time course of neuronal and glial apoptosis in neonatal rat dorsal root ganglia after sciatic nerve axotomy. *Eur J Neurosci*. 1998;10(11):3400-3408. doi:10.1046/j.1460-9568.1998.00346.x.
29. Schmalbruch H. Loss of sensory neurons after sciatic nerve section in the rat. *Anat Rec*. 1987;219(3):323-329. doi:10.1002/ar.1092190314.
30. Klusáková I, Dubový P. Experimental models of peripheral neuropathic pain based on traumatic nerve injuries – An anatomical perspective. *Ann Anat - Anat Anz*. 2009;191(3):248-259. doi:10.1016/j.aanat.2009.02.007.
31. Takahashi Y, Nakajima Y. Dermatomes in the rat limbs as determined by antidromic stimulation of sensory C-fibers in spinal nerves. *PAIN*. 1996;67(1):197-202. doi:10.1016/0304-3959(96)03116-8.
32. Asato F, Butler M, Blomberg H, Gordh T. Variation in rat sciatic nerve anatomy: Implications for a rat model of neuropathic pain. *J Peripher Nerv Syst*. 2000;5(1):19-21. doi:10.1046/j.1529-8027.2000.00155.x.
33. Swett JE, Torigoe Y, Elie VR, Bourassa CM, Miller PG. Sensory neurons of the rat sciatic nerve. *Exp Neurol*. 1991;114(1):82-103. doi:10.1016/0014-4886(91)90087-S.
34. Wall PD, Devor M, Inbal R, Scadding JW, Schonfeld D, Seltzer Z, Tomkiewicz MM. Autotomy following peripheral nerve lesions: experimental anesthesia dolorosa. *Pain*. 1979;7(2):103-113. doi:10.1016/0304-3959(79)90002-2.
- 35.Coderre TJ, Grimes RW, Melzack R. Deafferentation and chronic pain in animals: An evaluation of evidence suggesting autotomy is related to pain. *Pain*. 1986;26(1):61-84. doi:10.1016/0304-3959(86)90174-0.
36. Bennett GJ, Xie YK. A peripheral mononeuropathy in rat that produces disorders of pain sensation like those seen in man. *Pain*. 1988;33(1):87-107.
37. Clatworthy AL, Illich PA, Castro GA, Walters ET. Role of peri-axonal inflammation in the development of thermal hyperalgesia and guarding behavior in a rat model of neuropathic pain. *Neurosci Lett*. 1995;184(1):5-8. doi:10.1016/0304-3940(94)11154-B.
38. Kleinschnitz C, Hofstetter HH, Meuth SG, Braeuninger S, Sommer C, Stoll G. T cell infiltration after chronic constriction injury of mouse sciatic nerve is associated with interleukin-17 expression. *Exp Neurol*. 2006;200(2):480-485. doi:10.1016/j.expneurol.2006.03.014.
39. Maves TJ, Pechman PS, Gebhart GF, Meller ST. Possible chemical contribution from chronic gut sutures produces disorders of pain sensation like those seen in man. *Pain*. 1993;54(1):57-69. doi:10.1016/0304-3959(93)90100-4.
40. Mosconi T, Kruger L. Fixed-diameter polyethylene cuffs applied to the rat sciatic nerve induce a painful neuropathy: ultrastructural morphometric analysis of axonal alterations. *Pain*. 1996;64(1):37-57. doi:10.1016/0304-3959(95)00077-1.

41. Munger BL, Bennett GJ, Kajander KC. An experimental painful peripheral neuropathy due to nerve constriction. *Exp Neurol.* 1992;118(2):204-214. doi:10.1016/0014-4886(92)90037-Q.
42. Gautron M, Jazat F, Ratinahirana H, Hauw JJ, Guilbaud G. Alterations in myelinated fibres in the sciatic nerve of rats after constriction: possible relationships between the presence of abnormal small myelinated fibres and pain-related behaviour. *Neurosci Lett.* 1990;111(1-2):28-33. doi:10.1016/0304-3940(90)90339-B.
43. Seltzer Z, Dubner R, Shir Y. A novel behavioral model of neuropathic pain disorders produced in rats by partial sciatic nerve injury. *Pain.* 1990;43(2):205-218. doi:10.1016/0304-3959(90)91074-S.
44. Swett JE, Woolf CJ. The somatotopic organization of primary afferent terminals in the superficial laminae of the dorsal horn of the rat spinal cord. *J Comp Neurol.* 1985;231(1):66-77. doi:10.1002/cne.902310106.
45. Decosterd I, Woolf CJ. Spared nerve injury: an animal model of persistent peripheral neuropathic pain. *Pain.* 2000;87(2):149-158. doi:10.1016/S0304-3959(00)00276-1.
46. Bourquin A-F, Süveges M, Pertin M, Gilliard N, Sardy S, Davison AC, Spahn DR, Decosterd I. Assessment and analysis of mechanical allodynia-like behavior induced by spared nerve injury (SNI) in the mouse. *PAIN.* 2006;122(1):14.e1-14.e14. doi:10.1016/j.pain.2005.10.036.
47. Kim HS, Chung MJ. An experimental model for peripheral neuropathy produced by segmental spinal nerve ligation in the rat. *PAIN.* 1992;50(3):355-363. doi:10.1016/0304-3959(92)90041-9.
48. Tabo E, Jinks SL, Eisele JH, Carstens E. Behavioral manifestations of neuropathic pain and mechanical allodynia, and changes in spinal dorsal horn neurons, following L4-L6 dorsal root constriction in rats. *Pain.* 1999;80(3):503-520. doi:10.1016/S0304-3959(98)00243-7.
49. Hu S-J, Xing J-L. An experimental model for chronic compression of dorsal root ganglion produced by intervertebral foramen stenosis in the rat. *Pain.* 1998;77(1):15-23. doi:10.1016/S0304-3959(98)00067-0.
50. Cornefjord M, Sato K, Olmarker K, Rydevik B, Nordborg C. A Model for Chronic Nerve Root Compression Studies: Presentation of a Porcine Model for Controlled, Slow-Onset Compression With Analyses of Anatomic Aspects, Compression Onset Rate, and Morphologic and Neurophysiologic Effects. *Spine.* 1997;22(9):946.
51. Jancalek R, Dubovy P. An experimental animal model of spinal root compression syndrome: an analysis of morphological changes of myelinated axons during compression radiculopathy and after decompression. *Exp Brain Res.* 2007;179(1):111-119. doi:10.1007/s00221-006-0771-5.
52. Lombard MC, Nashold BS, Albe-Fessard D, Salman N, Sakr C. Deafferentation hypersensitivity in the rat after dorsal rhizotomy: a possible animal model of chronic pain. *Pain.* 1979;6(2):163-174.

53. Li Y, Dorsi MJ, Meyer RA, Belzberg AJ. Mechanical hyperalgesia after an L5 spinal nerve lesion in the rat is not dependent on input from injured nerve fibers. *Pain*. 2000;85(3):493-502. doi:10.1016/S0304-3959(00)00250-5.
54. Xu J-T, Xin W-J, Zang Y, Wu C-Y, Liu X-G. The role of tumor necrosis factor-alpha in the neuropathic pain induced by Lumbar 5 ventral root transection in rat. *PAIN*. 2006;123(3):306-321. doi:10.1016/j.pain.2006.03.011.
55. Dubový P, Tučková L, Jančálek R, Svíženská I, Klusáková I. Increased invasion of ED-1 positive macrophages in both ipsi- and contralateral dorsal root ganglia following unilateral nerve injuries. *Neurosci Lett*. 2007;427(2):88-93. doi:10.1016/j.neulet.2007.09.012.
56. Waller A. Experiments on the Section of the Glossopharyngeal and Hypoglossal Nerves of the Frog, and Observations of the Alterations Produced Thereby in the Structure of Their Primitive Fibres. *Philos Trans R Soc Lond*. 1850;140:423-429.
57. Salonen V, Aho H, Røyttä M, Peltonen J. Quantitation of Schwann cells and endoneurial fibroblast-like cells after experimental nerve trauma. *Acta Neuropathol (Berl)*. 1988;75(4):331-336. doi:10.1007/BF00687785.
58. Perry VH, Brown MC. Role of macrophages in peripheral nerve degeneration and repair. *BioEssays*. 1992;14(6):401-406. doi:10.1002/bies.950140610.
59. Mellick R, Cavanagh J. Changes in blood vessel permeability during degeneration and regeneration in peripheral nerves. *Brain*. 1968;91(1):141-160.
60. Tona A, Perides G, Rahemtulla F, Dahl D. Extracellular matrix in regenerating rat sciatic nerve: a comparative study on the localization of laminin, hyaluronic acid, and chondroitin sulfate proteoglycans, including versican. *J Histochem Cytochem*. 1993;41(4):593-599. doi:10.1177/41.4.8450198.
61. Cámara-Lemarroy CR, Garza FJG la, Fernández-Garza NE. Molecular Inflammatory Mediators in Peripheral Nerve Degeneration and Regeneration. *Neuroimmunomodulation*. 2010;17(5):314-324. doi:10.1159/000292020.
62. Saxena S, Caroni P. Mechanisms of axon degeneration: From development to disease. *Prog Neurobiol*. 2007;83(3):174-191. doi:10.1016/j.pneurobio.2007.07.007.
63. Mack TGA, Reiner M, Beirowski B, Mi W, Emanuelli M, Wagner D, Thomson D, Gillingwater T, Court F, Conforti L, Fernando FS, Tarlton A, Andressen C, Addicks K, Magni G, Ribchester RR, Perry VH, Coleman MP. Wallerian degeneration of injured axons and synapses is delayed by a *Ube4b/Nmnat* chimeric gene. *Nat Neurosci*. 2001;4(12):1199-1206. doi:10.1038/nn770.
64. Coleman M. Axon degeneration mechanisms: commonality amid diversity. *Nat Rev Neurosci*. 2005;6(11):889-898. doi:10.1038/nrn1788.
65. Beirowski B, Adalbert R, Wagner D, Grumme DS, Addicks K, Ribchester RR, Coleman MP. The progressive nature of Wallerian degeneration in wild-type and slow Wallerian degeneration (Wlds) nerves. *BMC Neurosci*. 2005;6:6. doi:10.1186/1471-2202-6-6.

66. Stoll G, Griffin JW, Li CY, Trapp BD. Wallerian degeneration in the peripheral nervous system: participation of both Schwann cells and macrophages in myelin degradation. *J Neurocytol.* 1989;18(5):671-683. doi:10.1007/BF01187086.
67. Brück W. The Role of Macrophages in Wallerian Degeneration. *Brain Pathol.* 1997;7(2):741-752. doi:10.1111/j.1750-3639.1997.tb01060.x.
68. Taskinen HS, Røyttä M. The dynamics of macrophage recruitment after nerve transection. *Acta Neuropathol (Berl).* 1997;93(3):252-259. doi:10.1007/s004010050611.
69. Omura T, Omura K, Sano M, Sawada T, Hasegawa T, Nagano A. Spatiotemporal quantification of recruit and resident macrophages after crush nerve injury utilizing immunohistochemistry. *Brain Res.* 2005;1057(1):29-36. doi:10.1016/j.brainres.2005.07.008.
70. Monk KR, Wu J, Williams JP, Finney BA, Fitzgerald ME, Filippi M-D, Ratner N. Mast cells can contribute to axon–glial dissociation and fibrosis in peripheral nerve. *Neuron Glia Biol.* 2007;3(3):233-244. doi:10.1017/S1740925X08000021.
71. Zuo Y, Perkins NM, Tracey DJ, Geczy CL. Inflammation and hyperalgesia induced by nerve injury in the rat: a key role of mast cells. *Pain.* 2003;105(3):467-479. doi:10.1016/S0304-3959(03)00261-6.
72. Moalem G, Tracey DJ. Immune and inflammatory mechanisms in neuropathic pain. *Brain Res Rev.* 2006;51(2):240-264. doi:10.1016/j.brainresrev.2005.11.004.
73. Barrientos S, Stojadinovic O, Golinko MS, Brem H, Tomic-Canic M. PERSPECTIVE ARTICLE: Growth factors and cytokines in wound healing. *Wound Repair Regen.* 2008;16(5):585-601. doi:10.1111/j.1524-475X.2008.00410.x.
74. Stoll G, Jander S, Myers RR. Degeneration and regeneration of the peripheral nervous system: From Augustus Waller's observations to neuroinflammation. *J Peripher Nerv Syst.* 2002;7(1):13-27. doi:10.1046/j.1529-8027.2002.02002.x.
75. Shamash S, Reichert F, Rotshenker S. The Cytokine Network of Wallerian Degeneration: Tumor Necrosis Factor- α , Interleukin-1 α , and Interleukin-1 β . *J Neurosci.* 2002;22(8):3052-3060.
76. Liefner M, Siebert H, Sachse T, Michel U, Kollias G, Brück W. The role of TNF- α during Wallerian degeneration. *J Neuroimmunol.* 2000;108(1):147-152. doi:10.1016/S0165-5728(00)00262-9.
77. Üçeyler N, Sommer C. Cytokine regulation in animal models of neuropathic pain and in human diseases. *Neurosci Lett.* 2008;437(3):194-198. doi:10.1016/j.neulet.2008.03.050.
78. Dubový P. Wallerian degeneration and peripheral nerve conditions for both axonal regeneration and neuropathic pain induction. *Ann Anat - Anat Anz.* 2011;193(4):267-275. doi:10.1016/j.aanat.2011.02.011.

79. Gölz G, Uhlmann L, Lüdecke D, Markgraf N, Nitsch R, Hendrix S. The cytokine/neurotrophin axis in peripheral axon outgrowth. *Eur J Neurosci*. 2006;24(10):2721-2730. doi:10.1111/j.1460-9568.2006.05155.x.
80. Woolf CJ. Dissecting out mechanisms responsible for peripheral neuropathic pain: Implications for diagnosis and therapy. *Life Sci*. 2004;74(21):2605-2610. doi:10.1016/j.lfs.2004.01.003.
81. Hanani M. Satellite glial cells in sensory ganglia: from form to function. *Brain Res Rev*. 2005;48(3):457-476. doi:10.1016/j.brainresrev.2004.09.001.
82. Humbertson A, Zimmermann E, Leedy M. A chronological study of mitotic activity in satellite cell hyperplasia associated with chromatolytic neurons. *Z Für Zellforsch Mikrosk Anat*. 1969;100(4):507-515. doi:10.1007/BF00344371.
83. Hu P, McLachlan EM. Macrophage and lymphocyte invasion of dorsal root ganglia after peripheral nerve lesions in the rat. *Neuroscience*. 2002;112(1):23-38. doi:10.1016/S0306-4522(02)00065-9.
84. Ramer MS, French GD, Bisby MA. Wallerian degeneration is required for both neuropathic pain and sympathetic sprouting into the DRG. *PAIN*. 1997;72(1):71-78. doi:10.1016/S0304-3959(97)00019-5.
85. Zhuang Z-Y, Kawasaki Y, Tan P-H, Wen Y-R, Huang J, Ji R-R. Role of the CX3CR1/p38 MAPK pathway in spinal microglia for the development of neuropathic pain following nerve injury-induced cleavage of fractalkine. *Brain Behav Immun*. 2007;21(5):642-651. doi:10.1016/j.bbi.2006.11.003.
86. Zhang J, Koninck YD. Spatial and temporal relationship between monocyte chemoattractant protein-1 expression and spinal glial activation following peripheral nerve injury. *J Neurochem*. 2006;97(3):772-783. doi:10.1111/j.1471-4159.2006.03746.x.
87. Hu P, McLachlan EM. Distinct functional types of macrophage in dorsal root ganglia and spinal nerves proximal to sciatic and spinal nerve transections in the rat. *Exp Neurol*. 2003;184(2):590-605. doi:10.1016/S0014-4886(03)00307-8.
88. Thacker MA, Clark AK, Marchand F, McMahon SB. Pathophysiology of peripheral neuropathic pain: Immune cells and molecules. *Anesth Analg*. 2007;105(3):838-847. doi:10.1213/01.ane.0000275190.42912.37.
89. Copray JCVM, Mantingh I, Brouwer N, Biber K, Küst BM, Liem RSB, Huitinga I, Tilders FJH, Van Dam A-M, Boddeke HWGM. Expression of interleukin-1 beta in rat dorsal root ganglia. *J Neuroimmunol*. 2001;118(2):203-211. doi:10.1016/S0165-5728(01)00324-1.
90. Sommer C, Kress M. Recent findings on how proinflammatory cytokines cause pain: peripheral mechanisms in inflammatory and neuropathic hyperalgesia. *Neurosci Lett*. 2004;361(1):184-187. doi:10.1016/j.neulet.2003.12.007.

91. Sommer C, Petrusch S, Lindenlaub T, Toyka KV. Neutralizing antibodies to interleukin 1-receptor reduce pain associated behavior in mice with experimental neuropathy. *Neurosci Lett.* 1999;270(1):25-28. doi:10.1016/S0304-3940(99)00450-4.
92. Schäfers M, Sorkin LS, Geis C, Shubayev VI. Spinal nerve ligation induces transient upregulation of tumor necrosis factor receptors 1 and 2 in injured and adjacent uninjured dorsal root ganglia in the rat. *Neurosci Lett.* 2003;347(3):179-182. doi:10.1016/S0304-3940(03)00695-5.
93. Ohtori S, Takahashi K, Moriya H, Myers RR. TNF- α and TNF- α receptor type 1 upregulation in glia and neurons after peripheral nerve injury: studies in murine DRG and spinal cord. *Spine.* 2004;29(10):1082-1088.
94. Dubový P, Jančálek R, Kubek T. Role of inflammation and cytokines in peripheral nerve regeneration. *Int Rev Neurobiol.* 2013;108:173-206. doi:10.1016/B978-0-12-410499-0.00007-1.
95. George A, Buehl A, Sommer C. Tumor necrosis factor receptor 1 and 2 proteins are differentially regulated during Wallerian degeneration of mouse sciatic nerve. *Exp Neurol.* 2005;192(1):163-166. doi:10.1016/j.expneurol.2004.11.002.
96. Sorkin LS, Xiao W-H, Wagner R, Myers RR. Tumour necrosis factor- α induces ectopic activity in nociceptive primary afferent fibres. *Neuroscience.* 1997;81(1):255-262. doi:10.1016/S0306-4522(97)00147-4.
97. DeLeo JA, Colburn RW, Nichols M, Malhotra A. Interleukin-6-Mediated Hyperalgesia/Allodynia and Increased Spinal IL-6 Expression in a Rat Mononeuropathy Model. *J Interferon Cytokine Res.* 1996;16(9):695-700. doi:10.1089/jir.1996.16.695.
98. Cui J-G, Holmin S, Mathiesen T, Meyerson BA, Linderöth B. Possible role of inflammatory mediators in tactile hypersensitivity in rat models of mononeuropathy. *PAIN.* 2000;88(3):239-248. doi:10.1016/S0304-3959(00)00331-6.
99. Murphy PG, Ramer MS, Borthwick L, Gauldie J, Richardson PM, Bisby MA. Endogenous interleukin-6 contributes to hypersensitivity to cutaneous stimuli and changes in neuropeptides associated with chronic nerve constriction in mice. *Eur J Neurosci.* 1999;11(7):2243-2253. doi:10.1046/j.1460-9568.1999.00641.x.
100. Arruda JL, Sweitzer S, Rutkowski MD, DeLeo JA. Intrathecal anti-IL-6 antibody and IgG attenuates peripheral nerve injury-induced mechanical allodynia in the rat: possible immune modulation in neuropathic pain. Published on the World Wide Web on 28 August 2000. *Brain Res.* 2000;879(1):216-225. doi:10.1016/S0006-8993(00)02807-9.
101. Dubový P, Brázda V, Klusáková I, Hradilová-Svíženská I. Bilateral elevation of interleukin-6 protein and mRNA in both lumbar and cervical dorsal root ganglia following unilateral chronic compression injury of the sciatic nerve. *J Neuroinflammation.* 2013;10:55. doi:10.1186/1742-2094-10-55.
102. Eulenfeld R, Dittrich A, Khouri C, Müller PJ, Mütze B, Wolf A, Schaper F. Interleukin-6 signalling: More than Jaks and STATs. *Eur J Cell Biol.* 2012;91(6):486-495. doi:10.1016/j.ejcb.2011.09.010.

103. Chernoff AE, Granowitz EV, Shapiro L, Vannier E, Lonnemann G, Angel JB, Kennedy JS, Rabson AR, Wolff SM, Dinarello CA. A randomized, controlled trial of IL-10 in humans. Inhibition of inflammatory cytokine production and immune responses. *J Immunol Baltim Md 1950*. 1995;154(10):5492-5499.
104. Moore KW, de Waal Malefyt R, Coffman RL, O'Garra A. Interleukin-10 and the Interleukin-10 Receptor. *Annu Rev Immunol*. 2001;19(1):683-765. doi:10.1146/annurev.immunol.19.1.683.
105. Doron-Mandel E, Fainzilber M, Terenzio M. Growth control mechanisms in neuronal regeneration. *FEBS Lett*. 2015;589(14):1669-1677. doi:10.1016/j.febslet.2015.04.046.
106. Mason MRJ, Lieberman AR, Grenningloh G, Anderson PN. Transcriptional Upregulation of SCG10 and CAP-23 Is Correlated with Regeneration of the Axons of Peripheral and Central Neurons in Vivo. *Mol Cell Neurosci*. 2002;20(4):595-615. doi:10.1006/mcne.2002.1140.
107. Bonilla IE, Tanabe K, Strittmatter SM. Small Proline-Rich Repeat Protein 1A Is Expressed by Axotomized Neurons and Promotes Axonal Outgrowth. *J Neurosci*. 2002;22(4):1303-1315. doi:10.1523/JNEUROSCI.22-04-01303.2002.
108. Dubový P, Klusáková I, Hradilová-Svíženská I, Joukal M. Expression of Regeneration-Associated Proteins in Primary Sensory Neurons and Regenerating Axons After Nerve Injury-An Overview. *Anat Rec Hoboken NJ 2007*. May 2018. doi:10.1002/ar.23843.
109. Dubový P, Klusáková I, Hradilová-Svíženská I, Brázda V, Kohoutková M, Joukal M. A conditioning sciatic nerve lesion triggers a pro-regenerative state in primary sensory neurons also of dorsal root ganglia non-associated with the damaged nerve. *Front Cell Neurosci*. 2019;13. doi:10.3389/fncel.2019.00011.
110. Sun H, Ren K, Zhong CM, Ossipov MH, Malan TP, Lai J, Porreca F. Nerve injury-induced tactile allodynia is mediated via ascending spinal dorsal column projections. *Pain*. 2001;90(1):105-111. doi:10.1016/S0304-3959(00)00392-4.
111. Rexed B. The cytoarchitectonic organization of the spinal cord in the cat. *J Comp Neurol*. 1952;96(3):415-495. doi:10.1002/cne.900960303.
112. Woolf CJ, Shortland P, Coggeshall RE. Peripheral nerve injury triggers central sprouting of myelinated afferents. *Nature*. 1992;355(6355):75-78. doi:10.1038/355075a0.
113. Yamamoto Y, Terayama R, Kishimoto N, Maruhama K, Mizutani M, Iida S, Sugimoto T. Activated Microglia Contribute to Convergent Nociceptive Inputs to Spinal Dorsal Horn Neurons and the Development of Neuropathic Pain. *Neurochem Res*. 2015;40(5):1000-1012. doi:10.1007/s11064-015-1555-8.
114. Gao Y-J, Ji R-R. Targeting Astrocyte Signaling for Chronic Pain. *Neurotherapeutics*. 2010;7(4):482-493. doi:10.1016/j.nurt.2010.05.016.
115. Gao Y-J, Ji R-R. Chemokines, neuronal–glial interactions, and central processing of neuropathic pain. *Pharmacol Ther*. 2010;126(1):56-68. doi:10.1016/j.pharmthera.2010.01.002.

116. Hernangómez M, Klusáková I, Joukal M, Hradilová-Svíženská I, Guaza C, Dubový P. CD200R1 agonist attenuates glial activation, inflammatory reactions, and hypersensitivity immediately after its intrathecal application in a rat neuropathic pain model. *J Neuroinflammation*. 2016;13:43. doi:10.1186/s12974-016-0508-8.
117. Kim SU, Vellis J de. Microglia in health and disease. *J Neurosci Res*. 2005;81(3):302-313. doi:10.1002/jnr.20562.
118. Hanisch U-K, Kettenmann H. Microglia: active sensor and versatile effector cells in the normal and pathologic brain. *Nat Neurosci*. 2007;10(11):1387-1394. doi:10.1038/nn1997.
119. Hu P, Bembrick AL, Keay KA, McLachlan EM. Immune cell involvement in dorsal root ganglia and spinal cord after chronic constriction or transection of the rat sciatic nerve. *Brain Behav Immun*. 2007;21(5):599-616. doi:10.1016/j.bbi.2006.10.013.
120. Tanga FY, Raghavendra V, DeLeo JA. Quantitative real-time RT-PCR assessment of spinal microglial and astrocytic activation markers in a rat model of neuropathic pain. *Neurochem Int*. 2004;45(2):397-407. doi:10.1016/j.neuint.2003.06.002.
121. Mika J, Osikowicz M, Rojewska E, Korostynski M, Wawrzczak-Bargiela A, Przewlocki R, Przewlocka B. Differential activation of spinal microglial and astroglial cells in a mouse model of peripheral neuropathic pain. *Eur J Pharmacol*. 2009;623(1):65-72. doi:10.1016/j.ejphar.2009.09.030.
122. Ji R-R, Berta T, Nedergaard M. Glia and pain: Is chronic pain a gliopathy? *PAIN®*. 2013;154:S10-S28. doi:10.1016/j.pain.2013.06.022.
123. Scholz J, Woolf CJ. The neuropathic pain triad: neurons, immune cells and glia. *Nat Neurosci*. 2007;10(11):1361-1368. doi:10.1038/nn1992.
124. Abbadie C, Lindia JA, Cumiskey AM, Peterson LB, Mudgett JS, Bayne EK, DeMartino JA, MacIntyre DE, Forrest MJ. Impaired neuropathic pain responses in mice lacking the chemokine receptor CCR2. *Proc Natl Acad Sci*. 2003;100(13):7947-7952. doi:10.1073/pnas.1331358100.
125. Liu T, Gao Y-J, Ji R-R. Emerging role of Toll-like receptors in the control of pain and itch. *Neurosci Bull*. 2012;28(2):131-144. doi:10.1007/s12264-012-1219-5.
126. Tanga FY, Nutile-McMenemy N, DeLeo JA. The CNS role of Toll-like receptor 4 in innate neuroimmunity and painful neuropathy. *Proc Natl Acad Sci U S A*. 2005;102(16):5856-5861. doi:10.1073/pnas.0501634102.
127. Kim D, Kim MA, Cho I-H, Kim MS, Lee S, Jo E-K, Choi S-Y, Park K, Kim JS, Akira S, Na HS, Oh SB, Lee SJ. A critical role of toll-like receptor 2 in nerve injury-induced spinal cord glial cell activation and pain hypersensitivity. *J Biol Chem*. 2007;282(20):14975-14983. doi:10.1074/jbc.M607277200.
128. Garrison CJ, Dougherty PM, Kajander KC, Carlton SM. Staining of glial fibrillary acidic protein (GFAP) in lumbar spinal cord increases following a sciatic nerve constriction injury. *Brain Res*. 1991;565(1):1-7. doi:10.1016/0006-8993(91)91729-K.

129. Colburn RW, Rickman AJ, DeLeo JA. The Effect of Site and Type of Nerve Injury on Spinal Glial Activation and Neuropathic Pain Behavior. *Exp Neurol.* 1999;157(2):289-304. doi:10.1006/exnr.1999.7065.
130. Wang W, Wang W, Mei X, Huang J, Wei Y, Wang Y, Wu S, Li Y. Crosstalk between Spinal Astrocytes and Neurons in Nerve Injury-Induced Neuropathic Pain. *PLOS ONE.* 2009;4(9):e6973. doi:10.1371/journal.pone.0006973.
131. Guo W, Wang H, Watanabe M, Shimizu K, Zou S, LaGraize SC, Wei F, Dubner R, Ren K. Glial–Cytokine–Neuronal Interactions Underlying the Mechanisms of Persistent Pain. *J Neurosci.* 2007;27(22):6006-6018. doi:10.1523/JNEUROSCI.0176-07.2007.
132. Milligan ED, Twining C, Chacur M, Biedenkapp J, O’Connor K, Poole S, Tracey K, Martin D, Maier SF, Watkins LR. Spinal Glia and Proinflammatory Cytokines Mediate Mirror-Image Neuropathic Pain in Rats. *J Neurosci.* 2003;23(3):1026-1040. doi:10.1523/JNEUROSCI.23-03-01026.2003.
133. Zhang J-M, An J. Cytokines, Inflammation and Pain. *Int Anesthesiol Clin.* 2007;45(2):27-37. doi:10.1097/AIA.0b013e318034194e.
134. Yan HQ, Banos MA, Herregodts P, Hooghe R, Hooghe-Peters EL. Expression of interleukin (IL)-1 β , IL-6 and their respective receptors in the normal rat brain and after injury. *Eur J Immunol.* 1992;22(11):2963-2971. doi:10.1002/eji.1830221131.
135. Perkins MN, Kelly D. Interleukin-1 beta induced-desArg⁹bradykinin-mediated thermal hyperalgesia in the rat. *Neuropharmacology.* 1994;33(5):657-660.
136. Zhang L, Berta T, Xu Z-Z, Liu T, Park JY, Ji R-R. TNF-alpha contributes to spinal cord synaptic plasticity and inflammatory pain: Distinct role of TNF receptor subtypes 1 and 2. *PAIN®.* 2011;152(2):419-427. doi:10.1016/j.pain.2010.11.014.
137. Shubayev VI, Myers R. Anterograde TNF α Transport From Rat Dorsal Root Ganglion To Spinal Cord And Injured Sciatic Nerve. *J Peripher Nerv Syst.* 2002;7(3):210-210. doi:10.1046/j.1529-8027.2002.02026_19.x.
138. Milligan ED, Sloane EM, Langer SJ, Cruz PE, Chacur M, Spataro L, Wieseler-Frank J, Hammack SE, Maier SF, Flotte TR, Forsayeth JR, Leinwand LA, Chavez R, Watkins LR. Controlling neuropathic pain by adeno-associated virus driven production of the anti-inflammatory cytokine, interleukin-10. *Mol Pain.* 2005;1(1):9. doi:10.1186/1744-8069-1-9.
139. Üçeyler N, Topuzoğlu T, Schießler P, Hahnenkamp S, Sommer C. IL-4 Deficiency Is Associated with Mechanical Hypersensitivity in Mice. *PLOS ONE.* 2011;6(12):e28205. doi:10.1371/journal.pone.0028205.
140. Üçeyler N, Valenza R, Stock M, Schedel R, Sprotte G, Sommer C. Reduced levels of antiinflammatory cytokines in patients with chronic widespread pain. *Arthritis Rheum.* 2006;54(8):2656-2664. doi:10.1002/art.22026.
141. Thomson AW, Lotze MT. *The Cytokine Handbook, Two-Volume Set.* Elsevier; 2003.

142. Kraus J, Börner C, Giannini E, Hickfang K, Braun H, Mayer P, Hoehe MR, Ambrosch A, König W, Höllt V. Regulation of μ -Opioid Receptor Gene Transcription by Interleukin-4 and Influence of an Allelic Variation within a STAT6 Transcription Factor Binding Site. *J Biol Chem*. 2001;276(47):43901-43908. doi:10.1074/jbc.M107543200.
143. Börner C, Wöltje M, Höllt V, Kraus J. STAT6 transcription factor binding sites with mismatches within the canonical 5'-TTC...GAA-3' motif involved in regulation of δ - and μ -opioid receptors. *J Neurochem*. 2004;91(6):1493-1500. doi:10.1111/j.1471-4159.2004.02846.x.
144. Wieseler-Frank J, Maier SF, Watkins LR. Glial activation and pathological pain. *Neurochem Int*. 2004;45(2):389-395. doi:10.1016/j.neuint.2003.09.009.
145. Hatherley D, Lea SM, Johnson S, Barclay AN. Structures of CD200/CD200 Receptor Family and Implications for Topology, Regulation, and Evolution. *Structure*. 2013;21(5):820-832. doi:10.1016/j.str.2013.03.008.
146. Wright GJ, Cherwinski H, Foster-Cuevas M, Brooke G, Puklavec MJ, Bigler M, Song Y, Jenmalm M, Gorman D, McClanahan T, Liu M-R, Brown MH, Sedgwick JD, Phillips JH, Barclay AN. Characterization of the CD200 Receptor Family in Mice and Humans and Their Interactions with CD200. *J Immunol*. 2003;171(6):3034-3046. doi:10.4049/jimmunol.171.6.3034.
147. Hoek RM, Ruuls SR, Murphy CA, Wright GJ, Goddard R, Zurawski SM, Blom B, Homola ME, Streit WJ, Brown MH, Barclay AN, Sedgwick JD. Down-Regulation of the Macrophage Lineage Through Interaction with OX2 (CD200). *Science*. 2000;290(5497):1768-1771. doi:10.1126/science.290.5497.1768.
148. Meuth SG, Simon OJ, Grimm A, Melzer N, Herrmann AM, Spitzer P, Landgraf P, Wiendl H. CNS inflammation and neuronal degeneration is aggravated by impaired CD200-CD200R-mediated macrophage silencing. *J Neuroimmunol*. 2008;194(1):62-69. doi:10.1016/j.jneuroim.2007.11.013.
149. Jaggi AS, Singh N. Role of different brain areas in peripheral nerve injury-induced neuropathic pain. *Brain Res*. 2011;1381:187-201. doi:10.1016/j.brainres.2011.01.002.
150. Gosselin R-D, Bebbber D, Decosterd I. Upregulation of the GABA transporter GAT-1 in the gracile nucleus in the spared nerve injury model of neuropathic pain. *Neurosci Lett*. 2010;480(2):132-137. doi:10.1016/j.neulet.2010.06.023.
151. Gao X, Kim HK, Chung JM, Chung K. Enhancement of NMDA receptor phosphorylation of the spinal dorsal horn and nucleus gracilis neurons in neuropathic rats. *Pain*. 2005;116(1):62-72. doi:10.1016/j.pain.2005.03.045.
152. Terayama R, Omura S, Fujisawa N, Yamaai T, Ichikawa H, Sugimoto T. Activation of microglia and p38 mitogen-activated protein kinase in the dorsal column nucleus contributes to tactile allodynia following peripheral nerve injury. *Neuroscience*. 2008;153(4):1245-1255. doi:10.1016/j.neuroscience.2008.03.041.

153. Chen J-J, Lue J-H, Lin L-H, Huang C-T, Chiang RP-Y, Chen C-L, Tsai Y-J. Effects of pre-emptive drug treatment on astrocyte activation in the cuneate nucleus following rat median nerve injury. *PAIN*. 2010;148(1):158-166. doi:10.1016/j.pain.2009.11.004.
154. Tsai Y-J, Leong S-M, Day A-S, Wen C-Y, Shieh J-Y, Lue J-H. A time course analysis of the changes in neuropeptide Y immunoreactivity in the rat cuneate nucleus following median nerve transection. *Neurosci Res*. 2004;48(4):369-377. doi:10.1016/j.neures.2003.12.003.
155. Tsai Y-J, Lin C-T, Huang C-T, Wang H-Y, Tien L-T, Chen S-H, Lue J-H. Neuropeptide Y Modulates c-Fos Protein Expression in the Cuneate Nucleus and Contributes to Mechanical Hypersensitivity following Rat Median Nerve Injury. *J Neurotrauma*. 2009;26(9):1609-1621. doi:10.1089/neu.2008.0642.
156. Kincaid W, Neubert MJ, Xu M, Kim CJ, Heinricher MM. Role for Medullary Pain Facilitating Neurons in Secondary Thermal Hyperalgesia. *J Neurophysiol*. 2006;95(1):33-41. doi:10.1152/jn.00449.2005.
157. Porreca F, Ossipov MH, Gebhart GF. Chronic pain and medullary descending facilitation. *Trends Neurosci*. 2002;25(6):319-325. doi:10.1016/S0166-2236(02)02157-4.
158. Carlson JD, Maire JJ, Martenson ME, Heinricher MM. Sensitization of Pain-Modulating Neurons in the Rostral Ventromedial Medulla after Peripheral Nerve Injury. *J Neurosci*. 2007;27(48):13222-13231. doi:10.1523/JNEUROSCI.3715-07.2007.
159. Wei F, Guo W, Zou S, Ren K, Dubner R. Supraspinal Glial–Neuronal Interactions Contribute to Descending Pain Facilitation. *J Neurosci*. 2008;28(42):10482-10495. doi:10.1523/JNEUROSCI.3593-08.2008.
160. Leong ML, Gu M, Speltz-Paiz R, Stahura EI, Mottey N, Steer CJ, Wessendorf M. Neuronal Loss in the Rostral Ventromedial Medulla in a Rat Model of Neuropathic Pain. *J Neurosci*. 2011;31(47):17028-17039. doi:10.1523/JNEUROSCI.1268-11.2011.
161. Pertovaara A. Noradrenergic pain modulation. *Prog Neurobiol*. 2006;80(2):53-83. doi:10.1016/j.pneurobio.2006.08.001.
162. Sindrup SH, Otto M, Finnerup NB, Jensen TS. Antidepressants in the Treatment of Neuropathic Pain. *Basic Clin Pharmacol Toxicol*. 2005;96(6):399-409. doi:10.1111/j.1742-7843.2005.pto_96696601.x.
163. Moore A, Derry S, Wiffen P. Gabapentin for Chronic Neuropathic Pain. *JAMA*. 2018;319(8):818-819. doi:10.1001/jama.2017.21547.
164. Hayashida K, Obata H, Nakajima K, Eisenach JC. Gabapentin Acts within the Locus Coeruleus to Alleviate Neuropathic Pain. *Anesthesiol J Am Soc Anesthesiol*. 2008;109(6):1077-1084. doi:10.1097/ALN.0b013e31818dac9c.
165. Brightwell JJ, Taylor BK. Noradrenergic neurons in the locus coeruleus contribute to neuropathic pain. *Neuroscience*. 2009;160(1):174-185. doi:10.1016/j.neuroscience.2009.02.023.

166. Al-Adawi S, Dawe GS, Bonner A, Stephenson JD, Zarei M. Central noradrenergic blockade prevents autotomy in rat: implication for pharmacological prevention of postdenervation pain syndrome. *Brain Res Bull.* 2002;57(5):581-586. doi:10.1016/S0361-9230(01)00747-X.
167. Michele Basso D, Beattie MS, Bresnahan JC. Descending systems contributing to locomotor recovery after mild or moderate spinal cord injury in rats: experimental evidence and a review of literature. *Restor Neurol Neurosci.* 2002;20(5):189-218.
168. Muir GD, Whishaw IQ. Red nucleus lesions impair overground locomotion in rats: a kinetic analysis. *Eur J Neurosci.* 2000;12(3):1113-1122. doi:10.1046/j.1460-9568.2000.00987.x.
169. Yu J, Ding C-P, Wang J, Wang T, Zhang T, Zeng X-Y, Wang J-Y. Red nucleus glutamate facilitates neuropathic allodynia induced by spared nerve injury through non-NMDA and metabotropic glutamate receptors. *J Neurosci Res.* 2015;93(12):1839-1848. doi:10.1002/jnr.23671.
170. Ding C-P, Xue Y-S, Yu J, Guo Y-J, Zeng X-Y, Wang J-Y. The Red Nucleus Interleukin-6 Participates in the Maintenance of Neuropathic Pain Induced by Spared Nerve Injury. *Neurochem Res.* 2016;41(11):3042-3051. doi:10.1007/s11064-016-2023-9.
171. Li X, Wang J, Wang Z, Dong C, Dong X, Jing Y, Yuan Y, Fan G. Tumor necrosis factor- α of Red nucleus involved in the development of neuropathic allodynia. *Brain Res Bull.* 2008;77(5):233-236. doi:10.1016/j.brainresbull.2008.08.025.
172. Wang Z, Wang J, Li X, Yuan Y, Fan G. Interleukin-1 β of Red nucleus involved in the development of allodynia in spared nerve injury rats. *Exp Brain Res.* 2008;188(3):379. doi:10.1007/s00221-008-1365-1.
173. Jing Y-Y, Wang J-Y, Li X-L, Wang Z-H, Pei L, Pan M-M, Dong X-P, Fan G-X, Yuan Y-K. Nerve Growth Factor of Red Nucleus Involvement in Pain Induced by Spared Nerve Injury of the Rat Sciatic Nerve. *Neurochem Res.* 2009;34(9):1612-1618. doi:10.1007/s11064-009-9950-7.
174. Reynolds DV. Surgery in the Rat during Electrical Analgesia Induced by Focal Brain Stimulation. *Science.* 1969;164(3878):444-445. doi:10.1126/science.164.3878.444.
175. Sohn J-H, Lee BH, Park SH, Ryu J-W, Kim B-O, Park YG. Microinjection of opiates into the periaqueductal gray matter attenuates neuropathic pain symptoms in rats. *NeuroReport.* 2000;11(7):1413-1416. doi:10.1097/00001756-200005150-00012.
176. Milligan ED, Watkins LR. Pathological and protective roles of glia in chronic pain. *Nat Rev Neurosci.* 2009;10(1):23-36. doi:10.1038/nrn2533.
177. Blackbeard J, O'Dea KP, Wallace VCJ, Segerdahl A, Pheby T, Takata M, Field MJ, Rice ASC. Quantification of the rat spinal microglial response to peripheral nerve injury as revealed by immunohistochemical image analysis and flow cytometry. *J Neurosci Methods.* 2007;164(2):207-217. doi:10.1016/j.jneumeth.2007.04.013.

178. Iadarola MJ, Max MB, Berman KF, Byas-Smith MG, Coghill RC, Gracely RH, Bennett GJ. Unilateral decrease in thalamic activity observed with positron emission tomography in patients with chronic neuropathic pain. *Pain*. 1995;63(1):55-64. doi:10.1016/0304-3959(95)00015-K.
179. Jhaveri MD, Elmes SJR, Richardson D, Barrett DA, Kendall DA, Mason R, Chapman V. Evidence for a novel functional role of cannabinoid CB2 receptors in the thalamus of neuropathic rats. *Eur J Neurosci*. 2008;27(7):1722-1730. doi:10.1111/j.1460-9568.2008.06162.x.
180. Hains BC, Saab CY, Waxman SG. Alterations in burst firing of thalamic VPL neurons and reversal by Na(v)1.3 antisense after spinal cord injury. *J Neurophysiol*. 2006;95(6):3343-3352. doi:10.1152/jn.01009.2005.
181. Kupers RC, Gybels JM. Electrical stimulation of the ventroposterolateral thalamic nucleus (VPL) reduces mechanical allodynia in a rat model of neuropathic pain. *Neurosci Lett*. 1993;150(1):95-98. doi:10.1016/0304-3940(93)90116-3.
182. Saadé NE, Al Amin H, Abdel Baki S, Chalouhi S, Jabbur SJ, Atweh SF. Reversible attenuation of neuropathic-like manifestations in rats by lesions or local blocks of the intralaminar or the medial thalamic nuclei. *Exp Neurol*. 2007;204(1):205-219. doi:10.1016/j.expneurol.2006.10.009.
183. Loggia ML, Chonde DB, Akeju O, Arabasz G, Catana C, Edwards RR, Hill E, Hsu S, Izquierdo-Garcia D, Ji R-R, Riley M, Wasan AD, Zürcher NR, Albrecht DS, Vangel MG, Rosen BR, Napadow V, Hooker JM. Evidence for brain glial activation in chronic pain patients. *Brain*. 2015;138(3):604-615. doi:10.1093/brain/awu377.
184. Banati RB, Cagnin A, Brooks DJ, Gunn RN, Myers R, Jones T, Birch R, Anand P. Long-term trans-synaptic glial responses in the human thalamus after peripheral nerve injury. *Neuroreport*. 2001;12(16):3439-3442.
185. Takeda K, Muramatsu M, Chikuma T, Kato T. Effect of Memantine on the Levels of Neuropeptides and Microglial Cells in the Brain Regions of Rats with Neuropathic Pain. *J Mol Neurosci*. 2009;39(3):380. doi:10.1007/s12031-009-9224-5.
186. Jeong Y, Holden JE. The role of spinal orexin-1 receptors in posterior hypothalamic modulation of neuropathic pain. *Neuroscience*. 2009;159(4):1414-1421. doi:10.1016/j.neuroscience.2009.02.006.
187. Martínez-Lorenzana G, Espinosa-López L, Carranza M, Aramburo C, Paz-Tres C, Rojas-Piloni G, Condés-Lara M. PVN electrical stimulation prolongs withdrawal latencies and releases oxytocin in cerebrospinal fluid, plasma, and spinal cord tissue in intact and neuropathic rats. *PAIN*. 2008;140(2):265-273. doi:10.1016/j.pain.2008.08.015.
188. Condés-Lara M, Maie IAS, Dickenson AH. Oxytocin actions on afferent evoked spinal cord neuronal activities in neuropathic but not in normal rats. *Brain Res*. 2005;1045(1):124-133. doi:10.1016/j.brainres.2005.03.020.
189. Moisset X, Bouhassira D. Brain imaging of neuropathic pain. *NeuroImage*. 2007;37:S80-S88. doi:10.1016/j.neuroimage.2007.03.054.

190. Chudler EH, Dong WK. The role of the basal ganglia in nociception and pain. *Pain*. 1995;60(1):3-38. doi:10.1016/0304-3959(94)00172-B.
191. Pedersen LH, Scheel-Krüger J, Blackburn-Munro G. Amygdala GABA-A receptor involvement in mediating sensory-discriminative and affective-motivational pain responses in a rat model of peripheral nerve injury. *Pain*. 2007;127(1):17-26. doi:10.1016/j.pain.2006.06.036.
192. Gonçalves L, Silva R, Pinto-Ribeiro F, Pêgo JM, Bessa JM, Pertovaara A, Sousa N, Almeida A. Neuropathic pain is associated with depressive behaviour and induces neuroplasticity in the amygdala of the rat. *Exp Neurol*. 2008;213(1):48-56. doi:10.1016/j.expneurol.2008.04.043.
193. Hagelberg N, Jääskeläinen SK, Martikainen IK, Mansikka H, Forssell H, Scheinin H, Hietala J, Pertovaara A. Striatal dopamine D2 receptors in modulation of pain in humans: a review. *Eur J Pharmacol*. 2004;500(1):187-192. doi:10.1016/j.ejphar.2004.07.024.
194. Ansah OB, Leite-Almeida H, Wei H, Pertovaara A. Striatal dopamine D2 receptors attenuate neuropathic hypersensitivity in the rat. *Exp Neurol*. 2007;205(2):536-546. doi:10.1016/j.expneurol.2007.03.010.
195. Pertovaara A, Wei H. Dual influence of the striatum on neuropathic hypersensitivity. *PAIN®*. 2008;137(1):50-59. doi:10.1016/j.pain.2007.08.009.
196. Baliki MN, Chialvo DR, Geha PY, Levy RM, Harden RN, Parrish TB, Apkarian AV. Chronic Pain and the Emotional Brain: Specific Brain Activity Associated with Spontaneous Fluctuations of Intensity of Chronic Back Pain. *J Neurosci*. 2006;26(47):12165-12173. doi:10.1523/JNEUROSCI.3576-06.2006.
197. Park SI, Oh JH, Hwang YS, Kim SJ, Chang JW. Electrical stimulation of the anterior cingulate cortex in a rat neuropathic pain model. In: Chang JW, Katayama Y, Yamamoto T, eds. *Advances in Functional and Reparative Neurosurgery*. Acta Neurochirurgica Supplementum. Vienna: Springer Vienna; 2006:65-71. doi:10.1007/978-3-211-35205-2_13.
198. Tan W, Yao W-L, Zhang B, Hu R, Wan L, Zhang C-H, Zhu C. Neuronal loss in anterior cingulate cortex in spared nerve injury model of neuropathic pain. *Neurochem Int*. 2018;118:127-133. doi:10.1016/j.neuint.2018.06.003.
199. Kuzumaki N, Narita M, Narita M, Hareyama N, Niikura K, Nagumo Y, Nozaki H, Amano T, Suzuki T. Chronic pain-induced astrocyte activation in the cingulate cortex with no change in neural or glial differentiation from neural stem cells in mice. *Neurosci Lett*. 2007;415(1):22-27. doi:10.1016/j.neulet.2006.12.057.
200. Coffield JA, Bowen KK, Miletic V. Retrograde tracing of projections between the nucleus submedius, the ventrolateral orbital cortex, and the midbrain in the rat. *J Comp Neurol*. 1992;321(3):488-499. doi:10.1002/cne.903210314.
201. Xie Y, Huo F, Tang J. Cerebral cortex modulation of pain. *Acta Pharmacol Sin*. 2009;30(1):31-41. doi:10.1038/aps.2008.14.

202. Grachev ID, Fredrickson BE, Apkarian AV. Brain chemistry reflects dual states of pain and anxiety in chronic low back pain. *J Neural Transm.* 2002;109(10):1309-1334. doi:10.1007/s00702-002-0722-7.
203. Baliki M, Al-Amin HA, Atweh S, Jaber M, Hawwa N, Jabbur SJ, Apkarian AV, Saadé NE. Attenuation of neuropathic manifestations by local block of the activities of the ventrolateral orbito-frontal area in the rat. *Neuroscience.* 2003;120(4):1093-1104. doi:10.1016/S0306-4522(03)00408-1.
204. Xie YF, Wang J, Huo FQ, Jia H, Tang JS. μ but not δ and κ opioid receptor involvement in ventrolateral orbital cortex opioid-evoked antinociception in formalin test rats. *Neuroscience.* 2004;126(3):717-726. doi:10.1016/j.neuroscience.2004.04.013.
205. Fuccio C, Luongo C, Capodanno P, Giordano C, Scafuro MA, Siniscalco D, Lettieri B, Rossi F, Maione S, Berrino L. A single subcutaneous injection of ozone prevents allodynia and decreases the over-expression of pro-inflammatory caspases in the orbito-frontal cortex of neuropathic mice. *Eur J Pharmacol.* 2009;603(1):42-49. doi:10.1016/j.ejphar.2008.11.060.
206. Jasmin L, Granato A, Ohara PT. Rostral agranular insular cortex and pain areas of the central nervous system: A tract-tracing study in the rat. *J Comp Neurol.* 2004;468(3):425-440. doi:10.1002/cne.10978.
207. Derbyshire SWG, Jones AKP, Creed F, Starz T, Meltzer CC, Townsend DW, Peterson AM, Firestone L. Cerebral Responses to Noxious Thermal Stimulation in Chronic Low Back Pain Patients and Normal Controls. *NeuroImage.* 2002;16(1):158-168. doi:10.1006/nimg.2002.1066.
208. Coffeenl U, Ortega-Legaspil JM, López-Muñozl FJ, Simón-Arceol K, Jaimesl O, Pellicerl F. Insular cortex lesion diminishes neuropathic and inflammatory pain-like behaviours. *Eur J Pain.* 2011;15(2):132-138. doi:10.1016/j.ejpain.2010.06.007.
209. Baumgärtner U, Buchholz H-G, Bellosevich A, Magerl W, Siessmeier T, Rolke R, Höhnemann S, Piel M, Rösch F, Wester H-J, Henriksen G, Stoeter P, Bartenstein P, Treede R-D, Schreckenberger M. High opiate receptor binding potential in the human lateral pain system. *NeuroImage.* 2006;30(3):692-699. doi:10.1016/j.neuroimage.2005.10.033.
210. Burkey AR, Carstens E, Wenniger JJ, Tang J, Jasmin L. An Opioidergic Cortical Antinociception Triggering Site in the Agranular Insular Cortex of the Rat that Contributes to Morphine Antinociception. *J Neurosci.* 1996;16(20):6612-6623. doi:10.1523/JNEUROSCI.16-20-06612.1996.
211. Jasmin L, Rabkin SD, Granato A, Boudah A, Ohara PT. Analgesia and hyperalgesia from GABA-mediated modulation of the cerebral cortex. *Nature.* 2003;424(6946):316-320. doi:10.1038/nature01808.
212. Burkey AR, Carstens E, Jasmin L. Dopamine Reuptake Inhibition in the Rostral Agranular Insular Cortex Produces Antinociception. *J Neurosci.* 1999;19(10):4169-4179. doi:10.1523/JNEUROSCI.19-10-04169.1999.

213. Sowards TV, Sowards M. Separate, parallel sensory and hedonic pathways in the mammalian somatosensory system. *Brain Res Bull.* 2002;58(3):243-260. doi:10.1016/S0361-9230(02)00783-9.
214. Talbot JD, Marrett S, Evans AC, Meyer E, Bushnell MC, Duncan GH. Multiple representations of pain in human cerebral cortex. *Science.* 1991;251(4999):1355-1358. doi:10.1126/science.2003220.
215. Kuroda R, Kawao N, Yoshimura H, Umeda W, Takemura M, Shigenaga Y, Kawabata A. Secondary somatosensory cortex stimulation facilitates the antinociceptive effect of the NO synthase inhibitor through suppression of spinal nociceptive neurons in the rat. *Brain Res.* 2001;903(1):110-116. doi:10.1016/S0006-8993(01)02446-5.
216. Wrigley PJ, Press SR, Gustin SM, Macefield VG, Gandevia SC, Cousins MJ, Middleton JW, Henderson LA, Siddall PJ. Neuropathic pain and primary somatosensory cortex reorganization following spinal cord injury. *PAIN®.* 2009;141(1):52-59. doi:10.1016/j.pain.2008.10.007.
217. Neto FL, Schadrack J, Platzer S, Zieglgänsberger W, Tölle TR, Castro-Lopes JM. Up-regulation of metabotropic glutamate receptor 3 mRNA expression in the cerebral cortex of monoarthritic rats. *J Neurosci Res.* 2001;63(4):356-367. doi:10.1002/1097-4547(20010215)63:4<356::AID-JNR1030>3.0.CO;2-3.
218. Kanda T. Biology of the blood–nerve barrier and its alteration in immune mediated neuropathies. *J Neurol Neurosurg Psychiatry.* 2013;84(2):208-212. doi:10.1136/jnnp-2012-302312.
219. Olsson Y. Studies on vascular permeability in peripheral nerves. *Acta Neuropathol (Berl).* 1966;7(1):1-15. doi:10.1007/BF00686605.
220. Seitz RJ, Reiners K, Himmelmann F, Heininger K, Hartung H-P, Toyka KV. The blood–nerve barrier in Wallerian degeneration: A sequential long-term study. *Muscle Nerve.* 1989;12(8):627-635. doi:10.1002/mus.880120803.
221. Hirakawa H, Okajima S, Nagaoka T, Takamatsu T, Oyamada M. Loss and recovery of the blood–nerve barrier in the rat sciatic nerve after crush injury are associated with expression of intercellular junctional proteins. *Exp Cell Res.* 2003;284(2):194-208. doi:10.1016/S0014-4827(02)00035-6.
222. Omura K, Ohbayashi M, Sano M, Omura T, Hasegawa T, Nagano A. The recovery of blood–nerve barrier in crush nerve injury—a quantitative analysis utilizing immunohistochemistry. *Brain Res.* 2004;1001(1):13-21. doi:10.1016/j.brainres.2003.10.067.
223. Anzil AP, Blinzinger K, Herrlinger H. Fenestrated blood capillaries in rat cranio-spinal sensory ganglia. *Cell Tissue Res.* 1976;167(4):563-567.
224. Jimenez-Andrade JM, Herrera MB, Ghilardi JR, Vardanyan M, Melemedjian OK, Mantyh PW. Vascularization of the dorsal root ganglia and peripheral nerve of the mouse: Implications for chemical-induced peripheral sensory neuropathies. *Mol Pain.* 2008;4(1):10. doi:10.1186/1744-8069-4-10.

225. Hirakawa H, Okajima S, Nagaoka T, Kubo T, Takamatsu T, Oyamada M. Regional differences in blood-nerve barrier function and tight-junction protein expression within the rat dorsal root ganglion. *Neuroreport*. 2004;15(3):405-408. doi:10.1097/01.wnr.0000115812.26073.2a.
226. Jacobs JM, Macfarlane RM, Cavanagh JB. Vascular leakage in the dorsal root ganglia of the rat, studied with horseradish peroxidase. *J Neurol Sci*. 1976;29(1):95-107. doi:10.1016/0022-510X(76)90083-6.
227. Abram SE, Yi J, Fuchs A, Hogan QH. Permeability of injured and intact peripheral nerves and dorsal root ganglia. *Anesthesiology*. 2006;105(1):146-153.
228. Kubicek L, Kopacik R, Klusakova I, Dubovy P. Alterations in the vascular architecture of the dorsal root ganglia in a rat neuropathic pain model. *Ann Anat-Anat Anz*. 2010;192(2):101-106. doi:10.1016/j.aanat.2010.01.005.
229. McCabe JS, Low FN. The subarachnoid angle: An area of transition in peripheral nerve. *Anat Rec*. 1969;164(1):15-33. doi:10.1002/ar.1091640102.
230. Ohtani T, Taguchi T, Oda H, Shinoda K, Itoh Y, Toh S, Kawai S, Takahashi M. The Fine Structure of the Subarachnoid Angle in the Spinal Nerve Roots. *Orthop Traumatol*. 1990;39(2):586-589. doi:10.5035/nishiseisai.39.586.
231. Reina MA, Villanueva MC, Machés F, Carrera A, López A, De Andrés JA. The Ultrastructure of the Human Spinal Nerve Root Cuff in the Lumbar Spine: *Anesth Analg*. 2008;106(1):339-344. doi:10.1213/01.ane.0000295803.31074.dc.
232. Shanthaveerappa TR, Bourne GH. The 'perineural epithelium', a metabolically active, continuous, protoplasmic cell barrier surrounding peripheral nerve fasciculi. *J Anat*. 1962;96(Pt 4):527-537.
233. Engelhardt B, Sorokin L. The blood-brain and the blood-cerebrospinal fluid barriers: function and dysfunction. *Semin Immunopathol*. 2009;31(4):497-511. doi:10.1007/s00281-009-0177-0.
234. Sixt M, Engelhardt B, Pausch F, Hallmann R, Wendler O, Sorokin LM. Endothelial cell laminin isoforms, laminins 8 and 10, play decisive roles in T cell recruitment across the blood-brain barrier in experimental autoimmune encephalomyelitis. *J Cell Biol*. 2001;153(5):933-946.
235. Wolburg H, Lippoldt A. Tight junctions of the blood-brain barrier: development, composition and regulation. *Vascul Pharmacol*. 2002;38(6):323-337. doi:10.1016/S1537-1891(02)00200-8.
236. Balda MS, Whitney JA, Flores C, González S, Cerejido M, Matter K. Functional dissociation of paracellular permeability and transepithelial electrical resistance and disruption of the apical-basolateral intramembrane diffusion barrier by expression of a mutant tight junction membrane protein. *J Cell Biol*. 1996;134(4):1031-1049.
237. Luissint A-C, Artus C, Glacial F, Ganeshamoorthy K, Couraud P-O. Tight junctions at the blood brain barrier: physiological architecture and disease-associated dysregulation. *Fluids Barriers CNS*. 2012;9:23. doi:10.1186/2045-8118-9-23.

238. Wong V, Gumbiner BM. A synthetic peptide corresponding to the extracellular domain of occludin perturbs the tight junction permeability barrier. *J Cell Biol.* 1997;136(2):399-409.
239. Wolburg H, Wolburg-Buchholz K, Kraus J, Rascher-Eggstein G, Liebner S, Hamm S, Duffner F, Grote E-H, Risau W, Engelhardt B. Localization of claudin-3 in tight junctions of the blood-brain barrier is selectively lost during experimental autoimmune encephalomyelitis and human glioblastoma multiforme. *Acta Neuropathol (Berl).* 2003;105(6):586-592. doi:10.1007/s00401-003-0688-z.
240. Morita K, Sasaki H, Furuse M, Tsukita S. Endothelial claudin: claudin-5/TMVCF constitutes tight junction strands in endothelial cells. *J Cell Biol.* 1999;147(1):185-194.
241. Pfeiffer F, Schäfer J, Lyck R, Makrides V, Brunner S, Schaeren-Wiemers N, Deutsch U, Engelhardt B. Claudin-1 induced sealing of blood–brain barrier tight junctions ameliorates chronic experimental autoimmune encephalomyelitis. *Acta Neuropathol (Berl).* 2011;122(5):601. doi:10.1007/s00401-011-0883-2.
242. Beggs S, Liu XJ, Kwan C, Salter MW. Peripheral nerve injury and TRPV1-expressing primary afferent C-fibers cause opening of the blood-brain barrier. *Mol Pain.* 2010;6:74. doi:10.1186/1744-8069-6-74.
243. Winkler EA, Sengillo JD, Bell RD, Wang J, Zlokovic BV. Blood–Spinal Cord Barrier Pericyte Reductions Contribute to Increased Capillary Permeability. *J Cereb Blood Flow Metab.* 2012;32(10):1841-1852. doi:10.1038/jcbfm.2012.113.
244. Sauer R-S, Kirchner J, Yang S, Hu L, Leinders M, Sommer C, Brack A, Rittner HL. Blood-spinal cord barrier breakdown and pericyte deficiency in peripheral neuropathy. *Ann N Y Acad Sci.* 2017;1405(1):71-88. doi:10.1111/nyas.13436.
245. Abbott NJ. Inflammatory mediators and modulation of blood-brain barrier permeability. *Cell Mol Neurobiol.* 2000;20(2):131-147.
246. Abbott NJ, Rönnbäck L, Hansson E. Astrocyte–endothelial interactions at the blood–brain barrier. *Nat Rev Neurosci.* 2006;7(1):41-53. doi:10.1038/nrn1824.
247. Strazielle N, Ghersi-Egea JF. Choroid plexus in the central nervous system: biology and physiopathology. *J Neuropathol Exp Neurol.* 2000;59(7):561-574.
248. Wolburg H, Paulus W. Choroid plexus: biology and pathology. *Acta Neuropathol (Berl).* 2009;119(1):75-88. doi:10.1007/s00401-009-0627-8.
249. Sarin H. Physiologic upper limits of pore size of different blood capillary types and another perspective on the dual pore theory of microvascular permeability. *J Angiogenesis Res.* 2010;2:14. doi:10.1186/2040-2384-2-14.
250. Matyszak MK, Lawson LJ, Perry VH, Gordon S. Stromal macrophages of the choroid plexus situated at an interface between the brain and peripheral immune system constitutively express major histocompatibility class II antigens. *J Neuroimmunol.* 1992;40(2-3):173-181.

251. McMenamin PG, Wealthall RJ, Deverall M, Cooper SJ, Griffin B. Macrophages and dendritic cells in the rat meninges and choroid plexus: three-dimensional localisation by environmental scanning electron microscopy and confocal microscopy. *Cell Tissue Res.* 2003;313(3):259-269. doi:10.1007/s00441-003-0779-0.
252. Carpenter SJ, McCarthy LE, Borison HL. Electron microscopic study of the epiplexus (Kolmer) cells of the cat choroid plexus. *Z Für Zellforsch Mikrosk Anat Vienna Austria* 1948. 1970;110(4):471-486.
253. Hosoya Y, Fujita T. Scanning Electron Microscope Observation of Intraventricular Macrophages (Kolmer Cells) in the Rat Brain. *Arch Histol Jpn.* 1973;35(2):133-140. doi:10.1679/aohc1950.35.133.
254. Shechter R, Miller O, Yovel G, Rosenzweig N, London A, Ruckh J, Kim K-W, Klein E, Kalchenko V, Bendel P, Lira SA, Jung S, Schwartz M. Recruitment of Beneficial M2 Macrophages to Injured Spinal Cord Is Orchestrated by Remote Brain Choroid Plexus. *Immunity.* 2013;38(3):555-569. doi:10.1016/j.immuni.2013.02.012.
255. Strazielle N, Creidy R, Malcus C, Boucraut J, Ghersi-Egea J-F. T-Lymphocytes Traffic into the Brain across the Blood-CSF Barrier: Evidence Using a Reconstituted Choroid Plexus Epithelium. *PLOS ONE.* 2016;11(3):e0150945. doi:10.1371/journal.pone.0150945.
256. Meeker RB, Williams K, Killebrew DA, Hudson LC. Cell trafficking through the choroid plexus. *Cell Adhes Migr.* 2012;6(5):390-396. doi:10.4161/cam.21054.
257. Lazarevic I, Engelhardt B. Modeling immune functions of the mouse blood–cerebrospinal fluid barrier in vitro: primary rather than immortalized mouse choroid plexus epithelial cells are suited to study immune cell migration across this brain barrier. *Fluids Barriers CNS.* 2016;13:2. doi:10.1186/s12987-016-0027-0.
258. Redzic Z. Molecular biology of the blood-brain and the blood-cerebrospinal fluid barriers: similarities and differences. *Fluids Barriers CNS.* 2011;8(1):3. doi:10.1186/2045-8118-8-3.
259. van Deurs B, Koehler JK. Tight junctions in the choroid plexus epithelium. A freeze-fracture study including complementary replicas. *J Cell Biol.* 1979;80(3):662-673.
260. Kratzer I, Vasiljevic A, Rey C, Fevre-Montange M, Saunders N, Strazielle N, Ghersi-Egea J-F. Complexity and developmental changes in the expression pattern of claudins at the blood-CSF barrier. *Histochem Cell Biol.* 2012;138(6):861-879. doi:10.1007/s00418-012-1001-9.
261. Furuse M, Hirase T, Itoh M, Nagafuchi A, Yonemura S, Tsukita S, Tsukita S. Occludin: a novel integral membrane protein localizing at tight junctions. *J Cell Biol.* 1993;123(6 Pt 2):1777-1788.
262. Wolburg H, Wolburg-Buchholz K, Liebner S, Engelhardt B. Claudin-1, claudin-2 and claudin-11 are present in tight junctions of choroid plexus epithelium of the mouse. *Neurosci Lett.* 2001;307(2):77-80.

263. Lippoldt A, Liebner S, Andbjør B, Kalbacher H, Wolburg H, Haller H, Fuxe K. Organization of choroid plexus epithelial and endothelial cell tight junctions and regulation of claudin-1, -2 and -5 expression by protein kinase C. *Neuroreport*. 2000;11(7):1427-1431.
264. Stevenson BR, Siliciano JD, Mooseker MS, Goodenough DA. Identification of ZO-1: a high molecular weight polypeptide associated with the tight junction (zonula occludens) in a variety of epithelia. *J Cell Biol*. 1986;103(3):755-766.
265. Anderson JM, Stevenson BR, Jesaitis LA, Goodenough DA, Mooseker MS. Characterization of ZO-1, a protein component of the tight junction from mouse liver and Madin-Darby canine kidney cells. *J Cell Biol*. 1988;106(4):1141-1149. doi:10.1083/jcb.106.4.1141.
266. Jesaitis LA, Goodenough DA. Molecular characterization and tissue distribution of ZO-2, a tight junction protein homologous to ZO-1 and the Drosophila discs-large tumor suppressor protein. *J Cell Biol*. 1994;124(6):949-961.
267. Gumbiner B, Lowenkopf T, Apatira D. Identification of a 160-kDa polypeptide that binds to the tight junction protein ZO-1. *Proc Natl Acad Sci U S A*. 1991;88(8):3460-3464.
268. Haskins J, Gu L, Wittchen ES, Hibbard J, Stevenson BR. ZO-3, a novel member of the MAGUK protein family found at the tight junction, interacts with ZO-1 and occludin. *J Cell Biol*. 1998;141(1):199-208.
269. Balda MS, Gonzalez-Mariscal L, Matter K, Cereijido M, Anderson JM. Assembly of the tight junction: the role of diacylglycerol. *J Cell Biol*. 1993;123(2):293-302.
270. González-Mariscal L, Betanzos A, Avila-Flores A. MAGUK proteins: structure and role in the tight junction. *Semin Cell Dev Biol*. 2000;11(4):315-324. doi:10.1006/scdb.2000.0178.
271. Itoh M, Furuse M, Morita K, Kubota K, Saitou M, Tsukita S. Direct Binding of Three Tight Junction-Associated Maguks, Zo-1, Zo-2, and Zo-3, with the CooH Termini of Claudins. *J Cell Biol*. 1999;147(6):1351-1363. doi:10.1083/jcb.147.6.1351.
272. Wolburg H, Paulus W. Choroid plexus: biology and pathology. *Acta Neuropathol (Berl)*. 2009;119(1):75-88. doi:10.1007/s00401-009-0627-8.

12. Collection of articles

(Arranged in order of appearance in text)

- A. Dubový P, Hradilová-Svíženská I, Klusáková I, Kokošová V, Brázda V, Joukal M. Bilateral activation of STAT3 by phosphorylation at the tyrosine-705 (Y705) and serine-727 (S727) positions and its nuclear translocation in primary sensory neurons following unilateral sciatic nerve injury. *Histochem Cell Biol.* 2018;1-11; doi:10.1007/s00418-018-1656-y
- B. Dubový P, Klusáková I, Hradilová-Svíženská I, Joukal M. Expression of Regeneration-Associated Proteins in Primary Sensory Neurons and Regenerating Axons After Nerve Injury-An Overview. *Anat Rec Hoboken NJ 2007.* 2018; doi:10.1002/ar.23843
- C. Dubový P, Klusáková I, Hradilová-Svíženská I, Brázda V, Kohoutková M, Joukal M. A conditioning sciatic nerve lesion triggers a pro-regenerative state in primary sensory neurons also of dorsal root ganglia non-associated with the damaged nerve. *Frontiers in Cellular Neuroscience.* 2019;13. doi:10.3389/fncel.2019.00011
- D. Hernangómez M, Klusáková I, Joukal M, Hradilová-Svíženská I, Guaza C, Dubový P. CD200R1 agonist attenuates glial activation, inflammatory reactions, and hypersensitivity immediately after its intrathecal application in a rat neuropathic pain model. *J Neuroinflammation.* 2016;13:43. doi:10.1186/s12974-016-0508-8
- E. Dubový P, Klusáková I, Hradilová-Svíženská I, Joukal M, Boadas-Vaello P. Activation of Astrocytes and Microglial Cells and CCL2/CCR2 Upregulation in the Dorsolateral and Ventrolateral Nuclei of Periaqueductal Gray and Rostral Ventromedial Medulla Following Different Types of Sciatic Nerve Injury. *Front Cell Neurosci.* 2018;12:40. doi:10.3389/fncel.2018.00040
- F. Joukal M, Klusáková I, Dubový P. Direct communication of the spinal subarachnoid space with the rat dorsal root ganglia. *Ann Anat - Anat Anz.* 2016;205:9-15. doi:10.1016/j.aanat.2016.01.004
- G. Joukal M, Klusáková I, Solár P, Kuklová A, Dubový P. Cellular reactions of the choroid plexus induced by peripheral nerve injury. *Neurosci Lett.* 2016;628:73-77. doi:10.1016/j.neulet.2016.06.019

A. Dubový P, Hradilová-Svíženská I, Klusáková I, Kokošová V, Brázda V, **Joukal M.**
Bilateral activation of STAT3 by phosphorylation at the tyrosine-705 (Y705) and serine-727 (S727) positions and its nuclear translocation in primary sensory neurons following unilateral sciatic nerve injury. *Histochem Cell Biol.* 2018:1-11; doi:10.1007/s00418-018-1656-y

Commentary: In this publication, we demonstrated that sciatic nerve injury induced activation of STAT3 in both lumbar and cervical DRG by phosphorylation at the tyrosine-705 and serine-727. Moreover, we found that STAT3 activation is closely related to IL-6 levels in cerebrospinal fluid. In addition, using IL-6 intrathecal application we showed that IL-6 released into the subarachnoid space can penetrate the DRG and subsequently activate STAT3.

IF (WOS, 2017): 2.164

Quartile (WOS, 2017): Microscopy Q1; Cell Biology Q4

Contribution of the author: Co-authorship. The author participated on performing of in vivo experiments, preparing samples for immunohistochemistry, western blot and writing of the corresponding texts.



Bilateral activation of STAT3 by phosphorylation at the tyrosine-705 (Y705) and serine-727 (S727) positions and its nuclear translocation in primary sensory neurons following unilateral sciatic nerve injury

Petr Dubový¹ · Ivana Hradilová-Svíženská¹ · Ilona Klusáková¹ · Viktoria Kokošová¹ · Václav Brázda¹ · Marek Joukal¹

Accepted: 24 February 2018

© Springer-Verlag GmbH Germany, part of Springer Nature 2018

Abstract

Unilateral sciatic nerve compression (SNC) or complete sciatic nerve transection (CSNT), both varying degrees of nerve injury, induced activation of STAT3 bilaterally in the dorsal root ganglia (DRG) neurons of lumbar (L4–L5) as well as cervical (C6–C8) spinal cord segments. STAT3 activation was by phosphorylation at the tyrosine-705 (Y705) and serine-727 (S727) positions and was followed by their nuclear translocation. This is the first evidence of STAT3(S727) activation together with the well-known activation of STAT3(Y705) in primary sensory neurons upon peripheral nerve injury. Bilateral activation of STAT3 in DRG neurons of spinal segments anatomically both associated as well as non-associated with the injured nerve indicates diffusion of STAT3 activation inducers along the spinal cord. Increased levels of IL-6 protein in the CSF following nerve injury as well as activation and nuclear translocation of STAT3 in DRG after intrathecal injection of IL-6 shows that this cytokine, released into the subarachnoid space can penetrate the DRG to activate STAT3. Previous results on increased bilateral IL-6 synthesis and the present manifestation of STAT3 activation in remote DRG following unilateral sciatic nerve injury may reflect a systemic reaction of the DRG neurons to nerve injury.

Keywords Dorsal root ganglia · Neuroinflammation · Systemic reaction · Peripheral nerve injury

Introduction

Primary sensory neurons with their cell bodies in the dorsal root ganglia (DRG) send off peripheral and central branches of afferent axons that display different responses to neuronal

injury. While injury to peripheral axonal branches results in profound molecular alterations involving activation of transforming factors (Patodia and Raivich 2012), no such changes are induced after intraspinal injury of central branches of afferent axons (Schwaiger et al. 2000).

In response to unilateral sciatic nerve injury, protein and mRNA levels of IL-6 and its receptors were enhanced bilaterally in primary sensory neurons not only in DRG of lumbar segments (L4–L5) associated with the injury, but also in cervical segments (C7–C8) not associated with the injured nerve (Dubovy et al. 2013; Brazda et al. 2013). Upon binding to its specific membrane-bound receptor (IL-6R), IL-6 brings together the intracellular regions of gp130 to initiate a signal transduction cascade via activation of signal transducer and activator of transcription 3 (STAT3) (Aaronson and Horvath 2002; Eulenfeld et al. 2012). Activation of STAT3 is by JAK2-dependent phosphorylation at the tyrosine-705 (Y705), and JAK2-independent phosphorylation mediated by mitogen-activated protein kinases (MAPKs) at the serine-727 (S727) position (Aaronson and Horvath 2002). Activation of STAT3 by phosphorylation at the Y705 position occurs in DRG neurons very early after a nerve

✉ Petr Dubový
pdubovy@med.muni.cz

Ivana Hradilová-Svíženská
isvizen@med.muni.cz

Ilona Klusáková
iklusak@med.muni.cz

Viktoria Kokošová
435583@mail.muni.cz

Václav Brázda
vabdna@gmail.com

Marek Joukal
mjoukal@med.muni.cz

¹ Department of Anatomy, Cellular and Molecular Research Group, Faculty of Medicine, Masaryk University, Kamenice 3, Brno 62500, Czech Republic

lesion and is mediated by neurotrophic cytokines including IL-6 (Miao et al. 2006; Schwaiger et al. 2000; Sheu et al. 2000; Qiu et al. 2005) and neurotrophins (Pellegrino and Habecker 2013; Ng et al. 2006b). Phosphorylated STAT3 dimers translocate to the nucleus and initiate transcription of target genes (Taga 1996; Eulendorf et al. 2012).

Activated STAT3 is a molecular mediator of IL-6 signaling, but it is not yet known if STAT3 is also activated bilaterally in both lumbar and cervical DRG neurons after unilateral sciatic nerve injury. Thus far, only activation of STAT3 by phosphorylation at the Y705 position has been detected in DRG neurons associated with injured nerve (Schwaiger et al. 2000; Sheu et al. 2000; Qiu et al. 2005). The goal of our present experiments was, therefore, to investigate activation of STAT3 by monitoring phosphorylation at both the Y705 and the S727 positions in DRG neurons associated and not associated with unilateral sciatic nerve injury. To explore if the IL-6 produced and released by lumbar DRG affected by sciatic nerve injury can induce activation of STAT3 in cervical DRG through cerebrospinal fluid of the subarachnoid space, we analyzed activation and nuclear translocation of STAT3(Y705) and STAT3(S727) in DRG after intrathecal IL-6 delivery.

Materials and methods

Animals and surgical treatment

The experiments were performed in 32 adult male rats (Wistar, 250–280 g, Anlab, Brno, Czech Republic) housed in 12 h light/dark cycles at a temperature of 22–24 °C under specific pathogen-free conditions in the animal housing facility of Masaryk University. Sterilized standard rodent food and water were available ad libitum. All experimental procedures were carried out under sterile conditions by the same person according to protocols approved by the Animal Investigation Committee of the Faculty of Medicine, Brno, Czech Republic. All surgical procedures were performed under anesthesia using a mixture of ketamine (40 mg/ml) and xylazine (4 mg/ml) administered intraperitoneally (0.2 ml/100 g body weight).

The right sciatic nerve was exposed in the mid-thigh, ligated using 2 ligatures and cut with a pair of sharp scissors (complete sciatic nerve transection, CSNT, $n=8$). The proximal nerve stump was buried and fixed in muscles to shield the distal stump from reinnervation. Alternatively, a longitudinally slit 2-mm silicone tube of 1 mm internal diameter was placed around the right sciatic nerve of rats to reduce nerve diameter (sciatic nerve constriction, SNC, $n=8$) (Schmid et al. 2013). The tube was tied in place with a sterile thread and closed to prevent the tube from opening. The muscles and skin were closed with 5/0 sutures. The

right sciatic nerve of sham-operated rats ($n=8$) was carefully exposed without any lesion. All operated and sham-operated rats were left to survive for 7 days. Eight other rats without any surgical treatment were used as naive control.

Quantitative immunohistochemical analysis

Naïve, sham-, SNC- and CSNT-operated rats ($n=4$ for each group) were deeply anesthetized with a lethal dose of sodium pentobarbital (70 mg/kg body weight, i.p.) and perfused transcardially with 500 ml phosphate-buffered saline (PBS, 10 mM sodium phosphate buffer, pH 7.4, containing 0.15 M NaCl) followed by 500 ml of Zamboni's fixative (Zamboni and Demartin 1967). The L4-L5 and C6-C8 DRG from both sides were detected within their intervertebral foramina following total laminectomy and foraminotomy. The DRG were removed, immersed separately in Zamboni's fixative at 4 °C overnight, and then divided into samples of ipsilateral (L-DRGi) and contralateral (L-DRGc) lumbar DRG as well as ipsilateral (C-DRGi) and contralateral (C-DRGc) cervical DRG separately for each group of rats (naïve, sham-, SNC-, and CSNT-operated). The DRG samples were washed in 20% phosphate-buffered sucrose for 12 h, blocked in Tissue-Tek® OCT compound (Miles, Elkhart, IN) and cut to prepare serial longitudinal cryostat sections (12 µm). The DRG sections were mounted on chrome-alum covered slides and processed for indirect immunohistochemical staining.

Briefly, DRG sections of lumbar and cervical segments of naïve, sham-, SNC- and CSNT-operated rats were immunostained simultaneously under the same conditions. Sections were washed with PBS containing 0.05% Tween 20 (PBS-T) and 1% bovine serum albumin (BSA) for 10 min, treated with 5% normal donkey serum in PBS-T for 30 min, then incubated with 25 µl of rabbit polyclonal antibody against STAT3(Y705) (1:100; Santa Cruz, USA) or rabbit polyclonal antibody against STAT3(S727) (1:200; Abcam, USA) in a humid chamber at room temperature (21–23 °C) for 12 h. The immunohistochemical reaction was visualized using TRITC-conjugated and affinity-purified donkey anti-rabbit secondary antibody (1:100; Millipore, USA) for 90 min at room temperature. The control sections were incubated either without the primary STAT3(Y705) or STAT3(S727) antibodies or by substituting the primary antibodies with the donkey IgG isotype. The sections were stained with Hoechst 33,342 to detect cell nuclei, mounted in aqueous mounting medium (Vectashield; Vector Laboratories, USA) and analyzed using an epifluorescence microscope (Nikon Eclipse) equipped with a Nikon DS-Ri1 camera (Nikon, Prague, Czech Republic) and a stabilized power supply for the lamp housing.

The STAT3(Y705) and STAT3(S727) immunofluorescence intensities in the nuclei of DRG neurons were measured using the NIS-Elements image analysis system (Nikon,

Czech Republic) according to our previously published protocols (Dubovy et al. 2002, 2013). At least 200 nuclei of DRG neuronal profiles were measured for each animal group. The immunofluorescence intensities were expressed as mean intensities \pm SD.

Double immunostaining

A portion of the sections was incubated with a mixture (1:1) of rabbit STAT3(Y705) polyclonal antibody (1:100; Santa Cruz, USA) and mouse monoclonal antibody against ATF3 (1:100; Santa Cruz, USA) as a marker of axotomized neurons (Tsujino et al. 2000). Another portion of DRG sections was incubated with mouse monoclonal (1:150, Acris, USA) or rabbit polyclonal antibody (1:200; Abcam, USA) against STAT3(S727) and rabbit monoclonal anti-Rab7 antibody (1:100, Cell Signaling Technology, The Netherlands) or mouse monoclonal anti-EEA antibody (1:50, Santa Cruz, USA) to detect STAT3(S727) in late or early endosomes, respectively.

A mixture (1:1) of affinity purified TRITC-conjugated donkey anti-rabbit and FITC-conjugated donkey anti-mouse secondary antibodies (1:100; Millipore) was applied at room temperature for 90 min. Control sections were incubated without individual primary antibodies.

Western blot analysis

To validate the STAT3(Y705) and STAT3(S727) levels in DRG neurons obtained by quantitative immunohistochemical analysis, protein levels were analyzed by Western blot. In addition, total non-phosphorylated STAT3 protein was quantified. The naïve rats, sham-, SNC- and CSNT-operated rats ($n=6$ for each group) were deeply anesthetized with a lethal dose of sodium pentobarbital (70 mg/kg body weight, i.p.) and DRG of both sides were removed under aseptic conditions, washed in protease and phosphatase inhibitor cocktails (both Roche, Germany), fast frozen in liquid nitrogen and stored at -80°C until analyzed further. The DRG of lumbar (L4-L5) and cervical (C6-C8) segments were separated into samples of ipsilateral (L-DRGi) and contralateral (L-DRGc) lumbar DRG as well as ipsilateral (C-DRGi) and contralateral (C-DRGc) cervical DRG for each group of rats (naïve, sham-, SNC- and CSNT-operated). The DRG samples were homogenized in PBS containing 0.1% Triton X-100 and cocktails of protease and phosphatase inhibitors (Roche, Germany) and centrifuged at 10,000 g for 5 min at 4°C . Proteins were separated by SDS-polyacrylamide gel electrophoresis (Brazda et al. 2006) and transferred to nitrocellulose membranes by electroblotting (BioRad). Blots were blocked using 1% BSA in PBST (3.2 mM Na_2HPO_4 , 0.5 mM KH_2PO_4 , 1.3 mM KCl, 135 mM NaCl, 0.05% Tween 20, pH 7.4) for 1 h and incubated with rabbit polyclonal antibody

against STAT3(Y705) (1:100; Santa Cruz, USA), rabbit polyclonal antibody against STAT3(S727) (1:200; Abcam, USA) or mouse monoclonal antibody against STAT3 (1:1000; Cell Signaling, UK) overnight. After washing in PBST, blots were incubated with peroxidase-conjugated anti-rabbit or anti-mouse IgG (1:1000; Sigma, USA) at room temperature for 1 h. Protein bands were visualized using the ECL detection kit (Amersham, USA) on the chemiluminescence reader LAS-3000 (Fuji, Japan) and analyzed using image densitometry software. The levels of proteins were normalized to the value of naïve lumbar and cervical DRG which were arbitrarily set to one.

Quantitative assay of IL-6 protein in the cerebrospinal fluid

Naïve rats and those subjected to SNC or sham-operation for 7 days ($n=6$ for each group) were sacrificed by CO_2 inhalation. Samples of the cerebrospinal fluid (CSF) were obtained by puncture of the cisterna magna and collected into tubes and stored at -80°C until analysis; care was taken to avoid blood contamination. The total protein concentration was measured by Nanodrop ND-1000 (Thermo Scientific) and the level of IL-6 protein was assessed by Quantibody® Rat Inflammation Array 1 (RayBiotech, GA, USA) according to the manufacturer's instructions. Each sample collected from the individual groups of animals was measured in quadruplicate and the data were expressed as mean \pm SEM of IL-6 protein (pg per ml of CSF or per μg of total protein).

Intrathecal IL-6 administration

Rats were anesthetized using a mixture of ketamine (40 mg/ml) and xylazine (4 mg/ml) administered intraperitoneally (0.2 ml/100 g body weight). IL-6 protein (R&D Systems) was dissolved in artificial cerebrospinal fluid (ACSF; Hylden and Wilcox 1980) at 20 ng/10 μl concentration. Solution of IL-6 (10 μl) or ACSF (10 μl) with a further 10 μl ACSF was injected via a micro syringe into the subarachnoid space of the cisterna magna (cervical, $n=4$) or between L2-L3 vertebrae (lumbar, $n=4$). Animals were sacrificed in CO_2 and perfused transcardially with Zamboni's fixative solution (Zamboni and Demartin.C 1967). Lumbar (L4-L5) and cervical (C6-C8) DRG were removed following laminectomy and foraminotomy, immersed in the Zamboni's fixative overnight and longitudinal cryostat sections (12 μm) were prepared. Activation and nuclear translocation of STAT3(Y705) and STAT3(S727) were detected and evaluated using image analysis of immunofluorescence staining.

Statistical analyses

The Mann–Whitney U test was used to assess statistical differences in the data of immunofluorescence intensities and western blot analysis between naïve DRG neurons and DRG neurons of sham-operated rats or DRG neurons after sciatic nerve injury. Statistical significance was considered to be indicated by a P value of <0.05 . All statistical analyses were performed using STATISTICA 9.0 software (StatSoft, Inc., USA).

Results

Lumbar and cervical DRG neurons from naïve rats displayed very low intensity of STAT3(Y705) immunofluorescence in both nuclei and the cytoplasm (Fig. 1a). The neuronal nuclei of both lumbar and cervical segments revealed a significant increase in STAT3(Y705) intensity after sham-operation compared to naïve rats (Fig. 1b; Table 1). In comparison to DRG from naïve and sham-operated rats, a marked intensity of STAT3(Y705) immunofluorescence was induced bilaterally in the nuclei of lumbar and cervical DRG neurons after both SNC and CSNT (Fig. 1c–j; Table 1). In addition, the cytoplasm of some small- and medium-sized DRG neurons showed a diffuse immunofluorescence after both types of sciatic nerve injury (Fig. 1c–j). A moderate STAT3(Y705) immunofluorescence was induced in the satellite glial cells surrounding mainly large-sized neurons as was described previously (Dubovy et al. 2010). We observed STAT3(Y705) immunostaining also in the plasma membrane of large- and medium-sized DRG neurons and their satellite glial cells (Figs. 1c, d, i, j, 5c, d).

The nuclei of DRG neurons of both lumbar and cervical segments removed from naïve and sham-operated rats displayed a moderate intensity of STAT3(S727) immunofluorescence with significantly higher levels in the neuronal nuclei of DRG from sham-operated rats (Fig. 2a, b; Table 2). The intensity of STAT3(S727) immunofluorescence was significantly increased in neuronal nuclei 7 days after both SNC and CSNT in comparison to sham-operated controls (Fig. 2c–j; Table 2). In contrast to STAT3(Y705) immunostaining results, the nuclei of DRG neurons of both lumbar and cervical segments displayed a higher intensity of STAT3(S727) immunofluorescence in the ipsilateral than contralateral side after CSNT, while the bilateral intensity of immunostaining following SNC was similar in the neuronal nuclei (Table 2).

No apparent difference in the pattern of nuclear immunostaining for STAT3(Y705) and STAT3(S727) was observed between DRG of lumbar and cervical segments in reaction to SNC and CSNT, even though only a part of the neurons (about 20%) of ipsilateral lumbar DRG were

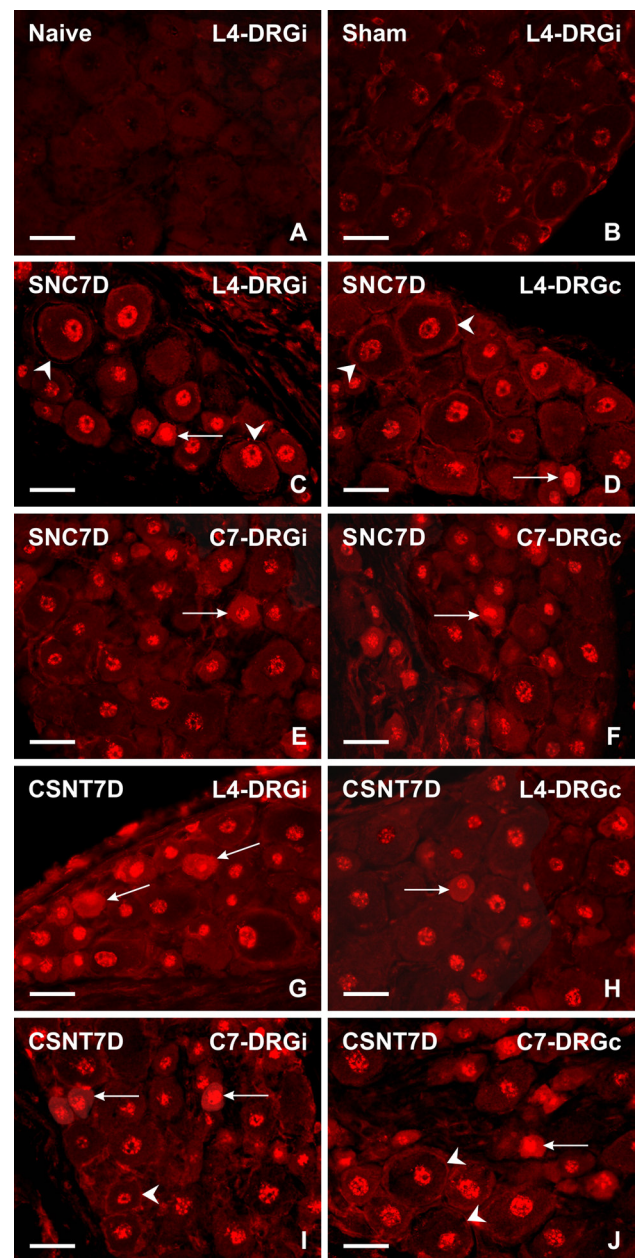


Fig. 1 Representative pictures of cryostat sections through the dorsal root ganglia (DRG) from naïve (Naïve), sham-operated (Sham) rats and rats with unilateral sciatic nerve compression (SNC) or complete sciatic nerve transection (CSNT) for 7 days. The sections of ipsilateral and contralateral DRG of the L4 spinal segment (L4-DRGi, L4-DRGc) as well as ipsilateral and contralateral DRG of the C7 spinal segment (C7-DRGi, C7-DRGc) were incubated under the same conditions with rabbit polyclonal antibody recognizing STAT3 phosphorylated in the Y705 position. In contrast to DRG of naïve and sham-operated rat (a, b), bilateral activation and nuclear translocation of STAT3Y705 was detected in the neurons of both L4- and C7-DRG 7 days after unilateral SNC or CSNT (c–j). Along with immunostained nuclei, a diffuse immunofluorescence was found in the cytoplasm of medium- and small-sized neuronal bodies (long arrows). In addition, STAT3(Y705) immunostaining was observed in the plasma membrane of large- and medium-sized DRG neurons and their satellite glial cells (arrowheads, c, d, i, j). Scale bars: 50 μ m

Table 1 Results of STAT3(Y705) immunofluorescence intensity measured in the neuronal nuclei of lumbar (L-DRG) and cervical (C-DRG) dorsal root ganglia of naïve rats (Naïve), ipsilateral (i) and contralateral (c) to sham-operation (Sham) and sciatic nerve compression (SNC) or complete sciatic nerve transection (CSNT) for 7 days ($n=6$ for each group)

	L-DRGi	L-DRGc	C-DRGi	C-DRGc
SNC	27.1 ± 6.0 ^{*a}	33.3 ± 3.9 ^{*a}	24.6 ± 7.3 ^{*a}	25.2 ± 6.1 ^{*a}
CSNT	22.5 ± 4.0 ^{*a}	29.5 ± 5.8 ^{*ab}	25.2 ± 4.1 ^{*a}	28.7 ± 4.3 ^{*a}
Sham	12.5 ± 2.6 ^a	12.7 ± 1.3 ^a	13.2 ± 2.6 ^a	13.9 ± 2.1 ^a
Naïve	7.6 ± 1.3		8.7 ± 1.7	

^aSignificant difference ($p < 0.05$) compared to Naïve

^bSignificant difference ($p < 0.05$) compared to the ipsilateral side

*Significant difference ($p < 0.05$) compared to Sham

simultaneously immunopositive for ATF3 - a marker of axon injury following SNC (Fig. 3a, b).

Besides nuclear translocation of STAT3(S727), the immunoreaction corresponding to the activated form of STAT3 was observed in vesicular structures in the cytoplasm of DRG neurons of both lumbar and cervical segments after SNC and CSNT (Fig. 2). Double immunostaining with mouse monoclonal STAT3(S727) and rabbit monoclonal Rab7 antibodies revealed activated STAT3 (phosphorylated at the S727 position) in late endosomes (Fig. 3c–e). However, no double immunofluorescence was observed when the DRG sections were immunostained simultaneously with STAT3(S727) antibody and antibody against the early endosomal antigen EEA (data not shown).

To verify the results of bilateral STAT3 activation in DRG neurons of both lumbar and cervical segments after unilateral sciatic nerve injury, STAT3(Y705) and STAT3(S727) protein levels were analyzed by Western blot. STAT3(Y705) protein levels were increased bilaterally in both lumbar and cervical DRG 7 days after unilateral SNC and CSNT when compared with controls from naïve or sham-operated rats. Only SNC induced a significantly higher STAT3(Y705) protein level in the ipsilateral rather than contralateral lumbar DRG, while cervical DRG of the same animals as well as both lumbar and cervical DRG after CSNT revealed bilaterally similar protein levels (Fig. 4a).

Protein levels of STAT3(S727) were also significantly increased in cervical and lumbar DRG of both sides after SNC and CSNT in comparison to controls from naïve or sham-operated rats. In contrast to differences between ipsilateral and contralateral lumbar and cervical DRG after CSNT in STAT3(S727) as measured by image analysis, no differences in whole STAT3(S727) protein levels were found by Western blot analysis (Fig. 4b).

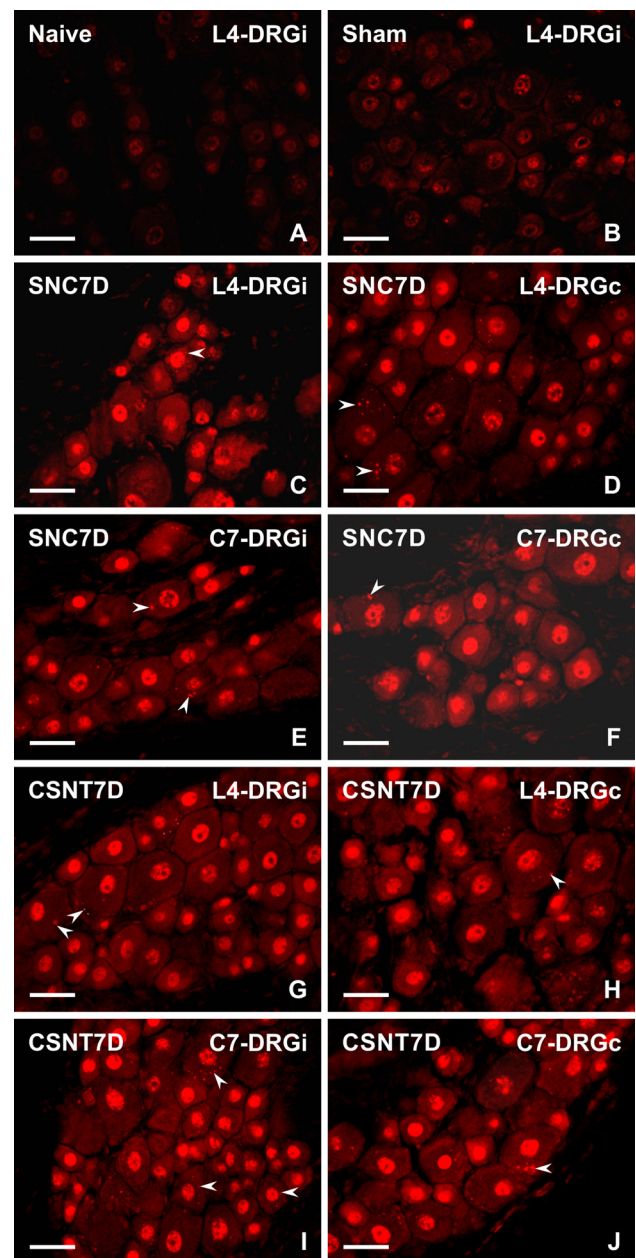


Fig. 2 Representative pictures of cryostat sections through the dorsal root ganglia (DRG) showing immunofluorescence staining of activated STAT3 by phosphorylation in the S727 position and its nuclear translocation. The DRG were from naïve (Naïve), sham-operated (Sham) rats and rats with unilateral sciatic nerve compression (SNC) or complete sciatic nerve transection (CSNT) for 7 days. The sections of ipsilateral and contralateral L4-DRG (L4-DRGi, L4-DRGc) as well as ipsilateral and contralateral C7-DRG (C7-DRGi, C7-DRGc) were incubated under the same conditions with rabbit polyclonal antibody specific to STAT3 phosphorylated at the S727 position. Scale bars: 50 μ m

Table 2 Results of STAT3(S727) immunofluorescence intensity measured in the neuronal nuclei of lumbar (L-DRG) and cervical (C-DRG) dorsal root ganglia of naïve rats (Naïve), ipsilateral (i) and contralateral (c) to sham-operation (Sham) and sciatic nerve compression (SNC) or complete sciatic nerve transection (CSNT) for 7 days ($n=6$ for each group)

	L-DRGi	L-DRGc	C-DRGi	C-DRGc
SNC	19.2±2.9* ^a	22.5±4.2* ^a	19.7±3.5* ^a	18.8±3.2* ^a
CSNT	18.1±2.3* ^{ab}	15.9±2.0* ^a	19.6±3.1* ^{ab}	16.4±1.7* ^a
Sham	13.5±1.6 ^a	13.7±2.8 ^a	15.2±1.8 ^a	14.6±2.0 ^a
Naïve	11.8±1.5		11.7±1.7	

^aSignificant difference ($p < 0.05$) compared to Naïve

^bSignificant difference ($p < 0.05$) compared to the contralateral side

*Significant difference ($p < 0.05$) compared to Sham

In contrast to STAT3(Y705) or STAT3(S727), protein levels of total STAT3 recognized by antibody against non-phosphorylated domains did not change in any DRG of naïve, sham-, SNC- or CSNT-operated rats (Fig. 4c).

IL-6 protein in the cerebrospinal fluid

The levels of IL-6 protein in CSF of naïve and sham-operated rats were undetectable with the method used, but IL-6 protein was increased to 450.8 ± 142.3 or 4331.8 ± 132.3 pg/ μ g total protein in rats with unilateral sciatic nerve injury.

Effect of intrathecal IL-6 injection on STAT3 activation and nuclear translocation in DRG neurons

Activation of STAT3 is implicated in the IL-6 signaling pathway. We, therefore, tested the nuclear translocation of activated STAT3 in the DRG neurons of both lumbar and cervical segments following intrathecal injection of IL-6. In comparison to ACSF injection (Fig. 5a, b, e, f), intrathecal application of IL-6 resulted in increased immunostaining for STAT3(Y705) (Fig. 5c, d) and STAT3(S727) (Fig. 5g, h) in neuronal DRG nuclei of both lumbar and cervical segments. These results demonstrate the activation and nuclear translocation of STAT3 by IL-6 diffusing from the CSF in the subarachnoid space along the spinal cord into DRG. No significant differences were observed in nuclear translocation of

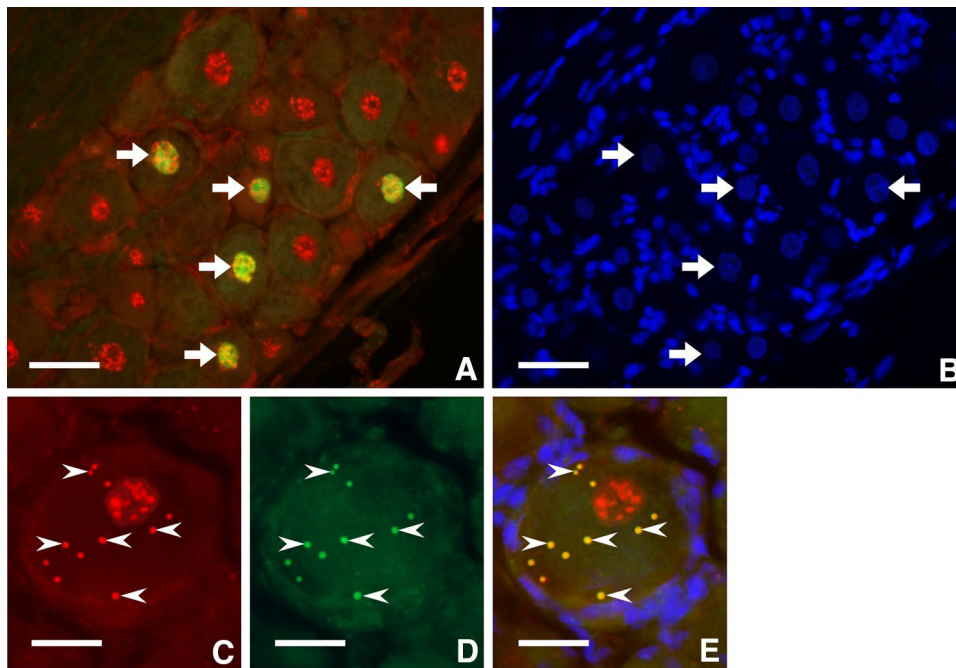


Fig. 3 **a, b** A cryostat section through the L4-DRG ipsilateral to SNC after double immunostaining for STAT3(Y705) (red) and ATF3 (green). Merged red and green immunofluorescence (**a**) indicates that only a portion of the neuronal nuclei displayed both STAT3(Y705) and ATF3 immunostaining (arrows) while rest are labeled only by STAT3(Y705) immunofluorescence and they did not express ATF3 as a marker of axon injury. The nuclei of the same section were stained with Hoechst (**b**). **c–e** A cryostat section through the L4-DRG neu-

ron ipsilateral to SNC for 7 days following double immunostaining for detection of STAT3(S727) by mouse monoclonal antibody (red, **c**) and Rab7 by rabbit monoclonal antibody (green, **d**) with Hoechst staining of nuclei (blue). Merged immunofluorescence (**e**) indicates that STAT3(S727) is localized in late endosomes (arrowheads) besides the neuronal nucleus. Scale bars: 50 μ m for **a, b** 20 μ m for **c–e**

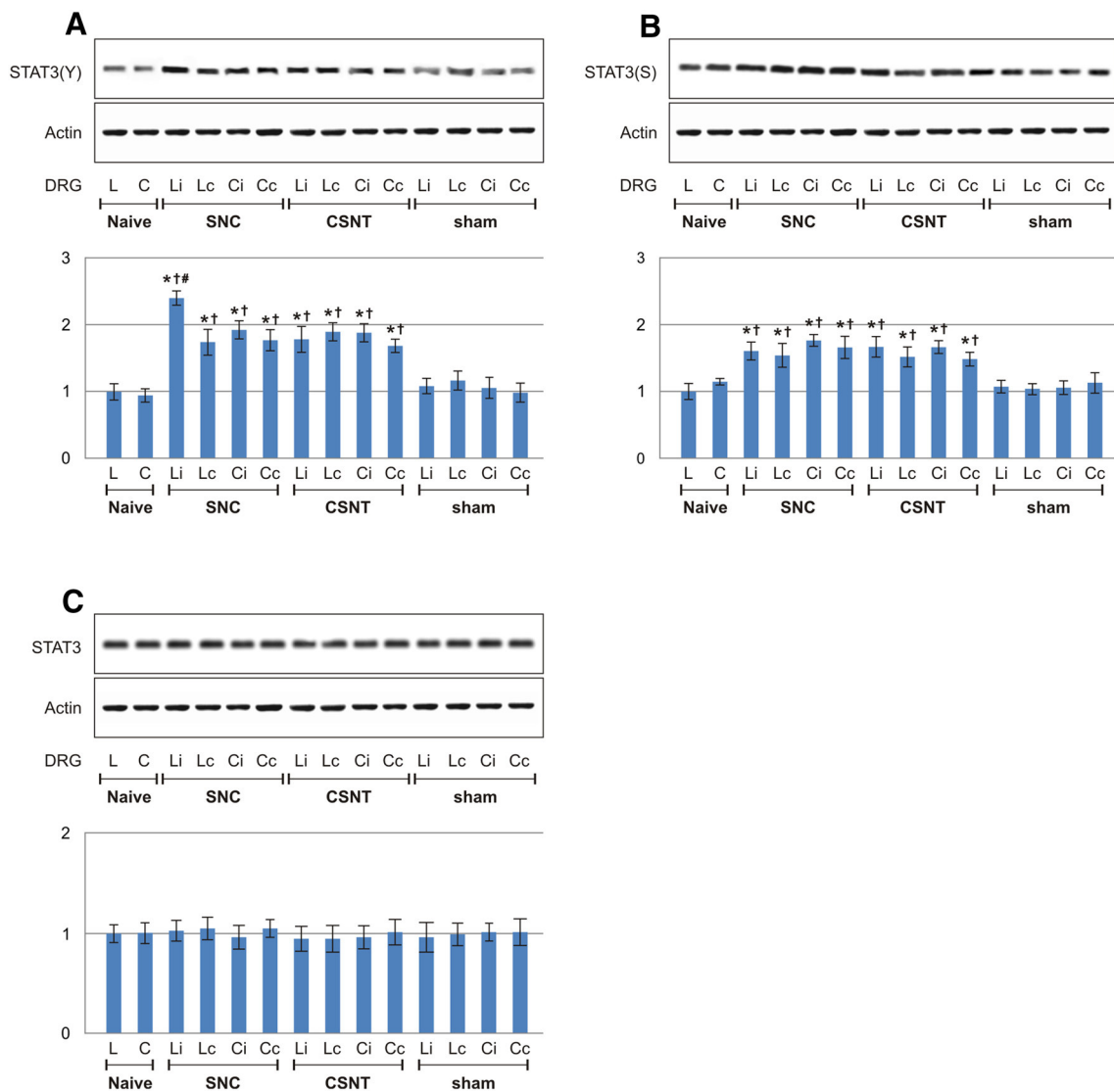


Fig. 4 Results of Western blot analysis of STAT3Y (a), STAT3S (b) and STAT3 (c) protein levels in DRG of L4-L5 (l) and C6-C8 (c) segments removed from ipsilateral (i) and contralateral (c) sides of Naive as well as sham-, SNC- and CSNT-operated rats for 7 days. Upper panels illustrate representative Western blots of DRG from 6

naive rats and 6 rats for each period of survival. Equal loading of proteins was confirmed by actin levels (Actin). Lower panels show densitometry of individual STAT3Y, STAT3S and STAT3 protein bands after normalization to actin; the intensities of the STAT3Y, STAT3S and STAT3 bands from naive DRG were taken as 1

activated STAT3 between IL-6 delivery into CSF of cisterna magna or lumbar spinal cord segments.

Discussion

DRG neurons with the peripheral branches of their afferent axons in the peripheral nerve are frequently used as an in vivo model to study molecular mechanisms of neuronal reaction to injury. Nerve lesion injury of peripheral axonal branches induces upregulation of IL-6 and activation of STAT3 in the corresponding DRG (Dubovy et al. 2013; Miao et al. 2006; Murphy et al. 1999a).

We showed earlier that unilateral sciatic nerve injury can induce increased levels of IL-6 protein and mRNA bilaterally not only in DRG neurons associated with L4-L5 spinal cord segments but also in remote DRG of cervical segments (Dubovy et al. 2013). A similar bilateral increase of IL6R protein and mRNA was detected in DRG after SNC (Brazda et al. 2013). Therefore, a similar pattern of STAT3 activation was expected following unilateral SNC or CSNT.

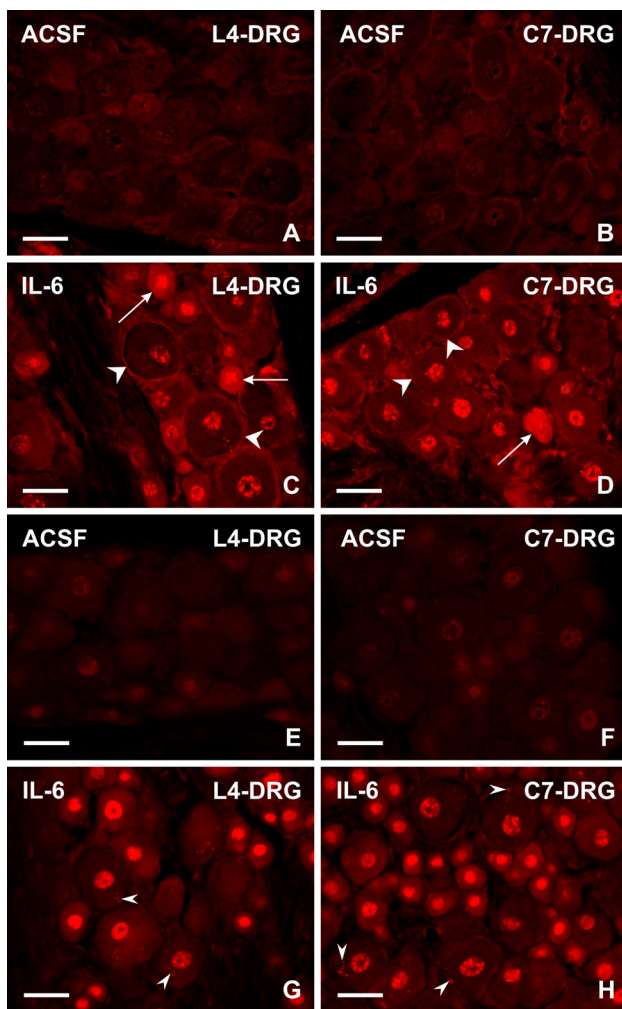


Fig. 5 Representative pictures of cryostat sections through the dorsal root ganglia (DRG) of L4 and C7 spinal segments from rats treated with intrathecal injection of artificial cerebrospinal fluid (**a, b, e, f**) or IL-6 (**c, d, g, h**) for 1 day. The cryostat sections were immunostained with rabbit polyclonal antibody recognizing STAT3 activated by phosphorylation at the Y705 (A-D) or S727 (E-H) positions. In contrast to sections through DRG of animals treated with artificial cerebrospinal fluid (ACSF), intrathecal IL-6 injection induced a strong increase of STAT3(Y705) and STAT3(S727) immunofluorescence in neuronal nuclei. Similarly to the DRG after SNC and CSNT, STAT3(S727) immunostaining was present also in vesicular structures of neurons (arrowheads) besides nuclear staining. The plasma membrane localization of STAT3(Y705) immunostaining was obvious in DRG neurons and their satellite glial cells after intrathecal injection of IL-6 (arrowheads, **c, d**). Scale bars: 50 μ m

Activation and translocation of STAT3Y705 and STAT3S727 in DRG after nerve injury

STAT3 has two conserved amino-acid residues (Y705 and S727), which are phosphorylated during STAT3 activation (Heinrich et al. 2003). Thus far, activation of STAT3 was detected only at the Y705 position in DRG neurons ipsilateral to peripheral nerve injury (Qiu et al. 2005; Wu et al.

2007; Bareyre et al. 2011). We present here, for the first time, activation of STAT3 also at the S727 position with the subsequent nuclear translocation in DRG neurons after two types of sciatic nerve injury. The coincident activation of STAT3 in the Y705 and S727 positions after two types of sciatic nerve injury in the DRG neurons was shown by immunohistochemical staining and Western blot analysis. Total STAT3 protein levels remained unaffected when compared to naïve, sham-, SNC- and CSNT-operated animals. The results suggest that the functional effect of STAT3 is elicited through post-translational modification and/or translocation, cytoplasmic translation and nuclear transcription (Nicolas et al. 2012; Haghikia et al. 2014).

Activation of STAT3 by phosphorylation at both the Y705 and S727 positions was also detected in motor neurons in vivo (Schwaiger et al. 2000) and PC12 line cells and sympathetic neurons in vitro (Pellegrino and Habecker 2013; Ng et al. 2006a). In contrast to STAT3(Y705) translocated into the nuclei of PC12 line cells, STAT3(S727) was found in axons and their growth cones (Ng et al. 2006a). Similarly, STAT3(S727) was detected in the axons and their growth cones of sympathetic neurons, and in their nuclei - which was not the case for PC12 line cells (Pellegrino and Habecker 2013).

As was expected, the STAT3(Y705) immunostaining was found predominantly in the neuronal nuclei of DRG indicating nuclear translocation of STAT3 activated in the Y705 position after sciatic nerve injury or intrathecal IL-6 injection. In addition, diffuse STAT3(Y705) immunofluorescence was present in the cytoplasm of some DRG neurons. STAT3(Y705) immunostaining was found also in the plasma membrane of some DRG neurons and their satellite glial cells—mainly after intrathecal injection of IL-6. Activated STAT3 has been reported to affect cell adhesion (Silver et al. 2004; Shah et al. 2006; Hombria and Sotillos 2008) and the plasma-membrane location of STAT3(Y705) in DRG is likely associated with the mutual contact of neurons and their satellite glial cells. Nevertheless, the precise functional involvement of membrane distribution of activated STAT3 in the DRG requires further experimental evidence. Besides neuronal nuclei, STAT3(S727) vesicular immunofluorescence was also found after both types of sciatic nerve injury and intrathecal IL-6 injection. Double immunostaining revealed that at least a part of vesicular immunoreactivity for STAT3 phosphorylated in the S727 position is present in late endosomes which also contain MAPKs (German et al. 2011). Thus, our immunohistochemical results showing different intracellular locations of STAT3 phosphorylated at the Y705 and S727 positions are consistent with a model of cytoplasmic and endocytic regulation of IL-6-induced STAT3 activation (Shah et al. 2006; German et al. 2011).

Functional involvement of STAT3(S727) is not completely clear until now. Activated STAT3 phosphorylated

at the S727 position may facilitate interaction with the transcriptional co-activators CBP and P300, maximizing the transcriptional activity of STAT3(Y705) (Schuringa et al. 2001). In addition, phosphorylation of the S727 position may modulate the duration of STAT3 transcriptional activity by promoting dephosphorylation of STAT3(Y705) (Wakahara et al. 2012). However, STAT3(S727) has also been suggested to mediate transcription activation without any detectable STAT3 phosphorylated at the Y705 position (Decker and Kovarik 2000). However, maximal sympathetic axon outgrowth requires phosphorylation of STAT3 at both positions (Pellegrino and Habecker 2013).

Activation of STAT3 in lumbar and cervical DRG following unilateral sciatic nerve injury and its possible functional involvement

The bilateral activation of STAT3 at both the Y705 and S727 positions and their nuclear translocation were detected in DRG neurons of both lumbar and cervical segments following unilateral SNC or CSNT. Double immunostaining for STAT3(Y705) and ATF3 in sections through lumbar DRG ipsilateral to SNC showed STAT3 activation also in the DRG neurons without any axonal injury. Moreover, activation and nuclear translocation of activated STAT3 in lumbar DRG neurons contralateral to nerve injury as well as in cervical segments of both sides, i.e., in DRG neurons without anatomical relation to the injured nerve, suggests the diffusion of signal molecules into DRG along the spinal cord. The cytokine IL-6 is a candidate signal molecule for spreading neuroinflammation after nervous system injury (Erta et al. 2012) and its increased synthesis was detected in the associated DRG but also in DRG not associated with the injured nerve (Dubovy et al. 2013). Although the expression of IL-6 in DRG associated with injured sciatic nerve correlated well with the duration of hypersensitivity (Murphy et al. 1999b), the possible involvement of increased IL-6 levels in remote DRG neurons in the induction or maintenance of neuropathic pain has not yet been demonstrated. The results seem to reflect rather a general neuroinflammatory reaction of DRG along the neural axis (Dubovy et al. 2013).

What is still unclear is the mechanism for the activation of STAT3 in DRG neurons not associated with unilateral peripheral nerve injury. We have detected a robust penetration of dextran molecules of molecular weight similar to IL-6 from CSF of the spinal subarachnoid space into DRG (Joukal et al. 2016). Intrathecal injection of IL-6 with subsequent activation of STAT3 presented here suggested that IL-6 in the CSF of perispinal subarachnoid space is a possible mediator of STAT3 activation in DRG neurons not associated with the injured nerve. If there is no barrier between DRG and the CSF of subarachnoid space, a nerve injury-induced increase of IL-6 in the corresponding

DRG can release IL-6 molecules into the subarachnoid space and their transport via CSF into remote DRG can activate STAT3 in their neurons. This is supported by the observation of increased IL-6 protein levels in CSF of rats with sciatic nerve injury. Moreover, STAT3 activated primarily by nerve injury-induced IL-6 may trigger further synthesis and release of IL-6 through the amplified feedback loop detected in various cell models (Murakami and Hirano 2012).

A further possible mechanism for the bilateral regulation of the IL-6/STAT3 pathway in both lumbar and cervical DRG neurons after unilateral sciatic nerve injury is suggested by published results from exosomes containing microRNAs (miRNAs) released after nerve injury. Various miRNAs were significantly increased in DRG neurons and released by exosomes after peripheral nerve injury (Wu et al. 2011; Hori et al. 2016; Chang et al. 2017). Notably, miR-21 was gradually increased in DRG in an IL-6-dependent manner and significantly increased in exosomes extracted from the blood of nerve-ligated mice (Hori et al. 2016). Moreover, it was demonstrated that miR-21 expression is strictly upregulated via an IL-6/STAT3 pathway (Loffler et al. 2007) and miRNAs may regulate transcription of STAT target genes (Pencik et al. 2016). However, any direct functional relationship between miR-21 and activated STAT3 in DRG neurons after nerve injury remains unconfirmed.

In conclusion, we detected STAT3 activation by phosphorylation at the Y705 and S727 positions in both lumbar and cervical DRG neurons after unilateral sciatic nerve injury of various types. We showed that IL-6 from the CSF in the perispinal subarachnoid space can mediate STAT3 activation in remote DRG neurons. These results indicate a systemic reaction of DRG neurons alongside the spinal cord induced by unilateral spinal nerve injury.

Acknowledgements We thank Ms. Dana Kutějová, Ms. Jitka Mikulášková, Ms. Marta Lněničková, Mgr. Jana Vachová and Mr. Lumír Trenčanský for their skillful technical assistance. Supported by grant 16-08508S of The Czech Science Foundation.

Compliance with ethical standards

Conflict of interest The authors declare that they have no competing interests.

References

- Aaronson DS, Horvath CM (2002) A road map for those who don't know JAK-STAT. *Science* 296:1653–1655. <https://doi.org/10.1126/science.1071545>
- Bareyre FM, Garzorz N, Lang C, Misgeld T, Buning H, Kerschensteiner M (2011) In vivo imaging reveals a phase-specific role of STAT3 during central and peripheral nervous system axon regeneration. *Proc Natl Acad Sci USA* 108:6282–6287. <https://doi.org/10.1073/pnas.1015239108>

- Brazda V, Muller P, Brozkova K, Vojtesek B (2006) Restoring wild-type conformation and DNA-binding activity of mutant p53 is insufficient for restoration of transcriptional activity. *Biochem Biophys Res Comm* 351:499–506. <https://doi.org/10.1016/j.bbrc.2006.10.065>
- Brazda V, Klusakova I, Svizenska IH, Dubovy P (2013) Dynamic response to peripheral nerve injury detected by in situ hybridization of IL-6 and its receptor mRNAs in the dorsal root ganglia is not strictly correlated with signs of neuropathic pain. *Mol Pain* <https://doi.org/10.1186/1744-8069-9-42>
- Chang HL, Wang HC, Chunag YT, Chou CW, Lin IL, Lai CS, Chang LL, Cheng KI (2017) miRNA expression change in dorsal root ganglia after peripheral nerve injury. *J Mol Neurosci* 61:169–177. <https://doi.org/10.1007/s12031-016-0876-7>
- Decker T, Kovarik P (2000) Serine phosphorylation of STATs. *Oncogene* 19:2628–2637. <https://doi.org/10.1038/sj.onc.1203481>
- Dubovy P, Klusakova I, Svizenska I (2002) A quantitative immunohistochemical study of the endoneurium in the rat dorsal and ventral spinal roots. *Histochem Cell Biol* 117:473–480. <https://doi.org/10.1007/200418-002-0411-5>
- Dubovy P, Klusakova I, Svizenska I, Brazda V (2010) Satellite glial cells express IL-6 and corresponding signal-transducing receptors in the dorsal root ganglia of rat neuropathic pain model. *Neuron Glia Biol* 6:73–83. <https://doi.org/10.1017/s1740925x10000074>
- Dubovy P, Brazda V, Klusakova I, Hradilova-Svizenska I (2013) Bilateral elevation of interleukin-6 protein and mRNA in both lumbar and cervical dorsal root ganglia following unilateral chronic compression injury of the sciatic nerve. *J Neuroinflamm* <https://doi.org/10.1186/1742-2094-10-55>
- Erta M, Quintana A, Hidalgo J (2012) Interleukin-6, a major cytokine in the central nervous system. *Int J Biol Sci* 8:1254–1266. <https://doi.org/10.7150/ijbs.4679>
- Eulenfeld R, Dittrich A, Khouri C, Muller PJ, Mutze B, Wolf A, Schaper F (2012) Interleukin-6 signalling: More than Jaks and STATs. *Eur J Cell Biol* 91:486–495. <https://doi.org/10.1016/j.ejcb.2011.09.010>
- German CL, Sauer BM, Howe CL (2011) The STAT3 beacon: IL-6 recurrently activates STAT 3 from endosomal structures. *Exp Cell Res* 317:1955–1969. <https://doi.org/10.1016/j.yexcr.2011.05.009>
- Haghikia A, Ricke-Hoch M, Stapel B, Gorst I, Hilfiker-Kleiner D (2014) STAT3, a key regulator of cell-to-cell communication in the heart. *Cardiovasc Res* 102:281–289. <https://doi.org/10.1093/cvr/cvu034>
- Heinrich PC, Behrmann I, Haan S, Hermanns HM, Muller-Newen G, Schaper F (2003) Principles of interleukin (IL)-6-type cytokine signalling and its regulation. *Biochem J* 374:1–20. <https://doi.org/10.1042/bj20020407>
- Hombria JCG, Sotillos S (2008) Disclosing JAK/STAT links to cell adhesion and cell polarity. *Semin Cell Dev Biol* 19:370–378. <https://doi.org/10.1016/j.semcdb.2008.06.002>
- Hori N, Narita M, Yamashita A, Horiuchi H, Hamada Y, Kondo T, Watanabe M, Igarashi K, Kawata M, Shibasaki M, Yamazaki M, Kuzumaki N, Inada E, Ochiya T, Iseki M, Mori T (2016) Changes in the expression of IL-6-mediated microRNAs in the dorsal root ganglion under neuropathic pain in mice. *Synapse* 70:317–324. <https://doi.org/10.1002/syn.21902>
- Hylden JLK, Wilcox GL (1980) Intrathecal morphine in mice—a new technique. *Eur J Pharmacol* 67:313–316. [https://doi.org/10.1016/0014-2999\(80\)90515-4](https://doi.org/10.1016/0014-2999(80)90515-4)
- Joukal M, Klusakova I, Dubovy P (2016) Direct communication of the spinal subarachnoid space with the rat dorsal root ganglia. *Ann Anat* 205:9–15. <https://doi.org/10.1016/j.aanat.2016.01.004>
- Loffler D, Brocke-Heidrich K, Pfeifer G, Stocsits C, Hacker-muller J, Kretschmar AK, Burger R, Gramatzki M, Blumert C, Bauer K, Cvijic H, Ullmann AK, Stadler PF, Horn F (2007) Interleukin-6-dependent survival of multiple myeloma cells involves the Stat3-mediated induction of microRNA-21 through a highly conserved enhancer. *Blood* 110:1330–1333. <https://doi.org/10.1182/blood-2007-03-081133>
- Miao T, Wu DS, Zhang Y, Bo XN, Subang MC, Wang P, Richardson PM (2006) Suppressor of cytokine signaling-3 suppresses the ability of activated signal transducer and activator of transcription-3 to stimulate neurite growth in rat primary sensory neurons. *J Neurosci* 26:9512–9519. <https://doi.org/10.1523/jneurosci.2160-06.2006>
- Murakami M, Hirano T (2012) The pathological and physiological roles of IL-6 amplifier activation. *Int J Biol Sci* 8:1267–1280. <https://doi.org/10.7150/ijbs.4828>
- Murphy PG, Borthwick LS, Johnston RS, Kuchel G, Richardson PM (1999a) Nature of the retrograde signal from injured nerves that induces interleukin-6 mRNA in neurons. *J Neurosci* 19:3791–3800
- Murphy PG, Ramer MS, Borthwick L, Gaudie J, Richardson PM, Bisby MA (1999b) Endogenous interleukin-6 contributes to hypersensitivity to cutaneous stimuli and changes in neuropeptides associated with chronic nerve constriction in mice. *Eur J Neurosci* 11:2243–2253. <https://doi.org/10.1046/j.1460-9568.1999.00641.x>
- Ng DCH, Lin BH, Lim CP, Huang GC, Zhang T, Poli V, Cao XM (2006a) Stat3 regulates microtubules by antagonizing the depolymerization activity of stathmin. *J Cell Biol* 172:245–257. <https://doi.org/10.1083/jcb.200503021>
- Ng YP, Cheung ZH, Ip NY (2006b) STAT3 as a downstream mediator of Trk signaling and functions. *J Biol Chem* 281:15636–15644. <https://doi.org/10.1074/jbc.M601863200>
- Nicolas CS, Peineau S, Amici M, Csaba Z, Fafouri A, Javalet C, Collet VJ, Hildebrandt L, Seaton G, Choi SL, Sim SE, Bradley C, Lee K, Zhuo M, Kaang BK, Gressens P, Dournaud P, Fitzjohn SM, Bortolotto ZA, Cho K, Collingridge GL (2012) The JAK/STAT pathway is involved in synaptic plasticity. *Neuron* 73:374–390. <https://doi.org/10.1016/j.neuron.2011.11.024>
- Patodia S, Raivich G (2012) Role of transcription factors in peripheral nerve regeneration. *Front Mol Neurosci*. <https://doi.org/10.3389/fnmol.2012.00008>
- Pellegrino MJ, Habecker BA (2013) STAT3 integrates cytokine and neurotrophin signals to promote sympathetic axon regeneration. *Mol Cell Neurosci* 56:272–282. <https://doi.org/10.1016/j.mcn.2013.06.005>
- Pencik J, Pham HTT, Schmoellerl J, Javaheri T, Schleder M, Culig Z, Merkel O, Moriggl R, Grebjen F, Kenner L (2016) JAK-STAT signaling in cancer: from cytokines to non-coding genome. *Cytokine* 87:26–36. <https://doi.org/10.1016/j.cyto.2016.06.017>
- Qiu J, Cafferty WBJ, McMahon SB, Thompson SWN (2005) Conditioning injury-induced spinal axon regeneration requires signal transducer and activator of transcription 3 activation. *J Neurosci* 25:1645–1653. <https://doi.org/10.1523/jneurosci.3269-04.2005>
- Schmid AB, Coppieters MW, Ruitenber MJ, McLachlan EM (2013) Local and remote immune-mediated inflammation after mild peripheral nerve compression in rats. *J Neuropath Exp Neurol* 72:662–680. <https://doi.org/10.1097/NEN.0b013e318298de5b>
- Schuringa JJ, Schepers H, Vellenga E, Kruijer W (2001) Ser727-dependent transcriptional activation by association of p300 with STAT3 upon IL-6 stimulation. *FEBS Lett* 495:71–76. [https://doi.org/10.1016/s0014-5793\(01\)02354-7](https://doi.org/10.1016/s0014-5793(01)02354-7)
- Schwaiger FW, Hager G, Schmitt AB, Horvat A, Streif R, Spitzer C, Gamal S, Breuer S, Brook GA, Nacimiento W, Kreutzberg GW (2000) Peripheral but not central axotomy induces changes in Janus kinases (JAK) and signal transducers and activators of transcription (STAT). *Eur J Neurosci* 12:1165–1176. <https://doi.org/10.1046/j.1460-9568.2000.00005.x>
- Shah M, Patel K, Mukhopadhyay S, Xu F, Guo G, Sehgal PB (2006) Membrane-associated STAT3 and PY-STAT3 in the cytoplasm.

- J Biol Chem 281:7302–7308. <https://doi.org/10.1074/jbc.M508527200>
- Sheu JY, Kulhanek DJ, Eckenstein FP (2000) Differential patterns of ERK and STAT3 phosphorylation after sciatic nerve transection in the rat. *Exp Neurol* 166:392–402. <https://doi.org/10.1006/exnr.2000.7508>
- Silver DL, Naora H, Liu JS, Cheng WJ, Montell DJ (2004) Activated signal transducer and activator of transcription (STAT) 3: Localization in focal adhesions and function in ovarian cancer cell motility. *Cancer Res* 64:3550–3558. <https://doi.org/10.1158/0008-5472.can-03-3959>
- Taga T (1996) gp130, a shared signal transducing receptor component for hematopoietic and neurotrophic cytokines. *J Neurochem* 67:1–10
- Tsujino H, Kondo E, Fukuoka T, Dai Y, Tokunaga A, Miki K, Yone-nobu K, Ochi T, Noguchi K (2000) Activating transcription factor 3 (ATF3) induction by axotomy in sensory and motoneurons: A novel neuronal marker of nerve injury. *Mol Cell Neurosci* 15:170–182. <https://doi.org/10.1006/mcne.1999.0814>
- Wakahara R, Kunimoto H, Tanino K, Kojima H, Inoue A, Shintaku H, Nakajima K (2012) Phospho-Ser727 of STAT3 regulates STAT3 activity by enhancing dephosphorylation of phospho-Tyr705 largely through TC45. *Genes Cells* 17:132–145. <https://doi.org/10.1111/j.1365-2443.2011.01575.x>
- Wu DS, Zhang Y, Bo XN, Huang WL, Xiao F, Zhang XY, Miao TZ, Magoulas C, Subang MC, Richardson PM (2007) Actions of neurotrophic cytokines and cyclic AMP in regenerative conditioning of rat primary sensory neurons. *Exp Neurol* 204:66–76. <https://doi.org/10.1016/j.expneurol.2006.09.017>
- Wu D, Raafat M, Pak E, Hammond S, Murashov AK (2011) Micro-RNA machinery responds to peripheral nerve lesion in an injury-regulated pattern. *Neuroscience* 190:386–397. <https://doi.org/10.1016/j.neuroscience.2011.06.017>
- Zamboni L, Demartin C (1967) Buffered picric acid-formaldehyde—a new rapid fixative for electron microscopy. *J Cell Biol* 35:A148

B. Dubový P, Klusáková I, Hradilová-Svíženská I, **Joukal M.** Expression of Regeneration-Associated Proteins in Primary Sensory Neurons and Regenerating Axons After Nerve Injury-An Overview. *Anat Rec Hoboken NJ 2007*. 2018; doi:10.1002/ar.23843

Commentary: In this publication, we summarized the critical issues of immunohistochemical detection of regeneration associated proteins in primary sensory neurons and axons. The overview was supplemented with our own results of GAP43 and SCG10 immunostaining in DRG after nerve injury.

IF (WOS, 2017): 1.373

Quartile (WOS, 2017): Anatomy and Morphology Q3

Contribution of the author: Co-authorship. The author participated on performing of in vivo experiments, preparing samples for immunohistochemistry and writing of the corresponding texts.



Expression of Regeneration-Associated Proteins in Primary Sensory Neurons and Regenerating Axons After Nerve Injury—An Overview

PETR DUBOVÝ ,* ILONA KLUSÁKOVÁ,
IVANA HRADILOVÁ-SVIŽENSKÁ, AND MAREK JOUKAL

Department of Anatomy, Cellular and Molecular Research Group, Masaryk University,
Brno, Czechia, Czech Republic

ABSTRACT

Peripheral nerve injury results in profound alterations of the affected neurons resulting from the interplay between intrinsic and extrinsic molecular events. Restarting the neuronal regenerative program is an important prerequisite for functional recovery of the injured peripheral nerve. The primary sensory neurons with their cell bodies in the dorsal root ganglia provide a useful *in vivo* and *in vitro* model for studying the mechanisms that regulate intrinsic neuronal regeneration capacity following axotomy. These studies frequently need to indicate the regenerative status of the corresponding neurons. We summarize the critical issues regarding immunohistochemical detection of several regeneration-associated proteins as markers for the initiation of the regeneration program in rat primary sensory neurons and indicators of axon regeneration in the peripheral nerves. This overview also includes our own results of GAP43 and SCG10 expression in different DRG neurons following double immunostaining with molecular markers of neuronal subpopulations (NF200, CGRP, and IB4) as well as transcription factors (ATF3 and activated STAT3) following unilateral sciatic nerve injury. *Anat Rec*, 301:1618–1627, 2018. © 2018 Wiley Periodicals, Inc.

Key words: peripheral nerve; regeneration; degeneration; therapies

Peripheral nerve injury results in profound alterations of metabolism, survival, excitability, and transmitter functions of the affected neurons. These processes result from the interplay between intrinsic and extrinsic molecular events (Fawcett and Keynes, 1990; Doron-Mandel et al., 2015); restarting the regenerative program and the capacity to survive injury are important prerequisites for functional recovery in injured peripheral nerves.

Primary sensory neurons with their cell bodies in the dorsal root ganglia (DRG) provide a useful *in vivo* and *in vitro* model to study the mechanisms regulating intrinsic neuronal regeneration capacity following axotomy. These studies frequently need to indicate the regenerative status of specific neurons using a simple and reliable method. The aim of the present overview is to critically summarize recent knowledge, combined with our own experience,

regarding the immunocytochemical detection of various regeneration-associated proteins to be used as markers labeling the initiation and progress of the regeneration

Grant sponsor: The Czech Science Foundation; Grant number: 16-08508S.

*Correspondence to: Petr Dubový, Professor and Head, Department of Anatomy, Faculty of Medicine, Kamenice 3, CZ-625 00 Brno, Czech Republic. Tel.: (420) 54949-1333 E-mail: pdubovy@med.muni.cz

Received 16 October 2017; Revised 9 November 2017; Accepted 8 December 2017.

DOI 10.1002/ar.23843

Published online 8 May 2018 in Wiley Online Library (wileyonlinelibrary.com).

program in primary sensory neurons as well as indicators of axon regeneration in peripheral nerves.

CLASSIFICATION OF NEURONS IN THE DRG

The DRG contain the bodies of primary sensory neurons that are markedly diverse as to their physiological function in afferent signaling and their reactions to a peripheral nerve injury. The subpopulations of DRG neurons can be classified according their size, cytological, chemical, and physiological properties (Lawson, 2002). Classically, DRG neurons are divided into large-, medium-, and small-sized (Lawson et al., 1974) and may be identified with further molecular phenotyping. The large neurons that send off heavy, myelinated axons also display strong immunostaining for NF200, while medium- and small-sized neurons give off lightly myelinated A δ and unmyelinated C axons, respectively (Lawson, 2002). The medium- and small-sized neurons that express substance-P and calcitonin gene-related peptide (CGRP) are classified as peptidergic, while small neurons free of CGRP but stained with *Griffonia simplicifolia* isolectin B4 (IB4) are denoted as nonpeptidergic nociceptive neurons (Lawson et al., 1993; Hunt and Mantyh, 2001). The IB4+ subpopulation differs from other neurons in expressing the receptor for glial cell line-derived neurotrophic factor (GDNF) rather than other neurotrophins (Molliver et al., 1997). A number of *in vivo* studies of the neuronal regenerative program were based on rat or mouse sciatic nerve injuries where nearly all (98%–99%) sciatic DRG neurons were located in the L4-L5 DRG of rat (Swett et al., 1991) or the L3-L4 DRG of mice (Rigaud et al., 2008).

REGENERATION-ASSOCIATED PROTEINS

Besides extrinsic factors produced by cells distal to the nerve injury, reactivation of a silent regenerative program of DRG neurons is needed for successful axon regeneration. The reactivation of the neuronal regeneration program can be detected by the expression of various regeneration-associated proteins like growth associated protein 43 (GAP43), cortical cytoskeleton associated protein 23 (CAP23), superior cervical ganglion 10 (SCG10), or small proline-rich repeat protein 1A (SPRR1A) that are important intrinsic determinants of the increased regenerative ability of DRG neurons (Bonilla et al., 2002; Mason et al., 2002).

Growth-Associated Protein 43

The prototypical growth-associated protein, GAP43, is a membrane- and cytoskeletal-associated phosphoprotein that is expressed at high levels in neurons during development and is concentrated in the axonal growth cone (Skene and Willard, 1981). Correlation between the expression of GAP43 and axonal growth has led to it being used as a marker for the regenerative state of neurons (Verge et al., 1990). GAP43 regulates the neuronal actin cytoskeleton and is a substrate for protein kinase C (PKC; Larsson, 2006) in promoting axonal growth (Laux et al., 2000). Removal of the distal nerve stump or blocking axonal transport does not alter GAP43 mRNA levels in DRG neurons indicating that molecular

inducers produced by nerve injury are not critical for GAP43 upregulation (Skene, 1989).

The DRG neurons of naïve rats display a low basal level of GAP43 immunostaining (Stewart et al., 1992; Schreyer and Skene, 1993) that is significantly increased mainly in large and medium-sized neurons after sciatic nerve injury (Table 1; Fig. 1A,D). In contrast to large NF200+ and medium sized CGRP+ neurons, small IB4+ neurons indeed did not display GAP43 after experimental nerve injury (Fig. 2). The absence of GAP43 protein in small IB4+ neurons is in accord with *in vitro* experiments that IB4-labeled primary sensory neurons do not express GAP43, and this is related to their impaired intrinsic axonal regeneration capacity (Leclere et al., 2007). Another explanation for these findings is that other proteins or signaling molecules, in addition to GAP43, are required for stimulation of axonal outgrowth. Moreover, axonal regeneration of IB4-labeled neurons can be intrinsically different from that of other classes of DRG neurons where SPRR1A is upregulated after sciatic nerve injury and that is also associated with axonal regeneration (Bonilla et al., 2002). Increased immunostaining for GAP43 can be stimulated over a long period also in DRG neurons that do not or cannot successfully regenerate their injured axons after nerve transection (Woolf et al., 1990). This indicates that the mere presence of GAP43 protein is not sufficient as proof of neuronal regeneration status.

It was found that only GAP43 immunoreactive neurons supported axon regrowth of 7 mm or longer within the first week following dorsal root injury. At later time points, axon regrowth was observed from neurons both with and without GAP43 immunoreactivity. The results suggest that axon regeneration is not absolutely dependent on the presence of GAP43 but rather its expression is correlated with a capacity for rapid outgrowth (Anderson and Schreyer, 1999).

GAP43 is activated by PKC-mediated phosphorylation at serine 41 (S41) that promotes the polymerization and stabilization of filamentous actin (F-actin) related to axon growth and sprouting (Tsai et al., 2007). The phosphorylated form is dephosphorylated by calcineurin, thus blocking F-actin polymerization and stabilization (Lautermilch and Spitzer, 2000). In contrast to immunostaining predominantly of large-sized neurons in naïve DRG by antibodies, recognizing both phosphorylated and unphosphorylated GAP43, an S41-GAP43-specific antibody immunostained mainly medium- and small-sized DRG neurons (Table 1; Fig. 1B). However, a more intense S41-GAP43 immunoreaction was induced by axotomy in all types of DRG neurons (Fig. 1C) indicating that immunostaining with S41-GAP43 antibody is a reliable indicator of the neuronal regeneration program.

Superior Cervical Ganglion 10 Protein

Superior cervical ganglion 10 (SCG10) protein, also known as stathmin 2 (STMN2), is a neuron-specific member of the stathmin family (Sugiura and Mori, 1995) whose members influence microtubule dynamics by promoting microtubule depolymerization (Riederer et al., 1997; Antonsson et al., 1998). Overexpression of SCG10 protein in neurons enhances axon outgrowth under *in vitro* (Riederer et al., 1997) as well as under *in vivo* conditions (Mason et al., 2002).

TABLE 1. Antibodies used for immunostaining of representative sections and summary of their cellular expression in DRG neurons or regenerated axons of the peripheral nerves

Marker	Host	Specificity	Dilution	Supplier	Immunofluorescence staining
GAP43	Mouse ^a	Phosphorylated and dephosphorylated	1:500	Sigma	GAP43 ^c in large and medium sized DRG neurons of the regenerative state, small IB4 ^c neurons are GAP43 ⁻ , GAP43 ^c in regenerated axons and activated Schwann cells
S41-GAP43	Rabbit ^b	Phosphorylated S41-GAP43	1:500	Thermo Fisher	S41-GAP43 ^c in all types of DRG neurons of the regenerative state
ATF3	Rabbit ^b	C-terminal peptide	1:200	Santa Cruz	ATF3 ^c in the nuclei of axotomized DRG neurons
ATF3	Mouse ^a	Internal region of ATF3	1:200	Santa Cruz	ATF3 ^c in the nuclei of axotomized DRG neurons
NF200	Rabbit ^b	Neurofilament H (200kD)	1:200	Sigma	NF200 ^c in large sized DRG neurons with heavy myelinated axons
CGRP	Rabbit ^b	CGRP	1:500	Acris	CGRP ^c in peptidergic subpopulation of medium and small sized DRG neurons
IB4-FITC	–	Isolectin B4	1:50	Vector	IB4 ^c in nonpeptidergic subpopulation of small sized DRG neurons
SCG10	Rabbit ^b	C-terminal peptide	1:1000	LSBio	SCG10 ^c in all types of DRG neurons of the regenerative state, SCG10 ^c in sensory regenerated axons also after a short period of nerve injury
Anti- β III tubulin	Mouse ^a	C-terminal peptide	1:500	Exbio	For double immunostaining with GAP43 or SCG10 to detect regenerated axons
SPRR1A	Rabbit ^b	Internal 40–89 amino acids	1:300	Abcam	SPRR1A ^c in all types of DRG neurons of the regenerative state
STAT3	Rabbit ^b	Phosphorylated at Y705	1:100	Santa Cruz	STAT3 ^c as a marker of regenerative state of DRG neurons

^aMonoclonal antibody.

^bPolyclonal antibody.

^cPositive immunoreaction and ⁻negative immunoreaction.

The binding of primary antibodies was visualized with donkey anti-mouse or anti-rabbit TRITC- or FITC-conjugated secondary antibodies (1:400; Millipore).

Upregulation of SCG10 mRNA could not be detected in ipsilateral axotomized sensory neurons one day after nerve transection, but became apparent only later during the first week after surgery (Voria et al., 2006). This is consistent with the results of Mason et al. (2002) who found increased SCG10 mRNA levels in DRG neurons and spinal motor neurons 3 days after nerve crush, but not at 1 day. In contrast, the intensity of SCG10 immunostaining was significantly increased in most neurons of the rat DRG within 1 day-crushed nerve (Table 1; Fig. 3A,B). This is in agreement with published results in mice (Shin et al., 2014). The discrepancy in the onset of SCG10 expression after nerve injury is probably due to differences in experimental animals, procedure for nerve crush and methods of SCG10 detection. It is important to note that in contrast to GAP43, all DRG neurons with activating transcription factor 3 (ATF3) immunopositive nuclei displayed SCG10 immunostaining 7 days after complete sciatic nerve transection (CSNT; Fig. 3C–E).

Differences of GAP43 and SCG10 as Markers of Neuronal Regenerative Status and Regenerating Axons

It was demonstrated that GAP43, CAP23, and SCG10 are coregulated in axotomized neurons and are correlated with the neuronal ability to regenerate their axons under *in vivo* conditions (Mason et al., 2002). However, other results of *in vivo* experiments also revealed upregulation of GAP43 in the DRG neurons without axotomy suggesting that increased GAP43 may not always be related to activation of the regeneration program of neurons, but is rather a metabolic sign of neuronal potential for plasticity and rapid axon regeneration (Benowitz and Routtenberg, 1997; Andersen and Schreyer, 1999). Moreover, as was mentioned above, injured IB4⁺ nociceptive neurons do not express GAP43 although the neurons displayed other molecules like SCG10 indicating their regenerative status (Bonilla et al., 2002). Double

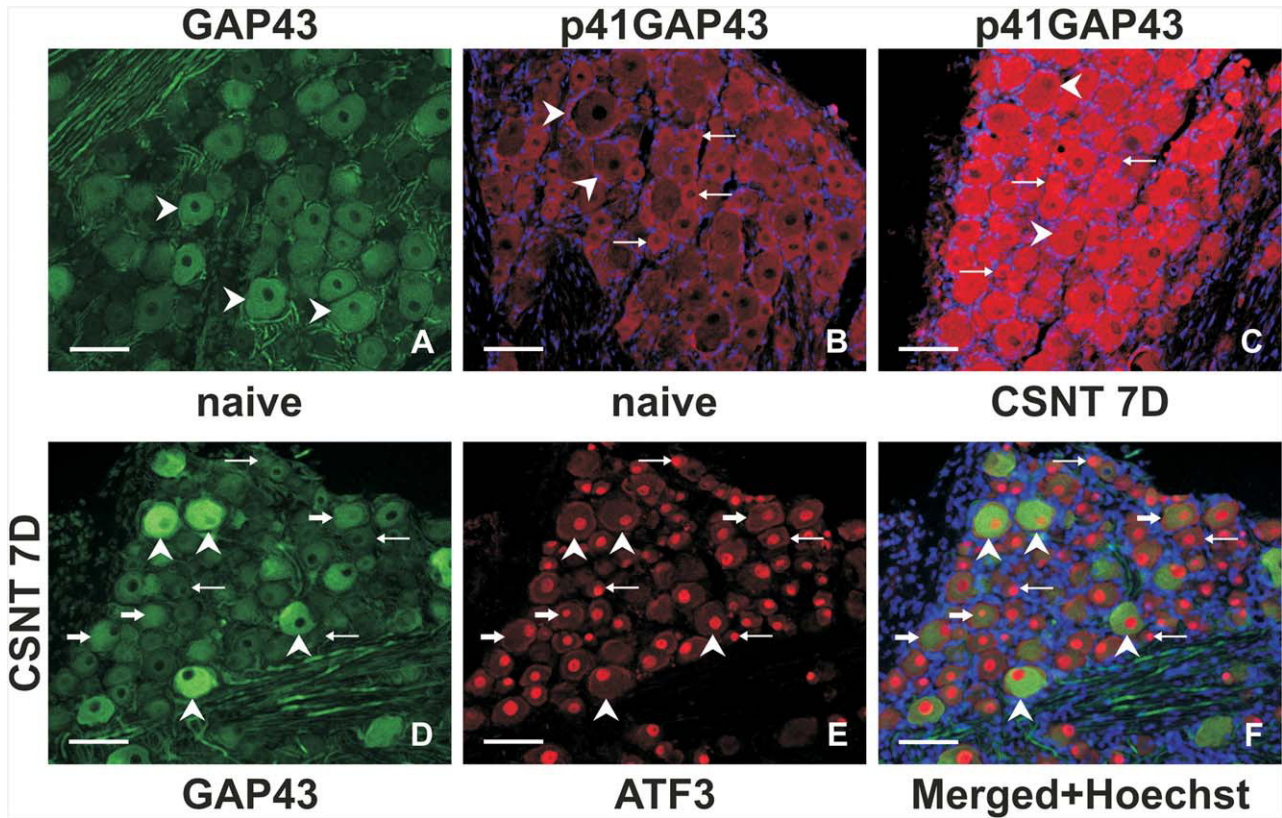


Fig. 1. Representative sections of L4-DRG of naïve rat (A, B) and from rat with CSNT for 7 days (C–F). The sections (A, D–F) were immunostained with mouse monoclonal anti-GAP43 antibody recognizing both phosphorylated and dephosphorylated forms. For double immunostaining (D–F), the section was further processed for immunostaining with rabbit polyclonal antibody against ATF3 and cell nuclei were stained by Hoechst 33342 (blue). Low intensity GAP43 immunofluorescence is seen mainly in large DRG neurons of naïve rat (A, arrowheads). Increased intensity of GAP43 is detected in large-sized neurons (arrowheads), while medium- (thick arrows) or small-sized neurons (slim arrows) display weak or no immunopositivity, respectively (D). Most neuronal nuclei were simultaneously decorated by ATF3 immunopositivity indicating injury to their axons (E), but the merged picture (F) illustrates that neurons with weak or no GAP43 immunostaining showed axon injury (thick and slim arrows). The sections of L4-DRG from naïve (B) and CSNT-operated (C) rat were immunostained for S41-GAP43 and cell nuclei were labeled by Hoechst 33342 (blue). Large neuronal bodies lack S41-GAP43 immunofluorescence, but they are enveloped by S41-GAP43+ satellite glial cells (B, arrowheads). In addition, medium- and small-sized neuronal bodies of naïve DRG displayed a low intensity of S41-GAP43 immunofluorescence (B, arrows). In contrast to GAP43, all DRG neurons including those with large (arrowheads) and medium or small bodies (arrows) display increased S41-GAP43 immunostaining after axotomy by CSNT (C). Scale bars: 135 μ m for A, B; 77 μ m for C–F.

immunofluorescence staining of DRG neurons after sciatic nerve injury demonstrated a higher amount of SCG10+ than GAP43+ neurons without differences in DRG subpopulations (Fig. 3F–H).

GAP43 is a widely used marker for regenerating axons, but besides regenerating axons, it is also upregulated in Schwann and Schwann-derived cells (Plantinga et al., 1993; Dubovy and Aldskogius, 1996). This GAP43 immunostaining of Schwann cells associated with regenerated axons make their detection difficult, especially during early periods of axon regeneration (Fig. 4A).

It was demonstrated that SCG10 is transported from the soma to the proximal axonal stump very early after axotomy, whereas it is rapidly lost in distal axon stumps due to phosphorylation by cJun N-terminal kinase (JNK; Tararuk et al., 2006; Shin et al., 2012, 2014). Thus, SCG10 immunostaining is rapidly increased in proximal axonal stumps and regenerating sprouts within 1 hr

after axotomy (Shin et al., 2012, 2014) in contrast to GAP43 labeling regenerated axons after 3 days (Shalom and Yaron, 2014). Therefore, detection of regenerated axons by SCG10 immunostaining is more useful mainly during early periods after nerve injury, for example, 1 day after nerve crush (Fig. 4B–D). In addition, SCG10 is a good marker for regenerated sensory axons, as its levels increase only in the proximal stumps of afferent but not motor axons of the injured sciatic nerve (Shin et al., 2014).

Small Proline-Rich Repeat Protein 1A

SPRR1A or Cornifin-A is one of a group of epithelial differentiation proteins that are induced in axotomized neurons. A very low level of SPRR1A is found in intact DRG neurons, but peripheral nerve injury induces a 60-fold increase of its expression in axotomized DRG

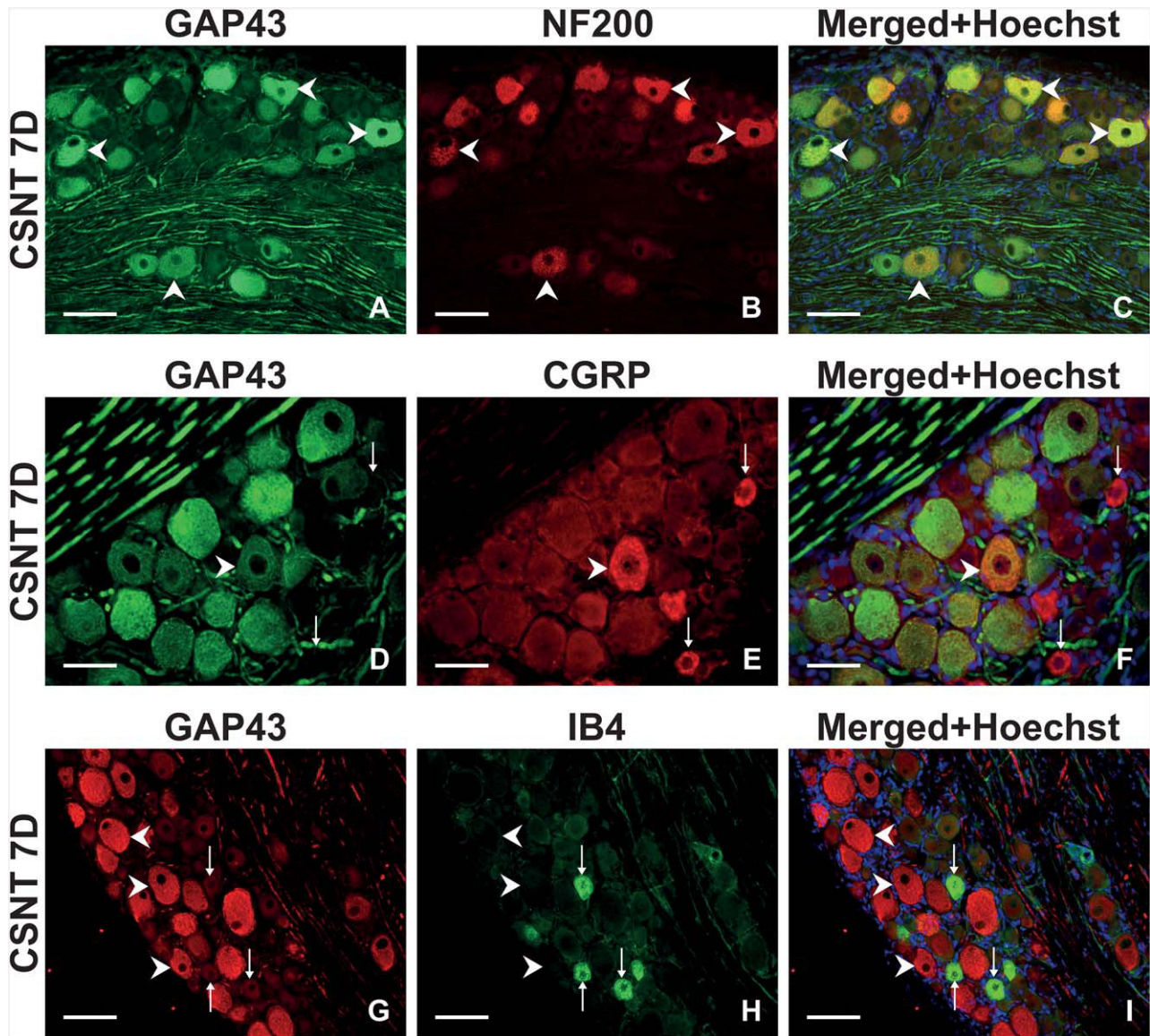


Fig. 2. Representative sections of L4-DRG ipsilateral to CSNT for 7 days double immunostained for GAP43 and NF200 (A–C) or CGRP (D–F) or stained with FITC labeled IB4 (G–I). The highest intensity GAP43 immunostaining is limited to NF200+ neurons with large-sized bodies (A–C, arrowheads). A weak GAP43 reaction is present in CGRP+ neurons of medium-sized bodies (D–F, arrowheads), but CGRP+ neurons of small-sized bodies are free of GAP43 immunostaining (D–F, arrows). In contrast to large neurons (arrowheads), no GAP43 immunofluorescence is observed in nonpeptidergic IB4+ neurons (G–I, arrows). Scale bars: 135 μ m for A–C, G–I; 77 μ m for D–F.

neurons. In addition, overexpression of SPRR1A colocalizes with F-actin in membrane folds of DRG neurons and significantly increases axon outgrowth *in vitro*, while knockdown of SPRR1A gene inhibits axon regeneration (Bonilla et al., 2002). Since SPRR1A is not normally present but is expressed *de novo* in DRG neurons following peripheral nerve injury at a time corresponding to rapid regeneration, it has been proposed as good marker for a reactivated neuronal regeneration program (Bonilla et al., 2002; Starkey et al., 2009).

However, immunohistochemical staining for SPRR1A in L4-DRG of mice undergoing sciatic nerve transection shows a smaller increase in immunofluorescence intensity in large neurons compared to small ones (Table 1; Fig. 5).

MOLECULAR MARKERS INVOLVED IN THE STRESS-RELATED RESPONSE OF AXOTOMIZED DRG AND THE ONSET OF THE AXON REGENERATION PROGRAM

In contrast to the regeneration-associated proteins mentioned above, another unique set of molecular markers can be used for monitoring the regenerative status of DRG neurons. This group of markers induced by axon injury includes transcription factors involved either in the stress-related response of axotomized neurons or contributing to the onset of axon regeneration. These markers include injury-induced molecules like ATF3 (Tsujino et al., 2000) or activated signal

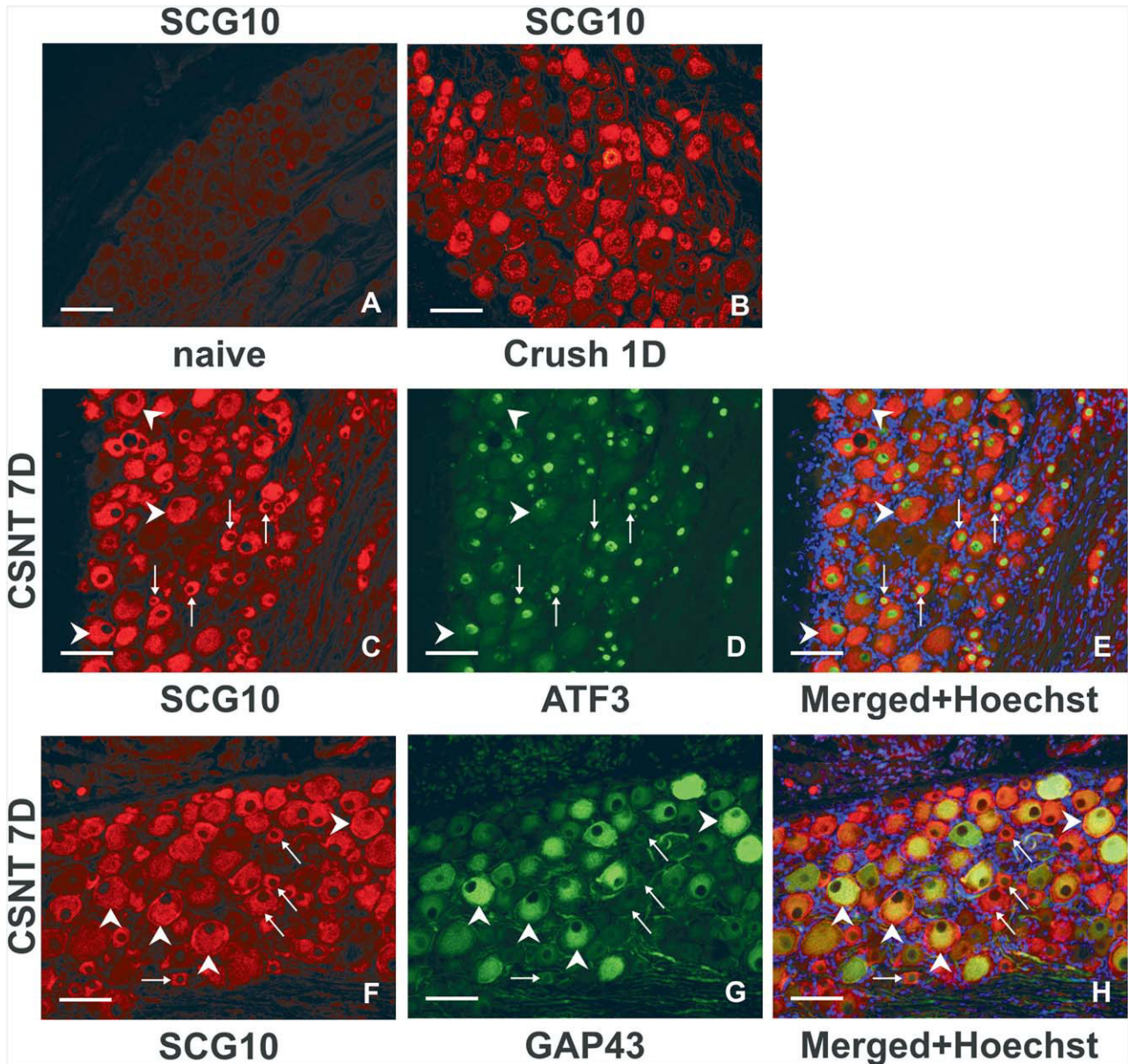


Fig. 3. Representative sections of L4-DRG from naïve rat (A) and rat operated on nerve crush for one day (B) or CSNT for 7 days (C–H). The sections were immunostained for detection of SCG10, and double immunostained with ATF3 (C–E) or GAP43 antibody (F–H). Cell nuclei were stained by Hoechst 33342 (blue). No SCG10 immunofluorescence can be seen in the L4-DRG of naïve rat (A). Increased SCG10 immunostaining in neuronal bodies is already seen one day after nerve crush (B). Most large (arrowheads), medium, and small (arrows) neuronal bodies show immunopositivity for both SCG10 and ATF3 indicating that neurons undergoing axotomy display the marker for neuronal regeneration (C–E). A merged picture (H) after double immunofluorescence staining for SCG10 (F) and GAP43 (G) shows that SCG10 immunostaining is present in most large neurons that are also GAP43+ (arrowheads), as well as in most medium and small neurons that display a negative reaction to GAP43 (arrows). In the L4-DRG after CSNT for 7 days only about one third (33%) of the neurons displayed positive immunostaining for both SCG10 and GAP43. Scale bars: 135 μ m.

transducer and activator of transcription 3 (STAT3) known to be among the molecular determinants associated with the onset of neuronal regeneration (Zigmond, 2012a).

Activating Transcription Factor 3

ATF3 is a member of the activating transcription factor/cAMP-responsive element binding protein (ATF/

CREB) family of transcription factors that is induced in a variety of stressed tissues (Hai et al., 1999, 2010). Since ATF3 is not expressed in intact DRG neurons and its occurrence is induced by nerve injury, it is regarded as a marker for identifying axotomized neurons. The time course of ATF3 induction depends on the distance between the injury site and the cell body (Tsujino et al., 2000). ATF3 represses transcription as a homodimer and

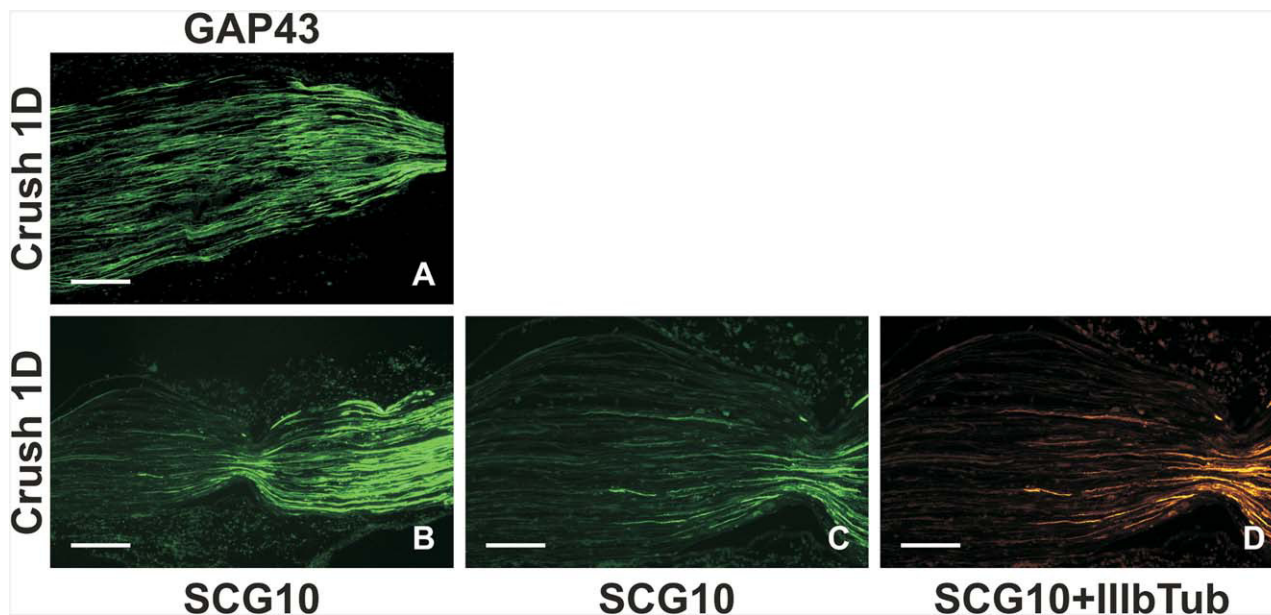


Fig. 4. Longitudinal cryostat sections of the rat ulnar nerve distal to one-day crush with clip immunostained for GAP43 (A) and SCG10 (B–D). The sections of ulnar nerve stump (A) were incubated with GAP43 antibody (A) or double immunostained for SCG10 and β III tubulin (B–D). It is impossible to detect a position of regenerating axons that are GAP43 immunopositive together with Schwann cells (A). In contrast, only regenerated axons are precisely decorated with SCG10 immunofluorescence (B, C). This is verified by colocalization with β III tubulin immunopositivity (D). Scale bars: 135 μ m.

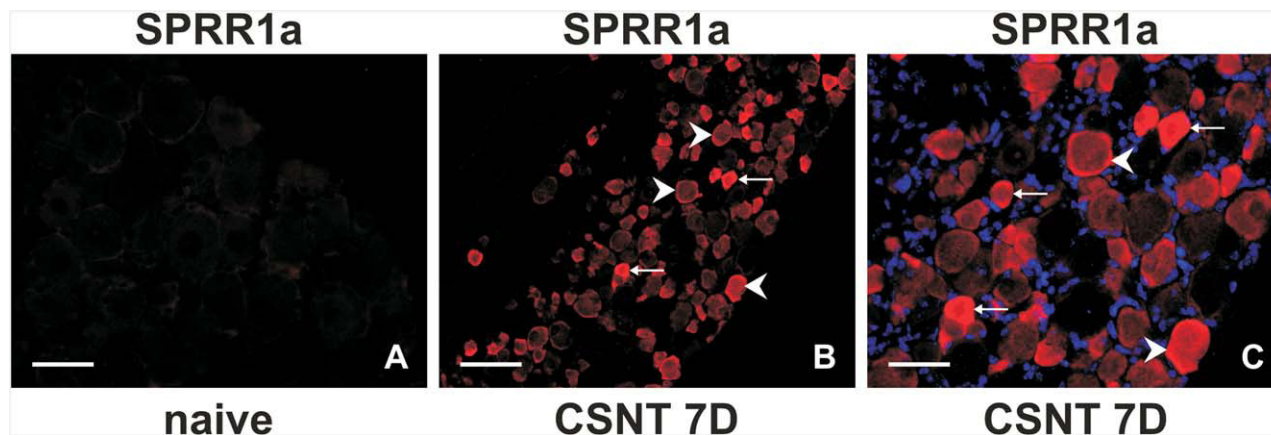


Fig. 5. Representative sections of L4-DRG from naïve mouse (A) and mouse operated on CSNT for 7 days (B, C) immunostained for SPRR1A. Cell nuclei were stained by Hoechst 33342 (C, blue). No SPRR1a immunopositivity can be seen in the section from naïve L4-DRG (A), while section of L4-DRG ipsilateral to CSNT demonstrates clear immunostaining in large (arrowheads), medium and small (arrows) neuronal bodies. Scale bars: 90 μ m for A, B; 45 μ m for C.

activates transcription as a heterodimer when coexpressed with its heterodimeric partners or other proteins like cJun (Hai et al., 1999). For ATF3 activation, cJun needs to be phosphorylated by JNK on serines at both positions 63 and 73 (Waetzig et al., 2006).

It was reported that the axon regeneration program is initiated when both ATF3 and phosphorylated cJun (pcJun) are upregulated in neurons in response to axotomy (Pearson et al., 2003; Lindwall et al., 2004). In contrast, there are data indicating that activation of cJun is not coincident with induction of ATF3 in injured DRG

neurons and that it is unlikely therefore that pcJun is necessary for ATF3 action in axotomized neurons (Seiffers et al., 2006). Moreover, experiments using ATF3-transgenic mice suggested that ATF3 overexpression results in an increase in axon outgrowth *in vitro* and regeneration after nerve injury *in vivo*. However, ATF3 alone in uninjured DRG neurons leads to a slight upregulation of some growth-associated gene targets, and ATF3 upregulation on its own is not enough to fully recapitulate the peripheral nerve regeneration program (Seiffers et al., 2007). Recent results indicate that the

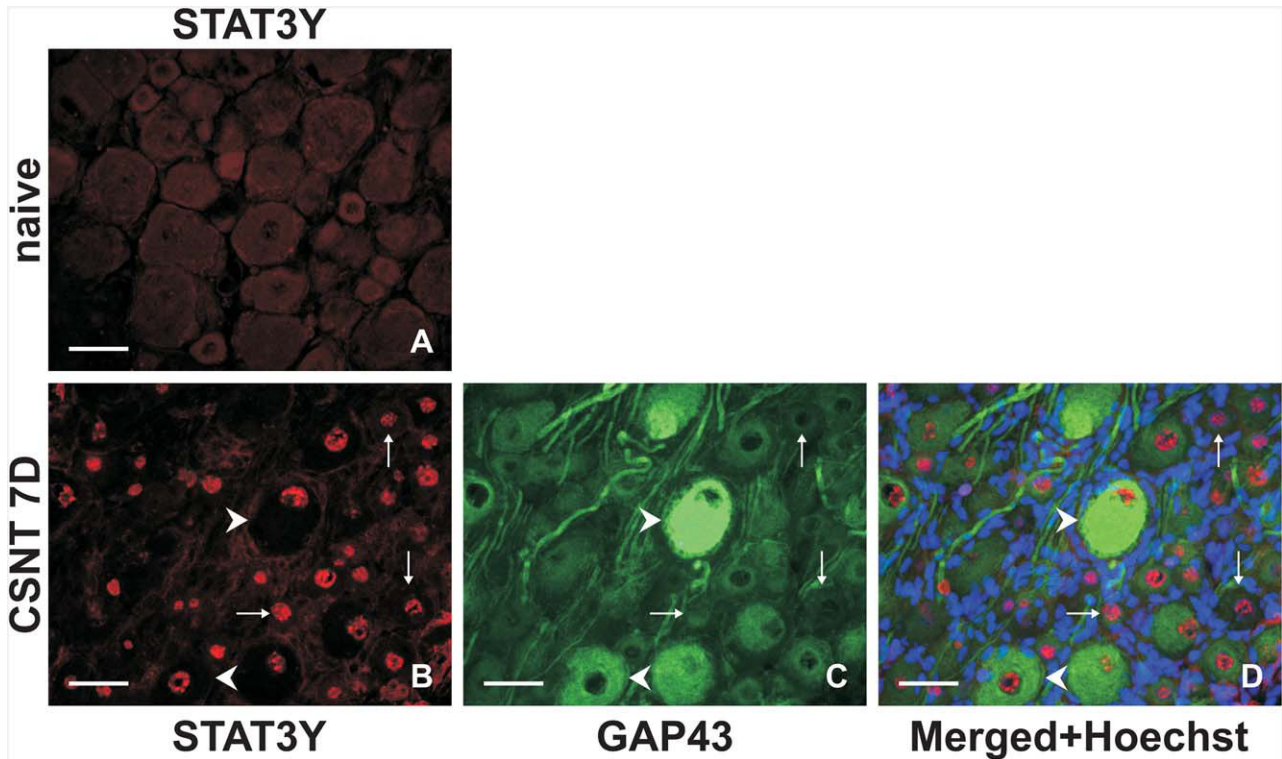


Fig. 6. Representative sections of L4-DRG from naïve rat (A) and rat treated with CSNT for 7 days (B–D). The sections were immunostained antibody recognizing STAT3 phosphorylated at Y705. For double immunostaining, the section was further incubated with GAP43 antibody recognizing both phosphorylated and dephosphorylated forms. Cell nuclei were stained by Hoechst 33342. Neurons and their nuclei in the section from naïve L4-DRG do not display STAT3Y immunostaining (A). Immunopositivity indicating nuclear translocation of STAT3Y705 in both large (arrowheads) and medium or small neuronal bodies (arrows) is detected in the section from L4-DRG ipsilateral to CSNT. However, only large neuronal bodies display a distinct GAP43 immunofluorescence. Scale bars: 135 μm .

ATF3 transcriptional activity might induce “effector” regeneration-associated genes like SPRR1A, Galanin, and GAP43 facilitating peripheral axon regeneration (Gey et al., 2016).

Besides the proregenerative role, ATF3 immunostaining of neuronal nuclei is a useful marker for axotomized DRG neurons. Colocalization of ATF3 with GAP43 or SCG10 in DRG neurons after nerve injury (Figs. 1 and 4) enables precise studies of axon regeneration following axotomy.

Signal Transducer and Activator of Transcription 3

STAT3, a member of the STAT family, is activated as part of Janus kinase (JAK)–STAT signaling pathway (Aaronson and Horvath, 2002). Activation of STAT3 is due to JAK2-dependent phosphorylation at the tyrosine-705 (Y705), and JAK2-independent phosphorylation at the serine-727 (S727) positions (Tsai et al., 2007). Phosphorylated STAT3 dimers translocate to the nucleus and initiate transcription of target genes (Eulendorf et al., 2012). STAT3 activation occurs in DRG neurons very early after a nerve lesion and the influence of neurotrophic cytokines (Zhong et al., 1999; Cafferty et al., 2001, 2004; Miao et al., 2006; Zigmond, 2012b) and neurotrophins (Pellegrino and Habecker, 2013) suggests the

involvement of STAT3 signaling in the promotion of axon growth (Lee et al., 2004; Zigmond, 2012b).

The activation of STAT3 associated with restoration of neuronal regeneration capacity is also supported by *in vitro* experiments with suppressor of cytokine signaling 3 (SOCS3), which provides feedback inhibition of STAT3 signaling. Overexpression of SOCS3 in primary sensory neurons blocks nuclear translocation of STAT3 and axonal growth while neutralization of SOCS3 stimulates axonal outgrowth (Miao et al., 2006).

Some studies demonstrate that STAT3 can transactivate GAP43 expression *in vivo* and *in vitro* (Wu and Bradshaw, 1996; Schwaiger et al., 2000). As was mentioned above, GAP43 promotes axon regeneration when phosphorylated at the S41 position by PKC that is also able to phosphorylate STAT3 at S727 (Tsai et al., 2007).

The DRG neurons of all size categories displayed nuclear translocation of immunostaining for STAT3-Y705 after nerve transections. The results of STAT3-Y705 colocalization with GAP43 indicate reactivation of the axon regeneration program even in DRG neurons with low or no immunoreactivity towards GAP43 (Table 1; Fig. 6).

SUMMARY AND CONCLUSION

Reactivation of neuronal regeneration is one of the most important conditions for successful reinnervation of injured peripheral nerves. DRG neurons are very useful

in studying the reactivation of the neuronal regeneration program, and are frequently used as *in vivo* and *in vitro* models. However, different populations of DRG neurons behave differently with respect to their regeneration capacity as well as the expression of molecular markers. This presents a problem for effective and reliable experimentation. Both published and original results presented here suggest that immunohistochemical detection of GAP43 by antibodies recognizing both phosphorylated and dephosphorylated forms fail to identify all types of DRG neurons that regenerate their axons. Moreover, GAP43 immunostaining is also unsuitable to detect regenerated axons during early periods after nerve injury. SCG10, another protein related to the cytoskeletal dynamics of regenerating axons is a more reliable marker than GAP43 for visualization of the reactivating neuronal regeneration program with the added advantage of enabling the specific detection of regenerated sensory axons. Immunostaining for selected transcription factors closely associated with the induction of the regeneration program like ATF3 or STAT3 is a good alternative for detecting DRG neurons that regenerate their axons.

ACKNOWLEDGEMENTS

The authors thank Ms. Dana Kutějová, Ms. Marta Lněničková, Ms. Jitka Mikulášková, and Mgr. Jana Vachová for their skillful technical assistance.

LITERATURE CITED

- Aaronson DS, Horvath CM. 2002. A road map for those who don't know JAK-STAT. *Science* 296:1653–1655.
- Andersen LB, Schreyer DJ. 1999. Constitutive expression of GAP-43 correlates with rapid, but not slow regrowth of injured dorsal root axons in the adult rat. *Exp Neurol* 155:157–164.
- Antonsson B, Kassel DB, Di Paolo G, Lutjens R, Riederer BM, Grenningloh G. 1998. Identification of *in vitro* phosphorylation sites in the growth cone protein SCG10 - Effect of phosphorylation site mutants on microtubule-destabilizing activity. *J Biol Chem* 273:8439–8446.
- Benowitz LI, Routtenberg A. 1997. GAP-43: An intrinsic determinant of neuronal development and plasticity. *Trends Neurosci* 20: 84–91.
- Bonilla IE, Tanabe K, Strittmatter SM. 2002. Small proline-rich repeat protein 1A is expressed by axotomized neurons and promotes axonal outgrowth. *J Neurosci* 22:1303–1315.
- Cafferty WBJ, Gardiner NJ, Das P, Qiu J, McMahon SB, Thompson SWN. 2004. Conditioning injury-induced spinal axon regeneration fails in interleukin-6 knock-out mice. *J Neurosci* 24:4432–4443.
- Cafferty WBJ, Gardiner NJ, Gavazzi I, Powell J, McMahon SB, Heath JK, Munson J, Cohen J, Thompson SWN. 2001. Leukemia inhibitory factor determines the growth status of injured adult sensory neurons. *J Neurosci* 21:7161–7170.
- Doron-Mandel E, Fainzilber M, Terenzio M. 2015. Growth control mechanisms in neuronal regeneration. *FEBS Lett* 589:1669–1677.
- Dubovy P, Aldskogius H. 1996. Growth-associated protein (GAP-43) in terminal Schwann cells of rat Pacinian corpuscles. *Neuroreport* 7:2147–2150.
- Eulenfeld R, Dittrich A, Khouri C, Muller PJ, Mutze B, Wolf A, Schaper F. 2012. Interleukin-6 signalling: More than Jaks and STATs. *Eur J Cell Biol* 91:486–495.
- Fawcett JW, Keynes RJ. 1990. Peripheral-nerve regeneration. *Ann Rev Neurosci* 13:43–60.
- Gey M, Wanner R, Schilling C, Pedro MT, Sinske D, Knoll B. 2016. Atf3 mutant mice show reduced axon regeneration and impaired regeneration-associated gene induction after peripheral nerve injury. *Open Biol* 6:160091.
- Hai T, Wolfgang CD, Marsee DK, Allen AE, Sivaprasad U. 1999. ATF3 and stress responses. *Gene Expr* 7:321–335.
- Hai T, Wolford CC, Chang YS. 2010. ATF3, a hub of the cellular adaptive-response network, in the pathogenesis of diseases: Is modulation of inflammation a unifying component? *Gene Expr* 15: 1–11.
- Hunt SP, Mantyh PW. 2001. The molecular dynamics of pain control. *Nat Rev Neurosci* 2:83–91.
- Larsson C. 2006. Protein kinase C and the regulation of the actin cytoskeleton. *Cell Signal* 18:276–284.
- Lautermilch NJ, Spitzer NC. 2000. Regulation of calcineurin by growth cone calcium waves controls neurite extension. *J Neurosci* 20:315–325.
- Laux T, Fukami K, Thelen M, Golub T, Frey D, Caroni P. 2000. GAP43, MARCKS, and CAP23 modulate PI(4,5)P-2 at plasmalemmal rafts, and regulate cell cortex actin dynamics through a common mechanism. *J Cell Biol* 149:1455–1471.
- Lawson SN. 2002. Phenotype and function of somatic primary afferent nociceptive neurones with C-, A delta- or A alpha/beta-fibres. *Exp Physiol* 87:239–244.
- Lawson SN, Caddy KWT, Biscoe TJ. 1974. Development of rat dorsal root ganglion neurones. Studies of cell birthdays and changes in mean cell diameter. *Cell Tissue Res* 153:399–413.
- Lawson SN, Perry MJ, Prabhakar E, McCarthy PW. 1993. Primary sensory neurons - neurofilament, neuropeptides, and conduction-velocity. *Brain Res Bull* 30:239–243.
- Leclere PG, Norman E, Groutsi F, Coffin R, Mayer U, Pizzey J, Tonge D. 2007. Impaired axonal regeneration by isolectin B4-binding dorsal root ganglion neurons *in vitro*. *J Neurosci* 27: 1190–1199.
- Lee N, Neitzel KL, Devlin BK, MacLennan AJ. 2004. STAT3 phosphorylation in injured axons before sensory and motor neuron nuclei: Potential role for STAT3 as a retrograde signaling transcription factor. *J Comp Neurol* 474:535–545.
- Lindwall C, Dahlin L, Lundborg G, Kanje M. 2004. Inhibition of c-Jun phosphorylation reduces axonal outgrowth of adult rat nodose ganglia and dorsal root ganglia sensory neurons. *Mol Cell Neurosci* 27:267–279.
- Mason MRJ, Lieberman AR, Grenningloh G, Anderson PN. 2002. Transcriptional upregulation of SCG10 and CAP-23 is correlated with regeneration of the axons of peripheral and central neurons *in vivo*. *Mol Cell Neurosci* 20:595–615.
- Miao T, Wu DS, Zhang Y, Bo XN, Subang MC, Wang P, Richardson PM. 2006. Suppressor of cytokine signaling-3 suppresses the ability of activated signal transducer and activator of transcription-3 to stimulate neurite growth in rat primary sensory neurons. *J Neurosci* 26:9512–9519.
- Molliver DC, Wright DE, Leitner ML, Parsadanian AS, Doster K, Wen D, Yan Q, Snider WD. 1997. IB4-binding DRG neurons switch from NGF to GDNF dependence in early postnatal life. *Neuron* 19:849–861.
- Pearson AG, Gray CW, Pearson JF, Greenwood JA, During MJ, Dragunow M. 2003. ATF3 enhances c-Jun-mediated neurite sprouting. *Mol Brain Res* 120:38–45.
- Pellegrino MJ, Habecker BA. 2013. STAT3 integrates cytokine and neurotrophin signals to promote sympathetic axon regeneration. *Mol Cell Neurosci* 56:272–282.
- Plantinga LC, Verhaagen J, Edwards PM, Hol EM, Bar PR, Gispen WH. 1993. The expression of B-50/GAP-43 in Schwann cells is upregulated in degenerating peripheral nerve stumps following nerve injury. *Brain Res* 602:69–76.
- Riederer BM, Pellier V, Antonsson B, Di Paolo G, Stimpson SA, Lutjens R, Catsicas S, Grenningloh G. 1997. Regulation of microtubule dynamics by the neuronal growth-associated protein SCG10. *Proc Natl Acad Sci USA* 94:741–745.
- Rigaud M, Gemes G, Barabas ME, Chernoff DI, Abram SE, Stucky CL, Hogan QH. 2008. Species and strain differences in rodent sciatic nerve anatomy: Implications for studies of neuropathic pain. *Pain* 136:188–201.

- Schreyer DJ, Skene JHP. 1993. Injury-associated induction of GAP-43 expression displays axon branch specificity in rat dorsal root ganglion neurons. *J Neurobiol* 24:959–970.
- Schwaiger FW, Hager G, Schmitt AB, Horvat A, Streif R, Spitzer C, Gamal S, Breuer S, Brook GA, Nacimiento W, et al. 2000. Peripheral but not central axotomy induces changes in Janus kinases (JAK) and signal transducers and activators of transcription (STAT). *Eur J Neurosci* 12:1165–1176.
- Seiffers R, Allchorne AJ, Woolf CJ. 2006. The transcription factor ATF-3 promotes neurite outgrowth. *Mol Cell Neurosci* 32:143–154.
- Seiffers R, Mills CD, Woolf CJ. 2007. ATF3 increases the intrinsic growth state of DRG neurons to enhance peripheral nerve regeneration. *J Neurosci* 27:7911–7920.
- Shalom HS, Yaron A. 2014. Marking axonal growth in sensory neurons: SCG10. *Exp Neurol* 254:68–69.
- Shin JE, Geisler S, DiAntonio A. 2014. Dynamic regulation of SCG10 in regenerating axons after injury. *Exp Neurol* 252:1–11.
- Shin JE, Miller BR, Babetto E, Cho Y, Sasaki Y, Qayum S, Russler EV, Cavalli V, Milbrandt J, DiAntonio A. 2012. SCG10 is a JNK target in the axonal degeneration pathway. *Proc Natl Acad Sci USA* 109:E3696–E3705.
- Skene JHP. 1989. Axonal growth-associated proteins. *Ann Rev Neurosci* 12:127–156.
- Skene JHP, Willard M. 1981. Axonally transported proteins associated with axon growth in rabbit central and peripheral nervous systems. *J Cell Biol* 89:96–103.
- Starkey ML, Davies M, Yip PK, Carter LM, Wong DJN, McMahon SB, Bradbury EJ. 2009. Expression of the Regeneration-Associated Protein SPRR1A in Primary Sensory Neurons and Spinal Cord of the Adult Mouse Following Peripheral and Central Injury. *J Comp Neurol* 513:51–68.
- Stewart HJS, Cowen T, Curtis R, Wilkin GP, Mirsky R, Jessen KR. 1992. GAP-43 immunoreactivity is widespread in the autonomic neurons and sensory neurons of the rat. *Neuroscience* 47:673–684.
- Sugiura Y, Mori N. 1995. SCG10 expresses growth-associated manner in developing rat brain, but shows a different pattern to p19 stathmin or GAP-43. *Dev Brain Res* 90:73–91.
- Swett JE, Torigoe Y, Elie VR, Bourassa CM, Miller PG. 1991. Sensory neurons of the rat sciatic nerve. *Exp Neurol* 114:82–103.
- Tararuk T, Ostman N, Li WR, Bjorkblom B, Padzik A, Zdrojewska J, Hongisto V, Herdegen T, Konopka W, Courtney MJ, et al. 2006. JNK1 phosphorylation of SCG10 determines microtubule dynamics and axodendritic length. *J Cell Biol* 173:821–277.
- Tsai SY, Yang LY, Wu CH, Chang SF, Hsu CY, Wei CP, Leu SJ, Liaw J, Lee YH, Tsai MD. 2007. Injury-induced janus kinase/protein kinase C-dependent phosphorylation of growth-associated protein 43 and signal transducer and activator of transcription 3 for neurite growth in dorsal root ganglion. *J Neurosci Res* 85:321–331.
- Tsujino H, Kondo E, Fukuoka T, Dai Y, Tokunaga A, Miki K, Yonenobu K, Ochi T, Noguchi K. 2000. Activating transcription factor 3 (ATF3) induction by axotomy in sensory and motoneurons: A novel neuronal marker of nerve injury. *Mol Cell Neurosci* 15:170–182.
- Verge VMK, Tetzlaff W, Richardson PM, Bisby MA. 1990. Correlation Between GAP43 and Nerve Growth Factor Receptors in Rat Sensory Neurons. *J Neurosci* 10:926–934.
- Voria I, Hauser J, Axis A, Schenker M, Bichet S, Kuntzer T, Grenningloh G, Barakat-Walter I. 2006. Improved sciatic nerve regeneration by local thyroid hormone treatment in adult rat is accompanied by increased expression of SCG10. *Exp Neurol* 197:258–267.
- Waetzig V, Zhao Y, Herdegen T. 2006. The bright side of JNKs - Multitalented mediators in neuronal sprouting, brain development and nerve fiber regeneration. *Prog Neurobiol* 80:84–97.
- Woolf CJ, Reynolds ML, Molander C, O'Brien C, Lindsay RM, benowitz LI. 1990. The growth-associated protein GAP-43 appears in dorsal root ganglion cells and in the dorsal horn of the rat spinal cord following peripheral nerve injury. *Neuroscience* 34:465–478.
- Wu YY, Bradshaw RA. 1996. Synergistic induction of neurite outgrowth by nerve growth factor or epidermal growth factor and interleukin-6 in PC12 cells. *J Biol Chem* 271:13033–13039.
- Zhong J, Dietzel ID, Wahle P, Kopf M, Heumann R. 1999. Sensory impairments and delayed regeneration of sensory axons in interleukin-6-deficient mice. *J Neurosci* 19:4305–4313.
- Zigmond RE. 2012a. Cytokines that promote nerve regeneration. *Exp Neurol* 238:101–106.
- Zigmond RE. 2012b. gp130 cytokines are positive signals triggering changes in gene expression and axon outgrowth in peripheral neurons following injury. *Front Mol Neurosci* 4:62.

C. Dubový P, Klusáková I, Hradilová-Svíženská I, Brázda V, Kohoutková M, **Joukal M.** A conditioning sciatic nerve lesion triggers a pro-regenerative state in primary sensory neurons also of dorsal root ganglia non-associated with the damaged nerve. *Frontiers in Cellular Neuroscience*. 2019;13. doi:10.3389/fncel.2019.00011

Commentary: In this publication, we demonstrated that sciatic nerve injury induced increased expression of SCG10 and GAP43 in the cervical DRG. The increase of regeneration-associated proteins corresponded with greater length of regenerating axons in the ulnar nerve 1 day after crush. In addition, we showed IL-6 signaling pathway as crucial for pro-regenerative state in remote DRG.

IF (WOS, 2017): 4.3

Quartile (WOS, 2017): Neurosciences Q1

Contribution of the author: Co-authorship. The author participated on performing of in vivo experiments, preparing samples for immunohistochemistry, western blot, RT-PCR and writing of the corresponding texts.



A Conditioning Sciatic Nerve Lesion Triggers a Pro-regenerative State in Primary Sensory Neurons Also of Dorsal Root Ganglia Non-associated With the Damaged Nerve

Petr Dubový*, Ilona Klusáková, Ivana Hradilová-Sviženská, Václav Brázda, Marcela Kohoutková and Marek Joukal

Department of Anatomy, Laboratory of Cellular and Molecular Neurobiology, Faculty of Medicine, Masaryk University, Brno, Czechia

OPEN ACCESS

Edited by:

Thomas Fath,
Macquarie University, Australia

Reviewed by:

Simone Di Giovanni,
Imperial College London,
United Kingdom
Stefania Raimondo,
University of Turin, Italy

*Correspondence:

Petr Dubový
pdubovy@med.muni.cz

Received: 08 October 2018

Accepted: 14 January 2019

Published: 04 February 2019

Citation:

Dubový P, Klusáková I, Hradilová-Sviženská I, Brázda V, Kohoutková M and Joukal M (2019) A Conditioning Sciatic Nerve Lesion Triggers a Pro-regenerative State in Primary Sensory Neurons Also of Dorsal Root Ganglia Non-associated With the Damaged Nerve. *Front. Cell. Neurosci.* 13:11. doi: 10.3389/fncel.2019.00011

The primary sensory neurons of dorsal root ganglia (DRG) are a very useful model to study the neuronal regenerative program that is a prerequisite for successful axon regeneration after peripheral nerve injury. Seven days after a unilateral sciatic nerve injury by compression or transection, we detected a bilateral increase in growth-associated protein-43 (GAP-43) and superior cervical ganglion-10 (SCG-10) mRNA and protein levels not only in DRG neurons of lumbar spinal cord segments (L4-L5) associated with injured nerve, but also in remote cervical segments (C6-C8). The increase in regeneration-associated proteins in the cervical DRG neurons was associated with the greater length of regenerated axons 1 day after ulnar nerve crush following prior sciatic nerve injury as compared to controls with only ulnar nerve crush. The increased axonal regeneration capacity of cervical DRG neurons after a prior conditioning sciatic nerve lesion was confirmed by neurite outgrowth assay of *in vitro* cultivated DRG neurons. Intrathecal injection of IL-6 or a JAK2 inhibitor (AG490) revealed a role for the IL-6 signaling pathway in activating the pro-regenerative state in remote DRG neurons. Our results suggest that the pro-regenerative state induced in the DRG neurons non-associated with the injured nerve reflects a systemic reaction of these neurons to unilateral sciatic nerve injury.

Keywords: unilateral nerve injury, primary sensory neurons, pro-regenerative state, GAP-43, SCG-10, IL-6, ulnar nerve crush, neurite outgrowth assay

INTRODUCTION

It is well-known that besides extrinsic factors, activation of a neuronal regenerative program is necessary for successful axon regeneration after peripheral nerve injury. The primary sensory neurons, whose bodies are in the dorsal root ganglia (DRG), are a useful model to study the mechanisms regulating the neuronal regeneration program after axotomy. The DRG neurons have peripheral and central branches of afferent axons with different responses to injury. Injury to peripheral axonal branches induces transcription-dependent changes of regeneration-associated

genes and proteins that promote axon regeneration by enhancing the regeneration potential of DRG neurons (Liu et al., 2011). In contrast, central axonal branches extending into the dorsal columns of the spinal cord fail to regenerate when injured because insufficient activation of the neuronal regeneration program (Schwaiger et al., 2000; Qiu et al., 2005). However, a conditioning lesion of the peripheral nerve, where peripheral axonal branches are injured beforehand, triggers a regenerative program in DRG neurons that is sufficient to allow regeneration also of central axonal branches (Neumann and Woolf, 1999). This phenomenon of a conditioning peripheral nerve lesion with the activation of the pro-regenerative state in DRG neurons is at least partly associated with upregulation of some neurotrophic cytokines including IL-6 (Cafferty et al., 2001; Zigmond, 2011, 2012). It was also shown that increased axon regeneration was conditioned in the homologous nerve contralateral to the injured nerve (Yamaguchi et al., 1999; Ryoike et al., 2000).

In our previous experiments we have found bilateral increased levels of IL6, as well as its receptor mRNA and protein, not only in DRG associated with the injured sciatic nerve, but also in remote cervical DRG (Brázda et al., 2013; Dubový et al., 2013). Moreover, unilateral sciatic nerve injury induced bilateral activation of STAT3 by phosphorylation at the tyrosine-705 (Y705) position in DRG neurons of both lumbar and cervical segments (Dubový et al., 2018a) that is a critical transforming factor of the neuronal pro-regenerative state (Bareyre et al., 2011; Zigmond, 2011). Based on our own and other previously published results, we hypothesize that nerve injury may stimulate the pro-regenerative state not only in the DRG neurons associated with damaged axons, but also in DRG neurons not directly associated with the injured nerve.

Activation of the neuronal pro-regenerative state is characterized by upregulation of various transforming factors, regeneration-associated genes and proteins which are important intrinsic determinants of neuronal regeneration capacity (Mar et al., 2014; Rishal and Fainzilber, 2014; Chandran et al., 2016). For example, phosphorylation and activation of the transcription factor cJun (Itoh et al., 2009; Frey et al., 2015) and the mitogen-activated protein kinase p38 (p38 MAPK; Verma et al., 2005; Nix et al., 2011) is associated with induction of the pro-regenerative state in DRG neurons following nerve injury.

Regeneration-associated proteins like growth-associated protein-43 (GAP-43) or superior cervical ganglion-10 (SCG-10) are generally used as markers for detecting the neuronal pro-regenerative state (Bonilla et al., 2002; Mason et al., 2002). GAP-43 is the prototypical GAP, is expressed at high levels in neurons during development and concentrated in the axonal growth cone (Skene and Willard, 1981). DRG neurons of naïve rats display a low basal level of GAP-43 that is significantly increased after nerve injury (Stewart et al., 1992; Schreyer and Skene, 1993; Liabotis and Schreyer, 1995). The SCG-10 protein, also known as stathmin 2, is a neuron-specific member of the stathmin family (Sugiura and Mori, 1995) that is upregulated specifically in primary sensory neurons regenerating their axons (Shin et al., 2014).

The goal of the present study was to investigate whether a sciatic nerve injury can activate the pro-regenerative state of DRG neurons not only in the corresponding lumbar but also in remote cervical spinal cord segments. The pro-regenerative state of DRG neurons was shown by the upregulation of GAP-43 and SCG-10 mRNAs and proteins as well as activation of cJun and p38 in correlation with the extent of regenerated axons after ulnar nerve crush following prior sciatic nerve injury. Increased axon regeneration capacity in cervical DRG neurons initiated by the conditioning sciatic nerve lesion was also confirmed by neurite outgrowth assay of *in vitro* cultivated DRG neurons. Moreover, intrathecal injection of IL-6 revealed that this cytokine can mediate this systemic reaction of DRG along the neuroaxis after unilateral sciatic nerve lesion.

MATERIALS AND METHODS

Animals and Surgical Treatment

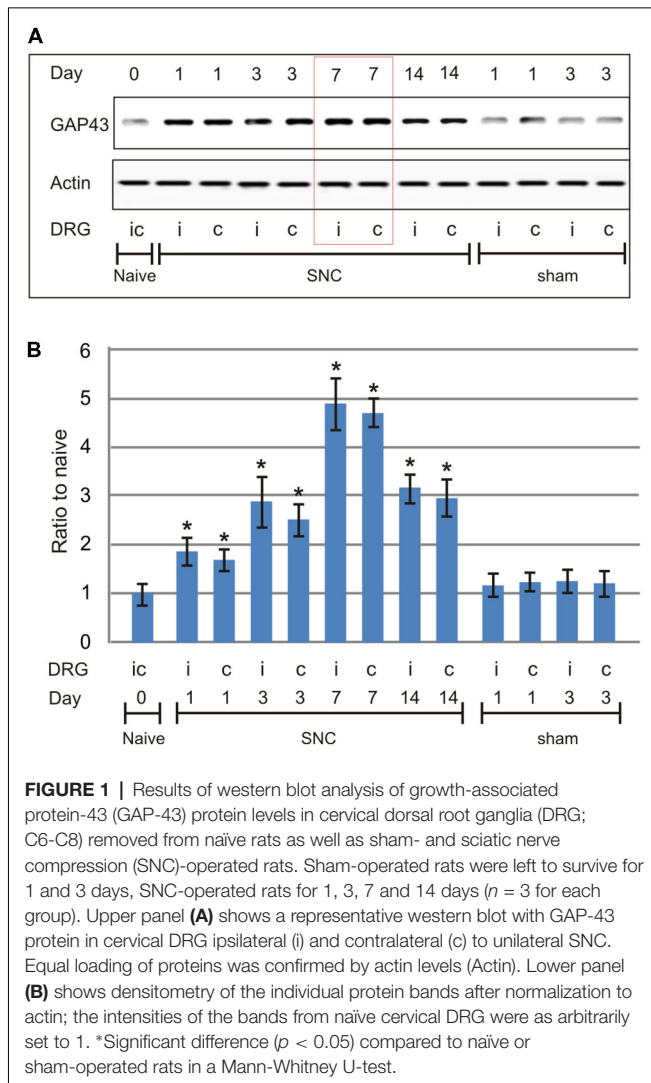
The experiments were performed in 194 adult male rats (Wistar, 250–280 g, Anlab, Brno, Czechia) housed in 12 h light/dark cycles at a temperature of 22–24°C under specific pathogen-free conditions in the animal housing facility of Masaryk University. Sterilized standard rodent food and water were available *ad libitum*. Animals for surgical treatments were anesthetized using a mixture of ketamine (40 mg/ml) and xylazine (4 mg/ml) administered intraperitoneally (0.2 ml/100 g body weight). All surgical procedures were carried out under sterile conditions by the same person according to protocols approved by the Animal Investigation Committee of the Faculty of Medicine, Brno, Czechia.

The right sciatic nerve of rats was exposed in mid-thigh, ligated with two ligatures and cut (complete sciatic nerve transection, CSNT). The proximal nerve stump was fixed in muscles to protect the distal stump from reinnervation. A longitudinally slit silicone tube of 2-mm length and 1 mm internal diameter was placed around the right sciatic nerve of rats to reduce the nerve diameter (sciatic nerve compression, SNC; Schmid et al., 2013). The tube was tied in place with a sterile thread to close and prevent tube from opening. The muscles and skin were closed with 5/0 sutures. The right sciatic nerve of sham-operated rats was carefully exposed without any lesion.

To determine the progression in time of the pro-regenerative state in cervical DRG after sciatic nerve lesion, a set of SNC-operated rats from the pilot study was left to survive for 1, 3, 7, and 14 days and compared with naïve rats or sham-operated rats surviving for 1 and 3 days ($n = 3$ for each group). Based on the pilot study in which GAP-43 peaked at 7 days after unilateral sciatic nerve lesion (Figure 1), further groups of operated and sham-operated rats were left to survive for 7 days after surgical treatment and used for bilateral analysis of the neuronal regeneration program in both lumbar and cervical DRG.

Quantitative Immunohistochemical Analysis

Naïve rats and sham-, SNC- and CSNT-operated rats ($n = 6$ for each group) were deeply anesthetized with a lethal dose of



sodium pentobarbital (70 mg/kg body weight, i.p.) and perfused transcardially with 500 ml phosphate-buffered saline (PBS, pH 7.4) followed by 500 ml of Zamboni's fixative (Zamboni and Demartin, 1967). The L4-L5 and C6-C8 DRG from both sides were detected in their intervertebral foramina following total laminectomy and foraminotomy. The DRG were removed, immersed separately in Zamboni's fixative at 4°C overnight, and then collected separately into samples of ipsilateral (L-DRGi) and contralateral (L-DRGc) lumbar as well as ipsilateral (C-DRGi) and contralateral (C-DRGc) cervical DRG for each group of rats (naïve, sham-, SNC-, and CSNT-operated).

The DRG samples were washed in 20% phosphate-buffered sucrose for 12 h, blocked in Tissue-Tek[®] OCT compound (Miles, Elkhart, IN, USA) and cut to prepare serial longitudinal cryostat sections (12 μ m). The DRG sections were mounted on chrome-alum covered slides and processed for indirect immunohistochemical staining for GAP-43 and SCG-10. Briefly, DRG sections of lumbar and cervical segments of naïve, sham-, SNC- and CSNT-operated rats were immunostained simultaneously under the same conditions. Sections were

washed with PBS containing 0.05% Tween 20 (PBS-T) and 1% bovine serum albumin (BSA) for 10 min, treated with 5% normal donkey serum in PBS-T for 30 min, then incubated with 25 μ l of mouse monoclonal antibody against GAP-43 (1:500; Sigma, Ronkonkoma, NY, USA) and rabbit polyclonal antibody against SCG-10 (1:1,000; LSBio, Seattle, WA, USA), phospho-cJun (1:100; Cell Signaling, New York, NY, USA) or phospho-p38 (1:200; Chemicon Int., Temecula, CA, USA) in a humid chamber at room temperature (21–23°C) for 12 h. The immunohistochemical reaction was visualized by treatment with FITC-conjugated and affinity-purified donkey anti-mouse or anti-rabbit secondary antibody (1:100; Millipore, USA) for 90 min at room temperature. The control sections were incubated without the primary antibody. Sections were stained with Hoechst 33342 to detect cell nuclei, mounted in aqueous mounting medium (Vectashield; Vector Laboratories, Burlingame, CA, USA) and analyzed using an epifluorescence microscope (Nikon Eclipse, Nikon, Czechia) equipped with a camera (DFC-480; Leica Microsystems) and a stabilized power supply for the lamp housing.

The neuronal diameter, GAP-43 and SCG-10 immunofluorescence intensities were measured using a NIS-Elements image analysis system (Nikon, Czechia) as previously (Dubový et al., 2002, 2013). At least 100 neuronal profiles containing nuclei were measured for each animal group. The sizes of DRG neurons in sections for immunofluorescence were categorized as small (<25 μ m), medium (25–40 μ m), and large (>40 μ m) according to their diameters calculated from the areas of neuronal profiles. The immunofluorescence intensities were expressed as mean intensity \pm SD.

Western Blot Analysis

In the pilot study, the cervical DRG (C6-C8) of naïve rats and rats surviving 1 and 3 days after sham-operation and 1, 3, 7 and 14 days after SNC-operation ($n = 3$ for each group) were removed bilaterally, flash-frozen in liquid nitrogen and stored at -80°C until western blot analysis of GAP-43.

The results of GAP-43 and SCG-10 levels obtained by quantitative immunohistochemistry in DRG neurons 7 days after sciatic nerve lesions were verified by western blot analysis. The DRG from lumbar (L4-L5) and cervical (C6-C8) levels ($n = 3$ for each group in three independent experiments) were collected as described under aseptic conditions. Samples of ipsilateral (L-DRGi) and contralateral (L-DRGc) lumbar DRG as well as ipsilateral (C-DRGi) and contralateral (C-DRGc) cervical DRG from each group of rats were flash-frozen in liquid nitrogen and stored at -80°C until analysis.

The DRG samples were homogenized in PBS containing protease inhibitors (LaRoche, Switzerland) with 0.1% Triton X-100, and centrifuged at 10,000 g for 5 min at 4°C. Proteins were separated by SDS-polyacrylamide gel electrophoresis (Brazda et al., 2006) and transferred to nitrocellulose membranes by electroblotting (BioRad). Blots were blocked using 1% BSA in PBST (3.2 mM Na_2HPO_4 , 0.5 mM KH_2PO_4 , 1.3 mM KCl, 135 mM NaCl, 0.05% Tween 20, pH 7.4) for 1 h and incubated with anti-GAP-43 mouse monoclonal (1:1,000; Sigma, Ronkonkoma, NY, USA), rabbit polyclonal anti-phosphorylated

S41-GAP43 (1:500; Thermo Fisher Scientific, Waltham, MA, USA) or anti-SCG-10 (1:500; LSBio, Seattle, WA, USA) antibodies overnight. Blots were washed in PBST and incubated with peroxidase-conjugated anti-mouse or anti-rabbit IgG (1:1,000; Sigma, Seattle, WA, USA) at room temperature for 1 h. Protein bands were visualized by the ECL detection kit (Amersham, USA) on the chemiluminometer reader LAS-3000 (Fuji, Japan) and analyzed using densitometry image software. The levels of proteins were normalized to the value of naïve DRG, which was arbitrarily set as one.

Real Time RT-PCR

The expression of GAP-43 and SCG-10 mRNAs in DRG was analyzed by real-time PCR (RT-PCR). Whole DRG from each group of rats ($n = 3$ for each group in three independent experiments) were removed under aseptic conditions from lumbar (L4-L5) and cervical (C6-C8) segments of both sides, collected as ipsilateral and contralateral samples and stored in RNA later (Thermo Fisher Scientific, Inc., Waltham, MA, USA) at 4°C. First-strand synthesis was performed using TaqMan[®] High Capacity RNA-to-cDNA Kit and the quality and concentration evaluated by optical density using NanoDrop. PCR amplification, in triplicate for each sample, was performed using ABI Prism 7300, TaqMan[®] Gene Expression Master Mix, and TaqMan[®] Gene Expression Assay Probes FAM[™] (Thermo Fisher Scientific, Inc., Waltham, MA, USA) for the target genes GAP-43 (assay ID—Rn01474579_m1) and SCG-10 (assay ID—Rn00584886_m1). Determinations were made with reference to the reporter gene encoding rat actin (actin, beta—Rn00667869_m1) Endogenous Control (VIC[®]). The polymerase activation step at 95°C for 15 min was followed by 40 cycles of 15 s at 95°C and 60 s at 60°C. The validity of the results was checked by running appropriate negative controls (water instead of cDNA by for PCR amplification; omitting reverse transcriptase for cDNA synthesis). Specific mRNA levels were calculated after normalizing to actin mRNA in each sample. Relative expression was determined using the Comparative Ct Model ($\Delta\Delta Ct$) with actin as the housekeeping gene. Data were presented as relative mRNA units compared with control values (expressed as fold over naïve value).

In vivo Assay of Axon Regeneration in Crushed Ulnar Nerve

Rats with prior operation on SNC ($n = 6$) or CSNT ($n = 6$) for 7 days were re-operated to expose and mobilize a short segment of the right ulnar nerve. The right ulnar nerve was also mobilized in a control group without any previous sciatic nerve injury ($n = 6$). The ulnar nerve was then crushed using a clamp of a defined force of 1.9 N for 2×1 min (Ronchi et al., 2009) under a stereoscopic microscope. The distal margin of the crush injury was indicated with a 10-0 epineurial suture and the skin wound was closed with 5/0 sutures.

To investigate peripheral axon regeneration, the ulnar nerves were removed 1 day after the crush injury following pericardial infusion with Zamboni fixative solution and ulnar nerve samples were fixed by immersion in Zamboni fixative solution overnight. After washing with 10% sucrose in PBS, longitudinal cryostat

sections of 10 μm thickness were cut and immunostained for SCG-10, which is a more selective marker of regenerating sensory axons than GAP-43 (Shin et al., 2014). SCG-10 fluorescence intensity was analyzed along the length of the nerve distal to the crush; the regeneration index was determined by measuring the length of the longest SCG-10 decorated axons from the crush site (Abe et al., 2010). The length of SCG-10+ axons was measured by a person blind to the experimental conditions in every third section using a NIS-Elements image analysis system (Nikon, Czechia).

In vitro Assay of Increased Axonal Outgrowth of Cervical DRG Neurons Induced by Sciatic Nerve Lesion

An *in vitro* culture of dissociated DRG neurons was prepared according to a modified protocol (Christie et al., 2010). Sham-operated rats ($n = 4$) and rats operated by SNC ($n = 4$) or CSNT ($n = 4$) for 7 days were deeply anesthetized by an intraperitoneal application of sodium pentobarbital (70 mg/kg) and killed by decapitation. The DRG of lumbar (L4-L5) and cervical (C6-C8) segments were removed bilaterally under aseptic conditions following laminectomy. The samples were collected in ice-cold $\text{Ca}^{2+}/\text{Mg}^{2+}$ -free Hank's buffered salt solution (CMF-HBSS, Sigma Aldrich), and the spinal roots and connective tissues were removed.

DRG were then dissociated by incubation in medium containing 0.1% collagenase type I (5,000 U/ml) for 90 min followed by 0.25% trypsin/EDTA at 37°C for 25 min. The DRG suspension was prepared by triturating through glass pipette tips, washed twice with Dulbecco's Modified Eagle's Medium/Nutrient F-12 Ham (DMEM/F12) supplemented with 10% fetal bovine serum (FBS; all from Sigma Aldrich) and the suspension was spun for 5 min at 1,500 rpm at 4°C. The cells were resuspended and placed into a culture medium of DMEM/F12 supplemented with 2 mM glutamine, 100 U/ml Penicillin and 100 $\mu\text{g}/\text{ml}$ Streptomycin (all from Sigma Aldrich), N2 and B27 (ThermoFisher Sci., diluted according to the manufacturer's instructions). The cells were re seeded at a density of 200 cells on glass cover slips previously coated with Geltrex[®] (ThermoFisher Sci.).

Cultures were incubated at 37°C in a humidified atmosphere containing 5% CO_2 for 2 days, washed in PBS, fixed by Zamboni solution for 20 min and immunostained with mouse anti- β tubulin III primary antibody (Sigma, 1:500) overnight at 4°C. The cells were then washed in PBS followed by incubation with goat anti-mouse TRITC-conjugated secondary antibody (Life Technologies, 1:1,000) for 90 min. Finally, cells were washed in PBS, stained with Hoechst 33342 to detect cell nuclei and mounted in a Vectashield aqueous mounting medium (Vector Laboratories, Burlingame, CA, USA). Three slides for each experimental group were analyzed under a Nikon Eclipse NI-E epifluorescence microscope equipped with a Nikon DS-Ri1 camera (Nikon, Prague, Czechia) using a 10 \times objective by a person blind to the experimental conditions.

To analyze neurite outgrowth and length, digital images of at least 100 randomly selected nucleate neurons per cover slip

were acquired. Neurites longer than the diameter of the neuronal bodies were analyzed in digital pictures converted to grayscale for better visualization. Neurite outgrowth initiation was quantified as the number of neurites per neuron counted using the Count and Taxonomy module of NIS-Elements software (Nikon, Prague, Czechia). Axonal elongation was analyzed by taking the total length of neurites per neuron when axons of individual neurons were traced and measured using the Neurite Tracer Plugin for ImageJ (Pool et al., 2008). The mean number of neurites per neuron and total neurite length per neuron were calculated from triplicate experiments and data were present as mean \pm SD.

***In vivo* Assay of Axon Regeneration in the Crushed Ulnar Nerve and Changes in the Pro-regenerative State of Cervical DRG Neurons After Intrathecal Injection of IL-6 or JAK2 Inhibitor AG490**

Recombinant rat IL-6 protein (R&D Systems) was dissolved in artificial cerebrospinal fluid (ACSF; Hylden and Wilcox, 1980) at 20 ng/10 μ l. AG490 (Sigma), an inhibitor of JAK2, was dissolved in ACSF at a concentration of 5 μ M.

A solution of IL-6 (10 μ l) or ACSF (10 μ l) along with a further 10 μ l ACSF was injected via a micro syringe into the lumbar subarachnoid space of intact rats ($n = 2$ for each group). Animals were left to survive for 1 day and cervical DRG (C6-C8) were removed following pericardial infusion with Zamboni fixative solution. Longitudinal DRG sections were double immunostained with mouse monoclonal antibody against GAP-43 (1:500; Sigma, USA) and rabbit polyclonal anti-STAT3 (Y705) antibody (1:100; Santa Cruz, CA, USA). The immunofluorescence reaction was visualized by treatment with FITC-conjugated donkey anti-mouse and TRITC-conjugated donkey anti-rabbit secondary antibodies (1:100; Millipore, USA) for 90 min at room temperature. Activation and nuclear translocation of STAT3 as well as GAP-43 immunofluorescence intensity were measured using a NIS-Elements image analysis system (Nikon, Czechia) as described previously.

To investigate *in vivo* the role of IL-6 in triggering the pro-regenerative state in cervical DRG, the right ulnar nerve was crushed as described ($n = 8$). A solution of IL-6 (10 μ l) or ACSF (10 μ l) along with a further 10 μ l ACSF was then injected via a micro syringe into the lumbar subarachnoid space ($n = 4$ for each group). The ulnar nerves were removed 1 day later (after the crush and intrathecal administration of IL-6) and fixed with Zamboni fixative solution. Axon regeneration was assessed on longitudinal cryostat sections (10 μ m thick) immunostained for SCG-10 and analyzed as described.

To test whether the JAK2/STAT3 signaling pathway is involved in inducing the pro-regenerative state of cervical DRG neurons after prior sciatic nerve injury, the right sciatic nerve of 8 rats was cut (CSNT). After 7 days, the rats with prior CSNT were re-operated to expose and crush the right ulnar nerve. 10 μ l of AG490 solution (5 μ M) or ACSF (10 μ l), along with a further 10 μ l ACSF was then injected via a micro syringe into the subarachnoid space of the cisterna magna ($n = 4$ for

each group). The length of regenerated SCG10+ axons was assessed on longitudinal cryostat sections (10 μ m thick) 1 day after the ulnar nerve crush and intrathecal injection of ACSF or AG490 as described above. In addition, cryostat sections of cervical DRG (C6-C8) ipsilateral to the ulnar nerve crush were double immunostained for GAP-43 and STAT3 and analyzed using a NIS-Elements image analysis system (Nikon, Czechia) as described above.

Enzyme-Linked Immunosorbent Assay (ELISA) of IL-6 in Rat Plasma

Three naïve rats and those operated on to create SNC or CSNT for 1, 3, and 7 days ($n = 3$ for each group), as well as sham-operated rats for 3 ($n = 3$) and 7 ($n = 3$) days were sacrificed by CO₂ inhalation. Blood samples were obtained by intracardiac puncture and collected into tubes containing heparin and protease inhibitor cocktail (LaRoche, Switzerland). Plasma was separated by centrifugation (2,500 g for 12 min) and stored at -60°C until analyzed. Total protein was measured by Nanodrop ND-1000 (Thermo Scientific) and the level of IL-6 protein was assessed using an ELISA kit with a sensitivity of 5 pg/ml (BioSource International, USA) according to the manufacturer's instructions. Measurement was carried out on a SUNRISE Basic microplate reader (Tecan, Salzburg, Austria) and the data were normalized as picograms of IL-6 protein to 100 μ g of total protein. IL-6 protein levels were compared to baseline values in plasma from naïve rats, which was arbitrarily set as one. Data were expressed as mean \pm SD.

Statistical Analyses

Statistical differences between data of immunofluorescence intensities, western blot analysis and RT-PCR of naïve DRG neurons and DRG neurons of sham-operated rats or rats with SNC and CSNT were tested using a Mann-Whitney U-test ($p < 0.05$). The same statistical analysis was used to compare IL-6 protein levels in plasma of naïve and sham-operated or SNC- and CSNT-operated rats. The mean number of neurites per neuron and total neurite length per neuron were compared between DRG neurons of sham- and SNC- or CSNT-operated rats using one-way ANOVA and Tukey's *post hoc* test to determine statistical significance. All statistical analyses were performed using STATISTICA 9.0 software (StatSoft, Inc., Tulsa, OK, USA).

RESULTS

Immunohistochemical and Western Blot Analysis of GAP-43 and SCG-10 Proteins

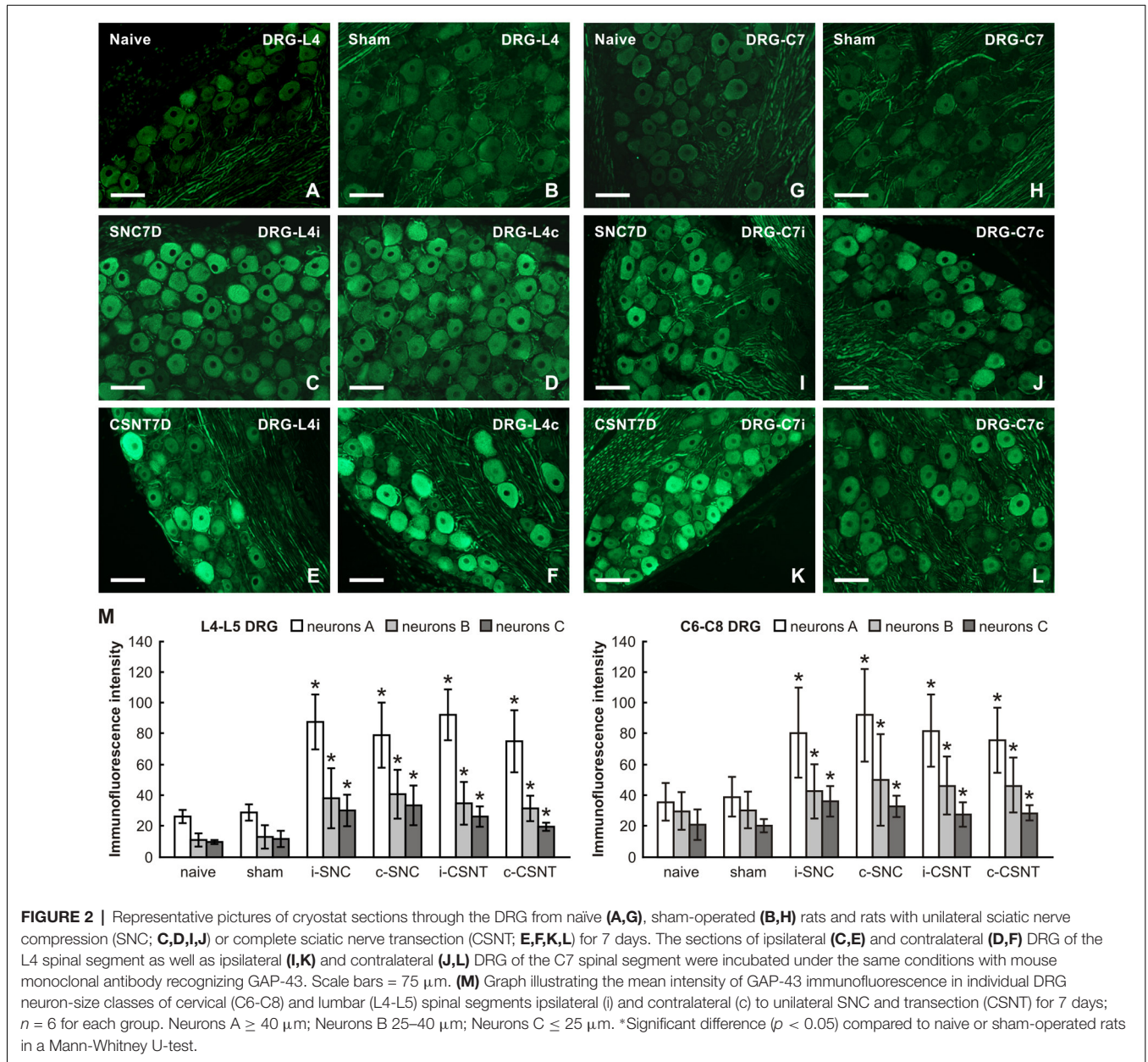
Western blot analysis of GAP-43 in cervical DRG of rats surviving 1, 3, 7, and 14 days after SNC showed the protein level peaked at 7 days with a drop at 14 days when compared to cervical DRG of naïve or sham-operated rats (Figure 1). Therefore, subsequent analyses illustrating the pro-regenerative state of cervical DRG neurons after sciatic nerve lesions were performed in rats 7 days after SNC or CSNT.

The lumbar and cervical DRG neurons of naïve and sham-operated rats displayed a low basal level of GAP-43 immunostaining. GAP-43 immunofluorescence increased strongly in large and medium-sized neurons of both ipsilateral and contralateral lumbar DRG 7 days after SNC and CSNT. Some medium- and small-sized neurons displayed only weak GAP-43 immunopositivity. Sections of cervical DRG also demonstrated a similar pattern of bilaterally increased GAP-43 immunofluorescence (Figure 2).

Image analysis revealed a bilateral increase of mean GAP-43 immunofluorescence intensity in all size-classes of neurons in both lumbar and cervical DRG after unilateral SNC and CSNT in comparison with naïve and sham-operated animals. Sciatic nerve injury induced a greater increase

in GAP-43 immunofluorescence intensity in large neurons than in medium- and small-sized neurons of both lumbar and cervical DRG. Further, a more significant increase in GAP-43 immunofluorescence was measured bilaterally in lumbar (3.3–2.6 times) than in cervical DRG neurons (2.5–1.9 times) compared to naïve or sham-operated rats. However, no significant differences were found between individual size-classes of neurons in the SNC and CSNT experimental groups (Figure 2M).

Basal SCG-10 immunofluorescence was very low or absent in the lumbar and cervical DRG neurons of naïve rats. Most neurons of all sizes in lumbar and cervical DRG of both sides displayed significantly enhanced SCG-10 immunofluorescence intensity 7 days after SNC and CSNT compared to DRG



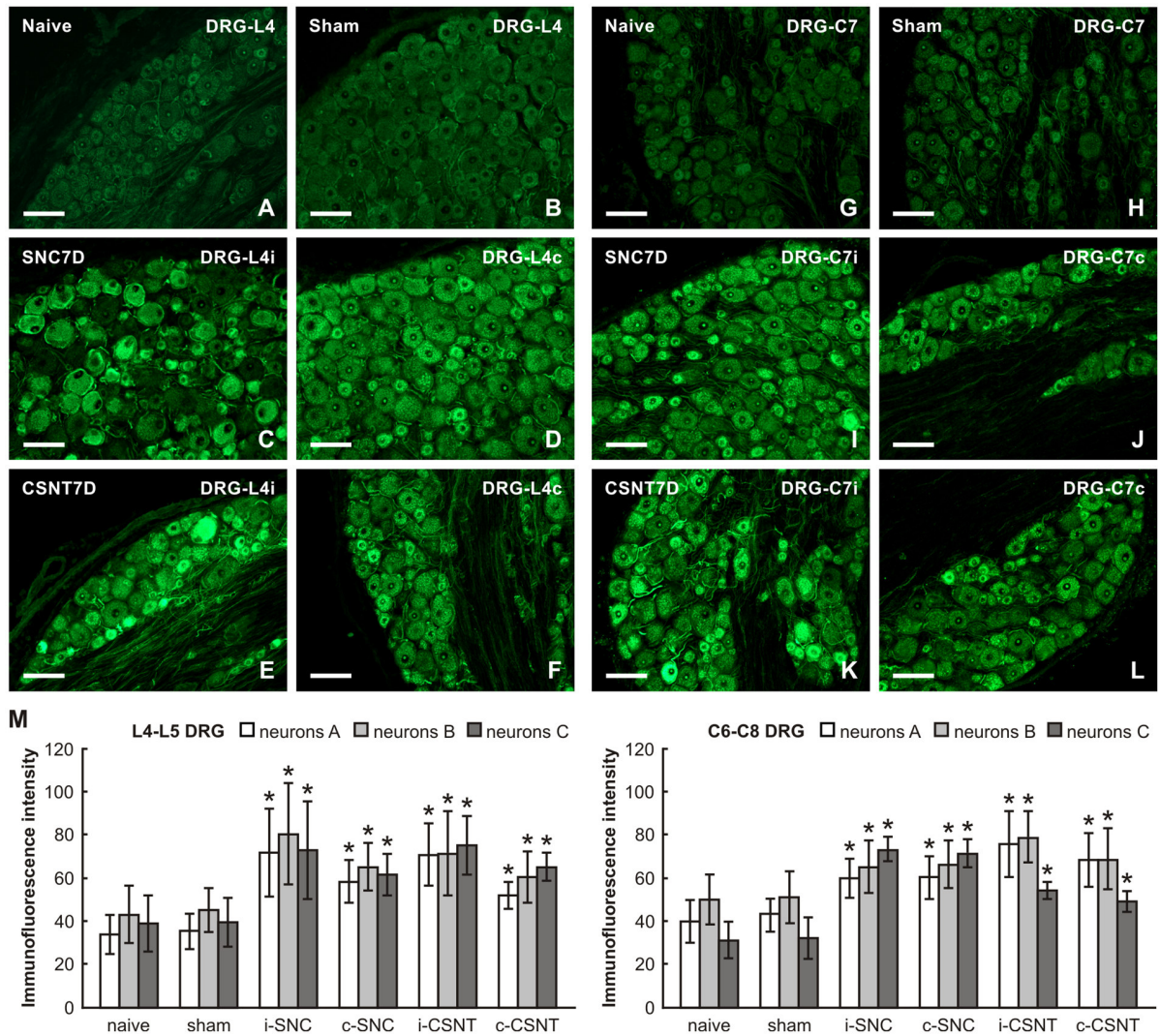


FIGURE 3 | Representative pictures of cryostat sections through the DRG from naïve (A,G), sham-operated (B,H) rats and rats with unilateral SNC (C,D,I,J) or CSNT (E,F,K,L) for 7 days. The sections of ipsilateral (C,E) and contralateral (D,F) DRG of the L4 spinal segment as well as ipsilateral (I,K) and contralateral (J,L) DRG of the C7 spinal segment were incubated under the same conditions with rabbit polyclonal antibody recognizing superior cervical ganglion-10 (SCG-10). Scale bars = 75 μm. (M) Graph illustrating the mean intensity of SCG-10 immunofluorescence measured in individual DRG neuron-size classes of cervical (C6-C8) and lumbar (L4-L5) spinal segments ipsilateral (i) and contralateral (c) to unilateral SNC and transection (CSNT) for 7 days; n = 6 for each group. Neurons A ≥ 40 μm; Neurons B 25–40 μm; Neurons C ≤ 25 μm. *Significant difference (p < 0.05) compared to naïve or sham-operated rats in a Mann-Whitney U-test.

from naïve or sham-operated rats. However, the increase in SCG-10 immunofluorescence intensity was lower than for GAP-43 (approximately 1.8–2 times in lumbar and 1.4–2.3 times in cervical DRG; Figures 3A–L). Moreover, image analysis of SCG-10 immunofluorescence intensity did not show any preferential increase among individual size-classes of DRG neurons (Figure 3M).

The increased levels of GAP-43 and SCG-10 proteins induced by SNC and CSNT and detected in the lumbar and cervical DRG of both sides by quantitative immunohistochemistry were verified by western blot analysis. Total GAP-43 and SCG-10 proteins were also significantly increased bilaterally in both lumbar and cervical DRG after unilateral SNC and CSNT for

7 days compared to naïve or sham-operated controls. Seven days after SNC or CSNT, the levels of GAP-43 protein were increased bilaterally in the lumbar and cervical DRG about two-to-three times compared to naïve and sham-operated controls. As was expected, GAP-43 protein levels shot up significantly in lumbar DRG after CSNT than SNC. Levels of GAP-43 protein in cervical DRG also increased significantly compared to controls, but the elevation was not to the extent seen in lumbar DRG (Figures 4A,B).

GAP-43 is activated by protein kinase C-mediated phosphorylation at serine 41 (S41) that promotes the polymerization and stabilization of filamentous actin (F-actin) related to axon growth and sprouting (Tsai et al., 2007).

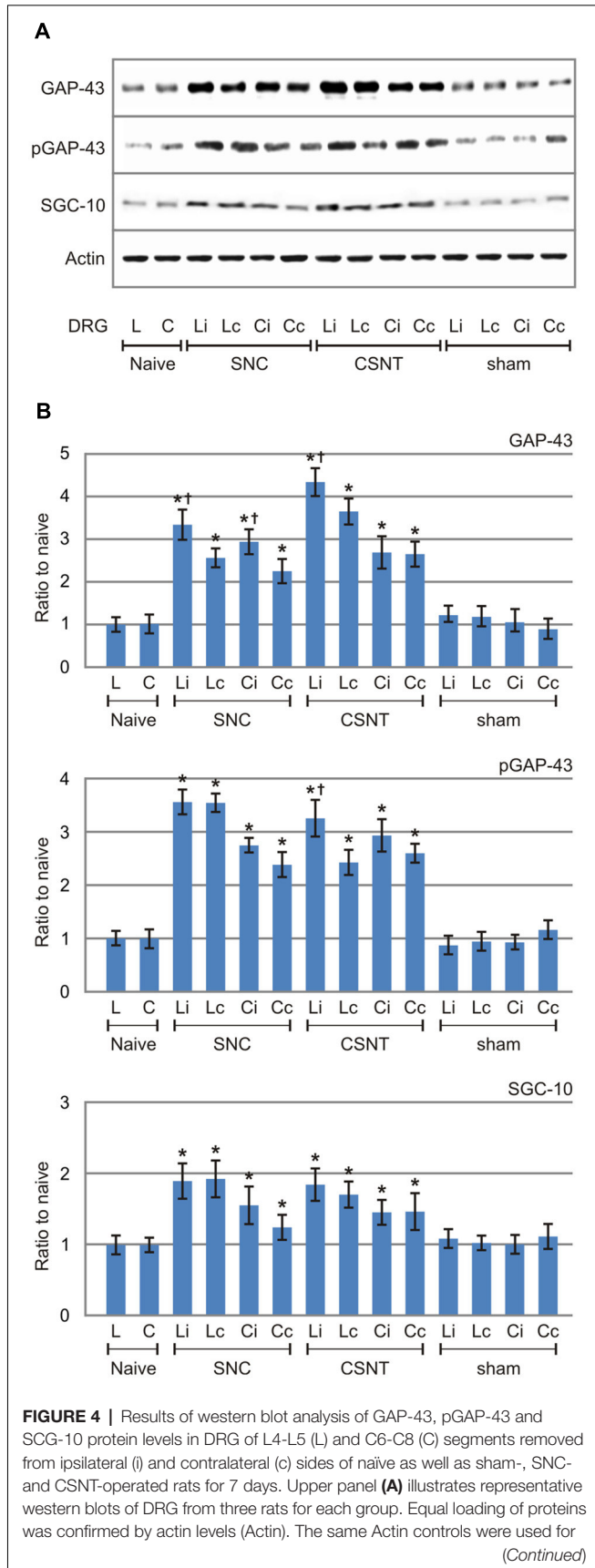


FIGURE 4 | Continued analysis of GAP-43, pGAP-43 and SCG-10 protein levels in this set representative western blots. Lower panels (B) show densitometry of individual protein bands after normalization to actin from three independent experiments; the intensities of the bands from naïve DRG were as arbitrarily set to 1. *Significant difference ($p < 0.05$) when compared to sham-operated rats; †Significant difference ($p < 0.05$) compared to contralateral DRG in a Mann-Whitney U-test.

Although in our experiments we used an antibody recognizing both unphosphorylated and phosphorylated GAP-43, the western blot analysis verified levels of activated GAP-43 using a specific antibody against phosphorylated GAP-43 (pGAP-43). The results demonstrated that activated pGAP-43 was increased bilaterally not only in lumbar but also in cervical DRG after SNC or CSNT compared to naïve or sham-operated controls. The magnitude of pGAP-43 increase was very similar to the increased GAP-43 levels. However, in contrast to significantly higher GAP-43 protein levels in ipsilateral than contralateral lumbar DRG after both SNC and CSNT, pGAP-43 protein level was significantly higher only in ipsilateral lumbar DRG after CSNT (Figures 4A,B).

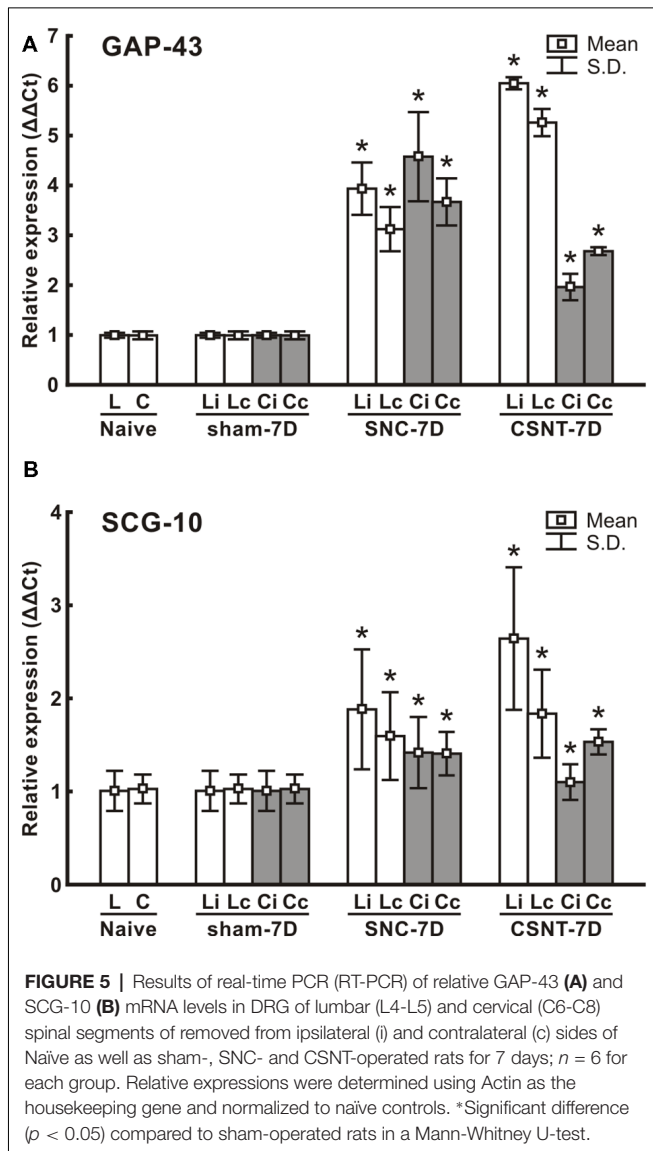
In contrast to GAP-43 and pGAP-43, the increase in levels of SCG-10 was less marked (about 1.5–1.8-fold) and the increase was more or less the same on both sides. Moreover, no significant differences in SCG-10 levels were found in lumbar DRG from SNC- and CSNT-operated animals. Similar protein levels of SCG-10 were also measured in cervical DRG after SNC and CSNT, as in the case of GAP-43 and pGAP-43 (Figures 4A,B).

RT-PCR Analysis of GAP-43 and SCG-10 mRNA

RT PCR was used to determine the levels of the relevant GAP-43 and SCG-10 mRNA in cervical and lumbar DRG 7 days after unilateral sciatic nerve injury by SNC or CSNT. Samples of cervical and lumbar DRG from sham-operated animals displayed no significant changes in SCG-10 and GAP-43 mRNA levels compared to naïve controls.

Levels of GAP-43 and SCG-10 mRNAs were significantly increased bilaterally in both cervical and lumbar DRG 1 week following sciatic nerve injury by SNC or CSNT compared to naïve or sham-operated controls. GAP-43 mRNA increased bilaterally in lumbar DRG to a higher level after CSNT than SNC. However, a statistically significant difference between ipsilateral and contralateral lumbar DRG was found only in the CSNT group. In contrast to lumbar DRG, cervical ones displayed a bilateral increase of GAP-43 mRNA that was greater after SNC than after CSNT.

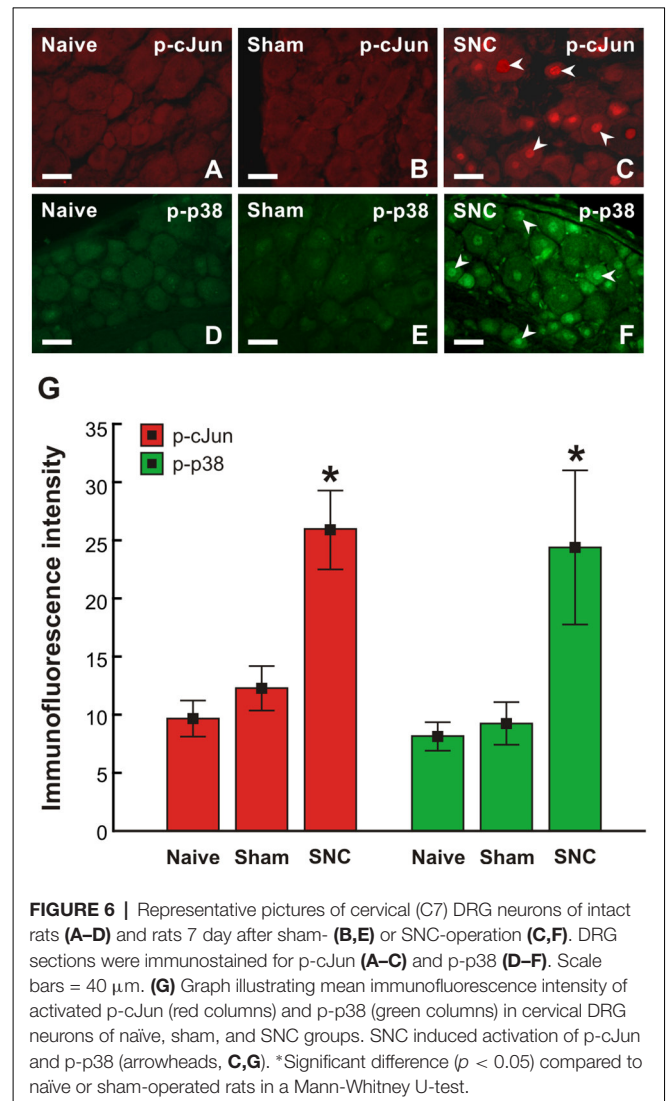
Similar to the GAP-43 and SCG-10 protein results, RT-PCR revealed a substantially smaller increase in SCG-10 mRNA levels in lumbar DRG (only up to 2.6-fold of sham-operated controls) than was measured for GAP-43 mRNA. Levels of SCG-10 mRNA were higher bilaterally in lumbar DRG after CSNT than after SNC, but the differences were not statistically significant. Both SNC and CSNT induced an approximately similar elevation of SCG-10 mRNA in cervical DRG of



both sides compared to naïve and sham-operated controls (Figure 5).

Sciatic Nerve Lesion Induced Activation of cJun and p38 MAPK in Cervical DRG Neurons

To confirm the sciatic nerve injury-induced pro-regenerative state of cervical DRG neurons demonstrated by GAP-43 and SCG10 analyses, activation of p-cJun and p-p38 MAPK was also investigated. Basal p-cJun and p-p38 MAPK immunofluorescence was very low in cervical DRG neurons of naïve and sham-operated rats. Sciatic nerve lesion increased immunofluorescence intensity of both p-cJun and p-p38 MAPK in the nuclei of cervical DRG neurons. Further, a higher intensity of p-p38 MAPK immunofluorescence was seen in the soma of neurons (Figure 6).

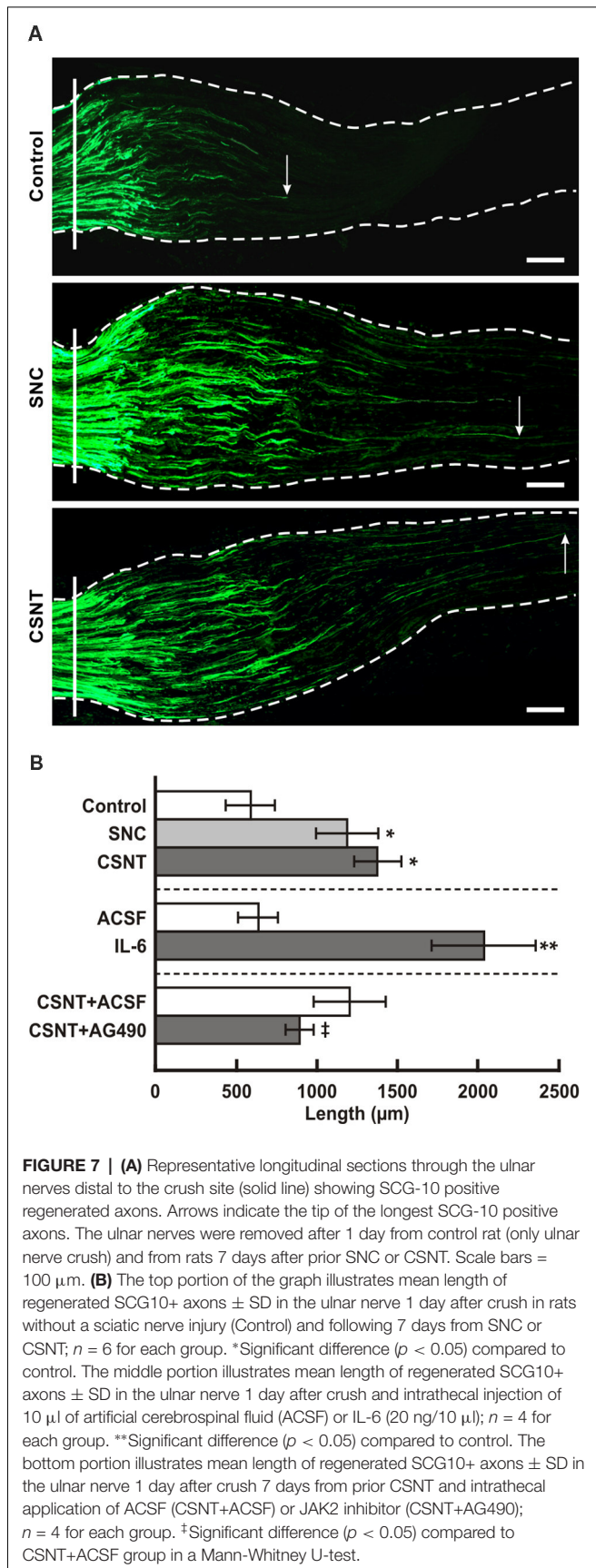


Axon Regeneration Assay in Crushed Ulnar Nerve After Prior Sciatic Nerve Injury

The axonal regeneration capacity of cervical DRG neurons was investigated in longitudinal sections of one-day-old crushed ulnar nerves by immunostaining for SCG-10—a specific marker for regenerated axons of primary sensory neurons (Shin et al., 2014). Axon regeneration index expressed as SCG-10+ axon extension from the point of nerve crush was greater in SNC- and CSNT-operated rats compared to control rats with only ulnar nerve crush (Figures 7A,B).

In vitro Assay of Axonal Outgrowth Capacity of Cervical DRG Neurons After Sciatic Nerve Injury

The increased capacity of cervical DRG neurons to regenerate their axons after prior sciatic nerve injury was verified by an *in vitro* assay of neurite outgrowth in DRG neurons taken from sham-, SNC- and CSNT-operated rats (Figures 8A–F). The diameter of neuronal bodies cultivated *in vitro* was between



25 and 45 μ m, thus encompassing all morphological classes of DRG neurons.

The mean number of neurites per neuronal body of cervical and lumbar DRG taken from sham-operated rats was very similar. Compared to cervical DRG neurons of sham-operated rats, the number of neurites sent off by cervical DRG neurons taken from SNC- and CSNT-operated rats was significantly higher. Surprisingly, cervical and contralateral lumbar DRG neurons displayed higher neurite outgrowth than lumbar DRG neurons ipsilateral to CSNT (7.0 ± 2.1 and 7.0 ± 1.7 compared to 4.6 ± 1.5 ; **Figure 8G**).

The total length of neurites per neuron was significantly larger in neurons from lumbar DRG of both sides and those cultivated from cervical DRG 7 days after SNC. Seven days after CSNT, the total neurite length per neuron was significantly larger in neurons cultivated from cervical and contralateral lumbar DRG, but not in neurons cultivated from ipsilateral lumbar DRG (**Figure 8H**).

IL-6 Protein Level in Plasma

IL-6 protein levels increased significantly in the plasma of sham-operated rats at 3 days but returned to normal by 7 days after treatment. Plasma IL-6 levels were elevated also in SNC and CSNT rats at 1 and 3 days but dropped back close to normal 7 days after sciatic nerve lesions (**Figure 9**). These IL-6 plasma level measurements are consistent with our previous results following SNC (Dubový et al., 2013) and indicate that IL-6 in the blood is likely not inducing the pro-regenerative state in cervical DRG neurons 7 days after sciatic nerve lesion.

Axon Regeneration Assay in Crushed Ulnar Nerve and Changes in the Pro-regenerative State in Cervical DRG Neurons After Intrathecal Application of IL-6 and JAK2 Inhibitor

To investigate if IL-6 is responsible for activation of the pro-regenerative state of rat cervical DRG neurons, we intrathecally applied IL-6. We showed previously that intrathecal application of IL-6 induced activation and nuclear translocation of STAT3 in DRG neurons (Dubový et al., 2018a). In the present experiments, we observed that intrathecal injection of IL-6 increased not only the activation of STAT3 but also the expression of GAP-43 in intact DRG neurons. In contrast, application of AG490 after CSNT and ulnar nerve crush resulted in decreased STAT3 activation and expression of GAP-43 in cervical DRG (**Figure 10**).

In addition, we measured the lengths of SCG-10+ regenerated axons distal to the ulnar nerve crush following intrathecal IL-6 application. The regenerated axons were significantly longer compared to control ulnar nerve crush or nerve crush and subsequent intrathecal injection of ACSF (**Figure 7B**, the middle portion). The pro-regenerative state of neurons is mediated by phosphorylation of STAT3 at the Y705 position by JAK2 (Schwaiger et al., 2000; Qiu et al., 2005; Niemi et al., 2016). When an inhibitor of JAK2 (AG490) was applied intrathecally in rats with ulnar nerve crush for a day following prior CSNT, SCG-10+ regenerated axons were significantly shorter compared to those

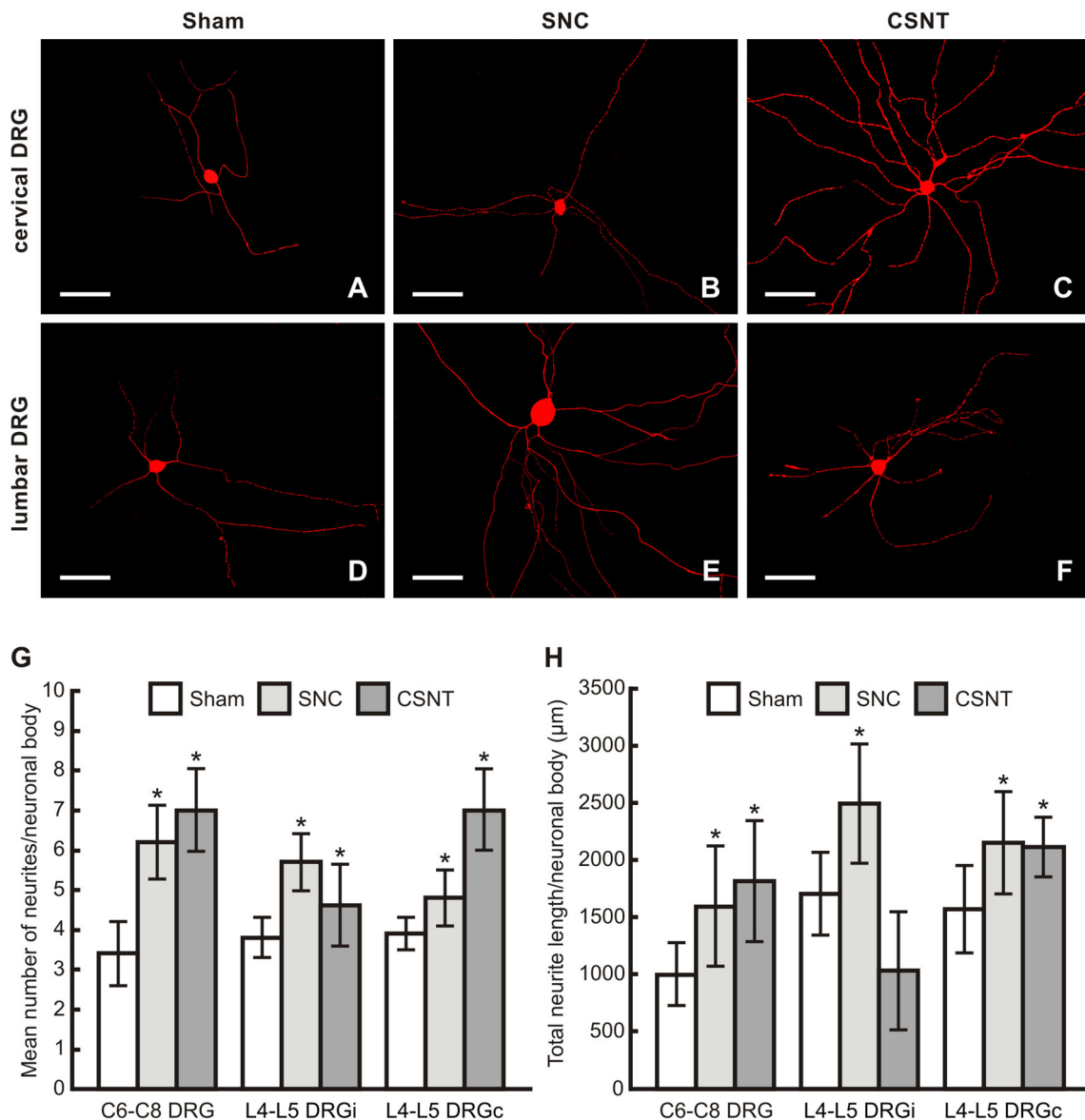


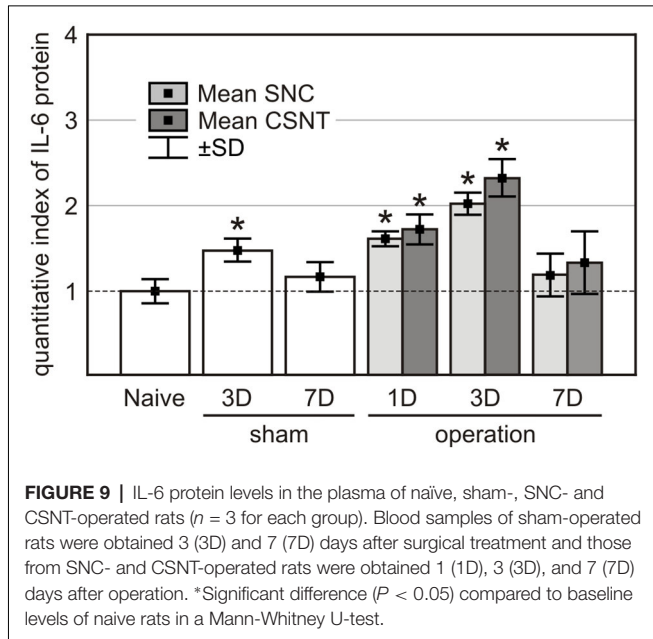
FIGURE 8 | (A–F) Representative pictures of cervical (C6–C8) and lumbar (L4–L5) DRG neurons of the ipsilateral side dissociated and cultured *in vitro* after removing of DRG from sham-, SNC- or CSNT-operated rats for 7 days. The DRG neurons were fixed and immunostained for β III-tubulin after 2 days of *in vitro* incubation. Scale bars = 75 μ m. The graphs illustrate mean number of neurites (**G**) and total neurite length (**H**) per neuronal body of *in vitro* cultivated DRG neurons of cervical (C6–C8) and lumbar (L4–L5) spinal segments from the ipsilateral (i) and contralateral (c) sides removed from sham-, SNC- and CSNT-operated rats ($n = 4$ for each group). At least 100 randomly selected neurons with nuclei per cover slip were measured. *Significant difference ($p < 0.05$) compared to sham-operated controls in a Mann-Whitney U-test.

of the rats subjected to CSNT and subsequent ulnar nerve crush and intrathecal injection only of ACSF (Figure 7B, the bottom portion).

DISCUSSION

Activation of the neuronal regenerative program after axon injury is an important prerequisite for useful reinnervation and functional recovery. This pro-regenerative status of the neurons is linked with the upregulation of regeneration-associated

molecules (Ma and Willis, 2015). For example, regeneration-associated proteins like GAP-43 and SCG-10 are frequently used as molecular markers of the pro-regenerative state of neurons induced by experimental nerve injury. The DRG neurons are a useful model for studying the induction of the regeneration-associated program marked by increased levels of GAP-43 and SCG-10 mRNA and protein (Mason et al., 2002; Shin et al., 2014). The DRG neurons of naïve rats display a low basal level of GAP-43 or SCG-10 immunostaining that is significantly increased in the neuronal bodies over a long period after sciatic



nerve injury (Stewart et al., 1992; Schreyer and Skene, 1993; Shin et al., 2014; Dubový et al., 2018b).

GAP-43 immunostaining is a widely used marker for regenerating axons in experimental models of peripheral nerve injury. Apart from regenerating axons, intense GAP-43 immunoreactivity is also present in Schwann and Schwann-derived cells (Plantinga et al., 1993; Dubovy and Aldskogius, 1996). This GAP-43 immunostaining of Schwann cells associated with regenerated axons makes their detection difficult, especially during early periods of axon regeneration (Dubový et al., 2018b). In contrast to GAP-43, SCG-10 is transported from the soma to the proximal axonal stump very early after axotomy, whereas it is rapidly lost in distal axon stumps (Tataruk et al., 2006; Shin et al., 2012, 2014). In contrast to GAP-43, which labels regenerated axons after 3 days (Sar Shalom and Yaron, 2014), SCG-10 immunostaining is rapidly increased in proximal axonal stumps and regenerating sprouts within hours after axotomy (Shin et al., 2012, 2014). Moreover, SCG-10 is a marker for regenerated sensory axons of injured peripheral nerves (Shin et al., 2014). Therefore, we monitored GAP-43 and SCG-10 mRNA and protein to prove the pro-regenerative state of DRG neurons, and SCG-10 was used to assess axon regeneration distal to ulnar nerve crush after 1 day.

Unilateral Sciatic Nerve Lesion Induced Pro-regenerative State in Both Lumbar and Cervical DRG

Subpopulations of rat DRG neurons can be classified according their size, their cytological, chemical and physiological properties (Lawson, 2002) and behave differently with respect to their regeneration capacity as well as the expression of molecular regeneration markers (Bonilla et al., 2002; Leclere et al., 2007; Shin and Cho, 2017). Classically, DRG neurons are divided into large-, medium- and small-sized (Lawson et al., 1974)

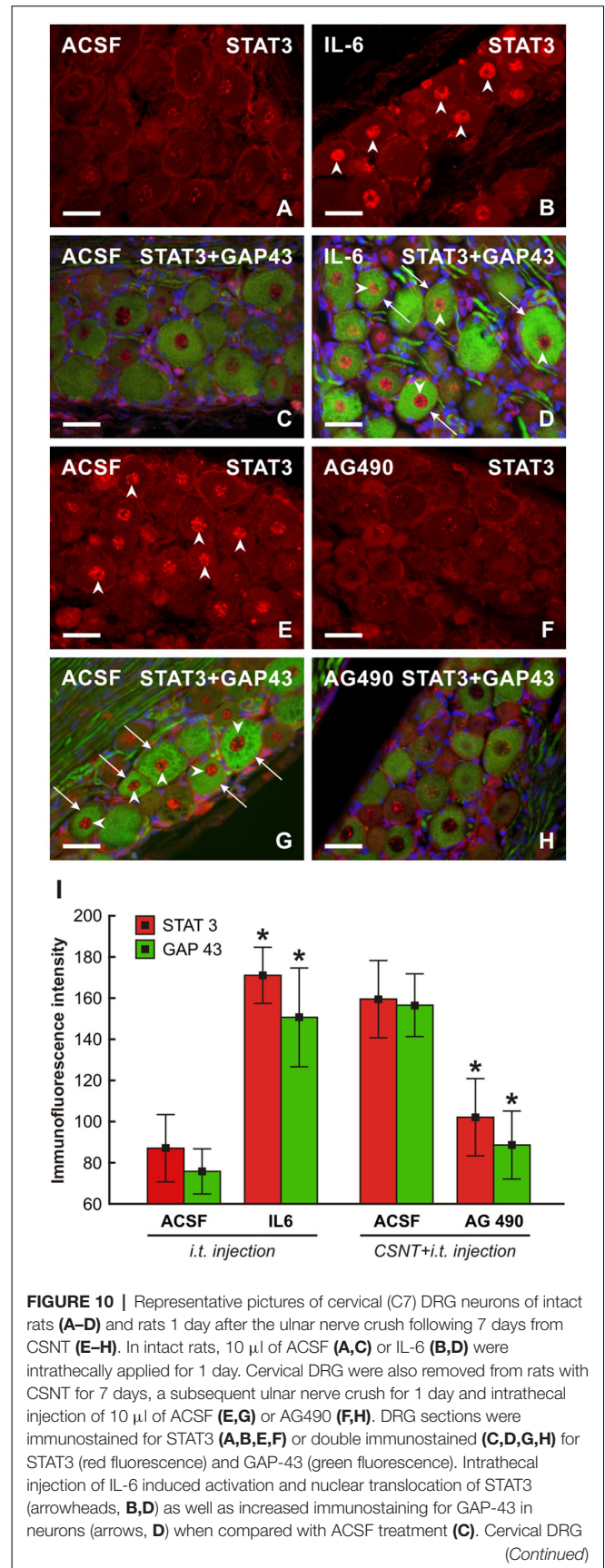


FIGURE 10 | Continued

neurons of rats following the ulnar nerve crush 7 days after CSNT displayed activation and nuclear translocation of STAT3 (**E,G**) and intense GAP-43 immunofluorescence in the neurons when injected with ACSF (**G**, arrowheads and arrows, respectively) while intrathecal application of AG490 resulted in a marked reduction of STAT3 activation and GAP-43 immunostaining (**F,H**). Scale bars = 40 μ m. (**I**) Graph illustrating mean immunofluorescence intensity of activated STAT3 and GAP-43 in cervical DRG neurons of intact rats following intrathecal application of ACSF or IL-6 for 1 day and rats with CSNT for 7 days and intrathecal injection of ACSF or AG490. *Significant difference ($P < 0.05$) compared with ACSF-treated rats in a Mann-Whitney U-test.

and may also be identified by further molecular phenotyping. Quantitative immunohistochemical staining revealed increased GAP-43 and SCG-10 immunofluorescence in both lumbar and cervical DRG neurons ipsilateral as well as contralateral to the SNC or CSNT. Detailed image analysis showed that the predominant increase of GAP-43 immunofluorescence intensity was seen in the large-sized neuronal subpopulation of both lumbar and cervical DRG. In contrast, a similar elevation of SCG-10 immunofluorescence intensity was observed in all size-classes neurons of DRG in the lumbar and cervical spinal cord segments. Principally, bilateral increase of GAP-43 and SCG-10 proteins detected by quantitative immunohistochemical staining in both lumbar and cervical DRG neurons after sciatic nerve lesion was verified by measuring whole GAP-43 and SCG-10 protein levels using western blot analysis. Further, it also revealed that unilateral sciatic nerve lesion induced bilateral elevation of activated (phosphorylated) GAP-43 in both lumbar and cervical DRG.

The pro-regenerative state of DRG neurons in both lumbar and cervical spinal cord segments was confirmed by increased levels of GAP-43 and SCG-10 mRNA. Although SCG-10 is considered a better marker of the pro-regenerative state of DRG neurons (Shin et al., 2014; Dubový et al., 2018b), increases in the levels of GAP-43 mRNA and protein were more distinct compared to naïve or sham-operated rats in both lumbar and cervical DRG after SNC or CSNT for 7 days. Our observation of a bilateral increase in GAP-43 and SCG-10 mRNA and proteins correlates well with published results indicating that NGF mRNA is bilaterally increased in both cervical and lumbar DRG after unilateral sciatic nerve crush (Heumann et al., 1987; Wells et al., 1994). These results suggest that upregulation of growth-associated molecules is not restricted to axotomized DRG neurons and probably reflects a systemic response of DRG neurons to unilateral sciatic nerve injury (Dubový et al., 2013, 2018a).

The expression of regeneration-associated proteins like GAP-43 or SCG10 is operated by transcription factors, such as c-Jun (Raivich et al., 2004; Frey et al., 2015; Valakh et al., 2015) or members of the MAPK family, e.g., p38 (Verma et al., 2005; Temporin et al., 2008; Nix et al., 2011; Law et al., 2016). Our results showing increased levels of GAP-43 and SCG10 as well as activation of p-cJun and p-p38 in cervical DRG after sciatic nerve injury suggested that the pro-regenerative program can be induced in remote cervical DRG neurons 7 days after sciatic nerve lesion.

Increased *in vivo* and *in vitro* Axon Regeneration Capacity of Cervical DRG Neurons Confirmed Their Pro-regenerative State Induced by Prior Sciatic Nerve Lesion

While SCG-10 increases only in the proximal stumps of afferent axons (Shin et al., 2014), we also measured SCG-10 in regenerated peripheral arms of afferent axons associated with cervical DRG neurons distal to the ulnar nerve crush. SCG-10 immunopositive axons displayed a significantly greater length from the point of ulnar nerve crush after prior SNC or CSNT than in controls without the conditioning lesion. These results demonstrated *in vivo* the enhanced pro-regenerative state of cervical DRG neurons corresponding with increased levels of GAP-43 or SCG-10 induced by the conditioning sciatic nerve lesion.

Neurite outgrowth assays are used to assess the effects of *in vivo* manipulations performed prior to removing DRG from animals (Frey et al., 2015; Al-Ali et al., 2017). In our *in vitro* assay, the number of neurites and their total lengths per neuron were significantly higher in cervical DRG neurons removed from rats subjected to SNC or CSNT than those from sham-operated controls. The results of the *in vitro* assay confirmed the enhanced capacity of cervical DRG neurons to regenerate their neurites after the conditioning sciatic nerve lesion.

Thus, the axon outgrowth tested *in vivo* and *in vitro* proves the initiation of pro-regenerative state in cervical DRG neurons non-associated with sciatic nerve lesion. Our present results extend previously published results that unilateral nerve injury affects the uninjured contralateral nerve with respect to expression of inflammatory mediators (Ruohonen et al., 2002) including *in vivo* promotion of axonal regeneration in the contralateral nerve associated with enhanced cytokine expression in the contralateral DRG (Ryoke et al., 2000).

IL-6 Is a Candidate for Signaling the Pro-regenerative Neuronal State in Remote DRG After Sciatic Nerve Lesion

In response to unilateral sciatic nerve injury, mRNA and protein levels of IL-6 and its receptors were enhanced bilaterally in primary sensory neurons not only in DRG of lumbar segments (L4-L5) associated with the injury, but also in cervical segments (C7-C8) not associated with the injured nerve (Brázda et al., 2013; Dubový et al., 2013). Upon binding to its membrane-bound receptor (IL-6R), IL-6 connects the intracellular regions of gp130 to initiate a signal transduction cascade by activating signal transducer and activator of transcription 3 (STAT3; Eulenfeld et al., 2012). Activation of STAT3 by JAK2-dependent phosphorylation at the tyrosine-705 (Y705) position occurs in DRG neurons after a nerve lesion and is mediated by neurotrophic cytokines including IL-6 (Schwaiger et al., 2000; Sheu et al., 2000; Qiu et al., 2005; Miao et al., 2006) and neurotrophins (Ng et al., 2006; Pellegrino and Habecker, 2013). We found STAT3 activation and nuclear translocation bilaterally in the DRG neurons of both lumbar and cervical spinal cord segments after unilateral SNC or CSNT. Moreover,

we also proved increased levels of IL-6 protein in the CSF following nerve injury as well as activation and nuclear translocation of STAT3 in DRG neurons along the neuroaxis after intrathecal injection of IL-6 (Dubový et al., 2018a). It is known that activation of STAT3 by JAK2 phosphorylation is a prerequisite for the synthesis of regeneration-associated proteins like GAP-43 or SCG-10 (Patodia and Raivich, 2012) and axon regeneration (Bareyre et al., 2011; Niemi et al., 2016). Intrathecal application of IL-6 in our present experiments increased STAT3 activation and GAP-43 expression in cervical DRG neurons, while a JAK2 inhibitor (AG490) decreased STAT3 activation and nuclear translocation as well as expression of GAP-43.

Intrathecal delivery of IL-6 promotes regeneration of the central arms of afferent axons into the spinal dorsal cord. This then activates the neuronal regeneration program in DRG neurons to overcome inhibitors of axon regeneration present in myelin (Cao et al., 2006). Therefore, in our experiments we tested *in vivo* the effect of intrathecal IL-6 and JAK2 inhibitor injection on axon regeneration after an ulnar nerve crush to illustrate the pro-regenerative state of cervical DRG neurons. Intrathecal IL-6 injection significantly increased the lengths of SCG-10+ regenerated axons distal to the ulnar nerve crush. In contrast, intrathecal application of AG490 reduced the lengths of regenerated axons after the ulnar nerve crush following prior unilateral SNC or CSNT. These results suggested a critical role for the JAK/STAT signaling pathway activated by IL-6 in inducing the pro-regenerative state in remote DRG neurons after unilateral sciatic nerve lesion.

What remains unclear is the mode of activation of remote DRG neurons following a conditioning unilateral sciatic nerve lesion. Axonal transport of local WD signaling molecules would be implicated only on the ipsilateral side of the compressed nerve (SNC) but can be excluded when the similar bilateral changes were found in CSNT group of rats. We observe bilateral changes in DRG of both lumbar and cervical segments, and this rather points towards a systemic pathway through either the blood stream or the CSF. The low level of IL-6 in the plasma of rats 7 days after SNC or CSNT suggests that it is more likely to be via the CSF. We found previously that rat DRG have no barrier to the CSF of the spinal subarachnoid space (Joukal et al., 2016). Therefore, intrathecal injection of IL-6 with subsequent activation of STAT3 in cervical DRG neurons (Dubový et al., 2018a) can trigger upregulation of GAP-43 and SCG-10 associated with the pro-regenerative state of these neurons. A unilateral sciatic nerve lesion induces increased IL-6 synthesis in the corresponding lumbar DRG (Murphy et al., 1995; Dubový et al., 2013) and the cytokine molecules can be released

into the subarachnoid space and transported via CSF into the remote DRG to activate STAT3 (Dubový et al., 2018a) and this then induces the neuronal pro-regenerative state.

Finally, our results indicate that the pro-regenerative state of cervical DRG neurons illustrates a systemic reaction along the neuroaxis to unilateral sciatic nerve injury, and that this reaction can be mediated by IL-6 and JAK2/STAT3 signaling. Moreover, the results suggest a role for inflammatory mediators in activating the neuronal pro-regenerative state without direct retrograde axonal transport of signaling molecules from the injured nerve.

CONCLUSION

In the present study, we have demonstrated that sciatic nerve lesion for 7 days triggers bilateral activation of a pro-regenerative state not only in the primary sensory neurons of lumbar DRG (L4-L5) associated with injured nerve but also in remote cervical DRG. The bilateral activation of the pro-regenerative state in DRG neurons anatomically non-associated with the injured nerve correlates well with our previous observation of bilateral expression of IL-6 and activation of STAT3. Taken together, these results indicate that the systemic reaction of DRG neurons to a unilateral nerve lesion along the neuroaxis can be mediated by IL-6 and JAK2/STAT3 signaling. This phenomenon can be activated also by other molecules released into the CSF of the perispinal subarachnoid space by neurons and non-neuronal cells in DRG associated with the injured nerve.

AUTHOR CONTRIBUTIONS

PD designed the research and wrote the article. IK, IH-S and MJ performed *in vivo* experiments and prepared samples for immunohistochemistry, western blot and RT-PCR and wrote the corresponding texts. MK performed *in vitro* experiments and prepared samples for immunohistochemistry and wrote the corresponding text. VB performed and analyzed western blot and RT-PCR data and wrote the corresponding text.

FUNDING

This work was supported by grant No. 16-08508S of The Czech Science Foundation (Grantová Agentura České Republiky).

ACKNOWLEDGMENTS

We thank Ms. Dana Kutějová, Ms. Marta Lněničková, Ms. Jitka Mikulášková, Mgr. Jana Vachová and Mr. Lumír Trenčanský for their skillful technical assistance.

REFERENCES

- Abe, N., Borson, S. H., Gambello, M. J., Wang, F., and Cavalli, V. (2010). Mammalian target of rapamycin (mTOR) activation increases axonal growth capacity of injured peripheral nerves. *J. Biol. Chem.* 285, 28034–28043. doi: 10.1074/jbc.m110.125336
- Al-Ali, H., Beckerman, S. R., Bixby, J. L., and Lemmon, V. P. (2017). *In vitro* models of axon regeneration. *Exp. Neurol.* 287, 423–434. doi: 10.1016/j.expneurol.2016.01.020
- Bareyre, F. M., Garzorz, N., Lang, C., Misgeld, T., Buning, H., and Kerschensteiner, M. (2011). *In vivo* imaging reveals a phase-specific role of STAT3 during central and peripheral nervous system axon regeneration. *Proc. Natl. Acad. Sci. U S A* 108, 6282–6287. doi: 10.1073/pnas.1015239108
- Bonilla, I. E., Tanabe, K., and Strittmatter, S. M. (2002). Small proline-rich repeat protein 1A is expressed by axotomized neurons and promotes axonal outgrowth. *J. Neurosci.* 22, 1303–1315. doi: 10.1523/jneurosci.22-04-01303.2002

- Brázda, V., Klusáková, I., Sviženská, I. H., and Dubovy, P. (2013). Dynamic response to peripheral nerve injury detected by *in situ* hybridization of IL-6 and its receptor mRNAs in the dorsal root ganglia is not strictly correlated with signs of neuropathic pain. *Mol. Pain* 9:42. doi: 10.1186/1744-8069-9-42
- Brazda, V., Muller, P., Brozkova, K., and Vojtesek, B. (2006). Restoring wild-type conformation and DNA-binding activity of mutant p53 is insufficient for restoration of transcriptional activity. *Biochem. Biophys. Res. Commun.* 351, 499–506. doi: 10.1016/j.bbrc.2006.10.065
- Cafferty, W. B. J., Gardiner, N. J., Gavazzi, I., Powell, J., McMahon, S. B., Heath, J. K., et al. (2001). Leukemia inhibitory factor determines the growth status of injured adult sensory neurons. *J. Neurosci.* 21, 7161–7170. doi: 10.1523/jneurosci.21-18-07161.2001
- Cao, Z. X., Gao, Y., Bryson, J. B., Hou, J. W., Chaudhry, N., Siddiq, M., et al. (2006). The cytokine interleukin-6 is sufficient but not necessary to mimic the peripheral conditioning lesion effect on axonal growth. *J. Neurosci.* 26, 5565–5573. doi: 10.1523/jneurosci.0815-06.2006
- Chandran, V., Coppola, G., Nawabi, H., Omura, T., Versano, R., Huebner, E. A., et al. (2016). A systems-level analysis of the peripheral nerve intrinsic axonal growth program. *Neuron* 89, 956–970. doi: 10.1016/j.neuron.2016.01.034
- Christie, K. J., Webber, C. A., Martinez, J. A., Singh, B., and Zochodne, D. W. (2010). PTEN inhibition to facilitate intrinsic regenerative outgrowth of adult peripheral axons. *J. Neurosci.* 30, 9306–9315. doi: 10.1523/jneurosci.6271-09.2010
- Dubovy, P., and Aldskogius, H. (1996). Growth-associated protein (GAP-43) in terminal Schwann cells of rat Pacinian corpuscles. *Neuroreport* 7, 2147–2150. doi: 10.1097/00001756-199609020-00017
- Dubový, P., Brázda, V., Klusáková, I., and Hradilová-Sviženská, I. (2013). Bilateral elevation of interleukin-6 protein and mRNA in both lumbar and cervical dorsal root ganglia following unilateral chronic compression injury of the sciatic nerve. *J. Neuroinflammation* 10:55. doi: 10.1186/1742-2094-10-55
- Dubový, P., Hradilová-Sviženská, I., Klusáková, I., Kokošová, V., Brázda, V., and Joukal, M. (2018a). Bilateral activation of STAT3 by phosphorylation at the tyrosine-705 (Y705) and serine-727 (S727) positions and its nuclear translocation in primary sensory neurons following unilateral sciatic nerve injury. *Histochem. Cell Biol.* 150, 37–47. doi: 10.1007/s00418-018-1656-y
- Dubový, P., Klusáková, I., Hradilová-Sviženská, I., and Joukal, M. (2018b). Expression of regeneration-associated proteins in primary sensory neurons and regenerating axons after nerve injury—An overview. *Anat. Rec.* 301, 1618–1627. doi: 10.1002/ar.23843
- Dubový, P., Klusáková, I., and Sviženská, I. (2002). A quantitative immunohistochemical study of the endoneurium in the rat dorsal and ventral spinal roots. *Histochem. Cell Biol.* 117, 473–480. doi: 10.1007/s00418-002-0411-5
- Eulenfeld, R., Dittrich, A., Khouri, C., Muller, P. J., Mutze, B., Wolf, A., et al. (2012). Interleukin-6 signalling: More than Jaks and STATs. *Eur. J. Cell Biol.* 91, 486–495. doi: 10.1016/j.ejcb.2011.09.010
- Frey, E., Valakh, V., Karney-Grobe, S., Shi, Y., Milbrandt, J., and DiAntonio, A. (2015). An *in vitro* assay to study induction of the regenerative state in sensory neurons. *Exp. Neurol.* 263, 350–363. doi: 10.1016/j.expneurol.2014.10.012
- Heumann, R., Lindholm, D., Bandtlow, C., Meyer, M., Radeke, M. J., Misko, T. P., et al. (1987). Differential regulation of messenger-rna encoding nerve growth-factor and its receptor in rat sciatic-nerve during development, degeneration and regeneration - role of macrophages. *Proc. Natl. Acad. Sci. U S A* 84, 8735–8739. doi: 10.1073/pnas.84.23.8735
- Hylden, J. L. K., and Wilcox, G. L. (1980). Intrathecal morphine in mice: a new technique. *Eur. J. Pharmacol.* 67, 313–316. doi: 10.1016/0014-2999(80)90515-4
- Itoh, A., Horiuchi, M., Bannerman, P., Pleasure, D., and Itoh, T. (2009). Impaired regenerative response of primary sensory neurons in ZPK/DLK gene-trap mice. *Biochem. Biophys. Res. Commun.* 383, 258–262. doi: 10.1016/j.bbrc.2009.04.009
- Joukal, M., Klusáková, I., and Dubový, P. (2016). Direct communication of the spinal subarachnoid space with the rat dorsal root ganglia. *Ann. Anat.* 205, 9–15. doi: 10.1016/j.aanat.2016.01.004
- Law, V., Dong, S., Rosaless, J. L., Jeong, M. Y., Zochodne, D., and Lee, K. Y. (2016). Enhancement of peripheral nerve regrowth by the purine nucleoside analog and cell cycle inhibitor, Roscovitine. *Front. Cell. Neurosci.* 10:238. doi: 10.3389/fncel.2016.00238
- Lawson, S. N. (2002). Phenotype and function of somatic primary afferent nociceptive neurones with C-, A δ - or A α/β -fibres. *Exp. Physiol.* 87, 239–244. doi: 10.1113/eph8702350
- Lawson, S. N., Caddy, K. W. T., and Biscoe, T. J. (1974). Development of rat dorsal root ganglion neurons. Studies of cell birthdays and changes in mean cell diameter. *Cell Tissue Res.* 153, 399–413. doi: 10.1007/bf00229167
- Leclere, P. G., Norman, E., Groutis, F., Coffin, R., Mayer, U., Pizzey, J., et al. (2007). Impaired axonal regeneration by isolectin B4-binding dorsal root ganglion neurons *in vitro*. *J. Neurosci.* 27, 1190–1199. doi: 10.1523/jneurosci.5089-06.2007
- Liabotis, S., and Schreyer, D. J. (1995). Magnitude of GAP-43 induction following peripheral axotomy of adult-rat dorsal-root ganglion neurons is independent of lesion distance. *Exp. Neurol.* 135, 28–35. doi: 10.1006/exnr.1995.1063
- Liu, K., Tedeschi, A., Park, K. K., and He, Z. (2011). Neuronal intrinsic mechanisms of axon regeneration. *Ann. Rev. Neurosci.* 34, 131–152. doi: 10.1146/annurev-neuro-061010-113723
- Ma, T. C., and Willis, D. E. (2015). What makes a RAG regeneration associated? *Front. Mol. Neurosci.* 8:43. doi: 10.3389/fnmol.2015.00043
- Mar, F. M., Bonni, A., and Sousa, M. M. (2014). Cell intrinsic control of axon regeneration. *EMBO Rep.* 15, 254–263. doi: 10.1002/embr.201337723
- Mason, M. R. J., Lieberman, A. R., Grenningloh, G., and Anderson, P. N. (2002). Transcriptional upregulation of SCG10 and CAP-23 is correlated with regeneration of the axons of peripheral and central neurons *in vivo*. *Mol. Cell. Neurosci.* 20, 595–615. doi: 10.1006/mcne.2002.1140
- Miao, T., Wu, D. S., Zhang, Y., Bo, X. N., Subang, M. C., Wang, P., et al. (2006). Suppressor of cytokine signaling-3 suppresses the ability of activated signal transducer and activator of transcription-3 to stimulate neurite growth in rat primary sensory neurons. *J. Neurosci.* 26, 9512–9519. doi: 10.1523/jneurosci.2160-06.2006
- Murphy, P. G., Grondin, J., Altares, M., and Richardson, P. M. (1995). Induction of interleukin-6 in axotomized sensory neurons. *J. Neurosci.* 15, 5130–5138. doi: 10.1523/jneurosci.15-07-05130.1995
- Neumann, S., and Woolf, C. J. (1999). Regeneration of dorsal column fibers into and beyond the lesion site following adult spinal cord injury. *Neuron* 23, 83–91. doi: 10.1016/s0896-6273(00)80755-2
- Ng, Y. P., Cheung, Z. H., and Ip, N. Y. (2006). STAT3 as a downstream mediator of Trk signaling and functions. *J. Biol. Chem.* 281, 15636–15644. doi: 10.1074/jbc.m601863200
- Niemi, J. P., DeFrancesco-Lisowitz, A., Cregg, J. M., Howarth, M., and Zigmund, R. E. (2016). Overexpression of the monocyte chemokine CCL2 in dorsal root ganglion neurons causes a conditioning-like increase in neurite outgrowth and does so via a STAT3 dependent mechanism. *Exp. Neurol.* 275, 25–37. doi: 10.1016/j.expneurol.2015.09.018
- Nix, P., Hisamoto, N., Matsumoto, K., and Bastiani, M. (2011). Axon regeneration requires coordinate activation of p38 and JNK MAPK pathways. *Proc. Natl. Acad. Sci. U S A* 108, 10738–10743. doi: 10.1073/pnas.1104830108
- Patodia, S., and Raivich, G. (2012). Role of transcription factors in peripheral nerve regeneration. *Cell Tissue Res.* 5:8. doi: 10.3389/fnmol.2012.00008
- Pellegrino, M. J., and Habecker, B. A. (2013). STAT3 integrates cytokine and neurotrophin signals to promote sympathetic axon regeneration. *Mol. Cell. Neurosci.* 56, 272–282. doi: 10.1016/j.mcn.2013.06.005
- Plantinga, L. C., Verhaagen, J., Edwards, P. M., Hol, E. M., Bär, P. R., and Gispen, W. H. (1993). The expression of B-50/GAP-43 in Schwann-cells is up-regulated in degenerating peripheral-nerve stumps following nerve injury. *Brain Res.* 602, 69–76. doi: 10.1016/0006-8993(93)90243-g
- Pool, M., Thiemann, J., Bar-Or, A., and Fournier, A. E. (2008). NeuriteTracer: a novel ImageJ plugin for automated quantification of neurite outgrowth. *J. Neurosci. Methods* 168, 134–139. doi: 10.1016/j.jneumeth.2007.08.029
- Qiu, J., Cafferty, W. B. J., McMahon, S. B., and Thompson, S. W. N. (2005). Conditioning injury-induced spinal axon regeneration requires signal transducer and activator of transcription 3 activation. *J. Neurosci.* 25, 1645–1653. doi: 10.1523/JNEUROSCI.3269-04.2005
- Raivich, G., Bohatschek, M., Da Costa, C., Iwata, O., Galiano, M., Hristova, M., et al. (2004). The AP-1 transcription factor c-jun is required for efficient axonal regeneration. *Neuron* 43, 57–67. doi: 10.1016/j.neuron.2004.06.005
- Rishal, I., and Fainzilber, M. (2014). Axon-soma communication in neuronal injury. *Nat. Rev. Neurosci.* 15, 32–42. doi: 10.1038/nrn3609

- Ronchi, G., Nicolino, S., Raimondo, S., Tos, P., Battiston, B., Papalia, B., et al. (2009). Functional and morphological assessment of a standardized crush injury of the rat median nerve. *J. Neurosci. Methods* 179, 51–57. doi: 10.1016/j.jneumeth.2009.01.011
- Ruohonen, S., Jagodi, M., Khademi, M., Taskinen, H. S., Ojala, P., Olsson, T., et al. (2002). Contralateral non-operated nerve to transected rat sciatic nerve shows increased expression of IL-1 β , TGF- β 1, TNF- α , and IL-10. *J. Neuroimmunol.* 132, 11–17. doi: 10.1016/s0165-5728(02)00281-3
- Ryoke, K., Ochi, M., Iwata, A., Uchio, Y., Yamamoto, S., and Yamaguchi, H. (2000). A conditioning lesion promotes *in vivo* nerve regeneration in the contralateral sciatic nerve of rats. *Biochem. Biophys. Res. Commun.* 267, 715–718. doi: 10.1006/bbrc.1999.2017
- Sar Shalom, H., and Yaron, A. (2014). Marking axonal growth in sensory neurons: SCG10. *Exp. Neurol.* 254, 68–69. doi: 10.1016/j.expneurol.2014.01.014
- Schmid, A. B., Coppieters, M. W., Ruitenber, M. J., and McLachlan, E. M. (2013). Local and remote immune-mediated inflammation after mild peripheral nerve compression in rats. *J. Neuropathol. Exp. Neurol.* 72, 662–680. doi: 10.1097/nen.0b013e318298de5b
- Schreyer, D. J., and Skene, J. H. P. (1993). Injury-associated induction of GAP-43 expression displays axon branch specificity in rat dorsal-root ganglion neurons. *J. Neurobiol.* 24, 959–970. doi: 10.1002/neu.480240709
- Schwaiger, F. W., Hager, G., Schmitt, A. B., Horvat, A., Streif, R., Spitzer, C., et al. (2000). Peripheral but not central axotomy induces changes in Janus kinases (JAK) and signal transducers and activators of transcription (STAT). *Eur. J. Neurosci.* 12, 1165–1176. doi: 10.1046/j.1460-9568.2000.00005.x
- Sheu, J. Y., Kulhanek, D. J., and Eckenstein, F. P. (2000). Differential patterns of ERK and STAT3 phosphorylation after sciatic nerve transection in the rat. *Exp. Neurol.* 166, 392–402. doi: 10.1006/exnr.2000.7508
- Shin, J. E., and Cho, Y. (2017). Epigenetic regulation of axon regeneration after neural injury. *Mol. Cells* 40, 10–16. doi: 10.14348/molcells.2017.2311
- Shin, J. E., Geisler, S., and DiAntonio, A. (2014). Dynamic regulation of SCG10 in regenerating axons after injury. *Exp. Neurol.* 252, 1–11. doi: 10.1016/j.expneurol.2013.11.007
- Shin, J. E., Miller, B. R., Babetto, E., Cho, Y., Sasaki, Y., Qayum, S., et al. (2012). SCG10 is a JNK target in the axonal degeneration pathway. *Proc. Natl. Acad. Sci. U S A* 109, E3696–E3705. doi: 10.1073/pnas.1216204109
- Skene, J. H. P., and Willard, M. (1981). Axonally transported proteins associated with axon growth in rabbit central and peripheral nervous systems. *J. Cell Biol.* 89, 96–103. doi: 10.1083/jcb.89.1.96
- Stewart, H. J. S., Cowen, T., Curtis, R., Wilkin, G. P., Mirsky, R., and Jessen, K. R. (1992). GAP-43 immunoreactivity is widespread in the autonomic neurons and sensory neurons of the rat. *Neuroscience* 47, 673–684. doi: 10.1016/0306-4522(92)90175-2
- Sugiura, Y., and Mori, N. (1995). SCG10 expresses growth-associated manner in developing rat brain, but shows a different pattern to p19 stathmin or GAP-43. *Dev. Brain Res.* 90, 73–91. doi: 10.1016/0165-3806(96)83488-2
- Tararuk, T., Ostman, N., Li, W. R., Björkblom, B., Padzik, A., Zdrojewska, J., et al. (2006). JNK1 phosphorylation of SCG10 determines microtubule dynamics and axodendritic length. *J. Cell Biol.* 173, 265–277. doi: 10.1083/jcb.200511055
- Temporin, K., Tanaka, H., Kuroda, Y., Okada, K., Yachi, K., Moritomo, H., et al. (2008). IL-1 β promotes neurite outgrowth by deactivating RhoA via p38 MAPK pathway. *Biochem. Biophys. Res. Commun.* 365, 375–380. doi: 10.1016/j.bbrc.2007.10.198
- Tsai, S. Y., Yang, L. Y., Wu, C. H., Chang, S. F., Hsu, C. Y., Wei, C. P., et al. (2007). Injury-induced janus kinase/protein kinase C-dependent phosphorylation of growth-associated protein 43 and signal transducer and activator of transcription 3 for neurite growth in dorsal root ganglion. *J. Neurosci. Res.* 85, 321–331. doi: 10.1002/jnr.21119
- Valakh, V., Frey, E., Babetto, E., Walker, L. J., and DiAntonio, A. (2015). Cytoskeletal disruption activates the DLK/JNK pathway, which promotes axonal regeneration and mimics a preconditioning injury. *Neurobiol. Dis.* 77, 13–25. doi: 10.1016/j.nbd.2015.02.014
- Verma, P., Chierzi, S., Codd, A. M., Campbell, D. S., Meyer, R. L., Holt, C. E., et al. (2005). Axonal protein synthesis and degradation are necessary for efficient growth cone regeneration. *J. Neurosci.* 25, 331–342. doi: 10.1523/JNEUROSCI.3073-04.2005
- Wells, M. R., Vaidya, U., and Schwartz, J. P. (1994). Bilateral phasic increases in dorsal-root ganglia nerve growth-factor synthesis after unilateral sciatic-nerve crush. *Exp. Brain Res.* 101, 53–58. doi: 10.1007/bf00243216
- Yamaguchi, H., Ochi, M., Mori, R., Ryoke, K., Yamamoto, S., Iwata, A., et al. (1999). Unilateral sciatic nerve injury stimulates contralateral nerve regeneration. *Neuroreport* 10, 1359–1362. doi: 10.1097/00001756-199904260-00037
- Zamboni, L., and Demartin, C. (1967). Buffered picric acid-formaldehyde—a new rapid fixative for electron microscopy. *J. Cell Biol.* 35:A148.
- Zigmond, R. E. (2011). gp130 cytokines are positive signals triggering changes in gene expression and axon outgrowth in peripheral neurons following injury. *Front. Mol. Neurosci.* 4:62. doi: 10.3389/fnmol.2011.00062
- Zigmond, R. E. (2012). Cytokines that promote nerve regeneration. *Exp. Neurol.* 238, 101–106. doi: 10.1016/j.expneurol.2012.08.017

Conflict of Interest Statement: The authors declare that the research was conducted in the absence of any commercial or financial relationships that could be construed as a potential conflict of interest.

Copyright © 2019 Dubový, Klusáková, Hradilová-Svženská, Brázda, Kohoutková and Joukal. This is an open-access article distributed under the terms of the Creative Commons Attribution License (CC BY). The use, distribution or reproduction in other forums is permitted, provided the original author(s) and the copyright owner(s) are credited and that the original publication in this journal is cited, in accordance with accepted academic practice. No use, distribution or reproduction is permitted which does not comply with these terms.

D. Hernangómez M, Klusáková I, **Joukal M**, Hradilová-Svíženská I, Guaza C, Dubový P. CD200R1 agonist attenuates glial activation, inflammatory reactions, and hypersensitivity immediately after its intrathecal application in a rat neuropathic pain model. *J Neuroinflammation*. 2016;13:43. doi:10.1186/s12974-016-0508-8

Commentary: In this publication, we demonstrated that intrathecal application of the CD200R1 agonist CD200Fc induces rapid suppression of behavioral signs of neuropathic pain after chronic constriction of the sciatic nerve. This was followed with suppression of glial activation, decreased proinflammatory and increased antiinflammatory cytokine mRNA levels.

IF (WOS, 2016): 5.102

Quartile (WOS, 2016): Immunology Q1, Neurosciences Q1

Contribution of the author: Co-authorship. The author conceived, designed, and carried out intrathecal administration and participated in acquiring and analyzing the presented data.

RESEARCH

Open Access



CD200R1 agonist attenuates glial activation, inflammatory reactions, and hypersensitivity immediately after its intrathecal application in a rat neuropathic pain model

Miriam Hernangómez¹, Ilona Klusáková^{1,2†}, Marek Joukal², Ivana Hradilová-Svíženská^{1,2†}, Carmen Guaza³ and Petr Dubový^{1,2*}

Abstract

Background: Interaction of CD200 with its receptor CD200R has an immunoregulatory role and attenuates various types of neuroinflammatory diseases.

Methods: Immunofluorescence staining, western blot analysis, and RT-PCR were used to investigate the modulatory effects of CD200 fusion protein (CD200Fc) on activation of microglia and astrocytes as well as synthesis of pro- (TNF, IL-1 β , IL-6) and anti-inflammatory (IL-4, IL-10) cytokines in the L4–L5 spinal cord segments in relation to behavioral signs of neuropathic pain after unilateral sterile chronic constriction injury (sCCI) of the sciatic nerve. Withdrawal thresholds for mechanical hypersensitivity and latencies for thermal hypersensitivity were measured in hind paws 1 day before operation; 1, 3, and 7 days after sCCI operation; and then 5 and 24 h after intrathecal application of artificial cerebrospinal fluid or CD200Fc.

Results: Seven days from sCCI operation and 5 h from intrathecal application, CD200Fc reduced mechanical and thermal hypersensitivity when compared with control animals. Simultaneously, CD200Fc attenuated activation of glial cells and decreased proinflammatory and increased anti-inflammatory cytokine messenger RNA (mRNA) levels. Administration of CD200Fc also diminished elevation of CD200 and CD200R proteins as a concomitant reaction of the modulatory system to increased neuroinflammatory reactions after nerve injury. The anti-inflammatory effect of CD200Fc dropped at 24 h after intrathecal application.

Conclusions: Intrathecal administration of the CD200R1 agonist CD200Fc induces very rapid suppression of neuroinflammatory reactions associated with glial activation and neuropathic pain development. This may constitute a promising and novel therapeutic approach for the treatment of neuropathic pain.

Keywords: Rat neuropathic pain model, Sterile nerve constriction, Neuroinflammation, Activated glial cells, Cytokines, Modulation

* Correspondence: pdubovy@med.muni.cz

[†]Equal contributors

¹Central European Institute of Technology (CEITEC), Masaryk University, Kamenice 3, 62500 Brno, Czech Republic

²Department of Anatomy, Division of Neuroanatomy, Faculty of Medicine, Masaryk University, Kamenice 3, 62500 Brno, Czech Republic

Full list of author information is available at the end of the article



Background

Peripheral neuropathic pain (PNP), manifesting as spontaneous pain, arises as a result of many forms of nerve damage, including traumatic nerve injury, diabetic neuropathy, HIV neuropathy, and drug-induced neuropathy [1, 2]. Among other effects, nerve injury-induced PNP is associated with inflammatory reaction and activation of glial cells in the corresponding spinal cord segments [1, 3, 4].

Experimental PNP models are predominantly based on injury to the sciatic nerve, wherein the maximum number of neuronal perikarya (98–99 %) is localized at the L4 and L5 segments [5]. Sterile chronic constriction injury (sCCI) of the sciatic nerve is a model for study of cellular and molecular changes inducing PNP after traumatic nerve injury with dominant molecular signaling from Wallerian degeneration [6]. It is well documented that hypersensitivity and ongoing pain due to peripheral nerve injury are associated with cellular and molecular changes in the dorsal horn (DH) of the spinal cord related to activation of microglial cells and astrocytes and alteration of pro- and anti-inflammatory cytokines produced by neurons, activated glia, and invaded immune cells [7–12]. There is a growing body of evidence that unilateral nerve injury results in bilateral neuroinflammatory reaction in the dorsal root ganglia and spinal cord DH [10, 13–15], thus illustrating signaling from the site of Wallerian degeneration to other compartments of the nervous system [16].

CD200 is a membrane glycoprotein of the immunoglobulin superfamily with immune suppression effect via its receptor CD200R. CD200 has an extracellular portion with two immunoglobulin domains, typical of proteins involved in cell-to-cell interaction. The CD200 receptor CD200R1 has a similar structure but with an additional intracellular domain that is susceptible to phosphorylation and involved in signal transduction [17, 18]. CD200 is highly expressed on neurons while CD200R is confined mainly to myeloid cells like macrophages and microglia [19–23]. In addition, CD200 is expressed in oligodendrocytes [23] and astrocytes [23, 24]. The interaction of CD200 with its receptor CD200R plays a significant role in maintaining microglia in a quiescent or resting state and attenuates various types of neuroinflammatory diseases [19, 25, 26]. It has been demonstrated that mice with levels of CD200 increased by spontaneous mutation in the *Wld* gene have less activated monocytes and increasing expression of IL-10 in the central nervous system following induction of experimental autoimmune encephalomyelitis [27]. Conversely, CD200^{-/-} mice have been shown to display myeloid cell dysregulation, enhanced susceptibility to experimental autoimmune encephalomyelitis [28], and microglial activation [29]. Furthermore, CD200R expression can be modulated by IL-4 and IL-13 [30, 31].

Experimental studies have demonstrated that soluble CD200 fusion protein (CD200Fc), containing the ectodomain of CD200 bound to a murine IgG2a module, attenuates inflammatory diseases and reduces microglial activation [32–36]. Nevertheless, our knowledge remains limited as to the effects of CD200Fc in attenuation of glial cell activation and alteration of pro- and anti-inflammatory cytokines in PNP induced by a peripheral nerve injury. Therefore, the goal of our present study was to explore whether intrathecal application of CD200Fc might attenuate activation of glial cells in the spinal cord, modify synthesis of pro- and anti-inflammatory cytokines, and reduce behavioral signs of PNP in the sCCI model. Our results provide the first evidence that CD200Fc administration induces rapid attenuation of glial activation and pro-inflammatory cytokine synthesis of the spinal cord in relation to reduction of neuropathic pain signs after experimental nerve injury.

Methods

Animals and surgical procedures

The experiments were carried out on 120 male Wistar rats weighing 240–250 g at the beginning of experiments. The animals were housed on 12 h light/dark cycles at temperature 22–24 °C under specific pathogen-free conditions in the animal housing facility of Masaryk University. All surgical procedures were performed by one person under aseptic conditions and deep anesthesia induced by a xylazine and ketamine cocktail injected intraperitoneally (xylazine 1.6 mg/kg; ketamine 64 mg/kg). Sterilized food and water were available ad libitum. Treatment of the animals was in accordance with the European Convention for the Protection of Vertebrate Animals Used for Experimental and Other Scientific Purposes and was supervised by the institutional Ethics Committee of Masaryk University in Brno (Czech Republic).

Six naïve rats treated with CD200Fc were used to demonstrate that the CD200R agonist has no effect on basal skin sensitivity, and 18 naïve rats were utilized for comparison of glial activation by immunohistochemistry, western blot analysis, and relative cytokine messenger RNA (mRNA) levels. The left sciatic nerve was exposed at mid-thigh and three silk ligatures (Ethicon 3–0) were applied to reduce the nerve diameter by one third in the rats undergoing sCCI ($n = 72$). The left sciatic nerves of 24 sham-operated rats were only exposed without any nerve lesion. Sham- and sCCI-operated animals were left to survive for 7 days.

Administration of CD200Fc and vehicle

At day 7 of sCCI operation, the rats were randomly divided into groups with intrathecal administration of CD200Fc for 5 h ($n = 18$; sCCI + CD200Fc5h) and 24 h ($n = 18$; sCCI + CD200Fc24h) as well as a control group

with intrathecal application of artificial cerebrospinal fluid (ACSF) for 5 h ($n = 18$; sCCI + ACSF5h) and 24 h ($n = 18$; sCCI + ACSF24h). CD200Fc (Cat. No. 3355-CD; R&D Systems, Minneapolis, MN, USA) was freshly prepared in sterile ACSF [37]. The single intrathecal injection was administered by introducing a hypodermic needle into the subarachnoid space of the cisterna magna for diffusion of CD200Fc (5 μ l; 2 μ g/ μ l) or sterile ACSF (5 μ l) throughout the spinal fluid over 30 s with another 30-s delay before removing the needle. To explore the effect of surgical approach on inflammatory reaction in the spinal cord, sham-operated rats were treated with ACSF (5 μ l) for 5 h ($n = 18$) and 24 h ($n = 6$, only for behavioral test). A direct effect of CD200Fc on basal sensitivity was tested in six naïve rats treated with CD200Fc (5 μ l; 2 μ g/ μ l) for 5 and 24 h.

Behavioral tests

Withdrawal thresholds for mechanical and thermal hypersensitivity were measured in ipsilateral hind paws using a dynamic plantar esthesiometer and plantar test (Ugo Basile), respectively. Rats were first acclimated in clear Plexiglas boxes for 30 min prior to testing. The paws were tested alternately with 5-min intervals between tests 1 day before operation; 1, 3, and 7 days after sCCI operation; and then 5 and 24 h after intrathecal ACSF or CD200Fc treatment. Six naïve rats were tested at 5 and 24 h after intrathecal administration to investigate a possible CD200Fc effect on basal sensitivity of animals. Five measurements were taken for each paw and test session. In the case of thermal hypersensitivity, withdrawal time was measured and the intensity radiance was set at value 50. Data for mechanical and thermal hypersensitivity were expressed as mean \pm SE of withdrawal thresholds in grams and withdrawal latency in seconds, respectively. All behavioral tests were conducted in a blind manner.

Immunohistochemical staining

The naïve rats and sCCI-operated rats treated with ACSF or CD200Fc for 5 and 24 h, as well as sham-operated and ACSF-treated rats ($n = 6$ for each group) were deeply anesthetized with a lethal dose of sodium pentobarbital (70 mg/kg body weight, i.p.) and perfused transcardially with 500 ml of heparinized (1000 units/500 ml) phosphate-buffered saline (PBS; 10 mM sodium phosphate buffer, pH 7.4, containing 0.15 M NaCl) followed by 500 ml of Zamboni's fixative [38]. The L4–L5 spinal cord segments were removed, immersed separately in Zamboni's fixative at 4 °C overnight, and then collected for each experimental group. The samples were washed in 20 % phosphate-buffered sucrose for 12 h and blocked in Tissue-Tek® OCT compound (Miles, Elkhart, Ind.). Serial transverse sections (12 μ m) of the L4–L5 spinal

cord segments were cut (Leica 1800 cryostat; Leica Microsystems, Wetzlar, Germany), collected on gelatin-coated microscopic slides, air-dried, then processed for immunohistochemical staining.

Briefly, the sections were washed with PBS containing 0.05 % Tween 20 (PBS-TW20) and 1 % bovine serum albumin for 10 min, then treated with 3 % normal donkey serum in PBS-TW20 for 30 min. The spinal cord sections were incubated with 25 μ l of mouse monoclonal anti-CD11b/c antibody (OX42, 1:50; AbD Serotec, Kidlington, UK) or rabbit polyclonal anti-gial fibrillary acidic protein (GFAP, 1:250; Dako, Glostrup, Denmark) in a humid chamber at room temperature (21–23 °C) overnight or for 180 min to identify activated microglial cells and astrocytes, respectively. The immunoreaction was visualized by treatment with FITC-conjugated affinity purified donkey anti-mouse or anti-rabbit secondary antibodies (1:400; Merck Millipore) for 90 min at room temperature. A part of sections was incubated overnight with mouse monoclonal anti-CD200 antibody (OX2, 1:100; Abcam) and treated with FITC-conjugated donkey anti-mouse (1:400; Merck Millipore) secondary antibody. Spinal cord distribution of CD200R was detected by immunostaining of sections with goat polyclonal anti-CD200R (OX2R, 1:200; Santa Cruz Biotechnology, Inc. USA) antibody and biotinylated donkey anti-goat secondary antibody (1:400; Santa Cruz Biotechnology, Inc. USA). Immunoreaction was visualized by TRITC-conjugated streptavidin (1:100; Jackson Laboratories, Inc. USA). The control sections were incubated with omission of the primary antibodies (data not shown). The cell nuclei were stained using Hoechst 33342 (Sigma; St. Louis, MO, USA). Sections were mounted in Vectashield aqueous mounting medium (Vector Laboratories; Burlingame, CA, USA) and then observed and analyzed using a Leica DMLB epifluorescence microscope equipped with a Leica DFC-480 camera (Leica Microsystems GmbH, Wetzlar, Germany).

Double immunofluorescence staining

To detect cellular localization of CD200 and CD200R proteins in the spinal cord, simultaneous immunostaining of CD200 or CD200R with corresponding cellular markers was carried out. Activated astrocytes and microglial cells were identified by immunostaining for GFAP and OX42, respectively (see above). Immunofluorescence staining with rabbit polyclonal NeuN antibody (1:500; Merck Millipore) was used to identify neurons of the spinal DH. Briefly, the spinal cord sections were immunostained for CD200 (see above), and after washing, the sections were immunolabeled with rabbit polyclonal anti-GFAP or NeuN antibody and TRITC-conjugated donkey anti-rabbit (1:400; Merck Millipore) secondary antibody. Other sections were incubated at first to

visualize distribution of CD200R and then for detection of activated microglial cells using mouse monoclonal OX42 antibody and FITC-conjugated donkey anti-mouse secondary antibody (see above). The control sections of the double immunostaining were incubated as described above but with omission of CD200 or CD200R antibodies. In the controls, no immunostaining for CD200 or CD200R was detected in the spinal cord sections.

To detect CD200R in activated astrocytes, the sections immunostained for CD200R using goat polyclonal antibody and biotin-streptavidin TRITC were next immunolabeled with rabbit anti-GFAP polyclonal antibody and FITC-conjugated donkey anti-rabbit secondary antibody (see above). The control sections were incubated with the goat anti-CD200R polyclonal antibody and FITC-conjugated donkey anti-rabbit secondary antibody or with rabbit anti-GFAP polyclonal antibody, and next, a biotin-streptavidin procedure was used for visualization of CD200R. No cross reaction between the secondary and primary antibodies was detected in these control sections. Double immunostained sections were mounted in Vectashield aqueous mounting medium and analyzed using a Nikon Eclipse epifluorescence microscope equipped with a DS-Ri1 camera (NIKON, Czech Republic).

Because detection of CD200R expression in activated astrocytes is not routine, the colocalization of CD200R and GFAP immunofluorescence was analyzed by colocalization module of NIS Elements software (Nikon, Czech Republic).

Image analysis

At least 10 sections (each separated from the next by an interval of about 80 μm) from each of the removed L4–L5 spinal cord segments for each animal per experimental group were selected for image analysis. Immunostaining area for OX42 or GFAP in spinal cord sections was measured using an NIS elements image analysis system (Laboratory Imaging Ltd, Prague, Czech Republic). Briefly, a box ($4 \times 10^4 \mu\text{m}^2$) was placed over the lateral, central, and medial areas of DH and OX42 or GFAP immunostained structures were detected by thresholding technique after subtraction of background. The area of immunostaining for OX42 or GFAP in corresponding DH was related to the area of interest ($4 \times 10^4 \mu\text{m}^2$) and expressed as the mean of relative area (%) \pm SD.

Western blot analysis

Rats were deeply anesthetized with a lethal dose of sodium pentobarbital (70 mg/kg body weight, i.p.). The L4–L5 spinal cord segments were detected following total laminectomy and rapidly removed, frozen in dry ice, then stored at -70°C until elaboration for western blot or reverse transcription (RT) and real-time polymerase chain reaction (PCR).

The fresh tissue samples of L4–L5 spinal cord segments from six animals for each group were homogenized in PBS containing 0.1 % Triton X-100 and protease inhibitors (LaRoche, Switzerland) and then centrifuged at 10,000g for 5 min at 4°C . Proteins were separated by SDS-polyacrylamide gel electrophoresis [39] and transferred to nitrocellulose membranes by electroblotting (Bio-Rad). Blots were blocked by 5 % milk-TBST for 1 h and incubated with mouse monoclonal OX42 antibody (1:300; AbD Serotec), rabbit polyclonal anti-GFAP (1:250; DAKO), goat polyclonal anti-CD200 (1:100; Santa Cruz Biotechnology), or anti-CD200R antibody (1:100; Santa Cruz Biotechnology) at 4°C for 18 h. Blots were washed in PBS-TW20 and incubated with secondary antibody (goat anti-mouse or anti-rabbit, 1:1000, Immunotech; anti-goat, 1:8000, Bio-Rad), at room temperature for 1 h. Protein bands were visualized using the ECL detection kit (Amersham) on an LAS-3000 chemiluminometer reader (Bouchet Biotech) and analyzed using densitometry image software. The blots were stripped in 62.5 mM Tris-HCl, pH 6.8, containing 2 % SDS and 0.7 % β -mercaptoethanol, and they were then reprobated with a monoclonal antibody against β -tubulin (1:5000; Exbio).

Reverse transcription and real-time polymerase chain reaction

The fresh tissue samples of L4–L5 spinal cord segments from six animals for each group were collected. Total RNA was extracted using RNeasy mini columns (Qiagen, Hilden, Germany). Contaminating genomic DNA was degraded by a treatment with DnaseI (Qiagen). The yield of RNA was determined using a Nanodrop[®] spectrophotometer (NanoDrop Technologies, Wilmington, DE, USA). Total RNA (1 μg in 20 μL) was reverse transcribed into complementary DNA (cDNA) using poly-dT primers and the Promega reverse transcription kit (Promega, Madrid, Spain). The oligonucleotide primer sequences used are given in Table 1. SYBR[®] PCR was performed using 1 μL of cDNA (corresponding to 50 ng RNA input) with 200 nM of the primers listed above (Invitrogen, Barcelona, Spain) in a Power SYBR[®] PCR Mastermix (Applied Biosystems, Foster City, CA, USA). Cycling conditions were as follows: 50°C for 2 min, 95°C for 10 min, and 40 amplification cycles of 95°C for 15 s and 60°C for 1 min. Samples were assayed using the Applied Biosystems PRISM 7500 sequence detection system, assaying each sample in triplicate and running a six-point standard curve in parallel. To ensure the absence of contamination with genomic DNA, a control sample using RNA as the template was run for each set of extractions. Relative quantification was obtained by calculating the ratio between the values obtained for each gene of interest and those of the 18S housekeeping gene with respect to the naïve animals.

Table 1 Rat primer sequences used in quantitative polymerase chain reactions

Genes	Forward	Reverse
IL-1 β	5'-TTGCTTCCAAGCCCTTGACT-3'	5'-CTCCACGGGCAAGACATAGG-3'
TNF- α	5'-CATGAGCAC GGAAAGCATGA-3'	5'-CCACGAGCAGGAATGAGAAGA-3'
IL-6	5'-AAGAAAGACAAAGCCAGAGTC-3'	5'-CACAACTGATATGCTTAGGC-3'
IL-4	5'-CCTTGCTGTACCCCTGTTCTG-3'	5'-TGCATGGAGTCCCTTTTCTG-3'
IL-10	5'-CAGTCAGCCAGACCCACAT-3'	5'-GCTCCACTGCCTTGCTTT-3'
18S	5'-ATGCTCTTAGCTGAGTGCCCG-3'	5'-ATTCTAGCTGCGGTATCCAGG-3'

Statistical analyses

Behavioral data were evaluated using Kruskal-Wallis one-way analysis with Bonferroni post hoc test and p values less than 0.05 were considered to be significant. To verify differences of immunostaining area, western blot and RT-PCR, a one-way ANOVA with subsequent post hoc t tests employing a correction of alpha according to Bonferroni for repeated measures was run with $p < 0.05$ as the level of significant differences between tested samples. Statistical differences between data of relative immunostaining area, western blot, and RT-PCR were tested by Mann-Whitney U test ($p < 0.05$). All statistical analyses were made using STATISTICA-12 software (StatSoft, Tulsa, OK, USA).

Results

CD200Fc reduces mechanical and thermal hypersensitivity of nerve-injured rats

As CD200Fc appears to be beneficial when administered in cases of various diseases with an inflammatory component [34, 36, 40], we investigated whether the CD200R1 agonist has effects on PNP behavioral signs in the sCCI model. No statistically significant changes of thresholds and withdrawal latencies were measured in the hind paws of naïve rats treated with CD200Fc for 5 and 24 h, thus indicating no influence of the CD200R agonist on basal sensitivity (data not shown). Sham-operated rats displayed a small but not statistically significant mechanical and thermal hypersensitivity at days 1 and 3 with no behavioral changes after 7 days and ACSF treatment for 5 or 24 h (Fig. 1a, b). All hind paws of rats subjected to sCCI of the sciatic nerve displayed significantly decreased thresholds of mechanical (Fig. 1a) and withdrawal latencies of thermal hypersensitivity (Fig. 1b) at days 1, 3, and 7 post-operation when compared with 1 day before operation.

Rats operated on sCCI with intrathecal administration of CD200Fc for 5 h displayed significant attenuation of mechanical and thermal hypersensitivity when compared with levels before CD200Fc injection or with ACSF-treated rats. Thresholds of mechanical and withdrawal latencies of thermal hypersensitivity did drop 24 h after CD200Fc administration, but the values remained still significantly higher when compared with levels before CD200Fc treatment (Fig. 1a, b).

CD200Fc attenuates activation of microglial cells and astrocytes in the spinal dorsal horn of nerve-injured rats

We investigated the regulatory effect of CD200Fc administration on microglial activation in the sCCI model of PNP because interaction of CD200 with CD200R decreases microglial activation [20, 33]. No significant difference of OX42 immunostaining was found between naïve and sham-operated rats (Fig. 2a, d, h). The OX42 immunoreactive area indicating activated microglial cells was markedly larger in ipsilateral DH of the spinal cord sections from sCCI-operated and ACSF-treated rats when compared with naïve or sham-operated animals (Fig. 2b, e). Microglial activation expressed by the OX42 immunoreactive area was significantly attenuated in ipsilateral DH sections prepared from the spinal cord of sCCI-operated rats and treated with CD200Fc for 5 h (Fig. 2c, f). However, 24 h after CD200Fc injection, the OX42 immunostaining area was enlarged, but it remained smaller than in control group of sCCI-operated and ACSF-treated rats (Fig. 2g). In contrast to ipsilateral DH, no significant extension of OX42 immunoreactive area was detected in the contralateral DH of sCCI-operated rats treated with ACSF or CD200Fc in comparison to naïve or sham-operated rats (Fig. 2i–k). The microglial cells immunostained for OX42 displayed the typical activated, amoeboid morphology in sections of L4–L5 spinal cord segments from rats sCCI-operated and treated with ACSF, whereas those in sections from CD200Fc-treated rats exhibited a ramified morphology similar to microglia of the naïve animals (insets in Fig. 2d–f). Quantitative changes of microglial activation detected by OX42 immunostaining area in the spinal cord sections of naïve, sham- and sCCI-operated, and ACSF- or CD200Fc-treated rats (Fig. 2l) were confirmed by western blot analysis of CD11b/c protein (Fig. 2m).

As CD200Fc appears to attenuate microglial activation in the sCCI-operated rats, we investigated whether intrathecal application of CD200Fc would also affect astroglial activation. Lumbar spinal cord sections prepared from rats 7 days after sCCI operation and treatment with ACSF displayed a bilateral enlargement of GFAP immunostaining area in DH when compared to the spinal cord sections of naïve or sham-operated rats (Fig. 3a–b, d–e, h–i). In comparison to ACSF treatment,

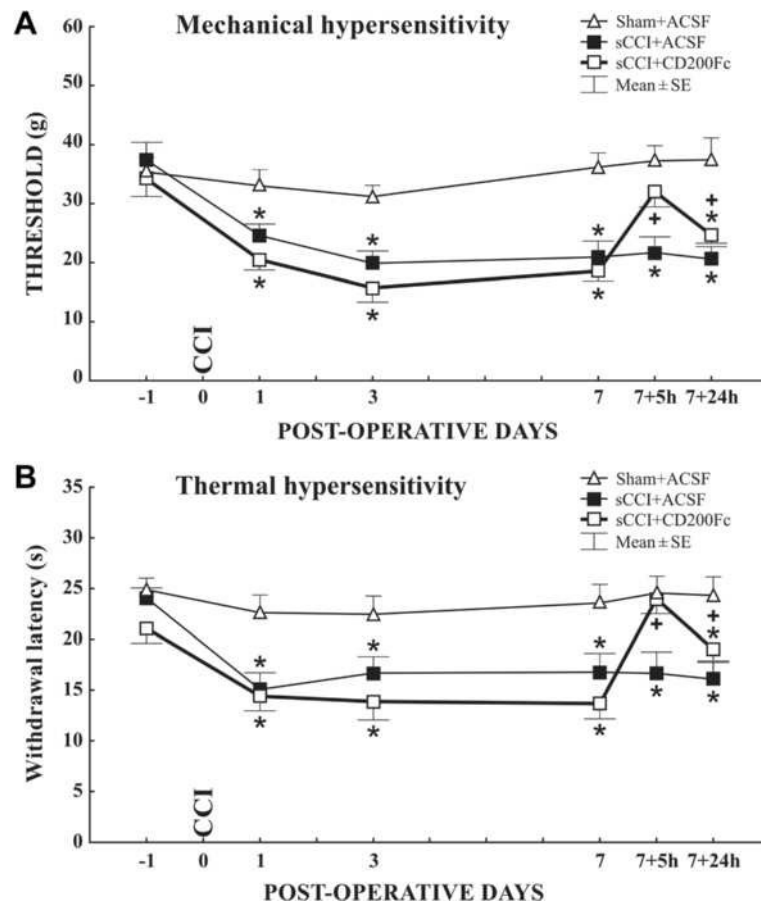


Fig. 1 Results of behavioral tests. Mechanical (a) and thermal hypersensitivity (b) in sCCI-operated rats treated with ACSF or CD200Fc. Withdrawal thresholds for mechanical hypersensitivity and latencies for thermal hypersensitivity were significantly decreased in the ipsilateral hind paws following sCCI when compared with 1 day before surgery, and CD200Fc treatment for 5 h was able to reverse these. Both behavioral signs of PNP were nevertheless significantly weaker 24 h from CD200Fc application, although they remained still higher than 7 days after sCCI operation but before CD200Fc application. All values in a and b represent mean \pm SE from six rats per group. Asterisk indicates statistically significant difference ($p < 0.001$) when compared with measurements 1 day before operation; Plus sign indicates statistical significant difference ($p < 0.01$) when compared to values of sCCI-operated animals before and after CD200Fc application. Kruskal-Wallis ANOVA followed by Mann-Whitney U test.

intrathecal administration of CD200Fc bilaterally reduced the extent of astroglial GFAP immunostaining in L4–L5 spinal cord sections from sCCI-operated rats (Fig. 3c, f, j). The GFAP-immunostained area of activated astrocytes was enlarged at 24 h after CD200Fc treatment, but it still remained lower than in the spinal cord of sCCI-operated and ACSF-treated rats. The quantitative changes of GFAP-immunoreactive areas (Fig. 3l) indicating activation state of astrocytes were confirmed by western blot analysis of GFAP protein in the spinal cord of naïve, sham-operated, and sCCI-operated and treated rats (Fig. 3m).

Cellular distribution and regulation of CD200 and CD200R1 levels in the spinal cord of nerve-injured and CD200Fc-treated rats

To determine precisely whether exogenous soluble CD200Fc might modify membrane-bound CD200 and CD200R1 expression in the spinal cord after sCCI

operation, we analyzed their proteins by immunofluorescence staining and western blotting in naïve and sham-operated rats in comparison with those of sCCI-operated animals after ACSF and CD200Fc administration for 5 h. The CD200 immunostaining was dominantly observed in DH with a higher intensity in the spinal cord sections from sCCI-operated and ACSF-treated rats when compared with that from sham-operated or sCCI-operated and CD200Fc-treated rats (Fig. 4a–c). Similarly, a distinctly increased immunostaining for CD200R1 was found in DH of spinal cord sections of sCCI-operated and ACSF-treated rats when compared with sections of the spinal cord from sham-operated rats (Fig. 4d–f). The increased CD200 and CD200R1 proteins in the spinal cord of sCCI-operated and ACSF-treated as well as the protein decrease after CD200Fc injection were confirmed by western blot analysis (Fig. 4g, h).

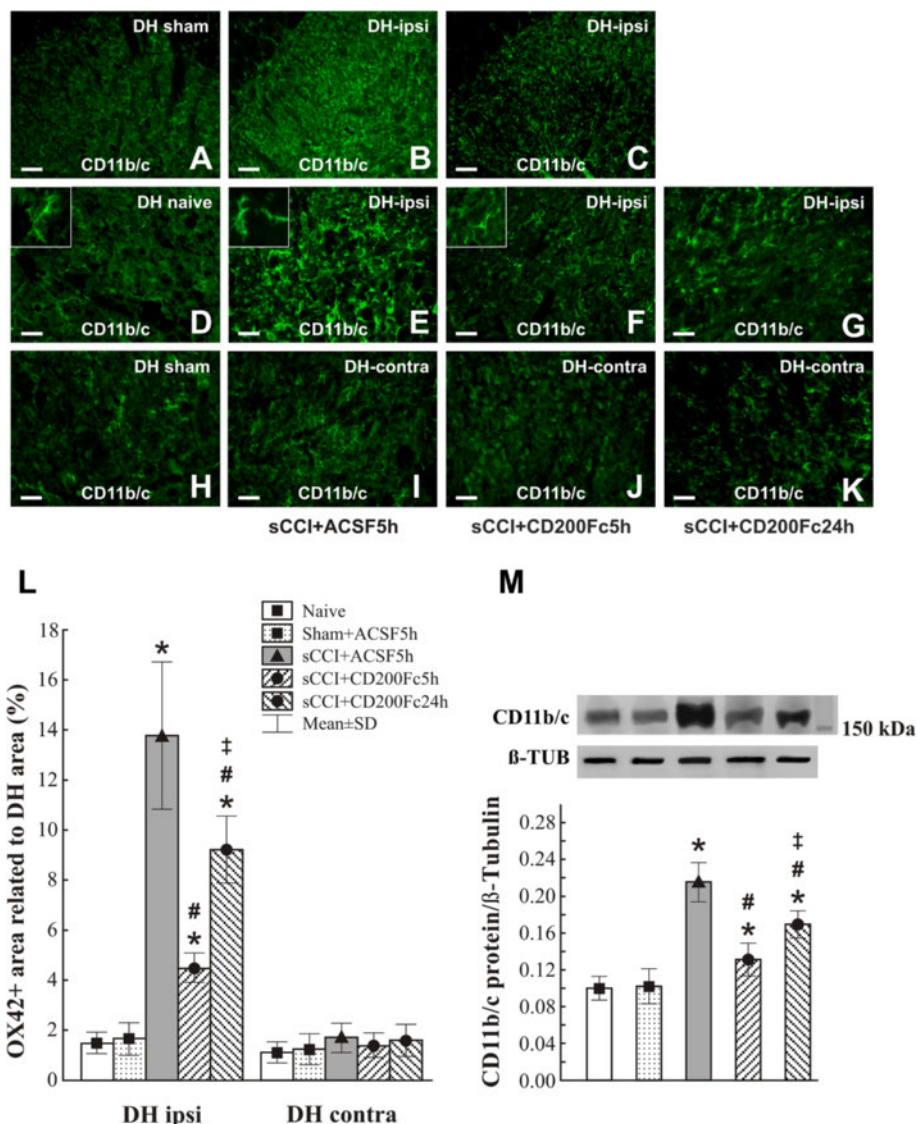


Fig. 2 Immunofluorescence staining and quantification of CD11b/c protein. OX42 (CD11b/c protein) immunofluorescence to detect microglia in the dorsal horn (DH) of sections through L4–L5 spinal cord segments from naïve and sham-operated rats as well as sCCI-operated rats treated with ACSF or CD200Fc. Representative pictures of OX42 immunofluorescence in ipsilateral DH of the spinal cord from sham- (a) and CCI-operated (b, c) rats 5 h after ACSF (a, b) or CD200Fc (c) injection. Scale bars = 75 μ m. A higher power magnification of OX42 immunofluorescence in DH of naïve (d) and sham-operated (h) rats and the ipsi- and contralateral DH (DH-ipsi, DH-contra) of sCCI-operated and ACSF-treated rats (e, i) as well as 5 (f, j) or 24 h (g, k) after injection with CD200Fc. Scale bars = 50 μ m. Insets in d–f show typical shape of OX42-labeled microglia in DH of naïve, ACSF-, and CD200Fc-treated rats, respectively. Scale bars for insets = 33 μ m. **l** Bar graph shows quantification of OX42 immunostaining area in DH of L4–L5 spinal cord segments from naïve and sham-operated rats as well as sCCI-operated rats for 7 days and 5 or 24 h after administration of CD200Fc or ACSF. **m** Western blot shows increased CD11b/c protein level in the spinal cord of sCCI-operated in comparison to naïve or sham-operated rats, whereas CD200Fc administration reduced this elevation. The data represent the mean \pm SD optical density normalized to tubulin from six animals in each group. * p < 0.05 when compared to DH of naïve or sham-operated rats; # p < 0.05 when compared to DH of sCCI + ACSF rats; ++ p < 0.05 when compared to 5-h treatment. Mann-Whitney U test

Double immunostaining of spinal cord sections of sCCI-operated and ACSF-treated rats revealed CD200 immunoreaction in both NeuN+ neurons and GFAP+ astrocytes (Fig. 5a–f). The CD200R immunofluorescence was detected in neuropil of the spinal cord sections and double immunostaining displayed colocalization of CD200R and

OX42 to illustrate presence of CD200R in activated microglial cells (Fig. 5g–i). When GFAP immunostaining corresponding with astrocyte activation was reduced after CD200Fc treatment, we sought to observe whether activated astrocytes could express CD200R1. Surprisingly, CD200R immunolabeling was colocalized with GFAP

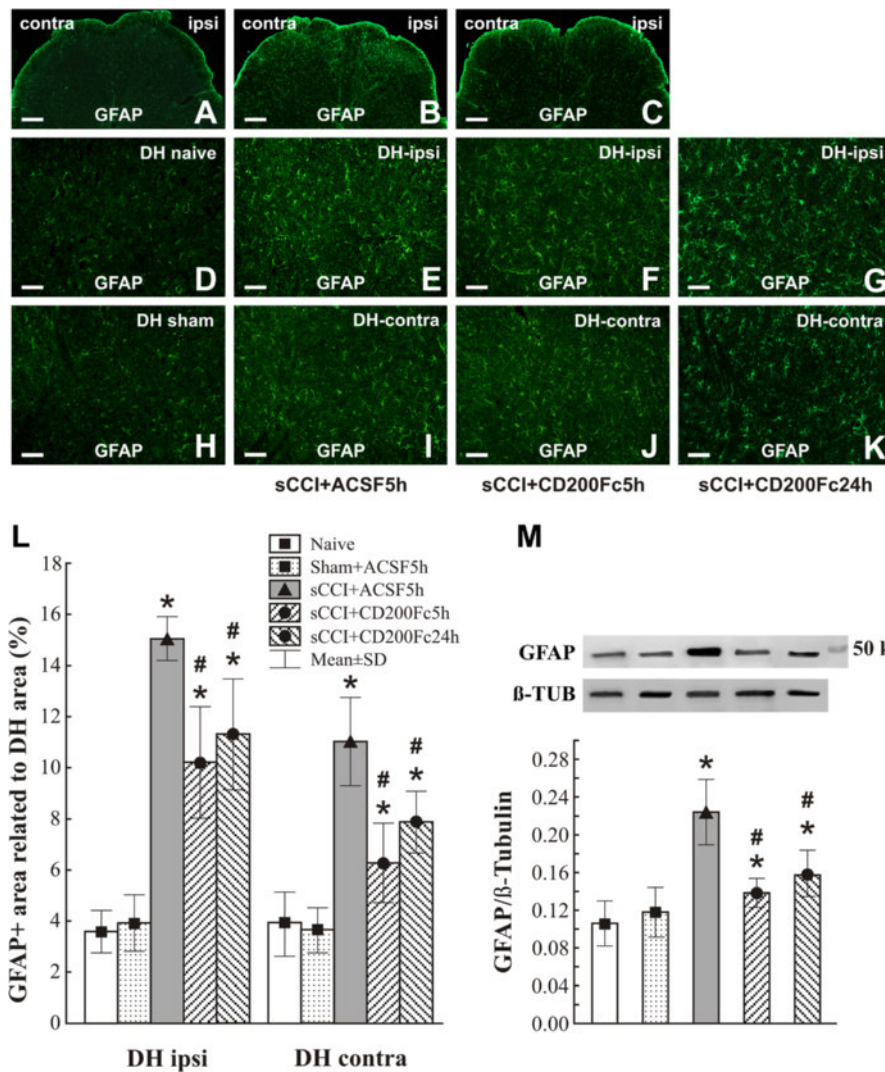


Fig. 3 Immunofluorescence staining and quantification of GFAP protein. GFAP-immunoreactive astrocytes in the dorsal horn (DH) of sections through L4–L5 spinal cord segments from naïve rats and sham-operated rats as well as sCCI-operated rats treated with ACSF or CD200Fc. Representative pictures of GFAP immunostaining in ipsilateral (ipsi) and contralateral (contra) DH of the spinal cord from sham- (a) and CCI-operated (b, c) rats 5 h after ACSF (a, b) or CD200Fc (c) injection. Scale bars = 100 μm. A higher power magnification of GFAP immunostaining in DH of naïve (d) and sham-operated (h) rats and the ipsi- and contralateral DH (DH-ipsi, DH-contra) of sCCI-operated and ACSF-treated rats (e, i) as well as rats 5 (f, j) or 24 h (g, k) after injection with CD200Fc. Scale bars = 50 μm. **l** Bar graph shows quantification of GFAP-immunoreactive area in DH of L4–L5 spinal cord segments from naïve and sham-operated rats as well as sCCI-operated rats for 7 days and 5 or 24 h after administration of CD200Fc or ACSF. **m** Western blot confirmed the increase of GFAP protein level in the spinal cord of sCCI-operated in comparison to naïve or sham-operated rats. The GFAP elevation was reduced by CD200Fc administration. The data represent the mean ± SE optical density normalized to tubulin from six animals in each group. **p* < 0.05 when compared to DH of naïve or sham-operated rats; #*p* < 0.05 when compared to DH of sCCI + ACSF rats. Mann-Whitney *U* test

immunostaining, indicating expression of the receptor in activated astrocytes of the spinal cord from sCCI-operated rats (Fig. 6a–f). The unexpected colocalization was verified by image analysis and measurement of indexes using NIS Elements. Mander’s overlap measured in double immunostained cells indicated by arrows (Fig. 6d–f) was 0.965265, 0.929336, and 0.960253. In addition, profile intensity of red (CD200R) and green (GFAP) channels in the

cells also indicated colocalization of CD200R and GFAP immunostaining (Fig. 6g).

Intrathecal CD200Fc administration reduces proinflammatory and enhances anti-inflammatory cytokine mRNAs in lumbar spinal cord segments of nerve-injured rats
To determine the immediate effect of CD200Fc treatment on cytokine synthesis in the spinal cord 7 days

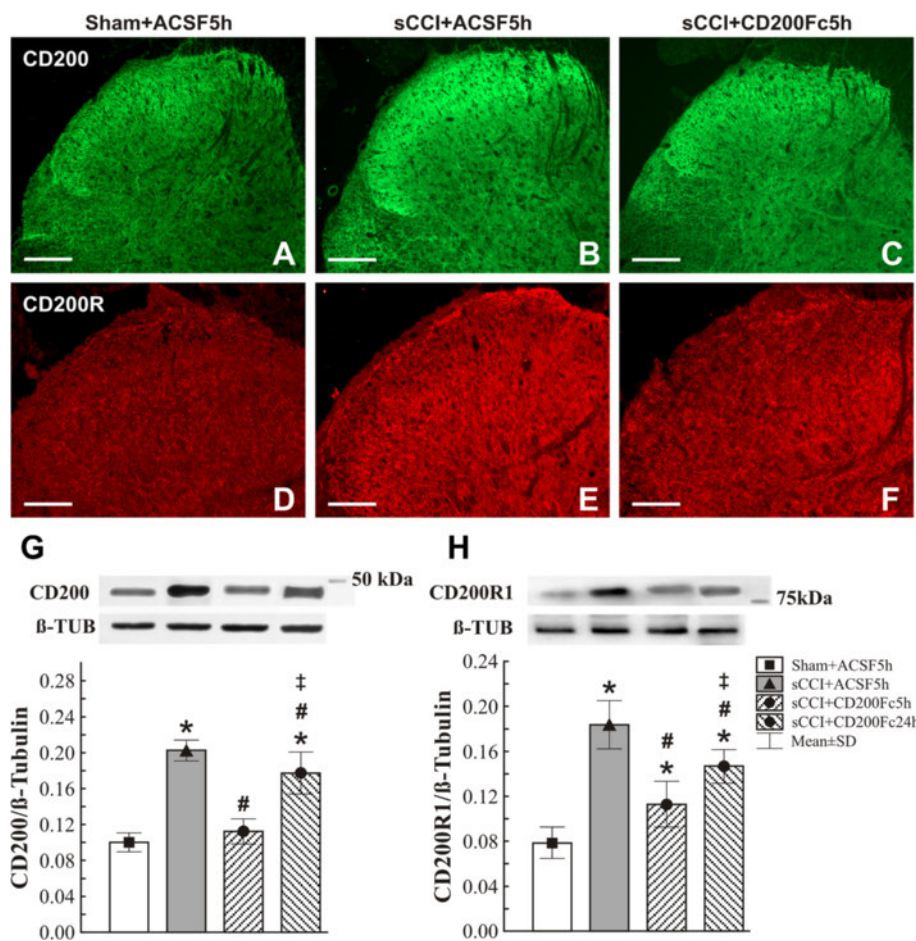


Fig. 4 Effect of CD200Fc on CD200 and CD200R1 protein levels. Effect of CD200Fc on CD200 and CD200R1 protein levels of the L4–L5 spinal cord segments from sCCI-operated rats. sCCI of the sciatic nerve and ACSF treatment increased intensity of CD200 and CD200R immunofluorescences in DH of spinal cord sections when compared with those from sham-operated rats. Intrathecal CD200Fc administration significantly attenuated elevation of CD200 and CD200R immunofluorescences in the spinal cord sections of sCCI-operated rats (**a–f**). Scale bars = 100 μ m. The CD200 and CD200R immunofluorescence changes were confirmed by western blot analysis of CD200 and CD200R proteins (**g, h**). Upper panels of **g** and **h** illustrate representative western blotting bands for CD200 and CD200R in the L4–L5 spinal cord segments from sham-operated (Sham), sCCI-operated and ACSF-treated (sCCI + ACSF5h) rats, as well as rats operated for sCCI and 5 (sCCI + CD200Fc5h) or 24 h (sCCI + CD200Fc24h) after administration of CD200Fc. Lower panels show mean density \pm SE of individual CD200 and CD200R1 protein bands in triplicate analysis of six animals after normalization to tubulin. * p < 0.05 when compared to naïve rats; # p < 0.05 when compared to sCCI + ACSF rats; ++ p < 0.05 when compared to 5 h after administration of CD200Fc. Mann-Whitney *U* test

after sCCI operation, RT-PCR was carried out using primers specific to pro- (TNF, IL-1 β , IL-6) and anti-inflammatory (IL-4, IL-10) cytokines.

As expected, L4–L5 segments of the spinal cord from sCCI-operated and ACSF-treated rats displayed robust elevation of relative mRNAs of proinflammatory (TNF, IL-1 β , IL-6) and a decrease of anti-inflammatory cytokines (IL-4, IL-10) when compared with spinal cord segments of naïve or sham-operated rats. After 5 h, intrathecal administration of CD200Fc produced normalization of TNF mRNA expression (Fig. 7a) and significant reduction in relative expression of IL-1 β and IL-6 mRNAs (Fig. 7b–c) in comparison with ACSF-treated rats. Conversely, relative levels of IL-4 and IL-10 mRNAs were simultaneously

increased close to (in the case of IL-4) or exceeding (for IL-10) those levels for spinal cord segments from naïve or sham-operated rats (Fig. 7d–e).

Discussion

Many experimental models of PNP are principally based on peripheral nerve injury providing a partial disconnection of axons from their neuronal bodies [6, 41]. The original model of CCI using four ligatures of chromic gut (4–0) loosely tied around the sciatic nerve [42] is not suitable for distinguishing neuroinflammatory reaction induced by a thread material [43] and/or Wallerian degeneration of injured axons [6]. Therefore, sCCI of the sciatic nerve in our experiments was prepared using

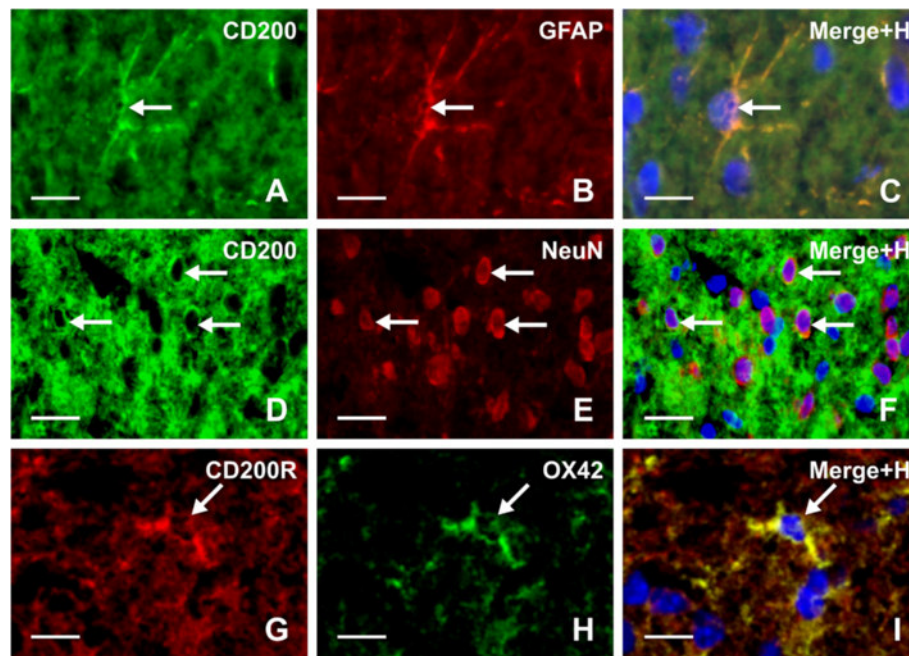


Fig. 5 Double immunostaining to detect CD200 protein in astrocytes and neurons as well as CD200R in microglia. Double immunostaining of sections through DH of L4–L5 spinal cord segments from sCCI-operated and ACSF-treated rats. Immunofluorescence for CD200 (a) and GFAP (b) are colocalized (c), evidencing that CD200 protein is expressed by astrocytes (arrows). In addition, double immunostaining for CD200 (d) and NeuN (e) detected a presence of CD200 protein also in neurons (f, arrows). Immunolabeling for CD200R (g) and OX42 (h) was colocalized, illustrating that activated microglial cells display CD200R protein (i, arrow). Merged figures (c, f, i) contain also blue channel of Hoechst stained nuclei. Scale bars = 30 μ m

3–0 sterilized thread (Ethicon) under aseptic conditions to study the effect of CD200Fc on spinal glial activation and cytokine reactions in consequent Wallerian degeneration induced by traumatic nerve compression. It is well known that PNP induced by nerve injury is related to activation of glial cells and upregulation of proinflammatory cytokines in the spinal cord, and their reduction has been associated with alleviation of behavioral signs [44–47].

CD200/CD200R is a regulatory system of inflammation that plays a relevant role in various diseases when CD200 ligand binding with its receptor is impaired [22, 25, 29]. In contrast, enhanced signaling of CD200R by CD200Fc treatment alleviates pathological effects of inflammation [32, 34–36]. However, the anti-neuroinflammatory effects of CD200Fc in neuropathic pain have not heretofore been investigated. The present study provides the first evidence that CD200Fc attenuates activation of glial cells and proinflammatory cytokines, as well as mechanical and thermal hypersensitivity in an experimental model of PNP immediately after its intrathecal administration.

CD200Fc has been applied intraperitoneally [35], subcutaneously [34], or intracerebroventricularly [32] in various experimental models of inflammatory diseases. As CD200Fc has a half life of just a few hours [48], we

applied the CD200R soluble ligand intrathecally to achieve direct and rapid diffusion of CD200Fc into DH of the rat spinal cord. We cannot exclude the possibility that a small portion of the drug administered into the cisterna magna will retrogradely reach the ventricular system and surrounding structures playing a role in the effects described here. However, decreased glial activation and modulation of cytokine mRNAs and CD200/CD200R changes revealed that CD200Fc diffused into the lumbar level of spinal cord.

CD200Fc attenuates glial activation of the spinal cord and neuropathic pain behavioral signs

Activation of microglial cells and astrocytes after nerve injury is strongly associated with induction and maintenance of mechanical and thermal hypersensitivity, and depression of the glial activities alleviates the behavioral signs of PNP [46, 49–51]. Microglial cells are accumulated in the spinal cord at the ipsilateral side to nerve injury and change their morphology from a “resting state” in which the cell bodies are small with long and thin processes into an “activated state” in which the cells present an amoeboid shape with their bodies enlarged and fine processes retracted [52, 53]. Microglial activation after peripheral nerve injury is generally detected by immunocytochemical staining using the OX42 antibody,

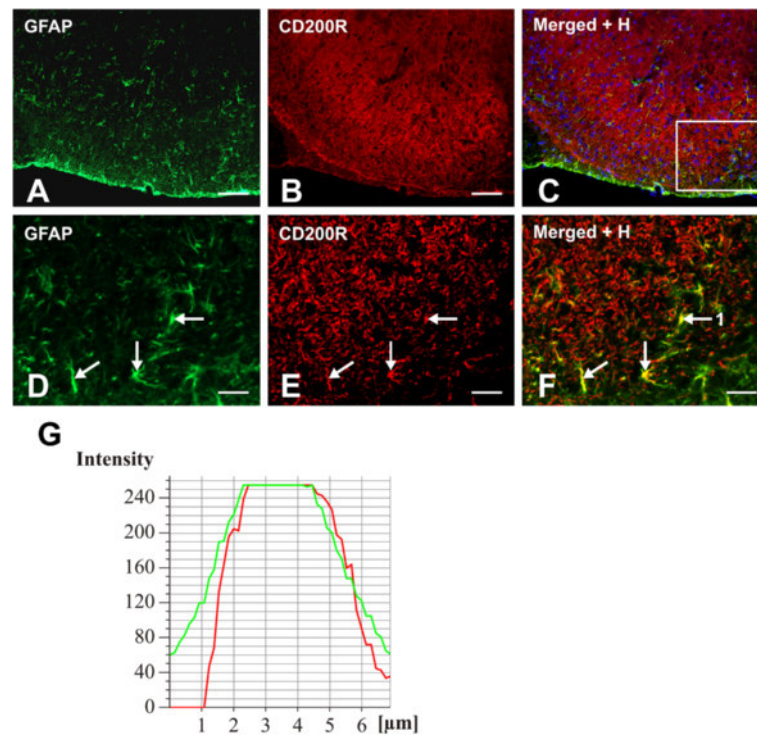


Fig. 6 Double immunostaining to detect CD200R protein in astrocytes. Double immunostaining of section through DH of L4–L5 spinal cord segments from sCCI-operated and ACSF-treated rats to detect CD200R protein in GFAP positive astrocytes. Immunofluorescence staining for GFAP (**a, d**) and CD200R (**b, e**) was colocalized as shown in merged figure (**c, f**). Scale bars = 100 μm. **d–f** illustrate a higher power magnification of area limited by a box in **c**. Evidence of CD200R in activated astrocytes was confirmed by image analysis of three cells in the section using NIS Elements software. Mander's overlap was 0.965265, 0.929336, and 0.960253 for cells indicated by arrows. Scale bars = 30 μm. **g** illustrates representative profile intensity of red (CD200R) and green (GFAP) channels in cell tagged 1

directed against a complement receptor 3 antigen (CD11b/c) or antibody against ionized calcium binding adapter molecule 1 (Iba1) [54, 55]. However, there is convincing evidence that enlarged OX42 immunostaining area measured by image analysis is related with microglial activation after nerve injury [53].

Ipsilateral DH of the spinal cord from sCCI + ACSF in contrast to naïve or sham-operated rats displayed enlarged areas of OX42 immunofluorescence and appearance of OX42+ microglial cells with the shapes indicating their activated state. The OX42 immunoreaction area was significantly reduced in DH of sCCI-operated and CD200Fc-treated rats, thus showing very rapid effect on the marker of activated microglia. The changes of microglial cell activation induced by CD200Fc were confirmed by western blot analysis of the CD11b/c protein. Our results are in agreement with other experimental studies in that CD200Fc rapidly reduced the markers of microglial activation [32, 34, 56].

Astrocytes are more dominant than microglia in the spinal cord, and they have been investigated predominantly in relation to their supportive functions for neurons [57]. Moreover, activated astrocytes are a major source of cytokines and may contribute significantly to

induction and maintenance of PNP [45, 49]. Astrocytes respond to various physiological or pathological stimuli with the increased expression of GFAP that is generally considered to be a marker for astrocyte activation [58]. It has been experimentally demonstrated that GFAP up-regulation in the spinal cord correlates well with nerve injury-induced PNP [49] and that suppression of astrocyte activation by fluorocitrate alleviates PNP symptoms [59]. In our experiments, as demonstrated by GFAP immunofluorescence areas and western blot analysis of GFAP protein, astrocytes became activated in sCCI-operated and ACSF-treated rats and were reduced bilaterally in DH of the spinal cord after treatment with CD200Fc. This suppression of activated astrocytes was much less than microglial cells which is in accordance with treatment by selective inhibitors of glial activation [55]. Our results of western blot analysis were obtained from whole L4–L5 segments containing possible changes also in the ventral horn of the spinal cord. However, OX42 and GFAP protein levels correlated with quantitative alterations of corresponding immunofluorescence were measured only in DH of the spinal cord.

Our present results evidence for the first time that intrathecal application of CD200Fc for 5 h diminished

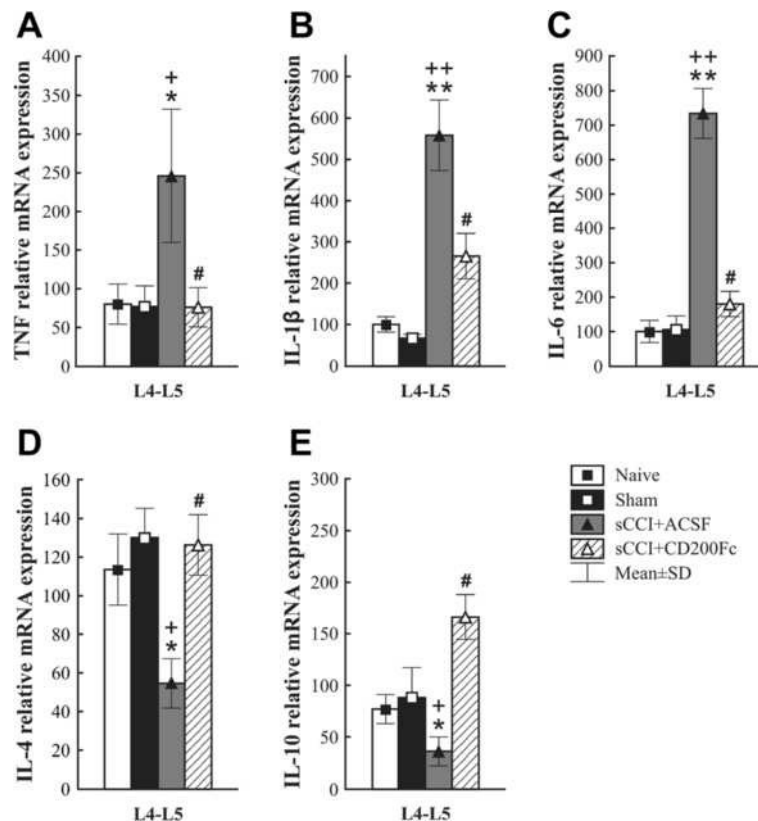


Fig. 7 RT-PCR analysis of cytokine RNAs in the spinal cord after CD200Fc administration. Effect of CD200Fc on TNF, IL-1 β , IL-6, IL-4, and IL-10 mRNAs expression in L4-L5 segments of spinal cord from sCCI-operated rats for 7 days. sCCI of the sciatic nerve and ACSF treatment increased levels of TNF (a), IL-1 β (b), and IL-6 (c) as well as decreased IL-4 (d) and IL-10 (e) mRNA expression in the lumbar spinal cord segments. Intrathecal CD200Fc administration prevented the increase of TNF, IL-1 β , and IL-6 as well as the decrease of IL-4 and IL-10 mRNAs expression in the lumbar spinal cord segments. The mRNA expression of each gene ($n = 6$ per group) was normalized to that of the 18S gene and the data represent the mean \pm SD. * $p < 0.05$, ** $p < 0.001$ when compared to naïve rats; + $p < 0.05$, ++ $p < 0.001$ when compared to sham-operated rats; # $p < 0.05$ when compared to sCCI + ACSF rats. Mann-Whitney U test

activation of both microglia and astrocytes in DH of the spinal cord after sciatic nerve injury. This rapid but reversible suppression of microglia and astrocyte activations runs in parallel with alleviation of both mechanical and thermal hypersensitivity. Because both activated microglial cells and astrocytes displayed CD200R, its activation by CD200Fc explains attenuation of the glial activation and consequent alleviation of nerve injury-induced PNP like in experimental studies using other modulators of glial activation [34, 46, 60]. Very rapid suppression of activated glial cells by CD200Fc was not surprising inasmuch as intrathecal injection of other drugs has been shown to abolish glial activation within hours [46, 61]. The CD200Fc effect was already weakened 24 h from single injection, however, thus indicating the necessity of repeated administration for longer PNP attenuation, as is usual for other molecules modulating neuroinflammation or pain [62, 63].

Expression of CD200 and CD200R in the dorsal horn of spinal cord

CD200 protein is constitutively expressed in neurons and to a lesser extent in reactive astrocytes while CD200R is expressed by microglia [21, 23]. The changes of CD200 and CD200R1 protein levels in the spinal cord after nerve injury and following administration of CD200Fc have not previously been described. The CD200 and CD200R immunostaining was predominantly found in the spinal dorsal horn and both immunofluorescence staining and western blot analysis revealed significantly higher levels of CD200 and CD200R proteins in the spinal cord after sCCI of the sciatic nerve. In contrast to neurodegenerative diseases [19, 25, 64], sciatic nerve injury probably activated endogenous regulatory mechanisms including upregulation of CD200/CD200R. Intrathecal CD200Fc treatment following sciatic nerve injury suppressed CD200 and CD200R proteins in the spinal cord to levels close to those of naïve

or sham-operated rats. The rapid regulation of the CD200 and CD200R proteins was parallel with activation or deactivation of microglia cells and astrocytes detected by CD11b/c or GFAP markers, respectively.

Using double immunostaining, we confirmed a presence of CD200 protein in neurons and astrocytes as well as CD200R in microglial cells as described earlier [21, 23]. However, there are no uncompromising results about expression of CD200R in astrocytes. We detected colocalization of GFAP and CD200R immunostaining in the spinal DH of sCCI-operated and ACSF-treated rats, thus indicating a presence of CD200R protein also in astrocytes activated by nerve injury. Activation of both microglia and astrocytes might therefore be directly modulated by CD200Fc through stimulation of CD200R. Intense cross talk between glial cells in the spinal DH is induced in the initiation phase of injury-induced PNP [8, 55, 65]. CD200/CD200R-mediated suppression of neuroinflammation may occur not only via neuron-microglia interactions but also via glia-glia interactions [23]. In addition to neurons, increased expression of CD200 in reactive astrocytes may contribute to control of microglial activation, while CD200R upregulation probably allows a modulation of astrocyte activation by contact with CD200+ neurons.

CD200Fc decreases proinflammatory and increases anti-inflammatory cytokine mRNAs in the spinal cord of nerve-injured rats

In the present time, there is no evidence about direct operation of CD200/CD200R dysbalance in neuropathic pain induction. It is generally accepted that CD200/CD200R modulatory system is involved in suppression of inflammation and glial activation. Although the recruitment of neutrophils, macrophages, and lymphocytes from blood might participate in the neuroimmune response of the spinal cord to nerve injury, the activation of microglia and astrocytes undoubtedly plays a pivotal role in production of cytokines and chemokines [10, 12, 54].

A nerve injury induces elevation of proinflammatory cytokine levels and their synthesis (mRNA) in the spinal cord associated with development and maintenance of PNP [66–68]. Experimental studies have demonstrated that suppression of proinflammatory cytokines like TNF, IL-1 β , and IL-6 is necessary for efficacious attenuation of mechanical and thermal hypersensitivity [67, 69, 70]. In contrast, increased synthesis or delivery of IL-10 has been shown to attenuate proinflammatory cytokine levels and alleviated PNP [71]. Similarly, other anti-inflammatory cytokines, such as IL-4, also have been decreased in the CCI model of PNP and IL-4 deficiency has been associated with mechanical hypersensitivity [72]. Accumulating evidence indicates that nerve injury induces upregulation of pro- and anti-inflammatory cytokines in activated microglia and astrocytes in relation

with development and maintenance of PNP [7, 10, 44]. Our results from RT-PCR showed increase of proinflammatory cytokine (TNF, IL-1 β , IL-6) and decrease of anti-inflammatory cytokine (IL-4, IL-10) mRNAs in the spinal cord of nerve-injured rats in comparison with naïve and sham-operated animals. Intrathecal CD200Fc treatment diminished elevation of proinflammatory cytokine (TNF, IL-1 β , IL-6) mRNAs and simultaneously ameliorated deficit of IL-4 and IL-10 mRNAs induced by unilateral sCCI of the sciatic nerve. This modulation of pro- and anti-inflammatory cytokine mRNAs by CD200Fc treatment was simultaneous with glia deactivation and attenuation of mechanical and thermal hypersensitivity.

CD200R1 stimulation suggests that CD200/CD200R1 interaction is involved in suppression of the proinflammatory phenotype of microglial cells [32–34, 73] and astrocytes. In addition, an *in vitro* study showed how microglia incubation with CD200-bearing astrocytic membrane preparations mitigates the LPS-induced increase in mRNA expression of the proinflammatory cytokines TNF, IL-1 β , and IL-6 [74]. In line with our findings, CD200Fc treatment significantly decreased the production of TNF and IL-6 but not of IL-10 or TGF- β in microglial cells of mice with experimental autoimmune encephalomyelitis [34]. Referring to anti-inflammatory cytokines, it has been pointed out that there is a possible involvement of CD200Fc in increasing IL-4 and IL-10 in microglia cells [33, 56]. Moreover, an increased expression of IL-10 in relation to enhanced neuronal levels of CD200 has been also found in the central nervous system of experimental autoimmune encephalomyelitis mice [27].

The present results indicate that sciatic nerve injury-induced upregulation of proinflammatory cytokines in parallel with elevation of the CD200/CD200R regulatory system. An enhanced signaling of CD200R1 by CD200Fc treatment attenuated activation of microglial cells and astrocytes simultaneously with a decrease of proinflammatory and increase of anti-inflammatory cytokine synthesis. Due to reduction of the inflammatory reaction by CD200Fc, expression of the CD200/CD200R regulatory system was diminished.

In conclusion, our results suggest that support of the CD200/CD200R regulatory system by administration of the CD200R1 agonist CD200Fc induces very rapid suppression of neuroinflammatory reactions associated with glial activation and PNP development. This may constitute a promising and novel therapeutic approach for the treatment of PNP. Additional experiments with nerve injury models are nevertheless needed, and particularly with repeated CD200Fc treatment to prolong its effect.

Conclusions

The present results indicate that sCCI of the sciatic nerve induced upregulation of proinflammatory cytokines in

parallel with elevation of the CD200/CD200R regulatory system. An enhanced signaling of CD200R1 by administration of the CD200R1 agonist CD200Fc induces very rapid suppression of glial activation in the spinal cord simultaneously with a decrease of proinflammatory and increase of anti-inflammatory cytokine synthesis associated with attenuation of PNP development. Due to reduction of the inflammatory reaction by CD200Fc, expression of the CD200/CD200R regulatory system was diminished.

Support of the CD200/CD200R regulatory system by administration of the CD200R1 agonist CD200Fc may constitute a promising and novel therapeutic approach for the treatment of PNP. Additional experiments with nerve injury models are nevertheless needed and particularly with repeated CD200Fc treatment to prolong its effect.

Competing interests

The authors declare that they have no competing interests.

Authors' contributions

MH conceived, designed the experiments, carried out behavioral tests, western blot, and RT-PCR analyses, and wrote the manuscript. IK, MJ, and IHS conceived, designed, and carried out intrathecal administration and participated in acquiring and analyzing the presented data. CG conceived and participated in acquiring and analyzing the RT-PCR data. PD conceived, designed and coordinated the study, and wrote the manuscript. All authors gave final approval to the version to be published.

Acknowledgements

We thank Dana Kutějová, Jitka Mikulášková, Marta Lněničková, Jana Vachová, and Lumír Trenčanský for their skillful technical assistance. This work was supported by the projects CEITEC from European Regional Development Fund (CZ.1.05/1.1.00/02.0068) and Employment of Newly Graduated Doctors of Science for Scientific Excellence (CZ.1.07/2.3.00/30.0009).

Author details

¹Central European Institute of Technology (CEITEC), Masaryk University, Kamenice 3, 62500 Brno, Czech Republic. ²Department of Anatomy, Division of Neuroanatomy, Faculty of Medicine, Masaryk University, Kamenice 3, 62500 Brno, Czech Republic. ³Department of Functional and Systems Neurobiology, Neuroimmunology Group, Cajal Institute, Consejo Superior de Investigaciones Científicas (CSIC), Madrid, Spain.

Received: 19 November 2015 Accepted: 10 February 2016

Published online: 18 February 2016

References

- Berger JV, Knaepen L, Janssen SPM, Jaken RJP, Marcus MAE, Joosten EAJ, et al. Cellular and molecular insights into neuropathy-induced pain hypersensitivity for mechanism-based treatment approaches. *Brain Res Rev.* 2011;67(1–2):282–310.
- Campbell JN, Meyer RA. Mechanisms of neuropathic pain. *Neuron.* 2006;52(1):77–92.
- Marchand F, Perretti M, McMahon SB. Role of the immune system in chronic pain. *Nature Rev Neurosci.* 2005;6(7):521–32.
- Watkins LR, Hutchinson MR, Ledebner A, Wieseler-Frank J, Milligan ED, Maier SF. Glia as the "bad guys": implications for improving clinical pain control and the clinical utility of opioids. *Brain Behav Immun.* 2007;21(2):131–46.
- Swett JE, Torigoe Y, Elie VR, Bourassa CM, Miller PG. Sensory neurons of the rat sciatic nerve. *Exp Neurol.* 1991;114(1):82–103.
- Klusakova I, Dubovy P. Experimental models of peripheral neuropathic pain based on traumatic nerve injuries—an anatomical perspective. *Ann Anat.* 2009;191(3):248–59.
- Moalem G, Tracey DJ. Immune and inflammatory mechanisms in neuropathic pain. *Brain Res Rev.* 2006;51(2):240–64.
- Choi H-S, Roh D-H, Yoon S-Y, Moon J-Y, Choi S-R, Kwon S-G, et al. Microglial interleukin-1 beta in the ipsilateral dorsal horn inhibits the development of mirror-image contralateral mechanical allodynia through astrocyte activation in a rat model of inflammatory pain. *Pain.* 2015;156(6):1046–59.
- Gao YJ, Ji RR. Targeting astrocyte signaling for chronic pain. *Neurotherapeutics.* 2010;7(4):482–93.
- Milligan ED, Twining C, Chacur M, Biedenkapp J, O'Connor K, Poole S, et al. Spinal glia and proinflammatory cytokines mediate mirror-image neuropathic pain in rats. *J Neurosci.* 2003;23(3):1026–40.
- Yamamoto Y, Terayama R, Kishimoto N, Maruhama K, Mizutani M, Iida S, et al. Activated microglia contribute to convergent nociceptive inputs to spinal dorsal horn neurons and the development of neuropathic pain. *Neurochem Res.* 2015;40(5):1000–12.
- Gao YJ, Ji RR. Chemokines, neuronal-glia interactions, and central processing of neuropathic pain. *Pharmacol Ther.* 2010;126(1):56–68.
- Brazda V, Klusakova I, Svizenska IH, Dubovy P. Dynamic response to peripheral nerve injury detected by in situ hybridization of IL-6 and its receptor mRNAs in the dorsal root ganglia is not strictly correlated with signs of neuropathic pain. *Mol Pain.* 2013;9:42.
- Dubovy P, Brazda V, Klusakova I, Hradilova-Svizenska I. Bilateral elevation of interleukin-6 protein and mRNA in both lumbar and cervical dorsal root ganglia following unilateral chronic compression injury of the sciatic nerve. *J Neuroinflamm.* 2013;10:55.
- Hatashita S, Sekiguchi M, Kobayashi H, Konno SI, Kikuchi SI. Contralateral neuropathic pain and neuropathology in dorsal root ganglion and spinal cord following hemilateral nerve injury in rats. *Spine.* 2008;33(12):1344–51.
- Dubovy P. Wallerian degeneration and peripheral nerve conditions for both axonal regeneration and neuropathic pain induction. *Ann Anat.* 2011;194(4):267–75.
- Wright GJ, Cherwinski H, Foster-Cuevas M, Brooke G, Puklavec MJ, Bigler M, et al. Characterization of the CD200 receptor family in mice and humans and their interactions with CD200. *J Immunol.* 2003;171(6):3034–46.
- Hatherley D, Lea SM, Johnson S, Barclay AN. Structures of CD200/CD200 receptor family and implications for topology, regulation, and evolution. *Structure.* 2013;21(5):820–32.
- Koning N, Bo L, Hoek RM, Huitinga I. Downregulation of macrophage inhibitory molecules in multiple sclerosis lesions. *Ann Neurol.* 2007;62(5):504–14.
- Dentesano G, Straccia M, Ejarque-Ortiz A, Tusell JM, Serratos J, Saura J, et al. Inhibition of CD200R1 expression by C/EBP beta in reactive microglial cells. *J Neuroinflamm.* 2012;9:165.
- Dentesano G, Serratos J, Tusell JM, Ramon P, Valente T, Saura J, et al. CD200R1 and CD200 expression are regulated by PPAR-gamma in activated glial cells. *Glia.* 2014;62(6):982–98.
- Gao S, Hao B, Yang XF, Chen WQ. Decreased CD200R expression on monocyte-derived macrophages correlates with Th17/Treg imbalance and disease activity in rheumatoid arthritis patients. *Inflamm Res.* 2014;63(6):441–50.
- Koning N, Swaab DF, Hoek RM, Huitinga I. Distribution of the immune inhibitory molecules CD200 and CD200R in the normal central nervous system and multiple sclerosis lesions suggests neuron-glia and glia-glia interactions. *J Neuroimmunol Exp Neurol.* 2009;68(2):159–67.
- Costello DA, Lyons A, Denieffe S, Browne TC, Cox FF, Lynch MA. Long term potentiation is impaired in membrane glycoprotein CD200-deficient mice. A role for toll-like receptor activation. *J Biol Chem.* 2011;286(40):34722–32.
- Walker DG, Dalsing-Hernandez JE, Campbell NA, Lue LF. Decreased expression of CD200 and CD200 receptor in Alzheimer's disease: a potential mechanism leading to chronic inflammation. *Exp Neurol.* 2009;215(1):5–19.
- Wang XJ, Ye M, Zhang YH, Chen SD. CD200-CD200R regulation of microglia activation in the pathogenesis of Parkinson's disease. *J Neuroimmunol Pharmacol.* 2007;2(3):259–64.
- Chitnis T, Imitola J, Wang Y, Elyaman W, Chawla P, Sharuk M, et al. Elevated neuronal expression of CD200 protects Wld(s) mice from inflammation-mediated neurodegeneration. *Am J Pathol.* 2007;170(5):1695–712.
- Hoek RM, Ruuls SR, Murphy CA, Wright GJ, Goddard R, Zurawski SM, et al. Down-regulation of the macrophage lineage through interaction with OX2 (CD200). *Science.* 2000;290(5497):1768–71.
- Meuth SG, Simon OJ, Gnimmm A, Melzer N, Herrmann AM, Spitzer P, et al. CNS inflammation and neuronal degeneration is aggravated by impaired CD200-CD200R-mediated macrophage silencing. *J Neuroimmunol.* 2008;194(1–2):62–9.

30. Lyons A, McQuillan K, Deighan BF, O'Reilly J-A, Downer EJ, Murphy AC, et al. Decreased neuronal CD200 expression in IL-4-deficient mice results in increased neuroinflammation in response to lipopolysaccharide. *Brain Beh Immun*. 2009;23(7):1020–7.
31. Koning N, van Eijk M, Pouwels W, Brouwer MSM, Voehringer D, Huitinga I, et al. Expression of the inhibitory CD200 receptor is associated with alternative macrophage activation. *J Innate Immun*. 2010;2(2):195–200.
32. Cox FF, Carney D, Miller AM, Lynch MA. CD200 fusion protein decreases microglial activation in the hippocampus of aged rats. *Brain Beh Immun*. 2012;26(5):789–96.
33. Hernangomez M, Mestre L, Correa FG, Loria F, Mecha M, Inigo PM, et al. CD200-CD200R1 interaction contributes to neuroprotective effects of anandamide on experimentally induced inflammation. *Glia*. 2012; 60(9):1437–50.
34. Liu YR, Bando Y, Vargas-Lowy D, Elyaman W, Khoury SJ, Huang T, et al. CD200R1 agonist attenuates mechanisms of chronic disease in a murine model of multiple sclerosis. *J Neurosci*. 2010;30(6):2025–38.
35. Simelyte E, Criado G, Essex D, Uger RA, Feldmann M, Williams RO. CD200-Fc, a novel antiarthritic biologic agent that targets proinflammatory cytokine expression in the joints of mice with collagen-induced arthritis. *Arthritis Rheum*. 2008;58(4):1038–43.
36. Ding Y, Yang H, Xiang W, He X, Liao W, Yi Z. CD200R1 agonist attenuates LPS-induced inflammatory response in human renal proximal tubular epithelial cells by regulating TLR4-MyD88-TAK1-mediated NF- κ B and MAPK pathway. *Biochem Biophys Res Comm*. 2015;460(2):287–94.
37. Hylden JK, Wilcox GL. Intrathecal morphine in mice—a new technique. *Eur J Pharmacol*. 1980;67(2–3):313–6.
38. Zamboni L, Demartin C. Buffered picric acid-formaldehyde—a new rapid fixative for electron microscopy. *J Cell Biol*. 1967;35(2P2):A148.
39. Brazda V, Muller P, Brozkova K, Vojtesek B. Restoring wild-type conformation and DNA-binding activity of mutant p53 is insufficient for restoration of transcriptional activity. *Biochem Biophys Res Comm*. 2006;351(2):499–506.
40. Ren Y, Yang B, Yin Y, Leng X, Jiang Y, Zhang L, et al. Aberrant CD200/CD200R1 expression and its potential role in Th17 cell differentiation, chemotaxis and osteoclastogenesis in rheumatoid arthritis. *Rheumatology*. 2015;54(4):712–21.
41. Austin PJ, Moalem-Taylor G. Animal models of neuropathic pain due to nerve injury. *NeuroMethods*. 2013;78:239–60.
42. Bennett GJ, Xie YK. A peripheral mononeuropathy in rat that produces disorders of pain sensation like those seen in man. *Pain*. 1988;33(1):87–107.
43. Maves TJ, Pechman PS, Gebhart GF, Meller ST. Possible chemical contribution from chronic gut sutures produces disorders of pain sensation like those seen in man. *Pain*. 1993;54(1):57–69.
44. Pineau I, Lacroix S. Endogenous signals initiating inflammation in the injured nervous system. *Glia*. 2009;57(4):351–61.
45. Guo W, Wang H, Watanabe M, Shimizu K, Zou SP, LaGraize SC, et al. Glial-cytokine-neuronal interactions underlying the mechanisms of persistent pain. *J Neurosci*. 2007;27(22):6006–18.
46. Clark AK, Yip PK, Grist J, Gentry C, Staniland AA, Marchand F, et al. Inhibition of spinal microglial cathepsin S for the reversal of neuropathic pain. *Proc Natl Acad Sci U S A*. 2007;104(25):10655–60.
47. Raghavendra V, Tanga F, DeLeo JA. Inhibition of microglial activation attenuates the development but not existing hypersensitivity in a rat model of neuropathy. *J Pharmacol Exp Ther*. 2003;306(2):624–30.
48. Gorczynski RM, Cattral MS, Chen ZG, Hu JA, Lei J, Min WP, et al. An immunoadhesin incorporating the molecule OX-2 is a potent immunosuppressant that prolongs allo- and xenograft survival. *J Immunol*. 1999;163(3):1654–60.
49. Wang W, Mei XP, Huang J, Wei YY, Wang YY, Wu SX, et al. Crosstalk between spinal astrocytes and neurons in nerve injury-induced neuropathic pain. *Plos One*. 2009;4(9):10.
50. Padi SSV, Kulkarni SK. Minocycline prevents the development of neuropathic pain, but not acute pain: possible anti-inflammatory and antioxidant mechanisms. *Eur J Pharmacol*. 2008;601(1–3):79–87.
51. Morioka N, Zhang FF, Nakamura Y, Kitamura T, Hisaoka-Nakashima K, Nakata Y. Tumor necrosis factor-mediated downregulation of spinal astrocytic connexin43 leads to increased glutamatergic neurotransmission and neuropathic pain in mice. *Brain Beh Immun*. 2015;49:293–310.
52. Beggs S, Salter MW. Stereological and somatotopic analysis of the spinal microglial response to peripheral nerve injury. *Brain Beh Immun*. 2007;21(5):624–33.
53. Blackbeard J, O'Dea KP, Wallace VCJ, Segerdahl A, Pheby T, Takata M, et al. Quantification of the rat spinal microglial response to peripheral nerve injury as revealed by immunohistochemical image analysis and flow cytometry. *J Neurosci Meth*. 2007;164(2):207–17.
54. Ji RR, Berta T, Nedergaard M. Glia and pain: is chronic pain a gliopathy? *Pain*. 2013;154:S10–28.
55. Mika J, Osikowicz M, Rojewska E, Korostynski M, Wawrzczak-Bargiela A, Przewlocki R, et al. Differential activation of spinal microglial and astroglial cells in a mouse model of peripheral neuropathic pain. *Eur J Pharmacol*. 2009;623(1–3):65–72.
56. Lyons A, Downer EJ, Crotty S, Nolan YM, Mills KHG, Lynch MA. CD200 ligand-receptor interaction modulates microglial activation in vivo and in vitro: a role for IL-4. *J Neurosci*. 2007;27(31):8309–13.
57. Cregg JM, DePaul MA, Filous AR, Lang BT, Tran A, Silver J. Functional regeneration beyond the glial scar. *Exp Neurol*. 2014;253:197–207.
58. Nolte C, Matyash M, Pivneva T, Schipke CG, Ohlemeyer C, Hanisch UK, et al. GFAP promoter-controlled EGFP-expressing transgenic mice: a tool to visualize astrocytes and astrogliosis in living brain tissue. *Glia*. 2001;33(1):72–86.
59. Lan L, Yuan H, Duan L, Cao R, Gao B, Shen J, et al. Blocking the glial function suppresses subcutaneous formalin-induced nociceptive behavior in the rat. *Neurosci Res*. 2007;57(1):112–9.
60. Mika J, Zychowska M, Popiolek-Barczyk K, Rojewska E, Przewlocka B. Importance of glial activation in neuropathic pain. *Eur J Pharmacol*. 2013; 716(1–3):106–19.
61. Feng XM, Zhang FJ, Dong R, Li WY, Liu J, Zhao X, et al. Intrathecal administration of clonidine attenuates spinal neuroimmune activation in a rat model of neuropathic pain with existing hyperalgesia. *Eur J Pharmacol*. 2009;614(1–3):38–43.
62. Kersten C, Cameron MG, Laird B, Mjaland S. Epidermal growth factor receptor—inhibition (EGFR-I) in the treatment of neuropathic pain. *Br J Anaesth*. 2015;115(5):761–7.
63. Xin Q, Cheng B, Pan Y, Liu H, Yang C, Chen J, et al. Neuroprotective effects of apelin-13 on experimental ischemic stroke through suppression of inflammation. *Peptides*. 2015;63:55–62.
64. Zhang S, Wang XJ, Tian LP, Pan J, Lu GQ, Zhang YJ, et al. CD200-CD200R dysfunction exacerbates microglial activation and dopaminergic neurodegeneration in a rat model of Parkinson's disease. *J Neuroinflamm*. 2011;8:154.
65. Narita M, Yoshida T, Nakajima M, Narita M, Miyatake M, Takagi T, et al. Direct evidence for spinal cord microglia in the development of a neuropathic pain-like state in mice. *J Neurochem*. 2006;97(5):1337–48.
66. Kleinschnitz C, Brinkhoff J, Sommer C, Stoll G. Contralateral cytokine gene induction after peripheral nerve lesions: dependence on the mode of injury and NMDA receptor signaling. *Mol Brain Res*. 2005;136(1–2):23–8.
67. Latremoliere A, Mauborgne A, Masson J, Bourgoin S, Kayser V, Hamon M, et al. Differential implication of proinflammatory cytokine interleukin-6 in the development of cephalic versus extracephalic neuropathic pain in rats. *J Neurosci*. 2008;28(34):8489–501.
68. Uceyler N, Tschärke A, Sommer C. Early cytokine gene expression in mouse CNS after peripheral nerve lesion. *Neurosci Lett*. 2008;436(2):259–64.
69. Sacerdote P, Franchi S, Moretti S, Castelli M, Procacci P, Magnaghi V, et al. Cytokine modulation is necessary for efficacious treatment of experimental neuropathic pain. *J Neuroimmun Pharmacol*. 2013;8(1):202–11.
70. Wilkerson JL, Gentry KR, Dengler EC, Wallace JA, Kerwin AA, Armijo LM, et al. Intrathecal cannabidiol CB2R agonist, AM1710, controls pathological pain and restores basal cytokine levels. *Pain*. 2012;153(5):1091–106.
71. Milligan ED, Sloane EM, Langer SJ, Cruz PE, Chacur M, Spataro L, et al. Controlling neuropathic pain by adeno-associated virus driven production of the anti-inflammatory cytokine, interleukin-10. *Mol Pain*. 2005;1:9.
72. Uceyler N, Topuzoglu T, Schiesser P, Hahnenkamp S, Sommer C. IL-4 deficiency is associated with mechanical hypersensitivity in mice. *Plos One*. 2011;6(12):e28205.
73. Lyons A, Downer EJ, Costello DA, Murphy N, Lynch MA. Dok2 mediates the CD200Fc attenuation of A beta-induced changes in glia. *J Neuroinflamm*. 2012;9:107.
74. Cox FF, Berezin V, Bock E, Lynch MA. The neural cell adhesion molecule-derived peptide, FGL, attenuates lipopolysaccharide-induced changes in glia in a cd200-dependent manner. *Neurosci*. 2013;235:141–8.

- E. Dubový P, Klusáková I, Hradilová-Svíženská I, **Joukal M**, Boadas-Vaello P. Activation of Astrocytes and Microglial Cells and CCL2/CCR2 Upregulation in the Dorsolateral and Ventrolateral Nuclei of Periaqueductal Gray and Rostral Ventromedial Medulla Following Different Types of Sciatic Nerve Injury. *Front Cell Neurosci.* 2018;12:40. doi:10.3389/fncel.2018.00040

Commentary: In this article, we demonstrated that chronic constriction injury and sciatic nerve transection induce activation glia and astrocytes in the periaqueductal gray and rostral ventromedial medulla. This activation is triggered by CCL2/CCR2 signaling involved in the neuron-glia and glia-glia interactions in both supraspinal regions suggesting its role in neuropathic pain maintenance.

IF (WOS, 2017): 4.3

Quartile (WOS, 2017): Neurosciences Q1

Contribution of the author: Co-authorship. The author participated in designing, performing the experiments as well as acquiring and analyzing the presented data.



Activation of Astrocytes and Microglial Cells and CCL2/CCR2 Upregulation in the Dorsolateral and Ventrolateral Nuclei of Periaqueductal Gray and Rostral Ventromedial Medulla Following Different Types of Sciatic Nerve Injury

Petr Dubový¹, Ilona Klusáková^{1†}, Ivana Hradilová-Sviženská^{1†}, Marek Joukal^{1†} and Pere Boadas-Vaello^{1,2*}

¹Department of Anatomy, Division of Neuroanatomy, Faculty of Medicine, Masaryk University, Brno, Czechia, ²Research Group of Clinical Anatomy, Embryology and Neuroscience (NEOMA), Department of Medical Sciences, Universitat de Girona, Girona, Spain

OPEN ACCESS

Edited by:

Flavia Trettel,
Sapienza Università di Roma, Italy

Reviewed by:

Ji Zhang,
McGill University, Canada
Guilherme Lucas,
University of São Paulo, Brazil

*Correspondence:

Pere Boadas-Vaello
pere.boadas@udg.edu

[†]These authors have contributed
equally to this work.

Received: 21 October 2017

Accepted: 01 February 2018

Published: 19 February 2018

Citation:

Dubový P, Klusáková I, Hradilová-Sviženská I, Joukal M and Boadas-Vaello P (2018) Activation of Astrocytes and Microglial Cells and CCL2/CCR2 Upregulation in the Dorsolateral and Ventrolateral Nuclei of Periaqueductal Gray and Rostral Ventromedial Medulla Following Different Types of Sciatic Nerve Injury. *Front. Cell. Neurosci.* 12:40. doi: 10.3389/fncel.2018.00040

Peripheral nerve injuries (PNIs) may result in cellular and molecular changes in supraspinal structures possibly involved in neuropathic pain (NPP) maintenance. Activated glial cells in specific supraspinal subregions may affect the facilitatory role of descending pathways. Sterile chronic compression injury (sCCI) and complete sciatic nerve transection (CSNT) in rats were used as NPP models to study the activation of glial cells in the subregions of periaqueductal gray (PAG) and rostral ventromedial medulla (RVM). Molecular markers for activated astrocytes (glial fibrillary acidic protein, GFAP) and microglial cells (OX42) were assessed by quantitative immunohistochemistry and western blotting. The cellular distribution of CCL2/CCR2 was monitored using immunofluorescence. sCCI induced both mechanical and thermal hypersensitivity from day 1 up to 3 weeks post-injury. Unilateral sCCI or CSNT for 3 weeks induced significant activation of astrocytes bilaterally in both dorsolateral (dIPAG) and ventrolateral PAG (vIPAG) compared to naïve or sham-operated rats. More extensive astrocyte activation by CSNT compared to sCCI was induced bilaterally in dIPAG and ipsilaterally in vIPAG. Significantly more extensive activation of astrocytes was also found in RVM after CSNT than sCCI. The CD11b immunopositive region, indicating activated microglial cells, was remarkably larger in dIPAG and vIPAG of both sides from sCCI- and CSNT-operated rats compared to naïve or sham-operated controls. No significant differences in microglial activation were detected in dIPAG or vIPAG after CSNT compared to sCCI. Both nerve injury models induced no significant differences in microglial activation in the RVM. Neurons and activated GFAP+ astrocytes displayed CCL2-immunoreaction, while activated OX42+ microglial cells were CCR2-immunopositive in both PAG and RVM after sCCI and CSNT. Overall, while CSNT induced robust astrogliosis in both PAG and RVM, microglial cell activation was similar in the supraspinal structures in both injury nerve models.

Activated astrocytes in PAG and RVM may sustain facilitation of the descending system maintaining NPP, while microglial activation may be associated with a reaction to long-lasting peripheral injury. Microglial activation via CCR2 may be due to neuronal and astrocyte release of CCL2 in PAG and RVM following injury.

Keywords: activated glial cells, CCL2/CCR2, neuroinflammation, periaqueductal gray, rostral ventromedial medulla, nerve injury, neuropathic pain model

INTRODUCTION

Peripheral nerve injuries (PNIs) due either to trauma, disease or surgical intervention, usually result in neuroplastic changes in the central nervous system (CNS) and pain (Berger et al., 2011). Such changes include the activation of endogenous glial cells of the CNS, like microglia (Streit et al., 1999; Hanisch and Kettenmann, 2007; Graeber and Streit, 2010) and astrocytes (Ridet et al., 1997; Pekny and Nilsson, 2005; Sofroniew and Vinters, 2010; Anderson et al., 2014; Pekny and Pekna, 2014). The activated glial cells facilitate pain neurotransmission and induce the central sensitization of spinal neurons located in the dorsal horn. Briefly, PNI causes the generation of ectopic discharges in the lesioned afferent nerve fibers and their neurons (Omana-Zapata et al., 1997; Woolf and Mannion, 1999; Liu et al., 2000; Schaible, 2007), triggering an increased release of excitatory neurotransmitters and neuromodulators onto spinal cord neurons and glial cells. These changes induce central sensitization, glial cell activation, and hyperexcitability of nociceptive spinal cord neurons that consequently increase their discharges through the ascending pain pathways (Zimmermann, 2001; Schaible, 2007; Latremoliere and Woolf, 2009; Woolf, 2011; Burnstock, 2016).

The cellular and molecular changes described till now have been extensively studied mainly in the dorsal horn of the spinal cord and its circuitry (Vranken, 2009, 2012; Boadas-Vaello et al., 2016), but much less is known about supraspinal changes associated with the induction and maintenance of neuropathic pain (NPP) and the underlying mechanisms. Neuroplastic processes in the spinal cord facilitate the generation and conduction of action potentials by the ascending pathways up to supraspinal structures, contributing to both sensory and pain behavior alterations. The periaqueductal gray (PAG) and rostral ventromedial medulla (RVM) are particularly interesting given their pivotal role in nociceptive modulation (Fields et al., 2006). The PAG has a columnar functional organization with discrete ventrolateral PAG (vlPAG) and dorsolateral PAG (dlPAG) columns that have differences in the antinociceptive effects with respect to their dependence on opiate mechanisms (Lane et al., 2004; Lovick and Bandler, 2005; Eidson and Murphy, 2013; Wilson-Poe et al., 2013) and the spinal projection of sciatic nerve (Keay et al., 1997).

Pre-clinical studies of nerve injury models demonstrated glial activation in PAG (Mor et al., 2010; Ni et al., 2016) and RVM (Wei et al., 2008; Guo et al., 2012) associated with changes in cytokines/chemokines (Wei et al., 2008; Norman et al., 2010; Chu et al., 2012; Guo et al., 2012). Moreover, the chemokine CCL2, also known as monocyte chemoattractant protein 1 (MCP-1), has been demonstrated to play a critical

role in NPP facilitation via its preferred receptor, CCR2 (Gao et al., 2009; Jung et al., 2009; Gao and Ji, 2010). It was demonstrated that PNI increases the release of CCL2 in the dorsal horn of the spinal cord (Van Steenwinckel et al., 2011; Clark et al., 2013) triggering the activation of microglial cells (Zhang and De Koninck, 2006; Thacker et al., 2009). The role of CCL2 signaling in supraspinal structures involved in pain modulation has still not been completely elucidated. Reactive microglia cells may synthesize and secrete more inflammatory mediators, which elicit increasing excitability of superficial dorsal horn neurons, and enhance secretion of CCL2 from spinal astrocytes (Clark et al., 2013). Similar processes may occur also in both PAG subregions as well as in the RVM which are involved in the alteration of descending pain modulation.

Overall, despite the available data regarding neuroplastic changes in supraspinal structures associated with nervous system injury-induced pathological pain (Boadas-Vaello et al., 2017), the cellular and molecular processes occurring in these structures as a consequence of PNI are not yet fully understood. Particularly, since distinct subregions of PAG may play different or specific roles in the descending modulation of pain (McMullan and Lumb, 2006; Eidson and Murphy, 2013), it is of interest to investigate whether dlPAG and vlPAG show different pathophysiological responses after PNI, and whether these responses appear in parallel with RVM glial activation, and to do so in distinct PNI models. To this end, the present work was designed to study glial activation in both PAG nuclei and RVM after two models of sciatic nerve injury, namely, sterile chronic constriction injury (sCCI) and complete sciatic nerve transection (CSNT). Moreover, considering the pivotal role of chemokines in CNS sensitization and NPP maintenance, the aim of experiments was also to explore associated chemokine signaling through monitoring the expression of CCL2/CCR2 which could be involved in supraspinal glial cross-talk after sciatic nerve injury.

MATERIALS AND METHODS

Animals and Surgical Procedures

The experiments were performed in 28 adult male rats (Wistar, 200–250 g, Anlab, a.s. Brno, Czech Republic). Animals were kept at 22°C and maintained on a 12 h light/dark cycle under specific pathogen-free conditions in the animal housing facility of the Masaryk University. Sterilized food and water were available *ad libitum*. All surgical treatments were carried out under sterile conditions by the same person in accordance with the European Convention for the Protection of

Vertebrate Animals Used for Experimental and Other Scientific Purposes and the protocol was approved by the Animal Investigation Committee of the Faculty of Medicine, Brno, Czech Republic.

Animals were anesthetized by intraperitoneal (i.p.) injection of ketamine (60 mg/kg) and xylazine (7.5 mg/kg) and the right sciatic nerve was exposed at the level of the mid-thigh by blunt dissection and separated from adhering tissue just proximal to its trifurcation. Three ligatures (3-0 Ethicon) were tied around the nerve with 1 mm spacing to reduce nerve diameter by approximately one third of its original diameter in the sCCI group ($n = 7$).

The right sciatic nerve was transected and the proximal stump was tightly ligated and turned back to prevent spontaneous reinnervation in the CSNT group ($n = 7$). The skin of the right paws of CSNT group animals was covered with picric acid solution to prevent autotomy. The right sciatic nerve was only exposed without any lesion in rats ($n = 7$) subjected to a sham operation. Retracted muscles and skin incision were closed with 3-0 silk sutures and the operated rats were left to survive for 3 weeks. Seven intact rats were used as naïve controls.

Behavioral Tests

Behavioral responses to noxious mechanical (paw withdrawal threshold, PWT) and thermal (paw withdrawal latency, PWL) stimuli were measured in both ipsi- and contralateral hind paws by Dynamic plantar esthesiometer and Plantar test (UGO BASILE), respectively. The location of measurement was in the glabrous skin of the hind paws in the portion of the dermatome innervated by the tibial nerve. Rats were first acclimated in clear Plexiglas boxes for 30 min prior to testing. In the case of thermal hyperalgesia, withdrawal time was measured and the intensity radiance was set to a value of 50. The paws were tested alternately with a 5 min interval between tests. Six PWT and PWL measurements were taken for each paw during each test session 1 day before and 1, 3, 7, 14 and 21 days after operation.

Data for mechanical allodynia and thermal hyperalgesia were expressed as mean \pm SD of PWT in grams and PWL in seconds, respectively. All behavioral tests were conducted in a blind manner.

After last behavioral tests at day 21 from operation, animals were sacrificed with a lethal dose of anesthetic and tissue samples were removed for immunohistochemical and western blot analysis.

Immunohistochemical Staining

Three naïve rats and three rats from the sCCI, CSNT and sham operation groups were deeply anesthetized with a lethal dose of sodium pentobarbital (70 mg/kg body weight, i.p.) and perfused transcardially with 500 ml phosphate-buffered saline (PBS, 10 mM sodium phosphate buffer, pH 7.4, containing 0.15 M NaCl) followed by 500 ml of Zamboni's fixative (Zamboni and Demartin, 1967).

Brainstem tissue between the superior and inferior colliculi was removed and immersed in Zamboni's fixative at 4°C overnight. The samples were washed in 20% phosphate-buffered

sucrose for 12 h and blocked in Tissue-Tek® OCT compound (Miles, Elkhart, IN, USA). Serial PAG coronal sections (12 μ m) from the central part of the superior colliculi to the upper edge of the inferior colliculi corresponding to PAG between 6.72–8.04 mm from the bregma (Paxinos and Watson, 1997) were cut (Leica 1800 cryostat; Leica Microsystems, Wetzlar, Germany). In the same brainstem tissue, coronal sections (12 μ m) through the medulla 1 mm from posterior edge of the inferior colliculi corresponding to RVM between –10.8 mm and –11.4 mm from the bregma (Paxinos and Watson, 1997) were also prepared. The sections were collected on gelatin-coated microscopic slides, air-dried and processed for immunohistochemical staining.

Increased expression and extent of GFAP and OX42 immunostaining are widely accepted markers of activated astrocytes (Pekny and Pekna, 2004) and microglial cells (Blackbeard et al., 2007), respectively. Therefore, indirect immunofluorescence staining for GFAP and OX42 was used to detect activation of astrocytes and microglial cells in PAG and RVM after sciatic nerve injury. Briefly, the sections were washed with PBS containing 0.05% Tween 20 (PBS-TW20) and 1% bovine serum albumin for 10 min, and then treated with 3% normal donkey serum in PBS-TW20 for 30 min. The sections were incubated with 50 μ l of mouse monoclonal anti-CD11b/c antibody (OX42), rabbit polyclonal anti-gial fibrillary acidic protein (GFAP) or rabbit polyclonal anti-CCL2 antibody in a humid chamber at room temperature (21–23°C) for 12 h to identify activated microglial cells, astrocytes or CCL2 expression, respectively. The immunoreaction was visualized by treatment with FITC- or TRITC-conjugated, affinity purified, donkey anti-mouse or anti-rabbit secondary antibodies for 90 min at room temperature. Cell nuclei were stained using Hoechst 33342 (Sigma, St. Louis, MO, USA) and the sections were mounted in Vectashield aqueous mounting medium (Vector Laboratories, Burlingame, CA, USA).

A set of PAG and RVM sections was double immunostained to detect cell types producing CCL2 or expressing CCR2. The sections were incubated with rabbit or chicken anti-GFAP antibody to detect activated astrocytes, with mouse monoclonal OX42 for co-localization in activated microglial cells and polyclonal or monoclonal NeuN antibody to identify neurons. The first incubations were combined with immunostaining with rabbit polyclonal anti-CCL2 antibody or goat polyclonal anti-CCR2 antibody. The binding of primary antibodies were visualized by appropriate FITC-, FITC- or AlexaFluor 647-conjugated secondary antibodies (Table 1).

Control sections were incubated by omitting the primary antibodies (data not shown). Cell nuclei were stained using Hoechst 33342 and sections were analyzed using a Nikon Eclipse NI-E epifluorescence microscope equipped with a Nikon DS-Ri1 camera driven by NIS-Elements software (Nikon, Prague, Czech Republic).

Image Analysis

At least 12 sections (separated from one another by an interval of about 80 μ m) of PAG or RVM for each animal were selected

TABLE 1 | List of primary and secondary antibodies used for immunofluorescence detection.

	Antibody	Source	Product	Dilution
GFAP	pAb	Rabbit	Dako	1:250
GFAP	pAb	Chicken	Abcam	1:500
OX42	mAb	Mouse	Serotec	1:50
NeuN	pAb	Rabbit	Millipore	1:500
NeuN	mAb	Mouse	Chemicon	1:500
CCL2	pAb	Rabbit	Serotec	1:250
CCR2	pAb	Goat	ThermoFisher	1:100
Anti-chicken	pAb	Goat	Abcam	1:200
Anti-rabbit	pAb	Donkey	Millipore	1:400
Anti-mouse	pAb	Donkey	Millipore	1:400
Anti-mouse	pAb	Goat	Millipore	1:400

pAb, polyclonal antibody; mAb, monoclonal antibody.

for image analysis. Immunopositive area for OX42 or GFAP was measured using the NIS-elements image analysis system (Laboratory Imaging Ltd., Prague, Czech Republic). Briefly, the area of interest (40,000 μm^2 for PAG; 70,000 μm^2 for RVM) was placed over the dIPAG and vIPAG) or over RVM and the GFAP- or OX-42-immunostained structures were detected by a thresholding technique after subtraction of background. The boundaries of dIPAG and vIPAG columns were defined according to the rat PAG map (Paxinos and Watson, 1997) and other anatomical criteria (Keay and Bandler, 2001). The area of immunostaining for OX42 or GFAP was related to the area of interest and expressed as the mean of relative area (%) \pm SD.

Western Blot Analysis

Naïve, sham-, sCCI- and CSNT-operated rats were used for western blot analysis (four rats for each group). Rats were killed with CO₂, decapitated and the brainstem was removed. A 2 mm thick coronal slice of the mesencephalon was rapidly removed at the position from the central part of the superior colliculi to the upper edge of the inferior colliculi corresponding to PAG between 6.72 mm and 8.04 mm from the Bregma (Paxinos and Watson, 1997). Radial segments corresponding approximately with ipsilateral and contralateral dIPAG and vIPAG were dissected under a stereomicroscope (see **Figure 2E**) according to the boundaries defined using anatomical criteria (Keay and Bandler, 2001).

A 2 mm coronal slice was cut through the medulla, 1 mm from posterior edge of the inferior colliculi corresponding approximately to 1 mm from the interaural line. This section corresponds to the RVM between -10.8 mm and -11.4 mm from the bregma (Paxinos and Watson, 1997). A tissue triangle was then dissected under a stereomicroscope to isolate the RVM area, including the nucleus raphe magnus, gigantocellularis, and gigantocellularis pars alpha (see **Figure 3E**). The RVM samples were not divided into ipsi- and contra-lateral sides because no differences were seen during image analysis of immunostained sections. Tissue samples were collected, frozen in liquid nitrogen, and stored at -80°C until further processing.

The PAG and RVM tissue samples of individual animals were homogenized in PBS containing 0.1% Triton X-100 and protease inhibitors (LaRoche, Switzerland), and centrifuged at 15,000 g for 20 min at 4°C . Protein concentration was measured in the

tissue supernatant by Nanodrop ND-1000 (Thermo Scientific) and normalized to the same levels. Each sample, containing 50 μg of protein, was separated by SDS-polyacrylamide gel electrophoresis (Wei et al., 2008) and transferred to nitrocellulose membranes by electroblotting (BioRad).

The membranes were blocked with 1% BSA in PBST (3.2 mM Na₂HPO₄, 0.5 mM KH₂PO₄, 1.3 mM KCl, 135 mM NaCl, 0.05% Tween 20, pH 7.4) for 1 h and incubated with mouse monoclonal anti-CD11b/c antibody (OX42; 1:50, AbD Serotec, Kidlington, UK) or rabbit polyclonal anti- GFAP (1:250, Dako, Glostrup, Denmark) overnight. Blots was washed in PBST and incubated with peroxidase-conjugated anti-mouse or anti-rabbit secondary antibodies (Sigma, 1:1000) at room temperature for 1 h. Equal loading of proteins was confirmed by b-actin staining. Protein bands were visualized using the ECL detection kit (Amersham) on an LAS-3000 chemiluminometer reader (Bouchet Biotech) and analyzed using densitometry image software. No differences were measured between samples of naïve and sham-operated rats, therefore, OX42 and GFAP protein data after normalization to actin were expressed as fold change relative to sham PAG or RVM, which were set to 1.

Statistical Analyses

Behavioral data among groups were evaluated using two-way analysis of variance (ANOVA) with repeated measurements. One-way ANOVA with Student–Newman–Keuls *post hoc* test was used for comparison at each time point and *p* values less than 0.05 were considered to be significant. Statistical differences between data for staining area and western blot analysis were tested using a Mann-Whitney U-test ($p < 0.05$). All statistical analyses were performed using STATISTICA 9.0 software (StatSoft, Inc., Tulsa, OK, USA).

RESULTS

Behavioral Tests

All rats operated on to create sCCI of the sciatic nerve displayed as signs of NPP, decreased thresholds of mechanical allodynia (PWT) and withdrawal latencies of thermal hyperalgesia (PWL) restricted to the hind paws ipsilateral to the nerve ligatures. Decreased PWT and PWL was induced at day 1 and maintained throughout the period of survival up to 3 weeks when compared

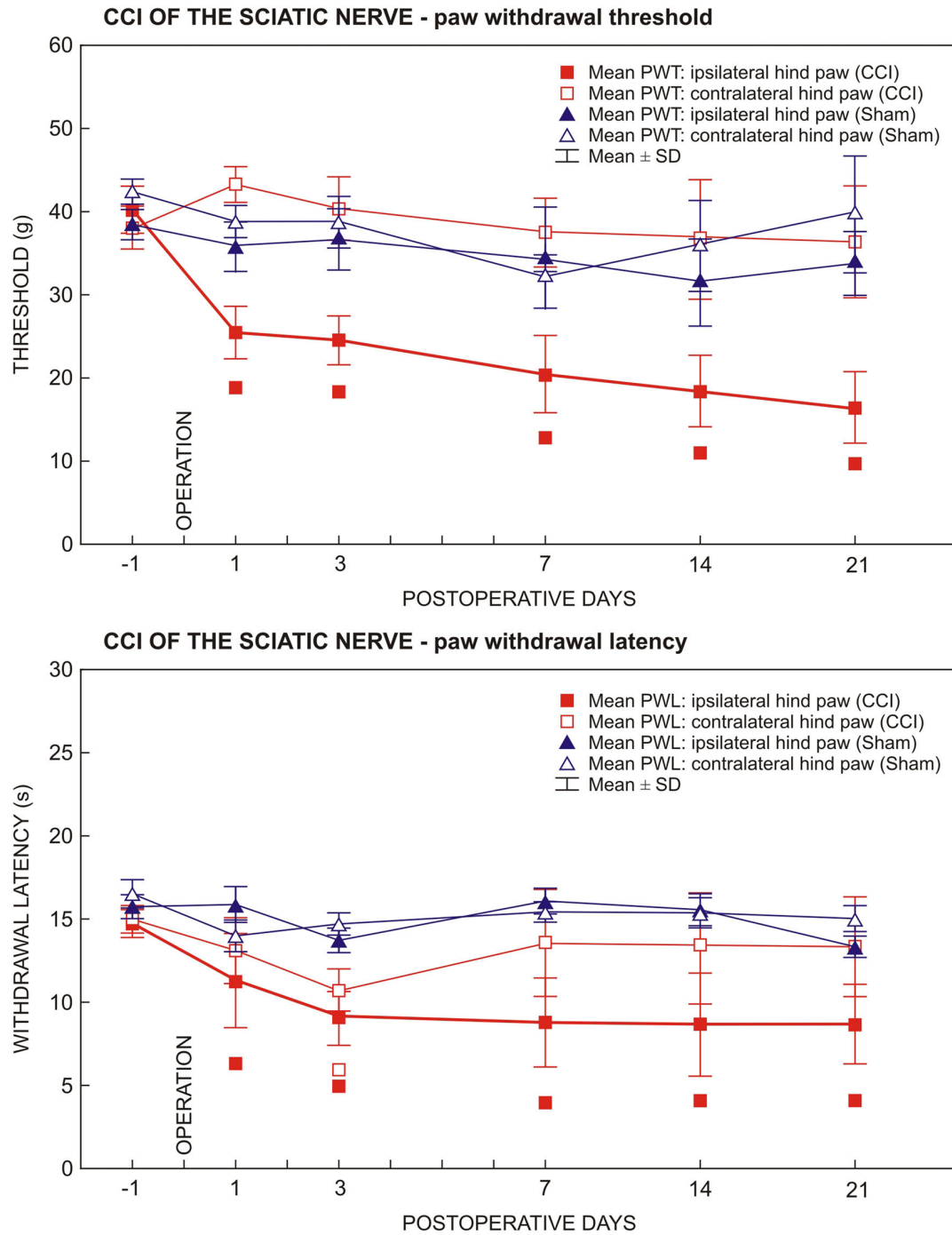


FIGURE 1 | Results of behavioral tests in rats operated upon to create unilateral sterile chronic compression injury (sCCI) of the sciatic nerve and sham-operated rats. Development and maintenance of paw withdrawal threshold (PWT) and paw withdrawal latency (PWL) was measured in the ipsilateral hind paws of sCCI-operated rats indicating mechanical allodynia and thermal hyperalgesia, respectively. Transient thermal hyperalgesia was measured bilaterally 3 days following sCCI. Data are expressed as mean \pm SD of PWT in grams and PWL in seconds for mechanical allodynia and thermal hyperalgesia, respectively. Symbols below the curves indicate a statistically significant difference ($p < 0.05$) compared to sham-operated rats.

with sham-operated rats. Hind paws contralateral to sCCI did not exhibit statistically significant changes of PWT and PWL when compared with 1 day before operation or with hind paws of sham-operated rats (Figure 1). In hind paws

of sham-operated animals, no significant changes in PWT and PWL data were measured compared to 1 day before operation. No autotomy was found in animals of the CSNT group.

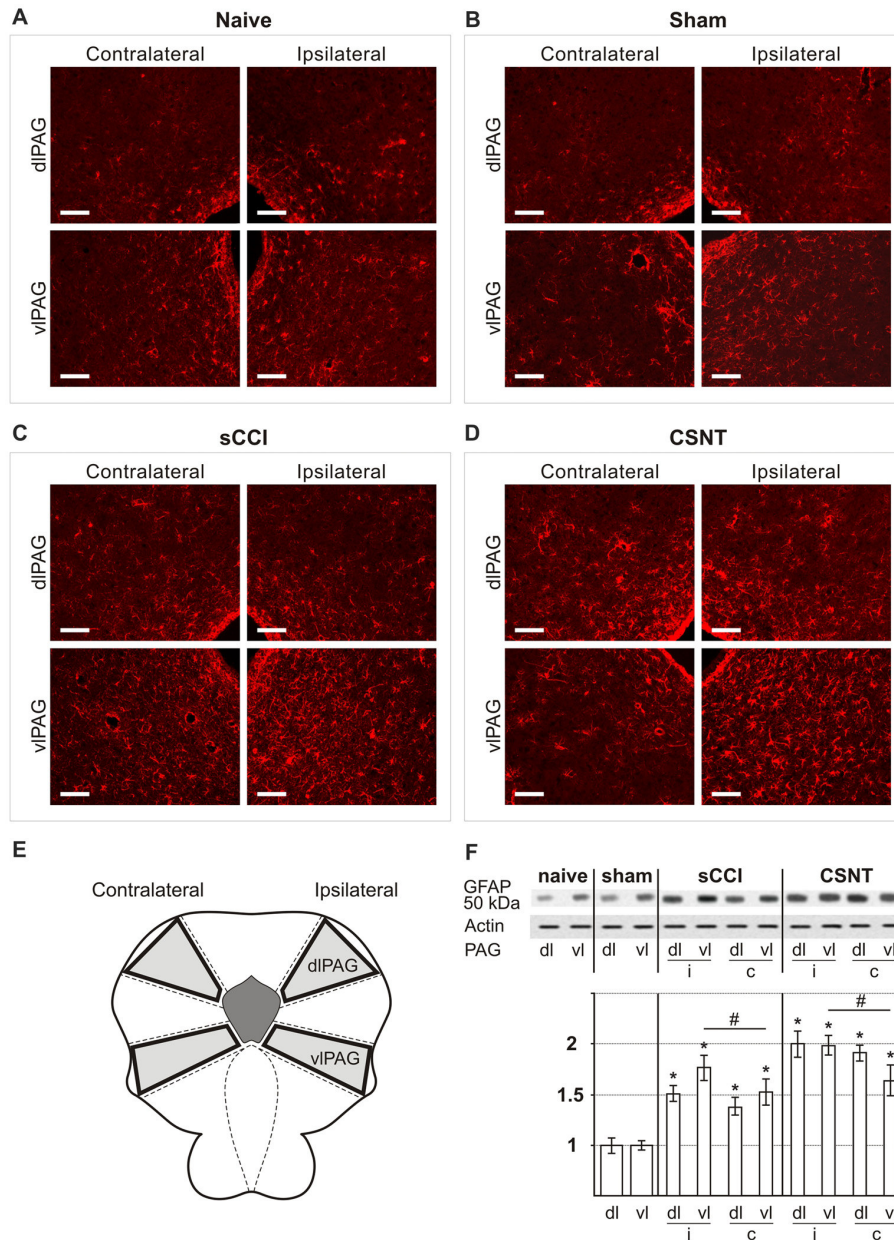


FIGURE 2 | Representative sections through dorsolateral periaqueductal gray (dIPAG) and ventrolateral PAG (vIPAG) of naïve (A), sham- (B), sCCI- (C) and complete sciatic nerve transection (CSNT)-operated (D) rats immunostained for glial fibrillary acidic protein (GFAP). The figures show a bilateral increase in the area containing activated GFAP+ astrocytes in both dIPAG and vIPAG after sCCI or CSNT for 3 weeks. Scale bars = 80 μ m. (E) Schematic representation of the location of dIPAG and vIPAG and their sampling for western blot analysis. (F) The top panel shows representative western blot of GFAP protein in PAG of naïve and sham-operated rats and 3 weeks after sCCI or CSNT. (i) indicates ipsilateral and (c) contralateral segments of dorsolateral (dl) and ventrolateral (vl) PAG. Graph below the blot illustrates density data obtained from three blots after normalization to actin, expressed as fold-change relative to those of sham-operated rats (set as 1). *Indicates a statistically significant difference ($p < 0.05$) compared to the value from sham-operated rats; # indicates a statistically significant difference ($p < 0.05$) between the values from ipsilateral and contralateral vIPAG.

Activation of Astrocytes in PAG and RVM after Chronic Compression Injury Compared to Complete Transection

Increased immunostaining for GFAP is frequently used to detect activation of astrocytes following various types of

nervous system injury (Pekny and Pekna, 2004). We found a significantly larger GFAP+ area corresponding to astrocytes in vIPAG than dIPAG in both naïve and operated rats. Sciatic nerve injury by sCCI or CSNT for 3 weeks induced increased GFAP intensity and a significant enlargement of

GFAP+ area bilaterally in both dIPAG and vIPAG when compared to naïve or sham-operated controls. In addition, CSNT gives rise to a larger GFAP+ area in bilateral dIPAG and only ipsilateral vIPAG when compared with sCCI. However, a significantly larger GFAP+ area was seen in vIPAG of the ipsilateral than the contralateral side (Figures 2A–D, Table 2).

Sections through RVM prepared from the same rats surviving for 3 weeks with sCCI or CSNT also displayed an increase in GFAP intensity and robust enlargement of the GFAP immunopositive area in comparison to RVM sections of naïve or sham-operated rats (Figures 3A–D). Similarly to PAG, CSNT gives rise to a larger GFAP+ area than in the same structures of animals subjected to sCCI (Table 2).

The increased activation of astrocytes in PAG and RVM after sCCI and CSNT detected by image analysis of GFAP immunofluorescence areas was confirmed by western blot analysis of the GFAP protein (Figures 2F, 3F).

Microglia Activation in PAG and RVM after Chronic Compression in Comparison to Transection

Activated microglial cells were identified by increased immunofluorescence staining for CD11b, detected using the antibody OX42 and by changes in their shape. Weak OX42 immunofluorescence and microglial cells with limited ramification occupied a similar proportion of immunostained areas in both vIPAG and dIPAG of naïve and sham-operated animals. The OX42 immunoreactive area indicating activated microglial cells was remarkably larger in vIPAG and dIPAG of both sides in PAG sections from sCCI- and CSNT-operated rats when compared to naïve or sham-operated ones. In contrast to GFAP+ astrocytes, no significant expansion of the OX42 immunoreactive area was detected in either dIPAG or vIPAG after CSNT when compared to sCCI of the sciatic nerve (Figures 4A–H, Table 3). Besides increased immunostaining intensity and enlargement of the OX42+ area, microglial activation was recognized by their changed morphology. In contrast to only a few processes in sections from naïve and sham-operated rats, activated microglial cells in PAG displayed more vigorous ramification along with upregulation of the constitutively expressed marker OX42 (Figures 4A–H, insets).

Increased OX42 immunostaining intensity and enlargement of the immunopositive area compared to RVM sections of naïve

or sham-operated rats was also observed in sections through RVM prepared from the same brainstems as for OX42 analysis in PAG. No significant increase in OX42+ areas was found in RVM after CSNT than sCCI of the sciatic nerve (Figures 5A–D, Table 3). Activated microglial cells in RVM after both types of sciatic nerve injury were not only highly ramified but some were also transformed morphologically to “bushy” type microglia (Figures 5A–D, insets).

Increased activation of microglial cells in PAG and RVM after sCCI and CSNT detected by image analysis of OX42 immunofluorescence areas was confirmed by western blot analysis of the OX42 protein (Figures 4I, 5E).

Neurons and Activated GFAP+ Astrocytes Display Immunostaining for CCL2 While Activated OX42+ Microglial Cells Are Immunopositive for CCR2 in Both PAG and RVM after Sciatic Nerve Injury

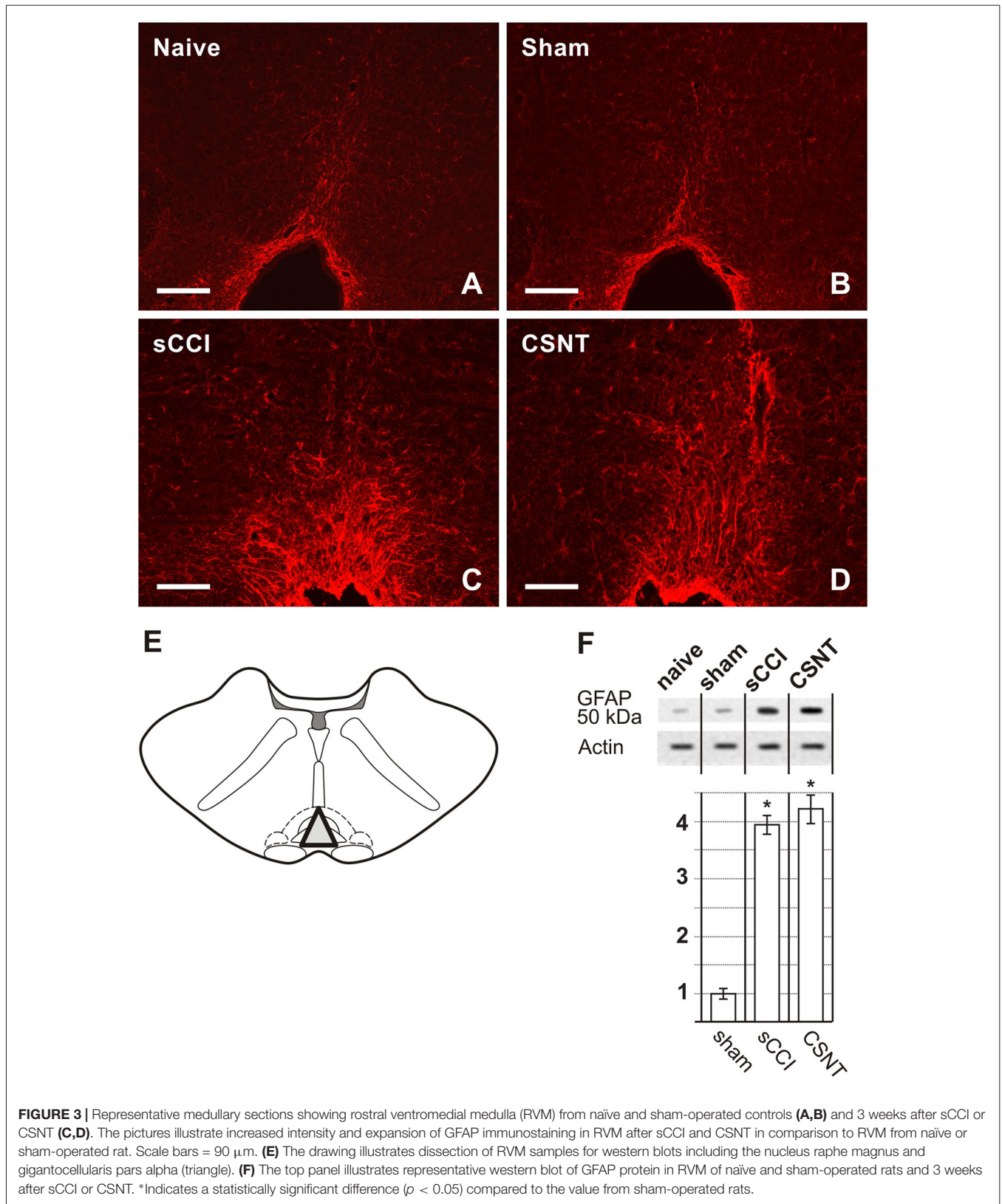
Sections through PAG from naïve and sham-operated rats show only weak CCL2 immunofluorescence in the cells present in the dIPAG and vIPAG columns. However, some cells in the narrow region at the Sylvian canal (aqueduct) displayed a higher intensity of CCL2 immunofluorescence than in the dIPAG and vIPAG area (Figures 6A–D). Sciatic nerve injury by sCCI and CSNT for 3 weeks induced a bilateral increase of CCL2 immunofluorescence intensity in cells of vIPAG and ipsilateral dIPAG, while the cells of contralateral dIPAG showed an intensity like that of naïve or sham-operated rats. Intense immunofluorescence intensity of CCL2 was found in the cells of vIPAG than dIPAG 3 weeks after sciatic nerve injury (Figures 6E–H). RVM sections of naïve and sham-operated rats displayed very faint CCL2 immunoreaction, but the intensity increased in the cells 3 weeks after sCCI or CSNT (Figures 7A–D).

To reveal the cellular origin of CCL2 protein, one set of sections were double immunostained for CCL2 and GFAP as marker of activated astrocytes or NeuN, a molecular marker of neurons. Double immunostaining showed the location of CCL2 protein in all GFAP+ astrocytes as well as NeuN+ neurons of PAG and RVM (Figures 7E, 8A–F), while OX42+ microglial cells were free of any CCL2 immunofluorescence (Figures 7F, 8G–I). The same cellular distribution of increased immunostaining for CCL2 was observed in PAG and RVM from animals subjected to both sCCI and CSNT for 3 weeks.

TABLE 2 | Percentage of glial fibrillary acidic protein (GFAP+) area \pm SD in rostral ventromedial medulla (RVM) and dorsolateral (dl) and ventrolateral (vl) periaqueductal gray (PAG) of naïve rats as well as in dIPAG and vIPAG of ipsilateral (ipsi) and contralateral (contra) sides from sham-operated rats and rats with sterile chronic compression injury (sCCI) and complete sciatic nerve transection (CSNT) for 3 weeks ($n = 6$ for each group).

	Naive	Sham		sCCI		CSNT	
		ipsi	contra	ipsi	contra	ipsi	contra
dIPAG	4.3 \pm 1.8	5.1 \pm 2.6	5.3 \pm 2.8	8.6 \pm 2.5*	7.9 \pm 2.3*	12.5 \pm 1.8*†	11.3 \pm 2.4*‡
vIPAG	10.3 \pm 2.2 ⁺	10.8 \pm 2.9 ⁺	10.9 \pm 2.4 ⁺	17.1 \pm 2.2 ^{++†}	13.8 \pm 2.8 ⁺⁺	23.6 \pm 3.5 ^{++††}	15.2 \pm 2.8 ⁺⁺
RVM	3.8 \pm 1.0	4.1 \pm 1.9		17.5 \pm 1.3*		20.8 \pm 2.1*‡	

⁺Significant difference ($p < 0.05$) compared to dIPAG. *Significant difference ($p < 0.05$) compared to Naive or Sham. †Significant difference ($p < 0.05$) compared to contralateral side. ‡Significant difference ($p < 0.05$) compared to sCCI.



Immunostaining for CCR2, a receptor of CCL2, was observed only in OX42+ microglial cells of both PAG and RVM

(**Figures 8J–L**), but no CCR2 immunoreaction was found in GFAP+ astrocytes.

DISCUSSION

The supraspinal modulatory system is differentially involved in descending facilitatory and inhibitory pathways to influence transmission of nociceptive inputs from the dorsal horn of the spinal cord to the upper structures of the CNS (Heinricher et al., 1989; Porreca et al., 2002). A fine equilibrium between the opposing descending controls exists under normal conditions. Sensitization may durably alter this balance in favor of facilitations that consequently give rise to a NPP state. The RVM and PAG of the brainstem are the principal (and the best studied) structures of the endogenous modulatory system that alter spinal dorsal horn processing of sensory input (Heinricher et al., 2009). Despite a growing body of evidence indicating a role for PAG and RVM in descending pain modulation, the precise underlying cellular and molecular mechanisms involved in descending facilitation and inhibition of the dorsal horn remain elusive.

Several animal models based on sciatic nerve injury are used to investigate NPP mechanisms and test novel analgesics. The chronic constriction injury of the sciatic nerve is most frequent model e included transection. The original CCI model created by four ligatures of chromic gut (4–0) loosely tied around the sciatic nerve results in inflammatory swelling with subsequent compression of the nerve (Bennett and Xie, 1988). However, Wallerian degeneration distal to traumatic nerve injury is considered to be neuroinflammation, and it is impossible to distinguish between nerve inflammation induced by chromic gut (Maves et al., 1993; Clatworthy et al., 1995) and proper inflammatory reactions as a consequence of Wallerian degeneration (Klusáková and Dubový, 2009). Therefore, we used sCCI of the sciatic nerve to study NPP and glial activation induced by traumatic nerve injury when damaged axons are mixed with spared ones influenced with inflammatory mediators produced only by Wallerian degeneration (Dubový, 2011). The CCI model is associated with symptoms of chronic nerve compression (Bennett and Xie, 1988), while the CSNT model is rather an experimental model to study neuropathic symptoms, such as “anesthesia dolorosa”, pain with reference to the area in the absence of any sensory signals (Devor, 1994). In the present study, we used the CSNT model primarily to compare glial reactions after total and partial (sCCI) nerve disconnection.

It is well-known that sensitization of the CNS at different levels by activation of glial cells can contribute to the development and/or maintenance of chronic pain states after a PNI (Suzuki et al., 2004). Most experimental results relating to the role of glial activation in induction and maintenance of NPP were observations made in the dorsal horn of the spinal cord (Blackbeard et al., 2007; Milligan and Watkins, 2009). Less attention has been paid to the activation of glial cells in supraspinal structures. For example, activated astrocytes were found in RVM after unilateral CCI of the rat infraorbital nerve (Wei et al., 2008) and in PAG following CCI of the sciatic nerve (Mor et al., 2010, 2011). In contrast to these separate studies in PAG and RVM of different

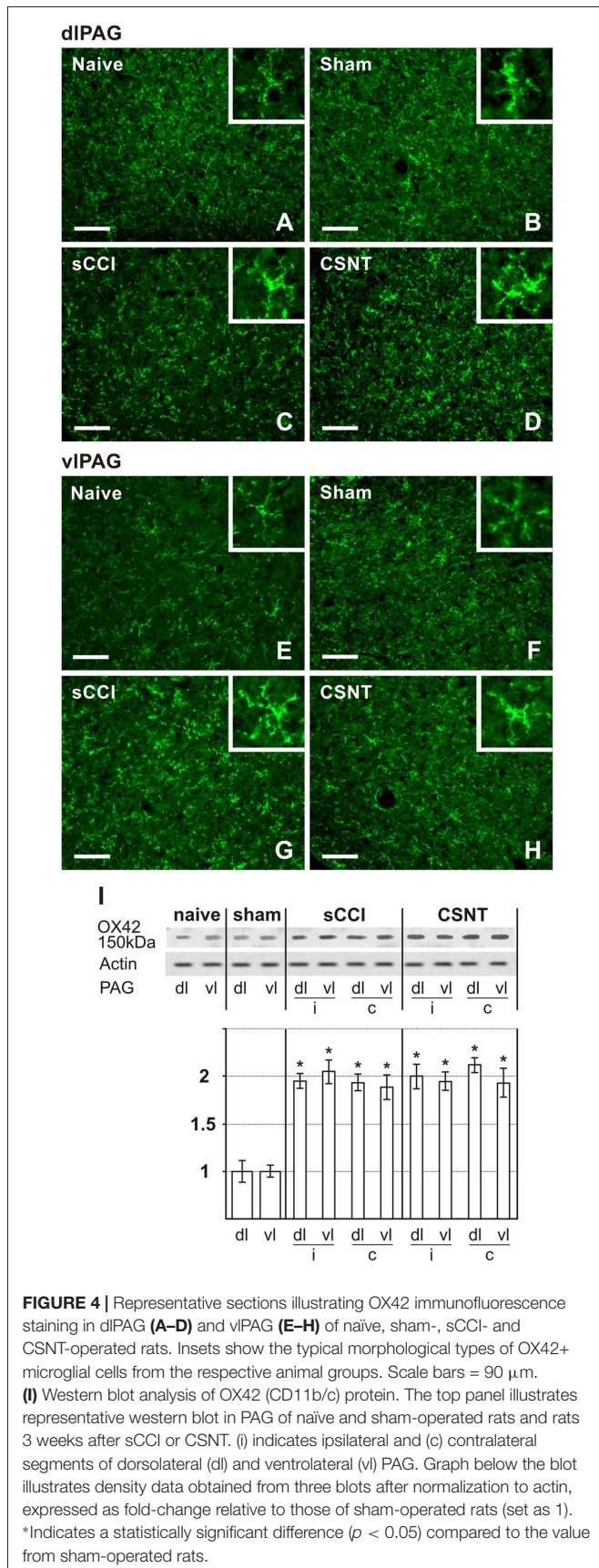
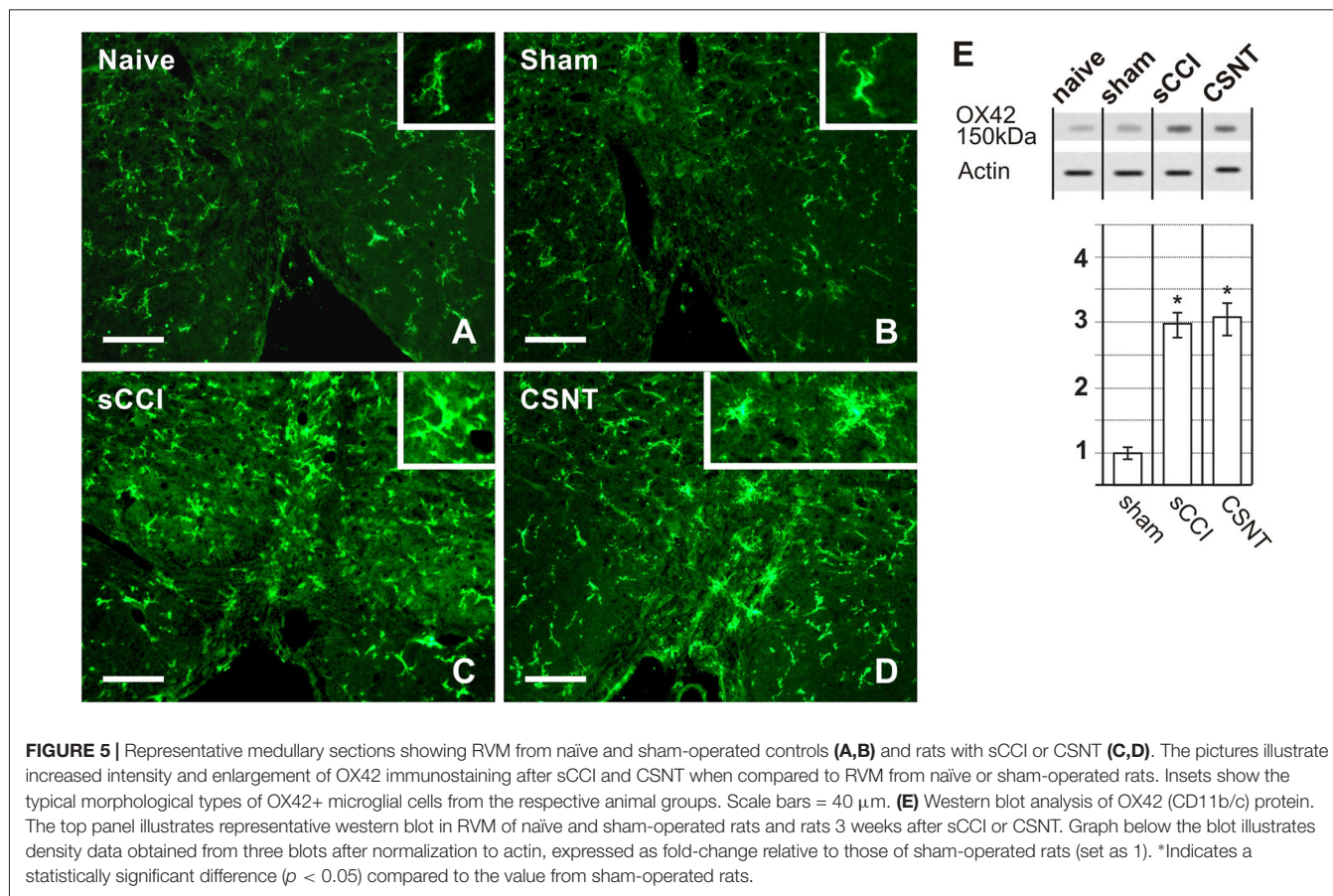


FIGURE 4 | Representative sections illustrating OX42 immunofluorescence staining in dIPAG (A–D) and vIPAG (E–H) of naïve, sham-, sCCI- and CSNT-operated rats. Insets show the typical morphological types of OX42+ microglial cells from the respective animal groups. Scale bars = 90 μm. (I) Western blot analysis of OX42 (CD11b/c) protein. The top panel illustrates representative western blot in PAG of naïve and sham-operated rats and rats 3 weeks after sCCI or CSNT. (i) indicates ipsilateral and (c) contralateral segments of dorsolateral (dl) and ventrolateral (vl) PAG. Graph below the blot illustrates density data obtained from three blots after normalization to actin, expressed as fold-change relative to those of sham-operated rats (set as 1). *Indicates a statistically significant difference ($p < 0.05$) compared to the value from sham-operated rats.

TABLE 3 | Percentage of OX-42+ area \pm SD in RVM and dorsolateral (dl) and ventrolateral (vl) PAG of naïve rats as well as in dlPAG and vlPAG of ipsilateral (ipsi) and contralateral (contra) sides from sham-operated rats and rats with sCCI and CSNT for 3 weeks.

	Naïve	Sham		sCCI		CSNT	
		ipsi	contra	ipsi	contra	ipsi	contra
dlPAG	6.9 \pm 0.9	7.2 \pm 1.5	7.0 \pm 1.2	13.1 \pm 1.8*	12.9 \pm 2.6*	13.9 \pm 2.5*	13.2 \pm 3.7*
vlPAG	7.9 \pm 2.7	8.3 \pm 2.6	8.1 \pm 2.9	13.4 \pm 2.4*	12.3 \pm 3.7*	13.2 \pm 2.4*	12.6 \pm 2.2*
RVM	0.7 \pm 0.2	0.8 \pm 0.2		3.6 \pm 1.2*		3.4 \pm 0.7*	

*Significant difference ($p < 0.05$) compared to Naïve or Sham ($n = 6$ for each group).



experimental models with varying times of survival, we used the sCCI and CSNT models for 3 weeks to compare long-lasting activation of astrocytes and microglial cells in both RVM and PAG depending on the extent of nerve injury.

Activation of Glial Cells in Ventrolateral and Dorsolateral Subregions of PAG

The vlPAG with the spinal projection of sciatic nerve (Keay et al., 1997) has a significant role in descending control of noxious afferentation via connections with RVM (Eidson and Murphy, 2013). In addition to descending control, vlPAG columns have projections to many CNS structures critical for the normal expression of sleep-wake cycles and social behaviors (Monassi et al., 2003; Mor et al., 2011). An increased number of GFAP+ astrocytes in vlPAG was mainly detected in a subset of rats

which displayed both NPP and disability following CCI of the sciatic nerve (Mor et al., 2011). In contrast, dlPAG column has projections primarily to the dorsolateral pons and the ventrolateral medulla that are implicated in autonomic control (Cameron et al., 1995). Moreover, descending control from dlPAG has different effects on nociceptive reflexes evoked by activation of C- and A-delta fibers (McMullan and Lumb, 2006).

Sciatic nerve injury by sCCI or CSNT for 3 weeks induced activation of astrocytes bilaterally in both dlPAG and vlPAG when compared to naïve or sham-operated control rats. Significantly more extensive activation of astrocytes was observed in vlPAG on the ipsilateral than the contralateral side in both models of unilateral sciatic nerve injury that can be related with the spinal projection of sciatic nerve (Keay et al., 1997). In contrast, ipsilateral dlPAG displayed

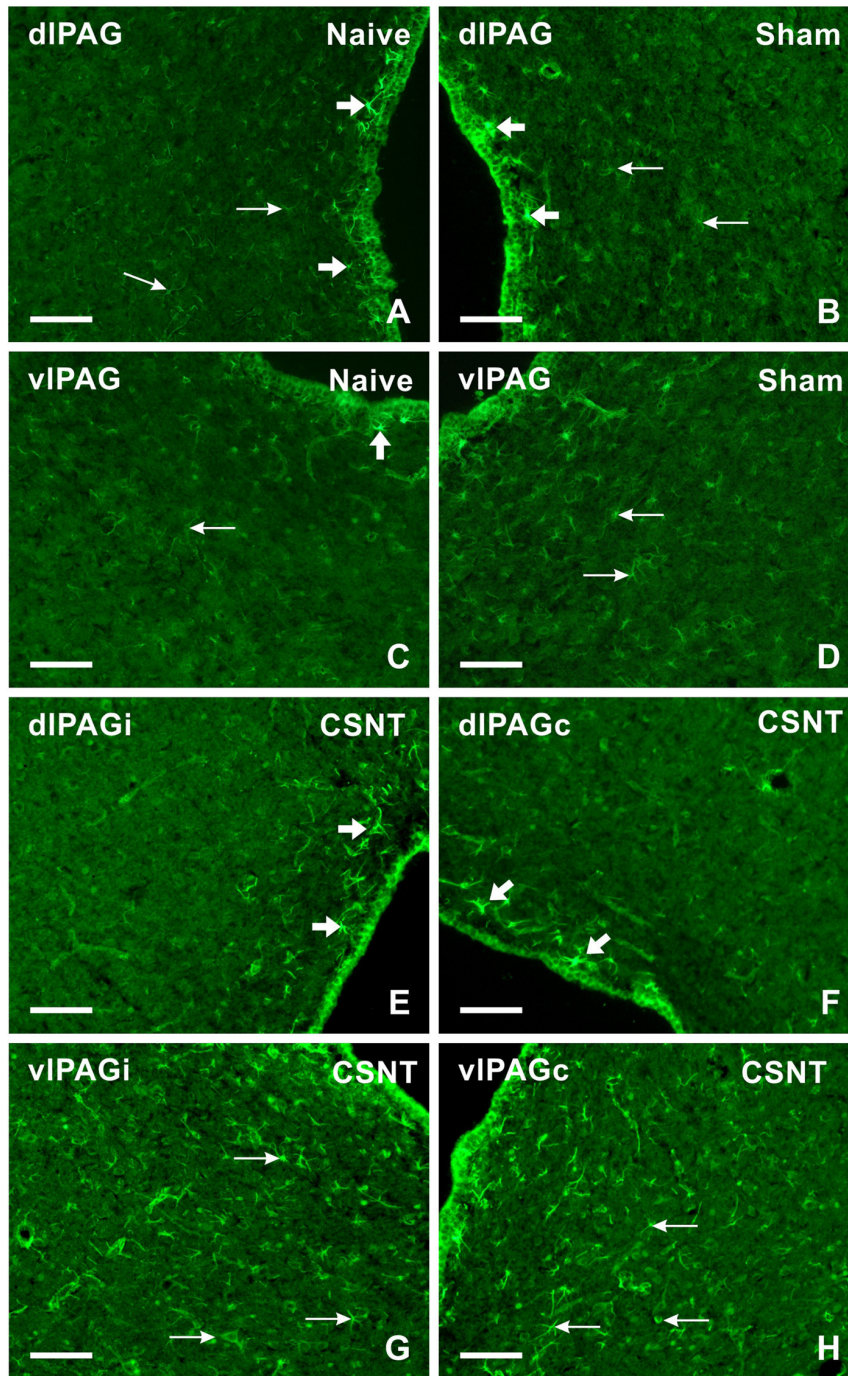


FIGURE 6 | Representative sections showing immunofluorescence staining for CCL2 in dIPAG and vIPAG of naïve (**A,C**), sham- (**B,D**) and CSNT-operated (**E–H**) rats. Weak CCL2 immunofluorescence was observed in the cells of both dIPAG and vIPAG from naïve and sham-operated controls (arrows in **A–D**). Only some cells located close to the ependymal layer displayed intense CCL2 immunostaining (broad arrows in **A–D**). Sciatic nerve injury for 3 weeks induced increased CCL2 immunofluorescence intensity in the cells (arrows) mainly in vIPAG of both ipsilateral (vIPAGi) and contralateral (vIPAGc) sides (**G,H**). Sections through dIPAG of the same animal (**E,F**) displayed distinct CCL2 immunofluorescence in a larger number of cells close to the ependymal layer (broad arrows) compared to naïve and sham-operated animals. Scale bars = 80 μ m.

a more extensive activation of astrocytes when compared to the contralateral column but this change was not significant. Our results also revealed a higher induction of

astroglial activation in PAG columns by CSNT than sCCI indicating a dependence on the extent of the sciatic nerve injury.

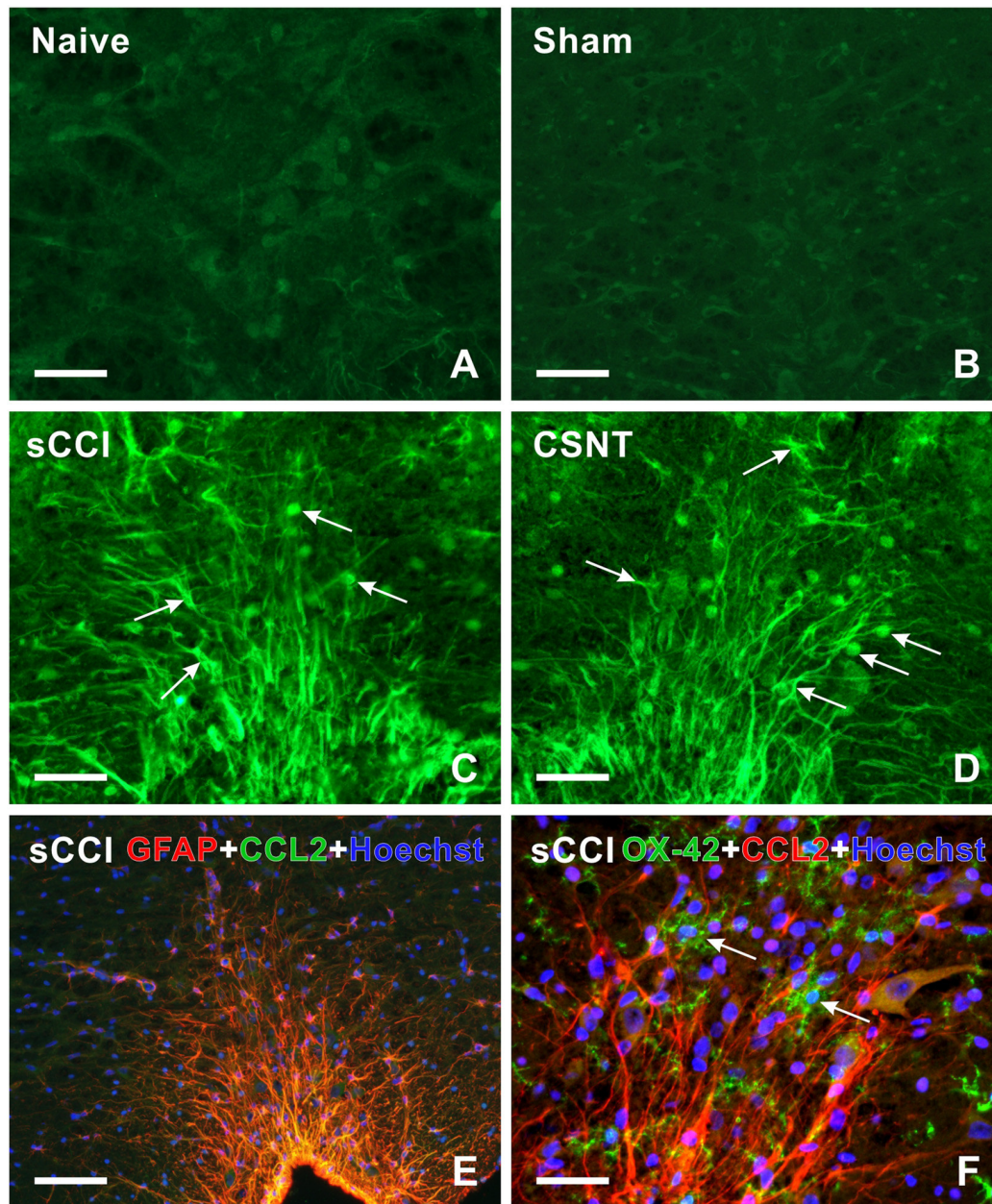


FIGURE 7 | (A–D) Representative medullary sections showing RVM from naïve **(A)** and sham-operated **(B)** controls as well as rats 3 weeks from sCCI **(C)** or CSNT **(D)** after immunostaining for CCL2. Compared to RVM of naïve and sham-operated rats **(A,B)**, CCL2 immunofluorescence intensity was significantly increased in cells (arrows) of RVM from rats with injured sciatic nerve **(C,D)**. **(E,F)** Representative pictures of double immunofluorescence for GFAP or OX42 and CCL2 in RVM after sCCI of the sciatic nerve for 3 weeks. **(E)** The section was double immunostained for GFAP (red) and CCL2 (green). The merged picture shows expression of CCL2 protein in all GFAP+ astrocytes of RVM; nuclei (blue) were stained with Hoechst. **(F)** The section was double immunostained for OX42 (green) and CCL2 (red). The merged picture shows the absence of CCL2 protein in OX42+ microglial cells (arrows); nuclei (blue) were stained with Hoechst. Scale bars = 90 μm in **(B,E)**; 40 μm in **(A,C,D,F)**.

In contrast to astrocytes, activation of microglial cells was similar in dIPAG and vlPAG of both sides in the sCCI and CSNT models of the sciatic nerve injury. This suggests that signaling leading to microglial activation is maintained bilaterally in both PAG columns 3 weeks after different types of sciatic nerve injury (sCCI and CSNT).

Taken together, these findings of activated astrocytes and microglial cells in vlPAG after sciatic nerve injury suggest a role for activated glial cells in the modulation of activity of this PAG column with respect to descending inhibition or facilitation of nociceptive input following nerve injury (Ni et al., 2016). It is clinically important that vlPAG and its

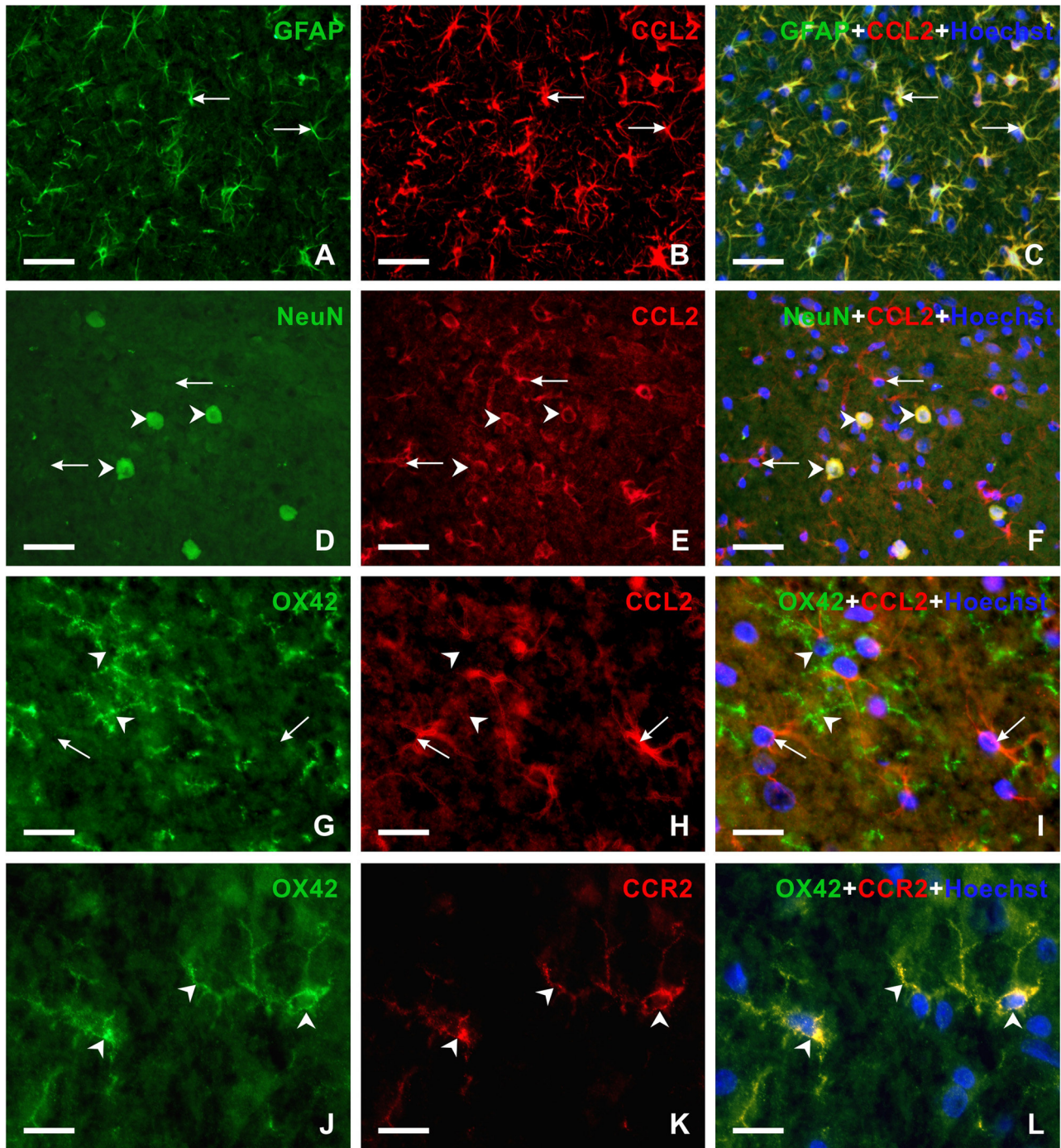


FIGURE 8 | Double immunofluorescence staining in vPAG of rats 3 weeks from sCCI. **(A–F)** Sections illustrating double immunofluorescence staining for CCL2 and GFAP or NeuN as markers of activated astrocytes or neurons, respectively. The merged pictures **(C,F)** show CCL2 protein in activated astrocytes (arrows) and neurons (arrowheads). **(G–L)** Double immunofluorescence staining for OX42 as a marker for microglial cells and CCL2 **(G–I)** or CCR2 **(J–L)**. The merged picture **(I)** shows the absence of CCL2 protein in microglial cells. Compare CCL2 positive astrocyte-like cells (arrows) with the absence of CCL2 immunoreaction in microglial cells (arrowheads). However, OX42+ microglial cells displayed CCR2 immunostaining (arrowheads in **L**). Scale bars = 40 μm for **(A–F)**; 75 μm for **(G–I)**; 15 μm for **(J–L)**.

descending projections to RVM comprise a neural circuit for opioid-mediated analgesia (Lane et al., 2004; Eidson and Murphy, 2013; Wilson-Poe et al., 2013). Increased activation of

microglial cells and astrocytes in vPAG was observed only in those animals made tolerant to morphine (Eidson and Murphy, 2013).

Unilateral sciatic nerve injury (sCCI and CSNT) induced bilateral activation of astrocytes and microglial cells in both dlPAG and vlPAG. These results are probably related with the bilateral projections from the spinal cord to PAG responses of which appear to be predominantly bilateral and non-somatotopic (Yeziarski and Mendez, 1991; Jones et al., 2003).

Activation of Glial Cells in RVM

The RVM provides the major common output of descending modulatory system that is critical in the maintenance of chronic pain states (Pertovaara et al., 1996; Porreca et al., 2002; Dubner and Ren, 2004; Gebhart, 2004; Vanegas and Schaible, 2004; Vera-Portocarrero et al., 2006; Bee and Dickenson, 2007). The RVM is a relay in the pathways from both vlPAG and dlPAG columns (Hudson and Lumb, 1996) with an important dlPAG connection involved in the modulation of endocannabinoid stress analgesia (Suplita et al., 2005). Early (1 and 3 days) and transient activation of microglia and prolonged reaction of astrocytes (14 days) were found in RVM in relation to long-lasting mechanical hyperalgesia after CCI of the rat infraorbital nerve (Wei et al., 2008). In contrast, a bilateral increase of astrocyte activation was demonstrated after 3 days with a decrease by day 10 following spinal nerve ligation (SNL). Conversely, although a weak immunofluorescence was observed at day 3, markedly stronger OX42 immunostaining was found at day 10 in rats operated on SNL (Leong et al., 2011). In our experiments, both types of sciatic nerve injury induced a strong activation of astrocytes and microglial cells in RVM, but no differences were found between the astrocyte- and the microglial activation induced by sCCI and CSNT. The results indicated that the intensity of glial activation in RVM after long-lasting nerve injury was not related to the extent of axotomy; this is consistent with the status of the RVM as a common output of descending modulatory system.

Retrograde neuronal death can be assumed as the initial signal for activation of glial cells after PNI (Flügel et al., 2001), but we did not investigate neuronal loss of RVM neurons in our experimental animals in relation to glial activation. However, there is some controversy about neuronal loss in RVM in different NPP models. While neuronal loss was found in RVM following spinal nerve ligation (Leong et al., 2011), it was absent after CCI or spared nerve injury (SNI) of the sciatic nerve (Leong et al., 2016). Therefore, other mechanisms of glial activation should be considered. Since CCL2 has a pivotal role in microglial cell activation in the dorsal horn after PNI (Zhang and De Koninck, 2006; Thacker et al., 2009; Van Steenwinckel et al., 2011; Clark et al., 2013), it is worth exploring the critical role of this chemokine also on supraspinal glial cross-talk which may exert NPP facilitation after sciatic nerve injury.

Expression of CCL2 and CCR2 in Activated Glial Cells of PAG and RVM

Activated glial cells upregulate synthesis and secretion of numerous cytokines and chemokines that are involved in the exchange of signals between neurons and the glial cells of CNS structures. It was also demonstrated that these inflammatory

mediators modulate nociceptive transmission and may influence NPP induction (DeLeo et al., 1996; Coyle, 1998; Colburn et al., 1999; DeLeo and Yeziarski, 2001; Watkins et al., 2003).

Several lines of evidence suggest that CCL2 and its receptor CCR2 are expressed in both neurons and glial cells in the dorsal horn of the spinal cord in animal NPP models (White et al., 2005; Dansereau et al., 2008; Abbadie et al., 2009; Jung et al., 2009). CCL2 was detected in primary sensory neurons and their afferents in the dorsal horn of the spinal cord (Tanaka et al., 2004; Dansereau et al., 2008; Jeon et al., 2009). Besides primary afferents, CCL2 protein was also found in GFAP+ astrocytes activated by SNL (Gao et al., 2009). In contrast, immunohistochemical staining localized the CCR2 protein in spinal microglia after partial sciatic nerve injury (Abbadie et al., 2003), whereas the CCR2 mRNA signal was also present in deep dorsal horn neurons 3 days after SNL (Gao et al., 2009). Upregulation of CCL2/CCR2 in the spinal dorsal horn of NPP models suggests an important role for signaling through this chemokine in the modulation of chronic pain induction (reviewed in White et al., 2007; Gosselin et al., 2008; White and Miller, 2010). This was also confirmed by attenuation of behavioral signs of NPP in CCR2 knock-out mice (Abbadie et al., 2003).

With respect to supraspinal structures, neuronal CCL2 and its receptor CCR2 associated with microglia were selectively upregulated in the RVM following SNL. Furthermore, injection of CCL2 into the RVM induced a dose-dependent hyperalgesia that was prevented by pretreatment with the CCL2 inhibitor RS-102895 (Guo et al., 2012). This showed that increased levels of CCL2 in RVM are related with descending facilitation of NPP. However, the precise cellular distribution of CCL2/CCR2 in PAG following PNI still remains unclear.

Our results revealed that neurons and activated astrocytes in both PAG and RVM displayed immunostaining for CCL2 protein, while activated microglial cells expressed CCR2 after chronic sciatic nerve injury. The results presented here and previously published studies of the cellular distribution of CCL2 and CCR2 suggest that CCL2/CCR2 signaling is involved in the neuron-glia and glia-glia interactions in both PAG and RVM after long-lasting nerve injury related to persistent pain. Based on the observed earlier activation of microglia, i.e., preceding astrocyte activation (Zhang and De Koninck, 2006; Hu et al., 2007), we can assume that the injury-associated nociceptive inputs trigger neuronal responses in PAG and RVM. Among these responses is the release of neuronal CCL2 that binds to CCR2 of microglia and promotes their activation (Zhang and De Koninck, 2006). Activated microglia may further stimulate astroglial activation through IL-18 and increase neuronal activity via CXCL1 (Abbadie et al., 2009; Gao and Ji, 2010). Furthermore, activated astrocytes may contribute to increased levels of CCL2 resulting in the augmentation of descending pain facilitation (Guo et al., 2012).

CONCLUSION

Partial sciatic nerve injury by sCCI results in early and more distinct mechanical and thermal hypersensitivity up to 3 weeks.

While CSNT induced a robust activation of astrocytes in both PAG and RVM, the activation of microglial cells was similar in these supraspinal structures after both types of sciatic nerve injury. This suggests that activated astrocytes in PAG and RVM may sustain the facilitation of the descending system to maintain NPP states, while activation of microglial cells may be associated with the reaction to long-lasting PNI. Furthermore, CCL2/CCR2 signaling may be involved in the neuron-glia and glia-glia interactions in both PAG and RVM after either sCCI or CSNT, triggering persistent NPP after PNI.

AUTHOR CONTRIBUTIONS

PD conceived, designed and coordinated the experiments, ensured quantitative immunohistochemical and western blot analyses and wrote the manuscript. PB-V conceived, designed

and coordinated the study and wrote the manuscript. IK, IH-S and MJ designed and performed the experiments and also participated in acquiring and analyzing the presented data. All authors have approved the final version for publication.

FUNDING

This work was supported by grant No. 16-08508S of the Czech Science Foundation and grants from the Vice-Chancellorship of Research of the University of Girona to PB-V (MOB2016 and MPCUdG2016/087).

ACKNOWLEDGMENTS

We thank Dana Kutějová, Jitka Mikulášková, Marta Lněničková, Jana Vachová and Lumír Trenčanský for their skillful technical assistance.

REFERENCES

- Abbadie, C., Bhargoo, S., De Koninck, Y., Malcangio, M., Melik-Parsadaniantz, S., and White, F. A. (2009). Chemokines and pain mechanisms. *Brain Res. Rev.* 60, 125–134. doi: 10.1016/j.brainresrev.2008.12.002
- Abbadie, C., Lindia, J. A., Cumiskey, A. M., Peterson, L. B., Mudgett, J. S., Bayne, E. K., et al. (2003). Impaired neuropathic pain responses in mice lacking the chemokine receptor CCR2. *Proc. Natl. Acad. Sci. U S A* 100, 7947–7952. doi: 10.1073/pnas.1331358100
- Anderson, M. A., Ao, Y., and Sofroniew, M. V. (2014). Heterogeneity of reactive astrocytes. *Neurosci. Lett.* 565, 23–29. doi: 10.1016/j.neulet.2013.12.030
- Bee, L. A., and Dickenson, A. H. (2007). Rostral ventromedial medulla control of spinal sensory processing in normal and pathophysiological states. *Neuroscience* 147, 786–793. doi: 10.1016/j.neuroscience.2007.05.004
- Bennett, G. J., and Xie, Y. K. (1988). A peripheral mononeuropathy in rat that produces disorders of pain sensation like those seen in man. *Pain* 33, 87–107. doi: 10.1016/0304-3959(88)90209-6
- Berger, J. V., Knaepen, L., Janssen, S. P. M., Jaken, R. J. P., Marcus, M. A. E., Joosten, E. A. J., et al. (2011). Cellular and molecular insights into neuropathy-induced pain hypersensitivity for mechanism-based treatment approaches. *Brain Res. Rev.* 67, 282–310. doi: 10.1016/j.brainresrev.2011.03.003
- Blackbeard, J., O'Dea, K. P., Wallace, V. C., Segerdahl, A., Pheby, T., Takata, M., et al. (2007). Quantification of the rat spinal microglial response to peripheral nerve injury as revealed by immunohistochemical image analysis and flow cytometry. *J. Neurosci. Methods* 164, 207–217. doi: 10.1016/j.jneumeth.2007.04.013
- Boadas-Vaello, P., Castany, S., Homs, J., Álvarez-Pérez, B., Deulofeu, M., and Verdú, E. (2016). Neuroplasticity of ascending and descending pathways after somatosensory system injury: reviewing knowledge to identify neuropathic pain therapeutic targets. *Spinal Cord* 54, 330–340. doi: 10.1038/sc.2015.225
- Boadas-Vaello, P., Homs, J., Reina, F., Carrera, A., and Verdú, E. (2017). Neuroplasticity of supraspinal structures associated with pathological pain. *Anat. Rec. (Hoboken)* 300, 1481–1501. doi: 10.1002/ar.23587
- Burnstock, G. (2016). Purinergic mechanisms and pain. *Adv. Pharmacol.* 75, 91–137. doi: 10.1016/bs.apha.2015.09.001
- Cameron, A. A., Khan, I. A., Westlund, K. N., and Willis, W. D. (1995). The efferent projections of the periaqueductal gray in the rat: a *Phaseolus vulgaris*-leucoagglutinin study. II. Descending projections. *J. Comp. Neurol.* 351, 585–601. doi: 10.1002/cne.903510408
- Chu, H., Sun, J., Xu, H., Niu, Z., and Xu, M. (2012). Effect of periaqueductal gray melanocortin 4 receptor in pain facilitation and glial activation in rat model of chronic constriction injury. *Neurol. Res.* 34, 871–888. doi: 10.1179/1743132812y.0000000085
- Clark, A. K., Old, E. A., and Malcangio, M. (2013). Neuropathic pain and cytokines: current perspectives. *J. Pain Res.* 6, 803–814. doi: 10.2147/JPR.S53660
- Clatworthy, A. L., Illich, P. A., Castro, G. A., and Walters, E. T. (1995). Role of peri-axonal inflammation in the development of thermal hyperalgesia and guarding behavior in a rat model of neuropathic pain. *Neurosci. Lett.* 184, 5–8. doi: 10.1016/0304-3940(94)11154-b
- Colburn, R. W., Rickman, A. J., and DeLeo, J. A. (1999). The effect of site and type of nerve injury on spinal glial activation and neuropathic pain behavior. *Exp. Neurol.* 157, 289–304. doi: 10.1006/exnr.1999.7065
- Coyle, D. E. (1998). Partial peripheral nerve injury leads to activation of astroglia and microglia which parallels the development of allodynic behavior. *Glia* 23, 75–83. doi: 10.1002/(sici)1098-1136(199805)23:1<75::aid-glia7>3.0.co;2-3
- Dansereau, M. A., Gosselin, R. D., Pohl, M., Pommier, B., Mechighel, P., Mauborgne, A., et al. (2008). Spinal CCL2 pronociceptive action is no longer effective in CCR2 receptor antagonist-treated rats. *J. Neurochem.* 106, 757–769. doi: 10.1111/j.1471-4159.2008.05429.x
- DeLeo, J. A., Colburn, R. W., Nichols, M., and Malhotra, A. (1996). Interleukin-6-mediated hyperalgesia/allodynia and increased spinal IL-6 expression in a rat mononeuropathy model. *J. Interferon Cytokine Res.* 16, 695–700. doi: 10.1089/jir.1996.16.695
- DeLeo, J. A., and Yeziarski, R. P. (2001). The role of neuroinflammation and neuroimmune activation in persistent pain. *Pain* 90, 1–6. doi: 10.1016/s0304-3959(00)00490-5
- Devor, M. (1994). “The pathophysiology of damaged peripheral nerves,” in *Textbook of Pain*, eds P. D. Wall and R. Melzack (New York, NY: Elsevier Churchill Livingstone), 79–101.
- Dubner, R., and Ren, K. (2004). Brainstem mechanisms of persistent pain following injury. *J. Orofac. Pain* 18, 299–305.
- Dubový, P. (2011). Wallerian degeneration and peripheral nerve conditions for both axonal regeneration and neuropathic pain induction. *Ann. Anat.* 193, 267–275. doi: 10.1016/j.aanat.2011.02.011
- Eidson, L. N., and Murphy, A. Z. (2013). Persistent peripheral inflammation attenuates morphine-induced periaqueductal gray glial cell activation and analgesic tolerance in the male rat. *J. Pain* 14, 393–404. doi: 10.1016/j.jpain.2012.12.010
- Fields, H. L., Basbaum, A. I., and Heinricher, M. M. (2006). “Central nervous system mechanisms of pain modulation,” in *Wall and Melzack's Textbook of Pain*, eds S. B. Mc Mahon and M. Koltzenburg (New York, NY: Elsevier Churchill Livingstone), 125–142.
- Flügel, A., Hager, G., Horvat, A., Spitzer, C., Singer, G. M., Graeber, M. B., et al. (2001). Neuronal MCP-1 expression in response to remote nerve injury. *J. Cereb. Blood Flow Metab.* 21, 69–76. doi: 10.1097/00004647-200101000-00009
- Gao, Y. J., and Ji, R. R. (2010). Targeting astrocyte signaling for chronic pain. *Neurotherapeutics* 7, 482–493. doi: 10.1016/j.nurt.2010.05.016

- Gao, Y. J., Zhang, L., Samad, O. A., Suter, M. R., Yasuhiko, K., Xu, Z. Z., et al. (2009). JNK-induced MCP-1 production in spinal cord astrocytes contributes to central sensitization and neuropathic pain. *J. Neurosci.* 29, 4096–4108. doi: 10.1523/JNEUROSCI.3623-08.2009
- Gebhart, G. F. (2004). Descending modulation of pain. *Neurosci. Biobehav. Rev.* 27, 729–737. doi: 10.1016/j.neubiorev.2003.11.008
- Gosselin, R. D., Dansereau, M. A., Pohl, M., Kitabgi, P., Beaudet, N., Sarret, P., et al. (2008). Chemokine network in the nervous system: a new target for pain relief. *Curr. Med. Chem.* 15, 2866–2875. doi: 10.2174/092986708786242822
- Graeber, M. B., and Streit, W. J. (2010). Microglia: biology and pathology. *Acta Neuropathol.* 119, 89–105. doi: 10.1007/s00401-009-0622-0
- Guo, W., Wang, H., Zou, S., Dubner, R., and Ren, K. (2012). Chemokine signaling involving chemokine (C-C motif) ligand 2 plays a role in descending pain facilitation. *Neurosci. Bull.* 28, 193–207. doi: 10.1007/s12264-012-1218-6
- Hanisch, U. K., and Kettenmann, H. (2007). Microglia: active sensor and versatile effector cells in the normal and pathologic brain. *Nat. Neurosci.* 10, 1387–1394. doi: 10.1038/nn1997
- Heinricher, M. M., Barbaro, N. M., and Fields, H. L. (1989). Putative nociceptive modulating neurons in the rostral ventromedial medulla of the rat: firing of on- and off-cells is related to nociceptive responsiveness. *Somatosens. Mot. Res.* 6, 427–439. doi: 10.3109/08990228909144685
- Heinricher, M. M., Tavares, I., Leith, J. L., and Lumb, B. M. (2009). Descending control of nociception: specificity, recruitment and plasticity. *Brain Res. Rev.* 60, 214–225. doi: 10.1016/j.brainresrev.2008.12.009
- Hu, P., Bembrick, A. L., Keay, K. A., and McLachlan, E. M. (2007). Immune cell involvement in dorsal root ganglia and spinal cord after chronic constriction or transection of the rat sciatic nerve. *Brain Behav. Immun.* 21, 599–616. doi: 10.1016/j.bbi.2006.10.013
- Hudson, P. M., and Lumb, B. M. (1996). Neurons in the midbrain periaqueductal grey send collateral projections to nucleus raphe magnus and the rostral ventrolateral medulla in the rat. *Brain Res.* 733, 138–141. doi: 10.1016/0006-8993(96)00784-6
- Jeon, S. M., Lee, K. M., and Cho, H. J. (2009). Expression of monocyte chemoattractant protein-1 in rat dorsal root ganglia and spinal cord in experimental models of neuropathic pain. *Brain Res.* 1251, 103–111. doi: 10.1016/j.brainres.2008.11.046
- Jones, A. K. P., Kulkarni, B., and Derbyshire, S. W. G. (2003). Pain mechanisms and their disorders. *Br. Med. Bull.* 65, 83–93. doi: 10.1093/bmb/65.1.83
- Jung, H., Bhangoo, S., Banisadr, G., Freitag, C., Ren, D., White, F. A., et al. (2009). Visualization of chemokine receptor activation in transgenic mice reveals peripheral activation of CCR2 receptors in states of neuropathic pain. *J. Neurosci.* 29, 8051–8062. doi: 10.1523/JNEUROSCI.0485-09.2009
- Keay, K. A., and Bandler, R. (2001). Parallel circuits mediating distinct emotional coping reactions to different types of stress. *Neurosci. Biobehav. Rev.* 25, 669–678. doi: 10.1016/s0149-7634(01)00049-5
- Keay, K. A., Feil, K., Gordon, B. D., Herbert, H., and Bandler, R. (1997). Spinal afferents to functionally distinct periaqueductal gray columns in the rat: an anterograde and retrograde tracing study. *J. Comp. Neurol.* 385, 207–229. doi: 10.1002/(sici)1096-9861(19970825)385:2<207::aid-cne3>3.0.co;2-5
- Klusáková, I., and Dubový, P. (2009). Experimental models of peripheral neuropathic pain based on traumatic nerve injuries—an anatomical perspective. *Ann. Anat.* 191, 248–259. doi: 10.1016/j.aanat.2009.02.007
- Lane, D. A., Tortorici, V., and Morgan, M. M. (2004). Behavioral and electrophysiological evidence for tolerance to continuous morphine administration into the ventrolateral periaqueductal gray. *Neuroscience* 125, 63–69. doi: 10.1016/j.neuroscience.2004.01.023
- Latremliere, A., and Woolf, C. J. (2009). Central sensitization: a generator of pain hypersensitivity by central neural plasticity. *J. Pain* 10, 895–926. doi: 10.1016/j.jpain.2009.06.012
- Leong, M. L., Gu, M., Speltz-Paiz, R., Stahura, E. I., Mottey, N., Steer, C. J., et al. (2011). Neuronal loss in the rostral ventromedial medulla in a rat model of neuropathic pain. *J. Neurosci.* 31, 17028–17039. doi: 10.1523/JNEUROSCI.1268-11.2011
- Leong, M. L., Speltz, R., and Wessendorf, M. (2016). Effects of chronic constriction injury and spared nerve injury, two models of neuropathic pain, on the numbers of neurons and glia in the rostral ventromedial medulla. *Neurosci. Lett.* 617, 82–87. doi: 10.1016/j.neulet.2016.02.006
- Liu, X., Eschenfelder, S., Blenk, K. H., Jänig, W., and Häbler, H. (2000). Spontaneous activity of axotomized afferent neurons after L5 spinal nerve injury in rats. *Pain* 84, 309–318. doi: 10.1016/s0304-3959(99)00211-0
- Lovick, T., and Bandler, R. (2005). “The organization of the midbrain periaqueductal grey and the integration of pain behaviours,” in *The Neurobiology of Pain*, eds S. P. Hunt and M. Koltzenburg (Oxford, UK: Oxford University Press), 267–287.
- Maves, T. J., Pechman, P. S., Gebhart, G. F., and Meller, S. T. (1993). Possible chemical contribution from chronic gut sutures produces disorders of pain sensation like those seen in man. *Pain* 54, 57–69. doi: 10.1016/0304-3959(93)90198-x
- McMullan, S., and Lumb, B. M. (2006). Midbrain control of spinal nociception discriminates between responses evoked by myelinated and unmyelinated heat nociceptors in the rat. *Pain* 124, 59–68. doi: 10.1016/j.pain.2006.03.015
- Milligan, E. D., and Watkins, L. R. (2009). Pathological and protective roles of glia in chronic pain. *Nat. Rev. Neurosci.* 10, 23–36. doi: 10.1038/nrn2533
- Monassi, C. R., Bandler, R., and Keay, K. A. (2003). A subpopulation of rats shows social and sleep-waking changes typical of chronic neuropathic pain following peripheral nerve injury. *Eur. J. Neurosci.* 17, 1907–1920. doi: 10.1046/j.1460-9568.2003.02627.x
- Mor, D., Bembrick, A. L., Austin, P. J., and Keay, K. A. (2011). Evidence for cellular injury in the midbrain of rats following chronic constriction injury of the sciatic nerve. *J. Chem. Neuroanat.* 41, 158–169. doi: 10.1016/j.jchemneu.2011.01.004
- Mor, D., Bembrick, A. L., Austin, P. J., Wyllie, P. M., Creber, N. J., Denyer, G. S., et al. (2010). Anatomically specific patterns of glial activation in the periaqueductal gray of the sub-population of rats showing pain and disability following chronic constriction injury of the sciatic nerve. *Neuroscience* 166, 1167–1184. doi: 10.1016/j.neuroscience.2010.01.045
- Ni, H. D., Yao, M., Huang, B., Xu, L. S., Zheng, Y., Chu, Y. X., et al. (2016). Glial activation in the periaqueductal gray promotes descending facilitation of neuropathic pain through the p38 MAPK signaling pathway. *J. Neurosci. Res.* 94, 50–61. doi: 10.1002/jnr.23672
- Norman, G. J., Karelina, K., Zhang, N., Walton, J. C., Morris, J. S., and Devries, A. C. (2010). Stress and IL-1 β contribute to the development of depressive-like behavior following peripheral nerve injury. *Mol. Psychiatry* 15, 404–414. doi: 10.1038/mp.2009.91
- Omana-Zapata, I., Khabbaz, M. A., Hunter, J. C., Clarke, D. E., and Bley, K. R. (1997). Tetrodotoxin inhibits neuropathic ectopic activity in neuromas, dorsal root ganglia and dorsal horn neurons. *Pain* 72, 41–49. doi: 10.1016/s0304-3959(97)00012-2
- Paxinos, G., and Watson, C. (1997). *The Rat Brain in Stereotaxic Coordinates*. San Diego, CA: Elsevier Academic Press.
- Pekny, M., and Nilsson, M. (2005). Astrocyte activation and reactive gliosis. *Glia* 50, 427–434. doi: 10.1002/glia.20207
- Pekny, M., and Pekna, M. (2004). Astrocyte intermediate filaments in CNS pathologies and regeneration. *J. Pathol.* 204, 428–437. doi: 10.1002/path.1645
- Pekny, M., and Pekna, M. (2014). Astrocyte reactivity and reactive astrogliosis: costs and benefits. *Physiol. Rev.* 94, 1077–1098. doi: 10.1152/physrev.00041.2013
- Pertovaara, A., Wei, H., and Hämläinen, M. M. (1996). Lidocaine in the rostromedial medulla and the periaqueductal gray attenuates allodynia in neuropathic rats. *Neurosci. Lett.* 218, 127–130. doi: 10.1016/s0304-3940(96)13136-0
- Porreca, F., Ossipov, M. H., and Gebhart, G. F. (2002). Chronic pain and medullary descending facilitation. *Trends Neurosci.* 25, 319–325. doi: 10.1016/s0166-2236(02)02157-4
- Ridet, J. L., Malhotra, S. K., Privat, A., and Gage, F. H. (1997). Reactive astrocytes: cellular and molecular cues to biological function. *Trends Neurosci.* 20, 570–577. doi: 10.1016/s0166-2236(97)01139-9
- Schaible, H. G. (2007). Peripheral and central mechanisms of pain generation. *Handb. Exp. Pharmacol.* 177, 3–28. doi: 10.1007/978-3-540-33823-9_1
- Sofroniew, M. V., and Vinters, H. V. (2010). Astrocytes: biology and pathology. *Acta Neuropathol.* 119, 7–35. doi: 10.1007/s00401-009-0619-8
- Streit, W. J., Walter, S. A., and Pennell, N. A. (1999). Reactive microgliosis. *Prog. Neurobiol.* 57, 563–581. doi: 10.1016/s0301-0082(98)00069-0
- Suplita, R. L. II., Farthing, J. N., Gutierrez, T., and Hohmann, A. G. (2005). Inhibition of fatty-acid amide hydrolase enhances cannabinoid stress-induced analgesia: sites of action in the dorsolateral periaqueductal gray and rostral

- ventromedial medulla. *Neuropharmacology* 49, 1201–1209. doi: 10.1016/j.neuropharm.2005.07.007
- Suzuki, R., Rahman, W., Hunt, S. P., and Dickenson, A. H. (2004). Descending facilitatory control of mechanically evoked responses is enhanced in deep dorsal horn neurons following peripheral nerve injury. *Brain Res.* 1019, 68–76. doi: 10.1016/j.brainres.2004.05.108
- Tanaka, T., Minami, M., Nakagawa, T., and Satoh, M. (2004). Enhanced production of monocyte chemoattractant protein-1 in the dorsal root ganglia in a rat model of neuropathic pain: possible involvement in the development of neuropathic pain. *Neurosci. Res.* 48, 463–469. doi: 10.1016/j.neures.2004.01.004
- Thacker, M. A., Clark, A. K., Bishop, T., Grist, J., Yip, P. K., Moon, L. D., et al. (2009). CCL2 is a key mediator of microglia activation in neuropathic pain states. *Eur. J. Pain* 13, 263–272. doi: 10.1016/j.ejpain.2008.04.017
- Van Steenwinckel, J., Reaux-Le Goazigo, A., Pommier, B., Mauborgne, A., Dansereau, M. A., Kitabgi, P., et al. (2011). CCL2 released from neuronal synaptic vesicles in the spinal cord is a major mediator of local inflammation and pain after peripheral nerve injury. *J. Neurosci.* 31, 5865–5875. doi: 10.1523/JNEUROSCI.5986-10.2011
- Vanegas, H., and Schaible, H. G. (2004). Descending control of persistent pain: inhibitory or facilitatory? *Brain Res. Rev.* 46, 295–309. doi: 10.1016/j.brainresrev.2004.07.004
- Vera-Portocarrero, L. P., Xie, J. Y., Kowal, J., Ossipov, M. H., King, T., and Porreca, F. (2006). Descending facilitation from the rostral ventromedial medulla maintains visceral pain in rats with experimental pancreatitis. *Gastroenterology* 130, 2155–2164. doi: 10.1053/j.gastro.2006.03.025
- Vranken, J. H. (2009). Mechanisms and treatment of neuropathic pain. *Cent. Nerv. Syst. Agents Med. Chem.* 9, 71–78. doi: 10.2174/187152409787601932
- Vranken, J. H. (2012). Elucidation of pathophysiology and treatment of neuropathic pain. *Cent. Nerv. Syst. Agents Med. Chem.* 12, 304–314. doi: 10.2174/187152412803760645
- Watkins, L. R., Milligan, E. D., and Maier, S. F. (2003). Glial proinflammatory cytokines mediate exaggerated pain states: Implications for clinical pain. *Adv. Exp. Med. Biol.* 521, 1–21.
- Wei, F., Guo, W., Zou, S., Ren, K., and Dubner, R. (2008). Supraspinal glial-neuronal interactions contribute to descending pain facilitation. *J. Neurosci.* 28, 10482–10495. doi: 10.1523/JNEUROSCI.3593-08.2008
- White, F. A., Jung, H., and Miller, R. J. (2007). Chemokines and the pathophysiology of neuropathic pain. *Proc. Natl. Acad. Sci. U S A* 104, 20151–20158. doi: 10.1073/pnas.0709250104
- White, F. A., and Miller, R. J. (2010). Insights into the regulation of chemokine receptors by molecular signaling pathways: functional roles in neuropathic pain. *Brain Behav. Immun.* 24, 859–865. doi: 10.1016/j.bbi.2010.03.007
- White, F. A., Sun, J., Waters, S. M., Ma, C., Ren, D., Ripsch, M., et al. (2005). Excitatory monocyte chemoattractant protein-1 signaling is up-regulated in sensory neurons after chronic compression of the dorsal root ganglion. *Proc. Natl. Acad. Sci. U S A* 102, 14092–14097. doi: 10.1073/pnas.0503496102
- Wilson-Poe, A. R., Pocius, E., Herschbach, M., and Morgan, M. M. (2013). The periaqueductal gray contributes to bidirectional enhancement of antinociception between morphine and cannabinoids. *Pharmacol. Biochem. Behav.* 103, 444–449. doi: 10.1016/j.pbb.2012.10.002
- Woolf, C. J. (2011). Central sensitization: implications for the diagnosis and treatment of pain. *Pain* 152, S2–S15. doi: 10.1016/j.pain.2010.09.030
- Woolf, C. J., and Mannion, R. J. (1999). Neuropathic pain: aetiology, symptoms, mechanisms, and management. *Lancet* 353, 1959–1964. doi: 10.1016/s0140-6736(99)01307-0
- Yeziarski, R. P., and Mendez, C. M. (1991). Spinal distribution and collateral projections of rat spinomesencephalic tract cells. *Neuroscience* 44, 113–130. doi: 10.1016/0306-4522(91)90254-1
- Zamboni, L., and Demartin, C. (1967). Buffered picric acid-formaldehyde—a new rapid fixative for electron microscopy. *J. Cell Biol.* 35:148A.
- Zhang, J., and De Koninck, Y. (2006). Spatial and temporal relationship between monocyte chemoattractant protein-1 expression and spinal glial activation following peripheral nerve injury. *J. Neurochem.* 97, 772–783. doi: 10.1111/j.1471-4159.2006.03746.x
- Zimmermann, M. (2001). Pathobiology of neuropathic pain. *Eur. J. Pharmacol.* 429, 23–37. doi: 10.1016/s0014-2999(01)01303-6

Conflict of Interest Statement: The authors declare that the research was conducted in the absence of any commercial or financial relationships that could be construed as a potential conflict of interest.

Copyright © 2018 Dubový, Klusáková, Hradilová-Svíženská, Joukal and Boadas-Vaello. This is an open-access article distributed under the terms of the Creative Commons Attribution License (CC BY). The use, distribution or reproduction in other forums is permitted, provided the original author(s) and the copyright owner are credited and that the original publication in this journal is cited, in accordance with accepted academic practice. No use, distribution or reproduction is permitted which does not comply with these terms.

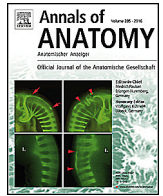
F. **Joukal M**, Klusáková I, Dubový P. Direct communication of the spinal subarachnoid space with the rat dorsal root ganglia. *Ann Anat - Anat Anz.* 2016;205:9-15. doi:10.1016/j.aanat.2016.01.004

Commentary: In this article, we demonstrated for the first time that the subarachnoid space anatomically reaches the DRG. We proved that intrathecal applied fluorescence-conjugated dextran diffuses to the DRG and induces inflammatory response expressed by presence of macrophages, dendritic cells and activation of satellite glial cells.

IF (WOS, 2016): 1.579

Quartile (WOS, 2016): Anatomy and Morphology Q1

Contribution of the author: First Author. The author designed and performed the experiments, analyzed the data and wrote manuscript.



Research article

Direct communication of the spinal subarachnoid space with the rat dorsal root ganglia



Marek Joukal, Ilona Klusáková, Petr Dubový*

Department of Anatomy, Division of Neuroanatomy, Faculty of Medicine, Masaryk University, CZ-625 00 Brno, Czech Republic

ARTICLE INFO

Article history:

Received 26 October 2015

Received in revised form

21 December 2015

Accepted 13 January 2016

Keywords:

Subarachnoid space

Cerebrospinal fluid

Dorsal root ganglia

Fluoro-emerald

Immunohistochemistry

Macrophages

ABSTRACT

The anatomical position of the subarachnoid space (SAS) in relation to dorsal root ganglia (DRG) and penetration of tracer from the SAS into DRG were investigated. We used intrathecal injection of methylene blue to visualize the anatomical position of the SAS in relation to DRG and immunostaining of dipeptidyl peptidase IV (DPP-IV) for detecting arachnoid limiting the SAS. Intrathecal administration of fluorescent-conjugated dextran (fluoro-emerald; FE) was used to demonstrate direct communication between the SAS and DRG. Intrathecal injection of methylene blue and DPP-IV immunostaining revealed that SAS delimited by the arachnoid was extended up to the capsule of DRG in a fold-like recess that may reach approximately half of the DRG length. The arachnoid was found in direct contact to the neuronal body-rich area in the angle between dorsal root and DRG as well as between spinal nerve roots at DRG. Particles of FE were found in the cells of DRG capsule, satellite glial cells, interstitial space, as well as in small and medium-sized neurons after intrathecal injection. Penetration of FE from the SAS into the DRG induced an immune reaction expressed by colocalization of FE and immunofluorescence indicating antigen-presenting cells (MHC-II+), activated (ED1+) and resident (ED2+) macrophages, and activation of satellite glial cells (GFAP+). Penetration of lumbar-injected FE into the cervical DRG was greater than that into the lumbar DRG after intrathecal injection of FE into the cisterna magna. Our results demonstrate direct communication between DRG and cerebrospinal fluid in the SAS that can create another pathway for possible propagation of inflammatory and signaling molecules from DRG primary affected by peripheral nerve injury into DRG of remote spinal segments.

© 2016 Elsevier GmbH. All rights reserved.

1. Introduction

The subarachnoid space (SAS) filled by cerebrospinal fluid (CSF) is much discussed clinically in the field of chronic pain. It is a common site for application of anesthetics (Czernicki et al., 2014) and sampling of CSF when assessing chronic pain (Zin et al., 2010). Moreover, neuroinflammatory reaction expressed by upregulation of cytokines (TNF α , IL-6 and IL-10) and chemokines (SDF1/CXCL12) has been detected in dorsal root ganglia (DRG) both associated and non-associated with damaged sciatic nerve. These findings suggest that signaling of the molecular changes might be propagated alongside the neuraxis from affected to remote DRG (Jancalék et al., 2010, 2011; Dubový et al., 2010, 2013). Moreover, various types of nerve injury-induced neuroinflammatory reactions have also been found in the central nervous system structures (Vania Apkarian et al., 2006). We hypothesize that direct communication

between the SAS and DRG could provide a pathway for propagation of signaling molecules alongside the neuraxis among DRG of different spinal segments via CSF. The first goal of our study, therefore, was to visualize the morphological position of the SAS in relation to rat DRG. Second, we investigated the penetration of 10 kDa fluorescent-conjugated dextran (fluoro-emerald; FE) from the SAS into DRG.

2. Materials and methods

2.1. Animals and surgical procedures

The experiments were performed on 20 adult male rats (Wistar, 200–250 g; Animal Breeding Facility of Masaryk University, Czech Republic). The animals were kept at 22 °C and maintained on a 12 h light/dark cycle under specific pathogen-free conditions in the animal housing area of Masaryk University. Sterilized food and water were available *ad libitum*. All experimental procedures were carried out aseptically and according to protocols approved by the Ethical Committee of Masaryk University, Brno and the Departmental

* Corresponding author. Tel.: +420 549 493 701; fax: +420 549 491 320.
E-mail address: pdubovy@med.muni.cz (P. Dubový).

Committee of the Ministry of Education, Youth and Sports of the Czech Republic.

2.2. Anatomical study of the SAS in relation to DRG

2.2.1. Intrathecal methylene blue injection

Although fusion of the meninges with DRG has been described (Shanthaveerappa and Bourne, 1962; McCabe and Low, 1969), a position of SAS in relation to rat DRG remained unclear. Therefore, we injected Methylene blue (MB) into SAS to macroscopically visualize the precise position of SAS in relation to DRG. Animals ($n = 5$) were anesthetized using a mixture of ketamine (40 mg/ml) and xylazine (4 mg/ml) administered intraperitoneally (0.2 ml/100 g body weight). MB was dissolved in artificial cerebrospinal fluid (ACSF; Hylden and Wilcox, 1980) at 1% concentration and 50 μ l of this solution was injected into the SAS of the cisterna magna. The micro syringe was inserted through the posterior atlanto-occipital membrane after skin incision and blunt reflection of paravertebral muscles. Animals were sacrificed in CO₂ and perfused transcardially with 4% paraformaldehyde. Lumbar (L4–L5) and cervical (C7–C8) DRG were detected *in situ* following laminectomy and foraminotomy conducted with great care not to damage the meninges. Microdissection and analysis were performed under a stereomicroscope (Leica M50 LED) equipped with a digital camera (Leica DFC 480, Leica Microsystems, Wetzlar, Germany).

2.2.2. Detection of the arachnoid by DPP-IV immunostaining

Five rats were sacrificed in CO₂ and perfused transcardially with Zamboni's fixative solution (Zamboni and de Martino, 1967). DRG of cervical (C7–C8) and lumbar (L4–L5) segments were removed and then immersed in Zamboni's fixative overnight. The DRG were then washed in 20% phosphate-buffered sucrose (pH 7.2) and embedded in Tissue-Tek OCT compound (Miles; Elkhart, IN, USA). Longitudinal cryostat sections (12 μ m) were then cut (Leica 1800 cryostat) and collected on gelatin-coated microscope slides. The sections were processed for indirect immunofluorescence staining to detect DPP-IV as a marker of the arachnoid (Haninec and Grim, 1990). Affinity purified secondary antibody conjugated with FITC was used for visualization of DPP-IV immunostaining (Table 1). Cell nuclei were stained with Hoechst 33342 (Sigma; St. Louis, MO, USA), the sections were mounted in a Vectashield aqueous mounting medium (Vector Laboratories; Burlingame, CA, USA) and analyzed using a Nikon Eclipse NI-E epifluorescence microscope equipped with a Nikon DS-R11 camera operated by a NIS-Elements software (Nikon, Prague, Czech Republic).

2.3. Penetration of labeled dextran (fluoro-emerald) from the SAS into DRG and immunodetection of loaded cells

Ten rats were deeply anesthetized using a mixture of ketamine (40 mg/ml) and xylazine (4 mg/ml) administered intraperitoneally (0.2 ml/100 g body weight). Fluorescent-conjugated dextran (fluoro-emerald, FE, MW = 10 kDa, lysine fixable, Molecular Probes, Eugene, OR, USA) was dissolved in ACSF (1.5 mg in 100 μ l).

The solution (50 μ l) was injected into the SAS using the micro syringe through the atlanto-occipital membrane to the cisterna magna (cervical, $n = 5$) or between the L2 and L3 vertebrae (lumbar, $n = 5$). All rats were left to survive for 20 h. They were then sacrificed in CO₂ and perfused transcardially with Zamboni's fixative solution (Zamboni and de Martino, 1967). Cervical (C7–C8) and lumbar (L4–L5) DRG were removed, immersed in Zamboni's fixative overnight. The samples were then washed in 20% phosphate-buffered sucrose for 12 h and longitudinal cryostat sections (12 μ m) were prepared. A part of the sections was stained using Hoechst 33342 (Sigma; St. Louis, MO, USA), mounted in a Vectashield aqueous mounting medium (Vector Laboratories; Burlingame, CA, USA), then analyzed using a Nikon epifluorescence microscope to examine FE penetration.

2.3.1. Immunofluorescence staining

To identify FE-loaded cells or cell reaction following FE penetration into DRG, the sections were processed for standard indirect immunofluorescence staining with ED1 and ED2 antibodies to detect activated and resident macrophages, respectively. In addition, MHC-II antibody was used to detect antigen-presenting cells (APC), GFAP antibody was applied as a marker of activated satellite glial cells (SGC), and Iba1 antibody was used to detect phagocytic activity of DRG cells. In addition, Ki-67 immunostaining was used to visualize proliferation activity of the cells. Primary and secondary antibodies and their concentrations are listed in Table 1. Briefly, the sections were washed with phosphate-buffered saline (PBS) containing 0.3% bovine serum albumin (BSA) and 0.1% Tween-20; treated with 3% normal goat or donkey serum for 30 min; then incubated with primary antibody at room temperature for an appropriate time and affinity purified secondary antibodies conjugated with TRITC were applied at room temperature for 90 min. The sections were washed in PBS, stained with Hoechst 33342, mounted in a Vectashield aqueous mounting medium, and then analyzed using a Nikon epifluorescence microscope. The control sections were incubated while omitting the primary antibodies.

2.3.2. Double immunostaining for GFAP and ED1

A part of DRG sections was double immunostained for GFAP and ED1 to detect positions of activated macrophages in relation to sensory neuron-SGC units. Sections were treated with a mixture of acetone and methanol (1:1) at -20°C for 5 min, washed with PBS containing 0.3% BSA and 0.1% Tween 20, then treated with 3% normal goat serum for 30 min. The sections were then incubated with mouse monoclonal anti-ED1 antibody at room temperature and TRITC-conjugated goat anti-mouse secondary antibody for 90 min. Next, simultaneous immunostaining was done by incubating the sections with rabbit polyclonal anti-GFAP antibody at room temperature. After thorough washing in PBS, the sections were treated with AlexaFluor 350-conjugated goat anti-rabbit secondary antibody for 90 min. Sections were mounted in a Vectashield aqueous mounting medium (Vector Laboratories; Burlingame, CA, USA) after washing in redistilled water.

Table 1
Primary and secondary antibodies, their dilutions and producers.

Primary antibody	Type of antibody	Dilution; incubation time	Producer	Secondary antibody	Dilution	Producer
DPP-IV	Mouse monoclonal	1:200; 240 min	Santa Cruz, USA	Goat anti-mouse	1:100	Chemicon
ED1	Mouse monoclonal	1:200; 240 min	Serotec, UK	Goat anti-mouse	1:50	Chemicon
ED2	Mouse monoclonal	1:200; 16 h	Serotec, UK	Goat anti-mouse	1:100	Chemicon
GFAP	Rabbit polyclonal	1:250; 180 min	Dako, Denmark	Goat anti-rabbit	1:100	Chemicon
				Donkey anti-rabbit	1:400	Jackson ImmunoResearch
Iba1	Goat polyclonal	1:50; 16 h	Abcam, UK	Biotinylated Donkey anti-goat	1:400	Santa Cruz
Ki-67	Rabbit polyclonal	1:500; 240 min	Vector, USA	Goat anti-rabbit	1:100	Chemicon
MHC-II	Mouse monoclonal	1:100; 240 min	Serotec, UK	Goat anti-mouse	1:100	Chemicon

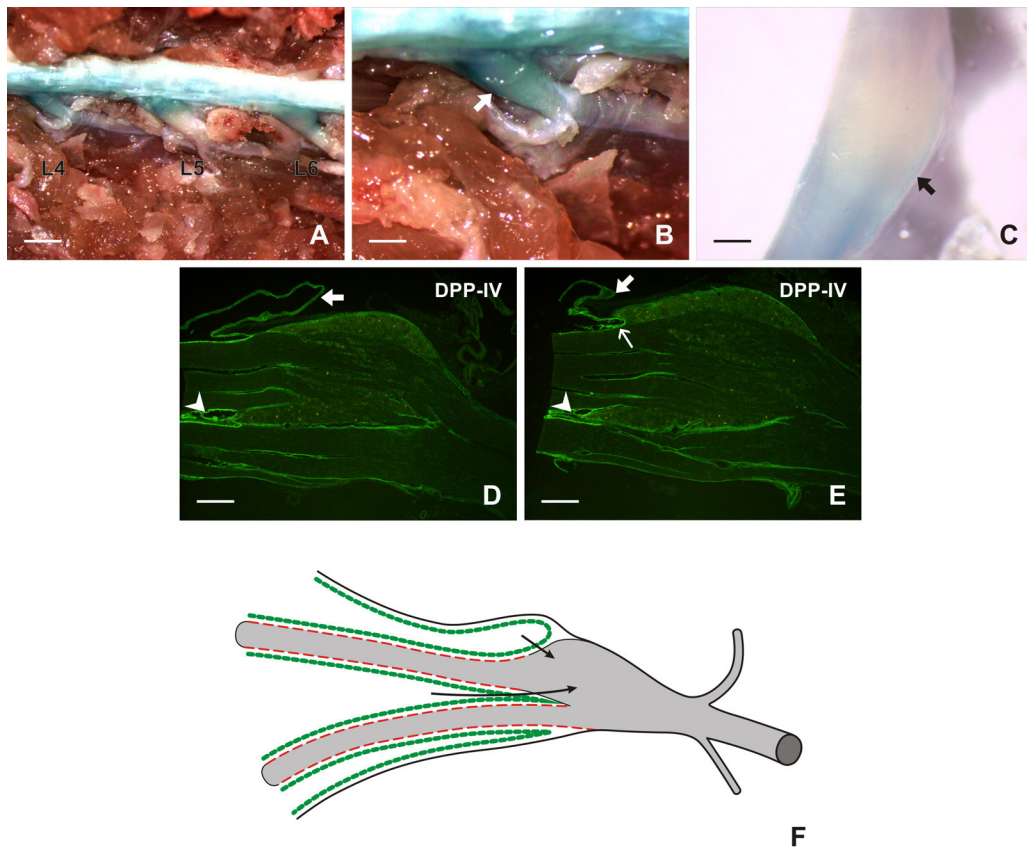


Fig. 1. Representative pictures of lumbar DRG after intrathecal injection of MB (A–C). Arrow indicates the SAS filled by MB as a blue stripe at the surface of DRG. The SAS was in some cases localized at approximately half of DRG length (B). Representative cryostat sections through lumbar DRG immunostained for DPP-IV as a marker of the arachnoid show the SAS delimited by the arachnoid as a fold-like recess reaching DRG (D and E, arrows). Furthermore, the SAS is in direct contact with DRG between the spinal nerve roots (D and E, arrowheads) and in the angle between the dorsal root and surface of DRG (E, open arrow). The schematic drawing (F) summarizes the aforementioned position of the SAS delimited by the arachnoid (dotted green line) in relation to DRG. Continuous black and dashed red lines indicate dura and pia mater, respectively. A possible route of molecule penetration from CSF into DRG is depicted by the arrows. Scale bar = 3 mm (A), 1 mm (B), 500 μm (C), 200 μm (D and E).

2.3.3. Double immunostaining for GFAP and Iba1

Phagocytic activity of GFAP+ SGC was proved by simultaneous reaction with Iba1 antibody as a marker for ionized calcium-binding adaptor molecule 1. A part of sections was pretreated (see above) and incubated with rabbit polyclonal anti-GFAP antibody at room temperature and Cy5-conjugated donkey anti-rabbit secondary antibody for 90 min. Then, goat polyclonal anti-Iba1 antibody at room temperature was applied overnight following inhibition of endogenous streptavidin–biotin interaction. After thorough washing in PBS, the sections were treated with biotinylated donkey anti-goat secondary antibody and TRITC-conjugated streptavidin (1:100; Jackson ImmunoResearch, USA) for 90 min. The sections were washed in PBS, stained with Hoechst 33342, mounted in a Vectashield aqueous mounting medium. TRITC and Cy5 fluorescence were detected by combination of C-FL Epi-FITRITC and Cy5 filter blocks, respectively. In the case of Iba1 immunostaining, monochromatic images were converted into purple pseudo color.

2.3.4. Quantitative analysis of FE penetration into DRG after lumbar and cervical administration

The FE+ areas were measured in neuronal body compartments of cervical and lumbar DRG after cervical or lumbar FE injection. Every third section was used to protect against measuring the same area twice. Two or three irregular areas of interest per section were circumscribed in at least 10 longitudinal sections of each DRG in neuronal body compartment and measured using NIS-Elements AR Analysis (version 4.20.00, Nikon, Prague, Czech Republic). The FE+

area was selected by thresholding technique (Dubovy et al., 2002). A percentage ratio of the FE+ area to total area of neuronal body compartment was counted and calculated for each picture. Results from four cervical and lumbar DRG were expressed as mean \pm SD and compared using Mann–Whitney *U* test (StatSoft, Tulsa, OK, USA) with $p < 0.05$ as the level of significance.

The categories of neuronal body sizes were determined by diameter calculated from areas measured using NIS-Elements AR Analysis. Only those neuronal profiles containing nuclei were counted. The sizes of DRG neurons were categorized as small ($< 25 \mu\text{m}$), medium (25–40 μm), and large ($> 40 \mu\text{m}$).

3. Results

3.1. Anatomical study of subarachnoid space in relation to DRG

Intrathecal application of MB was performed to investigate the *in situ* position of the SAS in relation to DRG. We found the SAS filled with MB as the blue color stripes indicating SAS extension to the surface of DRG in all spinal cord segments (Fig. 1A–C). Longitudinal cryostat sections of cervical and lumbar DRG immunostained for DPP-IV revealed a blind, fold-like recess delimited by the arachnoid and protruding up to the capsule surface of DRG. The extent of this recess varied from short in some sections to approximately half of DRG length in most cases. Nevertheless, the contact of the arachnoid with DRG capsule did not seem to be a place for communication between CSF and DRG. The place for direct communication between the SAS and DRG parenchyma is probably localized at the

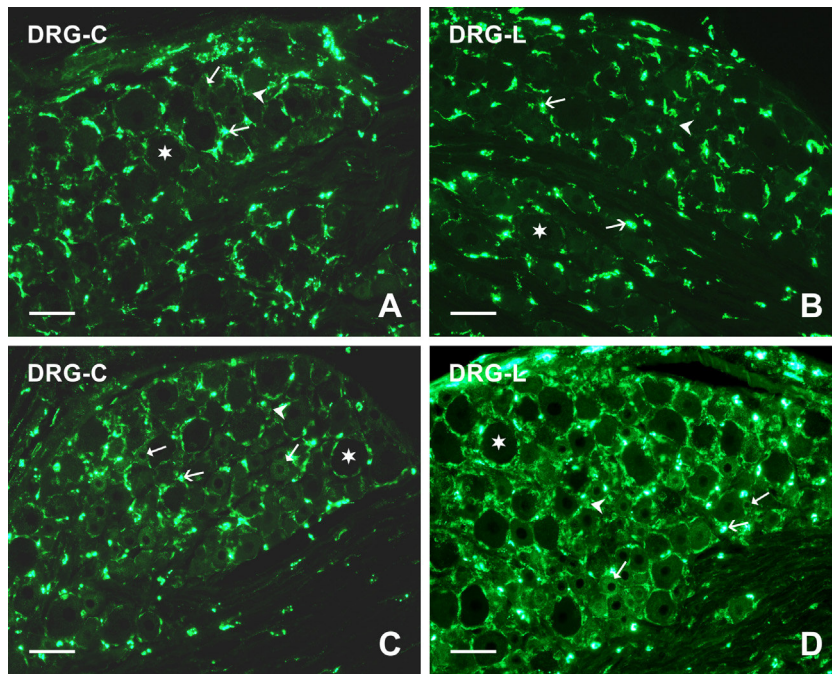


Fig. 2. Representative cryostat sections illustrate the amount of FE diffused into cervical (A and C) and lumbar (B and D) DRG after cervical (A and B) and lumbar application (C and D). Note the greater amount of FE particles in cervical DRG after lumbar application (C) compared to lumbar DRG after cervical application (B). Fluorescent particles penetrated into DRG and are dispersed in interstitial space (arrowheads) or loaded by interstitial cells (opened arrow). In addition, FE particles were found in small neurons (full arrow) in contrast to large neuronal bodies free of FE fluorescence (asterisks). Scale bar = 60 μm .

angle between the dorsal root and DRG surface where the arachnoid was in close contact with the surface of the neuronal body-rich area. In addition, the SAS of triangular shape limited by the DPP-IV+ arachnoid between the ventral and dorsal roots was also in close contact with DRG, thus forming another possible communication point between the SAS and DRG (Fig. 1D and E). The position of meninges and points of a possible communication between the SAS and DRG are shown schematically in Fig. 1F.

3.2. Penetration of FE from the SAS into DRG and immunophenotyping of loaded cells

A robust green fluorescence was found indicating diffusion of FE molecules from the subarachnoid space into DRG (Fig. 2A–D). The penetration of lumbar-injected FE into the cervical DRG was higher than into the lumbar DRG after intrathecal injection of FE into the cisterna magna (Fig. 2B and C; Table 2). Particles of FE were dispersed in the extracellular spaces of DRG, where they induced a strong immune reaction as expressed by macrophage invasion.

Immunostaining for ED1 suggested that most of the FE+ cells invading the interstitial space of both cervical and lumbar DRG were activated macrophages (Fig. 3A–C). As demonstrated by double immunostaining for GFAP and ED1 (Fig. 3D–G), some of the ED1+ cells additionally invaded the sensory neuron-SGC units. In comparison to ED1, only a few ED2+ macrophages were observed in the interstitial space of DRG. Round-shaped resident ED2+ macrophages were predominantly located in the neuronal

body-rich area of DRG and all of them were filled with FE (Fig. 3H–J). The cells immunolabeled for MHC-II+ found in the interstitial space of DRG were divided into a major population loaded with FE particles and a minor population without such particles (Fig. 4A–C). The FE particles were also observed in GFAP-immunostained SGC. Double immunostaining revealed that GFAP+ SGC loaded by FE particles also displayed immunofluorescence staining for Iba1 (Fig. 4D–F). In addition, the FE particles penetrated into the bodies of small and medium-sized neurons whereas the large neurons were free of FE fluorescence (Fig. 2D). A green FE fluorescence was also present in the capsule of DRG and attached meninges. The capsule of DRG and attached meninges displayed FE fluorescence and contained the cells loaded by FE particles that were recognized as activated (ED1+) and resident macrophages (ED2+) and APC (MHCII+) (Figs. 3A–C, H–J; 4A–C). Diffusion of FE particles induced a minimal proliferation activity of cells inside DRG and attached meninges, as illustrated by rare Ki-67 immunostaining (Fig. 4G–I). All Ki67+ cells were found to be free of FE particles.

4. Discussion

The relationship between arachnoid and DRG had been investigated by McCabe and Low (1969), who used the term “subarachnoid angle” to describe the place where meninges reach the surface of DRG. In addition, Shanthaveerappa and Bourne (1962) had postulated that the perineural epithelium of spinal nerve is in fact a prolongation of leptomeninges.

Our results from MB injection showed the blue stripes indicating enlargement of the SAS up to the surface of DRG. The SAS extension in the form of a fold-like recess was also detected by immunohistochemical staining for DPP-IV, used as a marker of the arachnoid (Haninec and Grim, 1990). Moreover, the SAS delimited by the DPP-IV+ arachnoid was found between the dorsal and ventral roots and as a sharp angle between the dorsal root and the neuronal body-rich area of DRG. These regions constitute a probable pathway for penetration of molecules from CSF of the SAS into DRG.

Table 2
Percentage value of FE+ area to the neuronal body-rich area of cervical (C-DRG) and lumbar DRG (L-DRG) after cervical or lumbar FE administration.

	C-DRG ($\bar{x} \pm \text{SD}$)	L-DRG ($\bar{x} \pm \text{SD}$)
Cervical FE administration	37.13 \pm 13.46	6.94 \pm 1.80
Lumbar FE administration	50.42 \pm 5.48*	69.30 \pm 11.29

* Significant difference ($p < 0.05$) when compared to L-DRG after cervical administration.

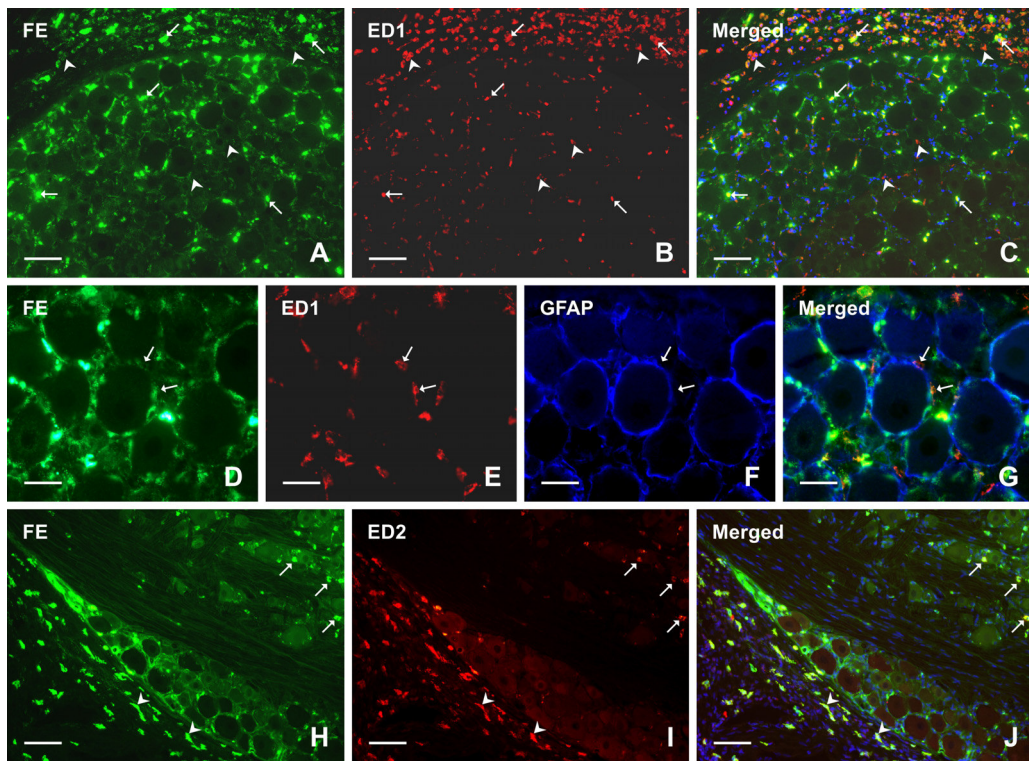


Fig. 3. Cryostat sections through lumbar DRG after lumbar application of FE illustrate the presence of activated (ED1) and resident (ED2) macrophages in DRG. Robust invasion of ED1+ macrophages is seen in DRG parenchyma, capsule and attached meninges (A–C). A part of activated macrophages (ED1+) are loaded (arrows) or free of FE particles (arrowheads). Double immunostaining for GFAP and ED1 reveal that some of activated macrophages invaded the sensory neuron-SGC unit and have become “satellite macrophages” (arrows, D–G). Resident macrophages (ED2+) loaded with FE were found in DRG capsule and attached meninges (H–J, arrowheads) as well as in DRG neuronal body-rich area (H–J, arrows). Cell nuclei were stained using Hoechst (C and J). Scale bar = 60 μm (A–C; H–J), 40 μm (D–G).

This is in accordance with [Abram et al. \(2006\)](#), who found fluorescein penetration into DRG near the subarachnoid angle 30 min after intrathecal injection but apparently paid little attention to this finding. [Hu and McLachlan \(2002\)](#) indirectly demonstrated diffusion of molecules from CSF into DRG in a region between the spinal nerve roots where the aggregation of APC was found. These previously published and our present results suggest that possible structural positions for communication between the SAS and DRG are localized in the area where the arachnoid attaches directly to the surface of neuronal body rich area at the angle between DRG and dorsal root and among the spinal nerve roots and DRG.

The SAS is a common site for intrathecal administration of anesthetics used in the treatment of neuropathic pain and for surgery ([Hawksworth and Serpell, 1998](#); [Czernicki et al., 2014](#)). In addition, the SAS may communicate with epidural space and anesthetics injected epidurally cross the arachnoid lamina and reach the SAS ([Ohtani et al., 1990](#); [Angel Reina et al., 2008](#)). The analgesic effect of anesthetics after intrathecal application is explained by their penetration into the dorsal roots ([Hamber and Viscomi, 1999](#)). However, our results after intrathecal FE application suggest a possible penetration of molecules including anesthetics from the SAS into DRG, where the primary sensory neurons could be affected. The effect of anesthetics on neurons has been investigated using patch clamp technique and explained by selective involvement of sodium and potassium channels ([Safonov et al., 1996](#); [Scholz et al., 1998](#); [Komai and McDowell, 2001](#)).

We used FITC-conjugated dextran (fluoro-emerald) as a tracer for studying direct communication between the SAS and DRG. Fluoro-emerald is lysine fixable conjugated dextran, and it is used extensively as a retrograde tracer to label neurons (e.g. after peripheral nerve lesions) or to study axonal sprouting after surgical nerve anastomoses ([Kubek et al., 2004](#); [Žele et al., 2010](#)).

In addition to neuronal tracing, dextrans are used in a wide variety of other applications, including fluid transport, intracellular communication, tracing cell lineage, probing membrane permeability and endocytosis ([Nasomphan et al., 2013](#); [Dai et al., 2014](#); [Hu et al., 2015](#)). Furthermore, dextrans have been used in clinical practice ([Lamke and Liljedahl, 1976](#)) despite the fact that they can induce anaphylactic reactions ([Zinderman et al., 2006](#)).

Although robust green FE fluorescence was found inside DRG after both cervical and lumbar intrathecal injection, the amount of FE diffused into cervical DRG after lumbar administration was obviously greater than that entering lumbar DRG after cervical injection. This is in agreement with the findings of [Kusmirek et al. \(1997\)](#), who found that intrathecal injection of opioid antagonist DAMGO administered both to the cervical and lumbar regions spreads alongside the neuraxis. However, identical doses of DAMGO administered to the lumbar SAS produced a suppression of both hind- and forepaw withdrawals in contrast to cervical administration where the withdrawals of hind paw were not suppressed.

Diffusion of FE into the arachnoid and DRG induced an immune reaction as demonstrated by immunostaining of FE-loaded cells for MHC-II, thus indicating APC, as well as for ED1 and ED2 indicating activated and resident macrophages, respectively ([Dijkstra et al., 1985](#); [Dijkstra and Damoiseaux, 1993](#); [Hu and McLachlan, 2003](#)). The presence of immune cells loaded by FE in the meninges corresponds with findings of [Wieseler-Frank et al. \(2007\)](#), who postulated that meninges are responsible for the immune reaction, including secretion of proinflammatory cytokines to the CSF after inflammatory stimulus. Intrathecal FE injection did not induce increased proliferation activity (Ki-67+) of the cells in the meninges and DRG of our experimental rats, thus indicating that most of activated ED1+ macrophages were blood-derived. Furthermore, the ED1+ macrophages loaded by

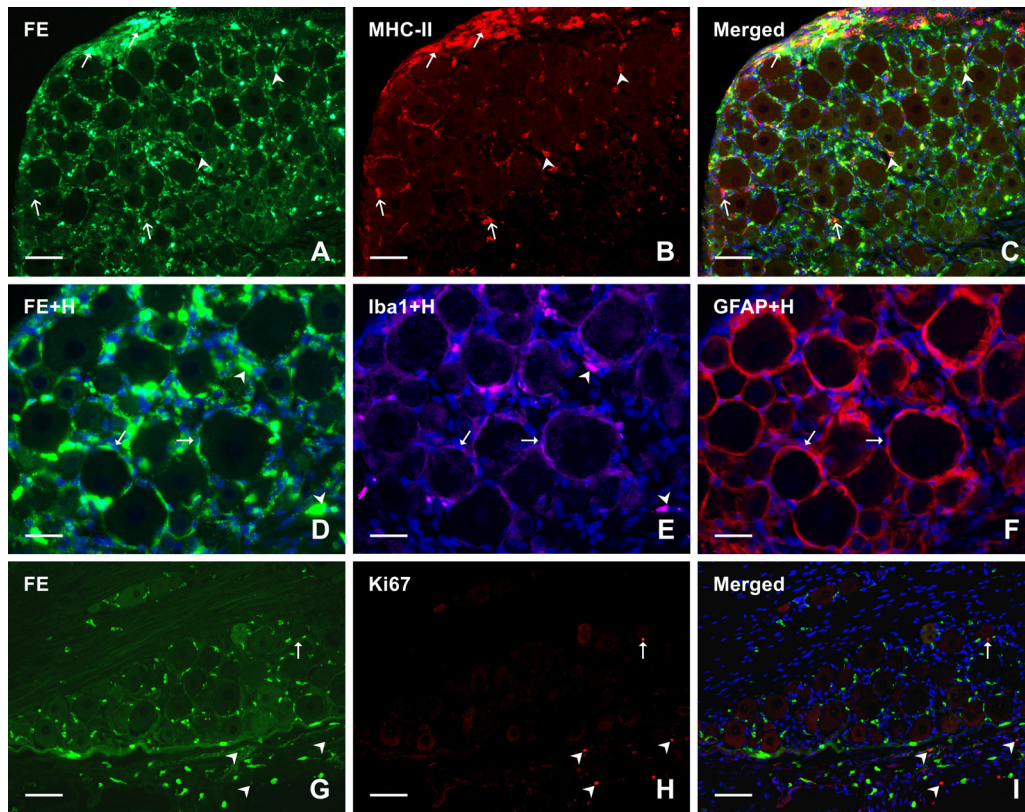


Fig. 4. Representative cryostat sections of lumbar DRG after lumbar FE injection. A–C illustrate presence of MHCII+ cells (APC) in DRG capsule and attached meninges (arrows) as well as in DRG neuronal body-rich area. The majority of APC were simultaneously loaded with FE (arrowhead) and a minority is without FE particles (open arrow). D–F demonstrate presence of FE particles in SGC double immunostained for GFAP and Iba1 (arrows) and in macrophages (arrowheads). G–I illustrate a minimal proliferation activity detected using immunostaining for Ki67 within DRG (arrow) and attached meninges (arrowheads). All Ki67+ cells were found free of FE particles. Cell nuclei were stained using Hoechst (C–F, I). Scale bar = 60 μm (A–C; G–I), 40 μm (D–F).

FE penetrated into the sensory neuron-SGC units to become the “satellite macrophage,” as has been described in an experimental neuropathic pain model (Dubovy et al., 2007).

Particles of FE diffused from the SAS into DRG also labeled SGC, which protect DRG neurons against foreign molecules (Hanani, 2005). FE induced activation of SGC which was confirmed by immunostaining for GFAP. As Iba1 is involved in regulation of membrane ruffling and phagocytosis (Imai and Kohsaka, 2002), positive double immunostaining for GFAP and Iba1 revealed phagocytic activation of SGC by FE particles. It is noteworthy that we found FE-loaded SGC mainly around large neurons the bodies of which were free of FE fluorescence. In contrast, FE particles penetrated and were observed within bodies of small and medium-sized neurons. This can be explained by differing numbers of SGC and their lamellae per neuron, which increase in proportion to neuronal volume (Pannese, 1980; Ledda et al., 2004). Therefore, smaller neurons have poor protection from fewer SGC and their cytoplasmic lamellae which would prevent penetration of FE molecules from interstitial space into DRG neurons.

Chronic constriction of the sciatic nerve has been shown to evoke cellular and molecular changes not only in DRG related to damaged nerve but also in contralateral and cervical DRG (Dubovy et al., 2013; Jancalek et al., 2011, 2010). There are several mechanisms for propagating these changes, which spread to the contralateral and remote structures after unilateral nerve damage. It has been strongly suggested that these changes are propagated via the commissural interneurons present in spinal cord and brainstem (Koltzenburg et al., 1999). However, molecules involved in Wallerian degeneration could alternatively be disseminated via

the blood stream to the remote structures (Dubovy et al., 2007). The present results suggest direct communication between the SAS filled with CSF and DRG alongside the neuraxis to make possible another non-synaptic pathway for exchange and spreading of molecules between primary affected DRG and those in remote spinal segments.

5. Conclusions

The anatomical position of the arachnoid and intrathecal injection of fluorescent-conjugated dextran indicate direct communication between the SAS and DRG and that the molecules of CSF could be directly diffused into DRG. A penetration of dextran molecules into DRG was confirmed also by loaded immune cells and activated SGC around large neurons. In addition, diffusion of dextran into small and medium-sized neurons suggests a possible modulation of their activity by molecules present in CSF or exogenous drugs after their intrathecal administration. Direct communication between the SAS and DRG creates another pathway for possible propagation of inflammatory and signaling molecules from DRG primary affected by peripheral nerve injury into DRG of remote spinal segments.

Acknowledgements

The authors thank D. Kutejova, J. Mikulaškova, L. Trencansky and J. Vachova for their skillful technical assistance. This work was supported by grant MUNI/A/1215/2014.

Appendix A. Supplementary data

Supplementary data associated with this article can be found, in the online version, at <http://dx.doi.org/10.1016/j.aanat.2016.01.004>.

References

- Abram, S.E., Yi, J., Fuchs, A., Hogan, Q.H., 2006. Permeability of injured and intact peripheral nerves and dorsal root ganglia. *Anesthesiology* 105, 146–153.
- Angel Reina, M., Concepcion Villanueva, M., Maches, F., Carrera, A., Lopez, A., Antonio De Andres, J., 2008. The ultrastructure of the human spinal nerve root cuff in the lumbar spine. *Anesth. Analg.* 106, 339–344, <http://dx.doi.org/10.1213/01.ane.0000295803.31074.de>.
- Czernicki, M., Sinovich, G., Mihaylov, I., Nejad, B., Kunnumpurath, S., Kodumudi, G., Vadivelu, N., 2014. Intrathecal Drug Delivery for Chronic Pain Management—Scope, Limitations and Future.
- Dai, T., Zhou, S., Yin, C., Li, S., Cao, W., Liu, W., Sun, K., Dou, H., Cao, Y., Zhou, G., 2014. Dextran-based fluorescent nanoprobe for sentinel lymph node mapping. *Biomaterials* 35, 8227–8235, <http://dx.doi.org/10.1016/j.biomaterials.2014.06.012>.
- Dijkstra, C.D., Damoiseaux, J.G., 1993. Macrophage heterogeneity established by immunocytochemistry. *Prog. Histochem. Cytochem.* 27, 1–65.
- Dijkstra, C.D., Döpp, E.A., Joling, P., Kraal, G., 1985. The heterogeneity of mononuclear phagocytes in lymphoid organs: distinct macrophage subpopulations in rat recognized by monoclonal antibodies ED1, ED2 and ED3. In: Klaus, G.G.B. (Ed.), *Microenvironments in the Lymphoid System*. Springer US, pp. 409–419.
- Dubový, P., Brázda, V., Klusáková, I., Hradilová-Svíženská, I., 2013. Bilateral elevation of interleukin-6 protein and mRNA in both lumbar and cervical dorsal root ganglia following unilateral chronic compression injury of the sciatic nerve. *J. Neuroinflamm.* 10, 55, <http://dx.doi.org/10.1186/1742-2094-10-55>.
- Dubový, P., Klusáková, I., Svíženská, I., Brázda, V., 2010. Spatio-temporal changes of SDF1 and its CXCR4 receptor in the dorsal root ganglia following unilateral sciatic nerve injury as a model of neuropathic pain. *Histochem. Cell Biol.* 133, 323–337, <http://dx.doi.org/10.1007/s00418-010-0675-0>.
- Dubový, P., Svíženská, I., Klusáková, I., 2002. Computer-assisted quantitative analysis of immunofluorescence staining of the extracellular matrix in rat dorsal and ventral spinal roots. *Acta Histochem.* 104, 371–374, <http://dx.doi.org/10.1078/0065-1281-00664>.
- Dubový, P., Tučková, L., Jančálek, R., Svíženská, I., Klusáková, I., 2007. Increased invasion of ED-1 positive macrophages in both ipsi- and contralateral dorsal root ganglia following unilateral nerve injuries. *Neurosci. Lett.* 427, 88–93, <http://dx.doi.org/10.1016/j.neulet.2007.09.012>.
- Hamber, E.A., Viscomi, C.M., 1999. Intrathecal lipophilic opioids as adjuncts to surgical spinal anesthesia. *Reg. Anesth. Pain Med.* 24, 255.
- Hanani, M., 2005. Satellite glial cells in sensory ganglia: from form to function. *Brain Res. Rev.* 48, 457–476, <http://dx.doi.org/10.1016/j.brainresrev.2004.09.001>.
- Haninec, P., Grim, M., 1990. Localization of dipeptidylpeptidase IV and alkaline phosphatase in developing spinal cord meninges and peripheral nerve coverings of the rat. *Int. J. Dev. Neurosci.* 8, 175–185, [http://dx.doi.org/10.1016/0736-5748\(90\)90008-P](http://dx.doi.org/10.1016/0736-5748(90)90008-P).
- Hawksworth, C., Serpell, M., 1998. Intrathecal anesthesia with ketamine. *Reg. Anesth. Pain Med.* 23, 283–288, [http://dx.doi.org/10.1016/S1098-7339\(98\)90056-6](http://dx.doi.org/10.1016/S1098-7339(98)90056-6).
- Hu, P., McLachlan, E.M., 2003. Distinct functional types of macrophage in dorsal root ganglia and spinal nerves proximal to sciatic and spinal nerve transections in the rat. *Exp. Neurol.* 184, 590–605, [http://dx.doi.org/10.1016/S0014-4886\(03\)00307-8](http://dx.doi.org/10.1016/S0014-4886(03)00307-8).
- Hu, P., McLachlan, E.M., 2002. Macrophage and lymphocyte invasion of dorsal root ganglia after peripheral nerve lesions in the rat. *Neuroscience* 112, 23–38, [http://dx.doi.org/10.1016/S0306-4522\(02\)00065-9](http://dx.doi.org/10.1016/S0306-4522(02)00065-9).
- Hu, X., Zhu, J., Li, X., Zhang, X., Meng, Q., Yuan, L., Zhang, J., Fu, X., Duan, X., Chen, H., Ao, Y., 2015. Dextran-coated fluorapatite crystals doped with Yb³⁺/Ho³⁺ for labeling and tracking chondrogenic differentiation of bone marrow mesenchymal stem cells in vitro and in vivo. *Biomaterials* 52, 441–451, <http://dx.doi.org/10.1016/j.biomaterials.2015.02.050>.
- Hylken, J.L., Wilcox, G.L., 1980. Intrathecal morphine in mice: a new technique. *Eur. J. Pharmacol.* 67, 313–316.
- Imai, Y., Kohsaka, S., 2002. Intracellular signaling in M-CSF-induced microglia activation: role of Iba1. *Glia* 40, 164–174, <http://dx.doi.org/10.1002/glia.10149>.
- Jancalek, R., Dubový, P., Svizenska, I., Klusakova, I., 2010. Bilateral changes of TNF-alpha and IL-10 protein in the lumbar and cervical dorsal root ganglia following a unilateral chronic constriction injury of the sciatic nerve. *J. Neuroinflamm.* 7, 11, <http://dx.doi.org/10.1186/1742-2094-7-11>.
- Jancalek, R., Svizenska, I., Klusakova, I., Dubovy, P., 2011. Bilateral changes of IL-10 protein in lumbar and cervical dorsal root ganglia following proximal and distal chronic constriction injury of peripheral nerve. *Neurosci. Lett.* 501, 86–91, <http://dx.doi.org/10.1016/j.neulet.2011.06.052>.
- Koltzenburg, M., Wall, P.D., McMahon, S.B., 1999. Does the right side know what the left is doing? *Trends Neurosci.* 22, 122–127, [http://dx.doi.org/10.1016/S0166-2236\(98\)01302-2](http://dx.doi.org/10.1016/S0166-2236(98)01302-2).
- Komai, H., McDowell, T.S., 2001. Local anesthetic inhibition of voltage-activated potassium currents in rat dorsal root ganglion neurons. *Anesthesiology* 94, 1089–1095.
- Kubek, T., Kyr, M., Haninec, P., Šámal, F., Dubový, P., 2004. Morphological evidence of collateral sprouting of intact afferent and motor axons of the rat ulnar nerve demonstrated by one type of tracer molecule. *Ann. Anat. Anat. Anz.* 186, 231–234, [http://dx.doi.org/10.1016/S0940-9602\(04\)80008-6](http://dx.doi.org/10.1016/S0940-9602(04)80008-6).
- Kusmirek, J., Owens, C.A., Mason, P., 1997. Lumbar but not cervical intrathecal DAMGO suppresses extrasegmental nociception in awake rats. *Brain Res.* 767, 375–379, [http://dx.doi.org/10.1016/S0006-8993\(97\)00786-5](http://dx.doi.org/10.1016/S0006-8993(97)00786-5).
- Lamke, L.-O., Liljedahl, S.-O., 1976. Plasma volume changes after infusion of various plasma expanders. *Resuscitation* 5, 93–101, [http://dx.doi.org/10.1016/0300-9572\(76\)90029-0](http://dx.doi.org/10.1016/0300-9572(76)90029-0).
- Ledda, M., De Palo, S., Pannese, E., 2004. Ratios between number of neuroglial cells and number and volume of nerve cells in the spinal ganglia of two species of reptiles and three species of mammals. *Tissue Cell* 36, 55–62, <http://dx.doi.org/10.1016/j.tice.2003.09.001>.
- McCabe, J.S., Low, F.N., 1969. The subarachnoid angle: an area of transition in peripheral nerve. *Anat. Rec.* 164, 15–33, <http://dx.doi.org/10.1002/ar.1091640102>.
- Nasomphan, W., Tangboriboonrat, P., Tanapongpipat, S., Smanmoo, S., 2013. Selective fluorescent detection of aspartic acid and glutamic acid employing dansyl hydrazine dextran conjugate. *J. Fluoresc.* 24, 7–11, <http://dx.doi.org/10.1007/s10895-013-1269-8>.
- Ohtani, T., Taguchi, T., Oda, H., Shinoda, K., Itoh, Y., Toh, S., Kawai, S., Takahashi, M., 1990. The fine structure of the subarachnoid angle in the spinal nerve roots. *Orthop. Traumatol.* 39, 586–589, <http://dx.doi.org/10.5035/nishiseisai.39.586>.
- Pannese, E., 1980. The satellite cells of the sensory ganglia. *Adv. Anat. Embryol. Cell Biol.* 65, 1–111.
- Safranov, B.V., Bischoff, U., Vogel, W., 1996. Single voltage-gated K⁺ channels and their functions in small dorsal root ganglion neurones of rat. *J. Physiol.* 493, 393–408.
- Scholz, A., Kuboyama, N., Hempelmann, G., Vogel, W., 1998. Complex blockade of TTX-resistant Na⁺ currents by lidocaine and bupivacaine reduce firing frequency in DRG neurons. *J. Neurophysiol.* 79, 1746–1754.
- Shanthaveerappa, T.R., Bourne, G.H., 1962. The 'perineural epithelium', a metabolically active, continuous, protoplasmic cell barrier surrounding peripheral nerve fasciculi. *J. Anat.* 96, 527–537.
- Vania Apkarian, A., Lavarello, S., Randolph, A., Berra, H.H., Chialvo, D.R., Besedovsky, H.O., del Rey, A., 2006. Expression of IL-1β in supraspinal brain regions in rats with neuropathic pain. *Neurosci. Lett.* 407, 176–181, <http://dx.doi.org/10.1016/j.neulet.2006.08.034>.
- Wieseler-Frank, J., Jekich, B.M., Mahoney, J.H., Bland, S.T., Maier, S.F., Watkins, L.R., 2007. A novel immune-to-CNS communication pathway: cells of the meninges surrounding the spinal cord CSF space produce proinflammatory cytokines in response to an inflammatory stimulus. *Brain. Behav. Immun.* 21, 711–718, <http://dx.doi.org/10.1016/j.bbi.2006.07.004>.
- Zamboni, L., de Martino, C., 1967. Buffered picric acid-formaldehyde: a new, rapid fixative for electron microscopy. *J. Cell Biol.* 35.
- Žele, T., Sketelj, J., Bajrović, F.F., 2010. Efficacy of fluorescent tracers in retrograde labeling of cutaneous afferent neurons in the rat. *J. Neurosci. Methods* 191, 208–214, <http://dx.doi.org/10.1016/j.jneumeth.2010.06.021>.
- Zin, C.S., Nissen, L.M., O'Callaghan, J.P., Moore, B.J., Smith, M.T., 2010. Preliminary study of the plasma and cerebrospinal fluid concentrations of IL-6 and IL-10 in patients with chronic pain receiving intrathecal opioid infusions by chronically implanted pump for pain management. *Pain Med.* 11, 550–561, <http://dx.doi.org/10.1111/j.1526-4637.2010.00821.x>.
- Zinderman, C.E., Landow, L., Wise, R.P., 2006. Clinical research study: anaphylactoid reactions to dextran 40 and 70: reports to the United States Food and Drug Administration, 1969 to 2004. *J. Vasc. Surg.* 43, 1004–1009, <http://dx.doi.org/10.1016/j.jvs.2006.01.006>.

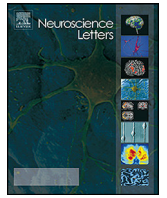
G. **Joukal M**, Klusáková I, Solár P, Kuklová A, Dubový P. Cellular reactions of the choroid plexus induced by peripheral nerve injury. *Neurosci Lett.* 2016;628:73-77. doi:10.1016/j.neulet.2016.06.019

Commentary: In this article, we demonstrated increased number of activated and resident macrophages in epiplexus position in rat choroid plexus after peripheral nerve injury. We found no proliferation in the choroid plexus after nerve injury suggesting that macrophages were recruited from circulated monocytes passing through altered blood-cerebrospinal fluid barrier.

IF (WOS, 2016): 2.180

Quartile (WOS, 2016): Neurosciences Q3

Contribution of the author: First Author. The author designed and performed the experiments, analyzed the data and wrote manuscript.



Research article

Cellular reactions of the choroid plexus induced by peripheral nerve injury



Marek Joukal, Ilona Klusáková, Peter Solár, Adéla Kuklová, Petr Dubový*

Department of Anatomy, Division of Neuroanatomy, Faculty of Medicine, Masaryk University, CZ-625 00 Brno, Czech Republic

HIGHLIGHTS

- Numbers of ED1+ and ED2+ epiplexus macrophages increased with duration of CCI.
- Sham-operated CP also displayed an increase in the number of epiplexus macrophages.
- No significant CP cell proliferation was found after either sham or CCI operation.
- Inflammatory reaction of CP was observed after both nerve injury as well as surgery.

ARTICLE INFO

Article history:

Received 11 April 2016
Received in revised form 7 June 2016
Accepted 8 June 2016
Available online 9 June 2016

Keywords:

Blood–cerebrospinal fluid barrier
Kolmer cells
Macrophages
Chronic constriction injury

ABSTRACT

The choroid plexus (CP) of brain ventricles forms the blood–cerebrospinal fluid (blood–CSF) barrier that is involved in many diseases affecting the central nervous system (CNS). We used ED1 and ED2 immunostaining to investigate epiplexus cell changes in rat CP after chronic constriction injury (CCI). In contrast to naïve CP, the CP of sham-operated rats showed an increase in the number of ED1+ cells of a similar magnitude during all periods of survival up to 3 weeks, while the number of ED2+ increased only at 3 days from operation. In comparison to naïve and sham-operated animals, the number of ED1+ and ED2+ cells in the epiplexus position increased with the duration of nerve compression. We detected no or negligible cell proliferation in the CP after sham- or CCI-operation. This suggests that increased number of ED1+ and ED2+ cells in the epiplexus position of the CP is derived from peripheral monocytes passing through altered blood–CSF barrier. The changes in epiplexus cells indicate that the CP reacts to tissue injury after the surgical approach itself and that the response to peripheral nerve lesion is greater. This suggests a role for an altered blood–CSF barrier allowing for propagation of signal molecules from damaged tissue and nerve to the CNS.

© 2016 Elsevier Ireland Ltd. All rights reserved.

1. Introduction

The choroid plexus (CP) in the brain ventricles consists of vascularized stroma and epithelial cells that constitute the blood–cerebrospinal fluid (blood–CSF) barrier. The vascularized stroma contains loose connective tissue, fenestrated capillaries, and macrophages. The ventricular side of the stroma is covered by epithelial cells that are responsible for secretion of cerebrospinal fluid (CSF). Choroidal epithelial cells are connected by tight junctions that are the main component of the blood–CSF barrier. The epiplexus or Kolmer cells adhere on the ventricular side of the CP epithelial cells and are regarded as part of the CP. These epiplexus cells display diverse morphologies ranging from round to polar

and stellate. They also have the typical cytological features of activated macrophages including vacuoles and lysosomes [1–3]. There is a growing body of evidence for a key CP role in many disorders including inflammatory, neurodegenerative, infectious, traumatic, neoplastic, as well as systemic diseases [1,2]. It has been found that peripheral inflammation caused by lipopolysaccharide induces molecular and cellular changes in the CP [4]. Wallerian degeneration of damaged nerve is considered to be aseptic inflammation [5] and produces damage associated molecular patterns (DAMPs) [6]. Moreover, Apkarian et al. [7] found an increased level of IL-1 beta in supraspinal structures after peripheral nerve injury. We hypothesize that Wallerian degeneration molecules, such as DAMPs, can affect the CP via the bloodstream. The aim of our study was to investigate whether a peripheral nerve injury can alter the epiplexus cell composition of the CP. Changes in the number of epiplexus cells may indicate a disruption of blood–CSF barrier and its role in the propagation of molecules from damaged peripheral nerve to CNS.

* Corresponding author.

E-mail address: pdubovy@med.muni.cz (P. Dubový).

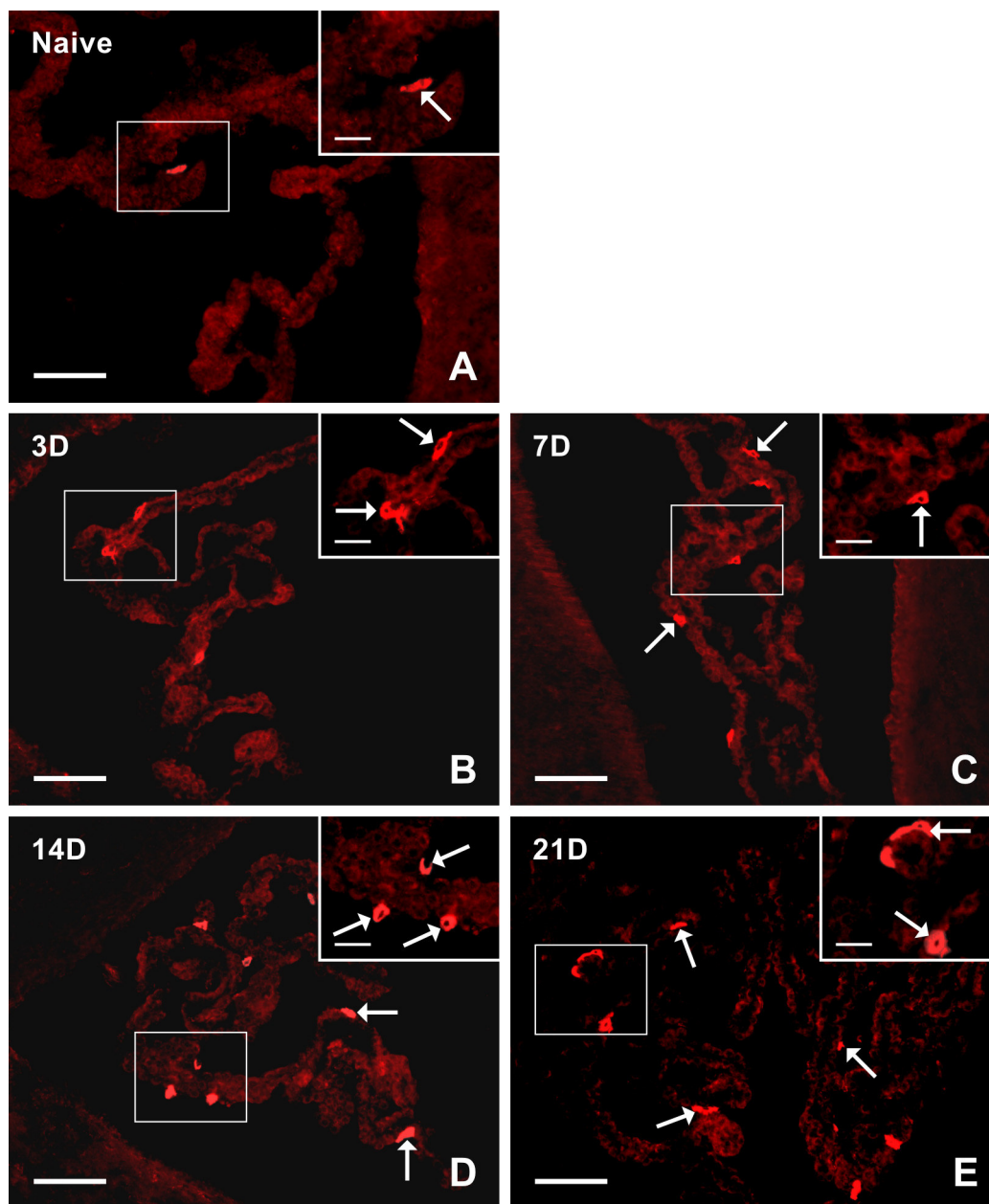


Fig. 1. Representative images showing immunostaining with ED1 antibody in the CP from naïve rats and operated rats at 3, 7, 14 and 21 days (3D, 7D, 14D and 21D) after CCI. Arrows indicate ED1+ epilexus cells. The insets on the upper right show, at higher magnification, the regions indicated by the box in the main part of the image. Scale bars = 80 μm (main image); 20 μm (insets).

2. Material and methods

2.1. Animals and surgical procedures

The experiments were performed on 52 adult male rats (Wistar, 200–250 g; Animal Breeding Facility, Masaryk University, Czech Republic). All experimental procedures were carried out aseptically and according to protocols approved by the Ethical Committee of

Table 1
Primary antibodies used, their dilutions, time of incubation, and suppliers.

Name	Type of antibody	Dilution	Incubation time	Supplier
ED1	Mouse monoclonal	1:200	240 min	Serotec
ED2	Mouse monoclonal	1:200	16 h	Serotec
Ki-67	Rabbit polyclonal	1:500	240 min	Vector Laboratories

Masaryk University, Brno and the Departmental Committee of the Ministry of Education, Youth and Sports, Czech Republic.

Rats were anesthetized with a mixture of 5% ketamine (100 mg/kg) and 2% xylazine (10 mg/kg) administered intraperitoneally. The chronic constriction injury (CCI) of the left sciatic nerve was created using three ligatures (3-0; Ethicon, Somerville, NJ) that reduced the nerve diameter by approximately one-third. The retracted muscles and skin incision were closed with 3-0 silk sutures and the animals were exposed to CCI for 3 (n=8), 7 (n=8), 14 (n=8), and 21 (n=8) days. The left sciatic nerve was merely exposed but left without any lesion in sham-operated rats surviving for 3 (n=4), 7 (n=4), 14 (n=4), and 21 (n=4) days.

The CCI- and sham-operated rats as well as naïve rats (n=4) were sacrificed using CO₂, then perfused transcardially with 500 ml heparinized (1000 units/500 ml) phosphate-buffered saline (pH 7.4) followed by 500 ml of Zamboni's fixative [8]. Brains were

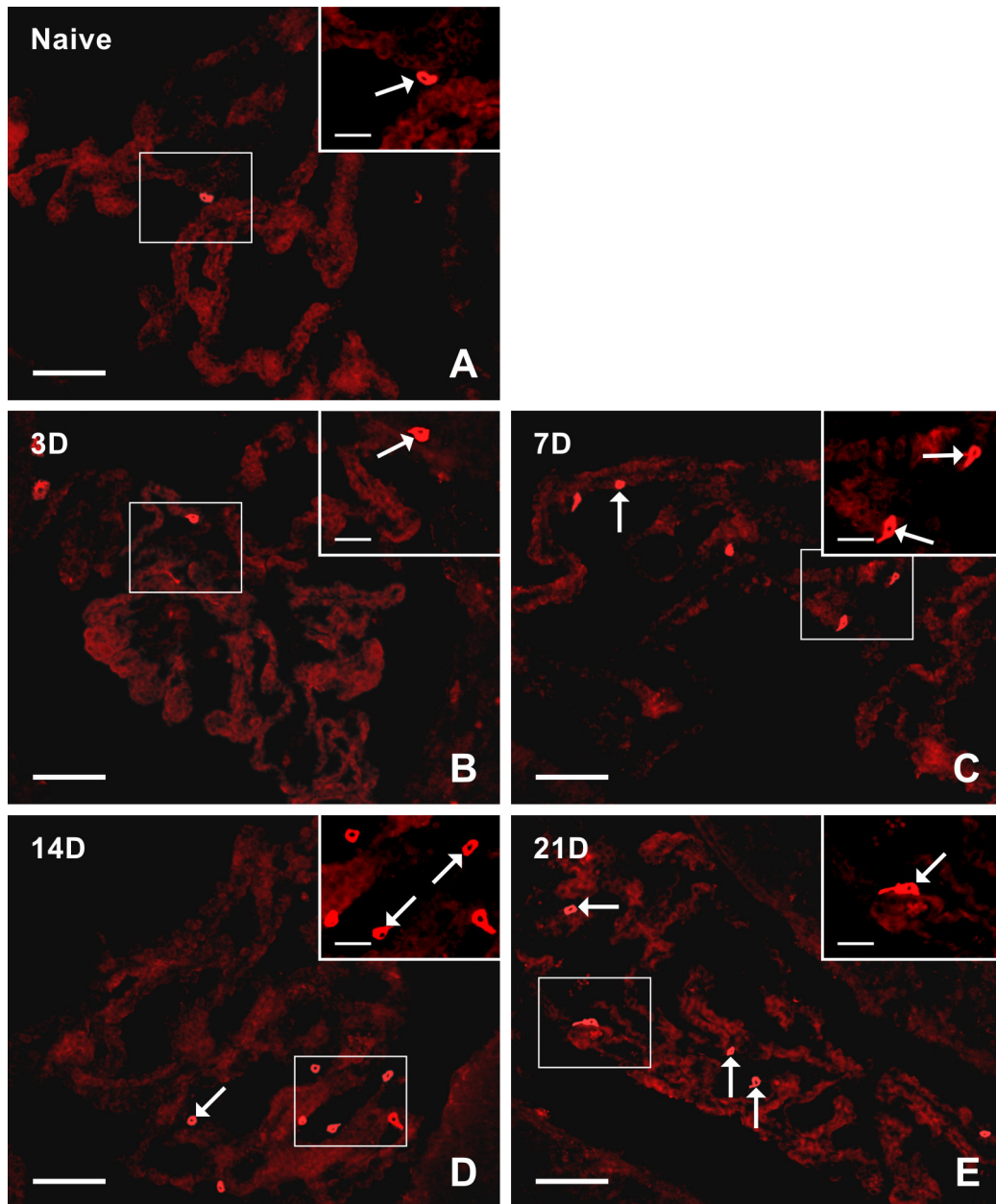


Fig. 2. Representative sections showing immunostaining with ED2 antibody in the CP from naïve rats and operated rats at 3, 7, 14 and 21 days (3D, 7D, 14D and 21D) after CCI. Arrows indicate ED2+ epiplexus cells. The insets on the upper right show, at higher magnification, the regions indicated by the box in the main part of the image. Scale bars = 80 μm (main image); 20 μm (insets).

removed and immersed in Zamboni's fixative for 3 days, then washed in 10% sucrose and embedded in Tissue-Tek OCT compound (Miles; Elkhart, IN). Coronal cryostat sections (20 μm) were cut (Leica 1800 cryostat; Leica Microsystems, Wetzlar, Germany) and mounted onto chrome-alum covered microscopic slides.

2.2. Immunohistochemical staining

The brain sections of naïve, sham- and CCI-operated animals were immunostained under identical conditions with ED1 (anti-CD68) and ED2 (anti-CD163) antibodies to detect macrophages with activated phagocytosis and resident tissue macrophages, respectively [9]. The proliferation of CP cells was assessed using Ki-67 immunostaining [10]. Sections were washed with phosphate-buffered saline containing 0.3% bovine serum albumin and 0.1% Tween-20, treated with 3% normal goat serum for 30 min, and

then incubated with the primary antibody at room temperature (Table 1). Affinity purified TRITC-conjugated goat anti-mouse or goat anti-rabbit secondary antibodies were applied at a final dilution of 1:100 at room temperature for 90 min. Control sections were incubated in parallel by omitting the primary antibodies. Immunostained sections were rinsed, stained with Hoechst 33342 (Sigma; St. Louis, MO) to detect positions of cell nuclei, and mounted in a Vectashield aqueous mounting medium (Vector Laboratories; Burlingame, CA). Immunofluorescence was observed and analyzed using a Nikon Eclipse NI-E epifluorescence microscope equipped with a Nikon DS-Ri1 camera (Nikon, Prague, Czech Republic).

2.3. Image analysis

At least 10 sections cut at 60 μm intervals through the brain ventricles containing the CP were analyzed in each group. The CP

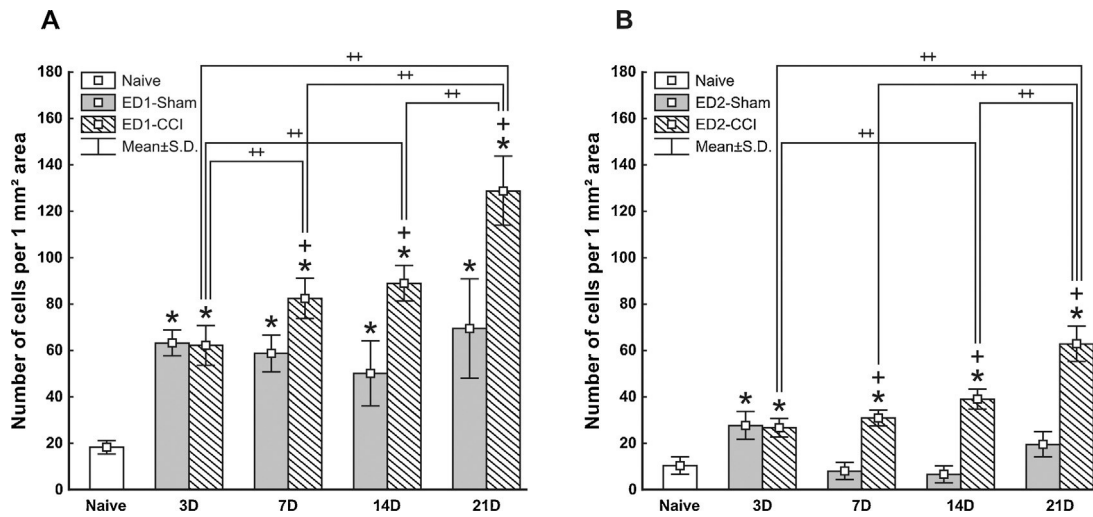


Fig. 3. Number of ED1+ (A) and ED2+ (B) macrophages per mm² of the CP area from naïve rats, sham- and CCI-operated rats at 3, 7, 14 and 21 days after operation. *Indicates significant difference ($p < 0.05$) when compared with the CP from naïve rats. +Indicates significant difference ($p < 0.05$) when compared with the CP from sham-operated rats. ++Indicates significant difference ($p < 0.05$) when comparing individual times of survival after CCI.

area was determined, manually edited when needed, and measured using the NIS-Elements AR Analysis (version 4.20.00, Nikon, Prague, Czech Republic). Numbers of ED1+ and ED2+ cells were manually counted in the defined area of the CP. The number of positive cells calculated for 1 mm² of CP area was presented as mean plus or minus standard deviation. Two independent investigators, who were blind to the group of animals, counted the number of immunofluorescence positive epilexus cells and no differences were observed between the two sets of values. The data were compared for CP sections from naïve, sham- and CCI-operated rats. To verify differences between groups, a Mann–Whitney *U*-test was performed using STATISTICA 5.5 software (StatSoft, Tulsa, OK, USA) with a significance level of $p < 0.05$ for differences between the tested samples.

3. Results

Immunostaining for ED1 and ED2 showed activated and resident macrophages, respectively in the epilexus position in all groups of animals. The numbers of ED1+ macrophages in the CP of sham-operated animals surviving for all investigated survival periods were significantly increased compared to the CP of naïve rats. In comparison with the CP of sham-operated rats, significantly increased numbers of ED1+ macrophages were found 7, 14 and 21 days after the CCI operation. At 3 days after sham and CCI surgery, the CP displayed similar numbers of ED1+ macrophages. The numbers of ED1+ cells were higher than naïve rats in the CP of CCI-operated and increased with time of survival (Figs. 1 and 3 A). No changes in ED1+ and ED2+ macrophages were observed in the CP stroma as well as in the meninges and blood vessels close to the CP in animals of all groups.

Epilexus cells immunostained for ED2 were significantly more numerous in the CP 3 days after sham operation when compared with the CP of naïve animals. In contrast to ED1+ cells however, the number of ED2+ cells dropped back to values close to naïve CP over time (7, 14 and 21 days of survival). After CCI, the numbers of both ED1+ and ED2+ macrophages gradually increased with time of survival (Figs. 2 and 3 B).

Immunostaining for Ki-67 showed no or very low proliferation of CP cells in all animal groups and periods of survival (results not shown).

4. Discussion

The presented results reveal that mere surgery including skin incision and retraction of muscles of sham-operated as well as peripheral nerve injury of CCI-operated rats affected the number of macrophages in the epilexus position (Kolmer cells) of the CP with higher numbers of ED1+ than ED2+ cells. This indicates that the surgical approach itself (even under aseptic conditions) may elicit recruitment of ED1+ and ED2+ cells into the epilexus position, but a larger increase was induced by nerve injury starting from 7 days. The cellular and molecular changes in nervous structures induced by a surgical approach itself have been described by other authors also [11,12].

A peripheral inflammatory stimulus by lipopolysaccharide induced the synthesis of pro-inflammatory cytokines in the CP, thus indicating that the structure must be considered a relevant mediator of immune signals between the periphery and the brain [13]. Moreover, an increased number of macrophages in the epilexus position of the CP was also found in the same model for peripheral inflammation [4].

Animal experiments revealed that nerve injury can induce inflammatory reactions in dorsal root ganglia unrelated to the injured nerve as well as in remote structures of the brainstem, thalamus, and prefrontal cortex [7,14–16]. The results presented here demonstrate that a nerve injury causes increased numbers of ED1+ and ED2+ epilexus cells and that this cell augmentation is not the result of their local proliferation. The question then arises as to what are the signaling pathways leading to these inflammatory cellular and molecular changes. Wallerian degeneration distal to a nerve injury is a source of DAMPs and inflammatory mediators. It is believed that the inflammatory reaction of remote structures not related to the primary injury can be induced by DAMPs released from damaged tissue and distributed via the bloodstream [15,17].

Increased number of immunoreactive CP cells could be due to *de novo* or enhanced synthesis of molecules recognized by ED1 and ED2 antibodies. However, it is more likely that these enhanced numbers of epilexus cells are the result of proliferation of local epilexus cells and/or infiltration of cells considered to be their precursors—circulatory monocytes [4]. Inasmuch as Ki-67 immunostaining in the CP of our experimental animals was not increased, we presume the enhanced numbers of epilexus macrophages both after surgery itself and after nerve injury are

derived from recruited monocytes. Migration of nerve injury-activated macrophages from the dorsal root ganglia via CSF [18–20] or through an altered blood-brain barrier [21] might be another source of the increased number of epilexus macrophages.

Alteration of tight junctions in the CP has been detected in various models of neuroinflammation [22]. There is speculation that cells from the bloodstream can reach the epilexus position via altered tight junctions and/or through the cytoplasm of epithelial cells by “emperipolesis,” as has been described in monkey [23]. We suggest that a peripheral nerve injury could alter tight junctions of CP epithelial cells, thereby resulting in penetration of circulating monocytes into the epilexus position. The monocyte recruitment may be stimulated by chemokines released by epithelial cells [24] as well as T-lymphocytes of the CP [25]. However, further experiments are needed to elucidate the precise mechanisms of the increase in epilexus macrophage numbers induced by surgical treatment or nerve injury.

5. Conclusion

To summarize, we demonstrated significant quantitative changes in ED1+ and ED2+ epilexus cells in the rat CP following chronic constriction injury of the sciatic nerve. A limited increase of the epilexus cells was found also after surgical treatment of sham-operated rats. The absence of accompanying changes in Ki-67 immunostained cells showed that enhanced epilexus cell number is not derived from local cell proliferation but points to a recruitment of cells derived from blood monocytes. We suggest that DAMPs released by damaged cells after surgery (sham-operation) and during Wallerian degeneration of injured nerve, are responsible for the alteration of the blood–CSF barrier leading to increased numbers of epilexus cells.

Acknowledgements

The authors thank M. Lněničková, J. Mikulášková, D. Kutějová, L. Trenčáský, and J. Vachová for their skillful technical assistance. This work was supported by grant MUNI/A/1268/2015 (Faculty of Medicine, Masaryk University).

References

- [1] H. Wolburg, W. Paulus, Choroid plexus: biology and pathology, *Acta Neuropathol.* 119 (2009) 75–88, <http://dx.doi.org/10.1007/s00401-009-0627-8>.
- [2] N. Strazielle, J.-F. Ghersi-Egea, Choroid plexus in the central nervous system: biology and physiopathology, *J. Neuropathol.* 59 (2000) 561–574.
- [3] S.A. Liddelow, Development of the choroid plexus and blood–CSF barrier, *Front. Neurosci.* 9 (2015) 32, <http://dx.doi.org/10.3389/fnins.2015.00032>.
- [4] J. Lu, C. Kaur, E.-A. Ling, Up-regulation of surface antigens on epilexus cells in postnatal rats following intraperitoneal injections of lipopolysaccharide, *Neuroscience* 63 (1994) 1169–1178, [http://dx.doi.org/10.1016/0306-4522\(94\)90581-9](http://dx.doi.org/10.1016/0306-4522(94)90581-9).
- [5] P. Dubový, R. Jančálek, T. Kubek, Role of inflammation and cytokines in peripheral nerve regeneration, *Int. Rev. Neurobiol.* 108 (2013) 173–206, <http://dx.doi.org/10.1016/B978-0-12-410499-0.00007-1>.
- [6] S.Y. Fu, T. Gordon, The cellular and molecular basis of peripheral nerve regeneration, *Mol. Neurobiol.* 14 (1997) 67–116, <http://dx.doi.org/10.1007/BF02740621>.
- [7] A.V. Apkarian, S. Lavarello, A. Randolph, H.H. Berra, D.R. Chialvo, H.O. Besedovsky, A. del Rey, Expression of IL-1beta in supraspinal brain regions in rats with neuropathic pain, *Neurosci. Lett.* 407 (2006) 176–181, <http://dx.doi.org/10.1016/j.neulet.2006.08.034>.
- [8] L. Zamboni, C. de Martino, Buffered picric acid-formaldehyde: a new, rapid fixative for electron microscopy, *J. Cell Biol.* 35 (1967).
- [9] C.D. Dijkstra, J.G. Damoiseaux, Macrophage heterogeneity established by immunocytochemistry, *Prog. Histochem. Cytochem.* 27 (1993) 1–65.
- [10] J. Gerdes, H. Lemke, H. Baisch, H.H. Wacker, U. Schwab, H. Stein, Cell cycle analysis of a cell proliferation-associated human nuclear antigen defined by the monoclonal antibody Ki-67, *J. Immunol.* 133 (1984) 1710–1715.
- [11] G. Wolf, D. Livshits, B. Beilin, R. Yirmiya, Y. Shavit, Interleukin-1 signaling is required for induction and maintenance of postoperative incisional pain: genetic and pharmacological studies in mice, *Brain Behav. Immun.* 22 (2008) 1072–1077, <http://dx.doi.org/10.1016/j.bbi.2008.03.005>.
- [12] C.E. Hill, B.J. Harrison, K.K. Rau, M.T. Houglund, M.B. Bunge, L.M. Mendell, J.C. Petruska, Skin incision induces expression of axonal regeneration-related genes in adult rat spinal sensory neurons, *J. Pain* 11 (2010) 1066–1073, <http://dx.doi.org/10.1016/j.jpain.2010.02.001>.
- [13] F. Marques, J.C. Sousa, G. Coppola, A.M. Falcao, A.J. Rodrigues, D.H. Geschwind, N. Sousa, M. Correia-Neves, J.A. Palha, Kinetic profile of the transcriptome changes induced in the choroid plexus by peripheral inflammation, *J. Cereb. Blood Flow Metab.* 29 (2009) 921–932, <http://dx.doi.org/10.1038/jcbfm.2009.15>.
- [14] R. Jancalek, P. Dubový, I. Svizenska, I. Klusakova, Bilateral changes of TNF-alpha and IL-10 protein in the lumbar and cervical dorsal root ganglia following a unilateral chronic constriction injury of the sciatic nerve, *J. Neuroinflamm.* 7 (2010) 11, <http://dx.doi.org/10.1186/1742-2094-7-11>.
- [15] P. Dubový, V. Brázda, I. Klusáková, I. Hradilová-Svíženská, Bilateral elevation of interleukin-6 protein and mRNA in both lumbar and cervical dorsal root ganglia following unilateral chronic compression injury of the sciatic nerve, *J. Neuroinflamm.* 10 (2013) 55, <http://dx.doi.org/10.1186/1742-2094-10-55>.
- [16] C.Y. Saab, B.C. Hains, Remote neuroimmune signaling: a long-range mechanism of nociceptive network plasticity, *Trends Neurosci.* 32 (2009) 110–117, <http://dx.doi.org/10.1016/j.tins.2008.11.004>.
- [17] Q. Zhang, M. Raouf, Y. Chen, Y. Sumi, T. Sursal, W. Junger, K. Brohi, K. Itagaki, C.J. Hauser, Circulating mitochondrial DAMPs cause inflammatory responses to injury, *Nature* 464 (2010) 104–107, <http://dx.doi.org/10.1038/nature08780>.
- [18] P. Hu, E.M. McLachlan, Distinct functional types of macrophage in dorsal root ganglia and spinal nerves proximal to sciatic and spinal nerve transections in the rat, *Exp. Neurol.* 184 (2003) 590–605, [http://dx.doi.org/10.1016/S0014-4886\(03\)00307-8](http://dx.doi.org/10.1016/S0014-4886(03)00307-8).
- [19] P. Hu, A.L. Bembrick, K.A. Keay, E.M. McLachlan, Immune cell involvement in dorsal root ganglia and spinal cord after chronic constriction or transection of the rat sciatic nerve, *Brain Behav. Immun.* 21 (2007) 599–616, <http://dx.doi.org/10.1016/j.bbi.2006.10.013>.
- [20] M. Joukal, I. Klusáková, P. Dubový, Direct communication of the spinal subarachnoid space with the rat dorsal root ganglia, *Ann. Anat. Anz.* 205 (2016) 9–15, <http://dx.doi.org/10.1016/j.aanat.2016.01.004>.
- [21] S. Beggs, X.J. Liu, C. Kwan, M.W. Salter, Peripheral nerve injury and TRPV1-expressing primary afferent C-fibers cause opening of the blood-brain barrier, *Mol. Pain* 6 (2010) 74, <http://dx.doi.org/10.1186/1744-8069-6-74>.
- [22] B. Shrestha, D. Paul, J.S. Pachter, Alterations in tight junction protein and IgG permeability accompany leukocyte extravasation across the choroid plexus during neuroinflammation, *J. Neuropathol. Exp. Neurol.* 73 (2014) 1047–1061, <http://dx.doi.org/10.1097/NEN.0000000000000127>.
- [23] E.A. Ling, Ultrastructure and mode of formation of epilexus cells in the choroid plexus in the lateral ventricles of the monkey (*Macaca fascicularis*), *J. Anat.* 133 (1981) 555–569.
- [24] J. Szymdynger-Chodobska, N. Strazielle, B.J. Zink, J.-F. Ghersi-Egea, A. Chodobski, The role of the choroid plexus in neutrophil invasion after traumatic brain injury, *J. Cereb. Blood Flow Metab.* 29 (2009) 1503–1516, <http://dx.doi.org/10.1038/jcbfm.2009.71>.
- [25] N. Strazielle, R. Creidy, C. Malcus, J. Boucraut, J.-F. Ghersi-Egea, T-Lymphocytes traffic into the brain across the blood–CSF barrier: evidence using a reconstituted choroid plexus epithelium, *PLoS One* 11 (2016) 1–17, <http://dx.doi.org/10.1371/journal.pone.0150945>.

13. Full list of author's publications in impacted journals

1. Dubový P, Hradilová-Svíženská I, Klusáková I, Brázda V, Joukal M*. Interleukin-6 contributes to initiation of neuronal regeneration program in the remote dorsal root ganglia neurons after sciatic nerve injury. *Histochem Cell Biol.* 2019. doi:10.1007/s00418-019-01779-3. (in press)
2. Dokoupil M, Marecová K, Uvíra M, Joukal M, Mrázková E, Chmelová J, Handlos P. Fatal delayed hemopericardium and hemothorax following blunt chest trauma. *Forensic Sci Med Pathol.* 2019. doi:10.1007/s12024-018-0069-5 (in press)
3. Dubový P, Klusáková I, Hradilová-Svíženská I, Brázda V, Kohoutková M, Joukal M. A conditioning sciatic nerve lesion triggers a pro-regenerative state in primary sensory neurons also of dorsal root ganglia non-associated with the damaged nerve. *Frontiers in Cellular Neuroscience.* 2019;13. doi:10.3389/fncel.2019.00011;
4. Korimová A, Klusáková I, Hradilová-Svíženská I, Kohoutková M, Joukal M, Dubový P. Mitochondrial Damage-Associated Molecular Patterns of Injured Axons Induce Outgrowth of Schwann Cell Processes. *Frontiers in Cellular Neuroscience.* 2018;12. doi:10.3389/fncel.2018.00457;
5. Dubový P, Klusáková I, Hradilová-Svíženská I, Joukal M. Expression of Regeneration-Associated Proteins in Primary Sensory Neurons and Regenerating Axons After Nerve Injury-An Overview. *Anatomical Records Hoboken NJ 2007.* 2018;301(10):1618-1627. doi:10.1002/ar.23843.
6. Dubový P, Hradilová-Svíženská I, Klusáková I, Kokošová V, Brázda V, Joukal M. Bilateral activation of STAT3 by phosphorylation at the tyrosine-705 (Y705) and serine-727 (S727) positions and its nuclear translocation in primary sensory neurons following unilateral sciatic nerve injury. *Histochemistry and Cell Biology.* February 2018;1-11. doi:10.1007/s00418-018-1656-y;
7. Handlos P, Uvíra M, Marecová K, Staňková M, Smatanová M, Dvořáček I, Joukal M*. Fatal Ingestion of Chlumsky Disinfectant Solution. *Journal of Forensic Sciences.* 2017;63(2):626-630. doi:10.1111/1556-4029.13539;
8. Dubový P, Klusáková I, Hradilová-Svíženská I, Joukal M, Boadas-Vaello P. Activation of Astrocytes and Microglial Cells and CCL2/CCR2 Upregulation in the Dorsolateral and Ventrolateral Nuclei of Periaqueductal Gray and Rostral Ventromedial Medulla Following Different Types of Sciatic Nerve Injury. *Frontiers in Cellular Neuroscience.* 2018;12:40. doi:10.3389/fncel.2018.00040;
9. Handlos P, Gruszka T, Staňková M, Marecová K, Joukal M*. Biventricular noncompaction cardiomyopathy with malignant arrhythmia as a cause of sudden

- death. *Forensic Science, Medicine and Pathology*. 2017;13(4):495-499.
doi:10.1007/s12024-017-9889-y;
10. Dubový P, Klusáková I, Kučera L, Osičková J, Chovancová J, Loja T, Mayer J, Doubek M, Joukal M. Local chemical sympathectomy of rat bone marrow and its effect on marrow cell composition. *Autonomic Neuroscience-Basic and Clinical*. 2017;206:19-27. doi:10.1016/j.autneu.2017.06.003;
 11. Handlos P, Světlík I, Dobiáš M, Smatanová M, Dvořáček I, Joukal M, Marecová K, Horáčková L. Dating of skeletal remains by radiocarbon method in a common part of forensic medical practice. *Chemické Listy*. 2017;111(7):445-448.
 12. Řehák Z, Šprláková-Puková A, Bortlíček Z, Fojtík Z, Kazda T, Joukal M, Koukalová R, Vašina J, Eremiášová J, Němec P. PET/CT imaging in polymyalgia rheumatica: praepubic 18F-FDG uptake correlates with pectineus and adductor longus muscles enthesitis and with tenosynovitis. *Radiology and Oncology*. 2017;51(1):8-14.
doi:10.1515/raon-2017-0001;
 13. Handlos P, Dokoupil M, Staňková M, Joukal M, Dvořáček I, Uvíra M, Smatanová M. Fluid content in the pleural cavity protects internal structures against heat. *Forensic Science, Medicine and Pathology*. 2016;12(4):497-501. doi:10.1007/s12024-016-9814-9;
 14. Joukal M, Klusáková I, Solár P, Kuklová A, Dubový P. Cellular reactions of the choroid plexus induced by peripheral nerve injury. *Neuroscience Letters*. 2016;628:73-77. doi:10.1016/j.neulet.2016.06.019;
 15. Hernangómez M, Klusáková I, Joukal M, Hradilová-Svíženská I, Guaza C, Dubový P. CD200R1 agonist attenuates glial activation, inflammatory reactions, and hypersensitivity immediately after its intrathecal application in a rat neuropathic pain model. *Journal of Neuroinflammation*. 2016;13:43. doi:10.1186/s12974-016-0508-8;
 16. Joukal M, Klusáková I, Dubový P. Direct communication of the spinal subarachnoid space with the rat dorsal root ganglia. *Annals of Anatomy - Anatomischer Anzeiger*. 2016;205:9-15. doi:10.1016/j.aanat.2016.01.004;
 17. Joukal M*, Frišhons J. A facial reconstruction and identification technique for seriously devastating head wounds. *Forensic Science International*. 2015;252:82-86.
doi:10.1016/j.forsciint.2015.04.027;

18. Vymazalová K, Vargová L, Joukal M. Variability of the pronator teres muscle and its clinical significance. *Romanian Journal of Morphology and Embryology*. 2015;56(3):1127-1135;
19. Vymazalová K, Vargová L, Joukal M. Uncommon course of the ulnar artery through the pronator teres muscle. *Journal of Nepal Medical Association*. 2014;52:946–948.